Faculty of Science and Engineering
Department of Civil Engineering

Experimental Study on Bentonite Stabilisation using Construction Waste and Slag

Umair Hasan

This thesis is presented for the Degree of
Master of Philosophy
of
Curtin University

August 2015

DECLARATION

To the best of my knowledge and belief this thesis contains no material previously published by any other person except where due acknowledgment has been made.

This thesis contains no material which has been accepted for the award of any other degree or diploma in any university.

Signature:

Date:

ABSTRACT

Due to ongoing rapid population growth it has become almost inevitable to carry out construction on ground with a weaker bearing capacity. The volumetric deviations in montmorillonite-rich clays like bentonite render such soils unsuitable to support overlying pavement and foundation structures and remedial measures such as soil stabilisation are often implemented. This study used experimental evaluation to conduct a feasibility analysis of an industrial by-product, ground granulated blast furnace slag, and recycled construction waste as effective expansive bentonite clay stabilisers. The unconfined compressive strength (UCS) and direct shear strength (DST) of samples at optimum moisture content was evaluated with 13 different combinations of slag (2% to 5% of the wt. of untreated clay) and construction waste (10%, 15% and 20% of the wt. of untreated clay), over six different curing periods (1, 3, 7, 14, 21 and 28 days). Scanning electron microscope (SEM), energy dispersive spectrometer (EDS) and x-ray diffraction (XRD) analyses were also conducted to determine the microstructural arrangement and mineralogical effect of the stabilisation treatment. The results indicated formation of structural bonds between admixtures and bentonite in stabilised specimens, as slag crystals and bentonite particles were observed to occupy the cavities and vesicles on the construction waste grains. Escalation in UCS values was observed with increased additive percentages and growing curing periods, with the optimum additive ratio calculated as 5% of slag and 20% of construction waste under all curing conditions. The results were more pronounced for all stabiliser combinations after 28 days of curing, probably due to the binding nature of slag. Direct shear tests were conducted based on the same controlling parameters under normal stresses of 50kPa, 100kPa and 20kPa. Results exhibit that shear strength parameters of cohesion, peak shear stress and internal friction angle increased with increasing stabiliser percentages and curing time. Sample with 5% slag and 20% construction waste (sample S3G5) also corresponded to the highest shear strength improvement. A strength development index (SDI) and a shear index (τ_I) was developed to assess the effects of the stabilisation process. The maximum SDI value, attributed to optimum compressive strength improvement was observed at 3.09 for S3G5. Minimum τ_I value, attributed to maximum improvement in shear strength was 0.71. Experimental data shows the

feasibility of using construction waste and slag mixture for the stabilisation of bentonite clays, in terms of shear and compressive strength improvement.

ACKNOWLEDGEMENT

"The essence of all beautiful art, all great art, is gratitude."

– Friedrich Nietzsche

There are many people whose contributions to this thesis exceed my ability to express my most humble gratitude. The first of those people is my supervisor Dr Amin Chegenizadeh, who has constantly supported my research through his excellent mentoring, enthusiasm, knowledge and perseverance to see the best in his students. I express my sincere gratitude to him for his guidance and friendship that has carved out a dedicated research student out of me. His supervision and valuable advice has immensely helped me to embark upon a path to academic career.

I would also like to express my sincerest gratitude and indebtedness to my co-supervisor Prof Hamid Nikraz for his support, inspiration and encouragement during the most difficult times of this research work. His assuring words and patient counsel kept me on track through the many personal, financial and educational obstacles that hurdled my way forward.

I also express my gratitude to Dr Andrew Whyte, Mrs Sucy Leong, Ms Cheryl Cheng, Frankie Sia and Mrs Diane Garth for their support in admin matters. I also extend my appreciations to Mark Whittaker, Darren Isaac and Mirzet Sehic at Geomechanics and Pavement Laboratories. I also thank Ms Elaine Miller, Dr Angela Halfpenny and Ms Veronica Avery at Department of Physics and Astronomy. I also extend my deepest appreciation to my friends and colleagues M. Arief Budihardjo, Yogie Rinaldy Ginting, Hassan Malekzehtab, Fariba Asadi, Behzad Ghadimi, Ainalem Nega, Md Abu Sayeed and Hamed Noohooji for their support and help in many technical and nontechnical matters.

Finally, I thank and express my love to my parents M. Riaz Usman and Rubina Riaz for being the architects of my every success and my sisters Zenab and Hira for being the elixirs of my life. I thank my family for being my companions through the thick and thin, the stress, hardship and fears that come with tough decisions and long journeys to success that come at the end of every decision.

DEDICATION

In the loving memory of my grandmother, Khursheed Bi,

and my secondary school English teacher, Mrs Sherwani,

for rekindling hope during the worst of times

PUBLICATIONS

The following publications have resulted from the work conducted as part of this research.

JOURNAL PUBLICATIONS

- Umair Hasan, Amin Chegenizadeh, Mochamad Arief Budihardjo, Hamid Nikraz, "A Review of the Stabilisation Techniques on Expansive Soils", Australian Journal of Basic and Applied Sciences, 9(7): 541-548, 2015.
- Umair Hasan, Amin Chegenizadeh, Mochamad Arief Budihardjo, Hamid Nikraz, "Experimental Evaluation of Construction Waste and Ground Granulated Blast Furnace Slag as Alternative Soil Stabilisers", Geotechnical and Geological Engineering: An International Journal (manuscript under review).
- Umair Hasan, Amin Chegenizadeh, Mochamad Arief Budihardjo, Hamid Nikraz, "Shear Strength Evaluation of Expansive Soil Stabilised from Recycled Materials", Engineering Geology (manuscript submitted).
- Mochamad Arief Budihardjo, Umair Hasan, Hamid Nikraz, "Prediction of the Migration of High Concentration of Cadmium (Cd) and Nickel (Ni) as an Effect of Climate Change from Landfill with Single and Double Liners System", Special Issue "Soil and Climate Change", International Journal of Ecosystem (manuscript submitted).
- Ghadhimi B., Mochamad Arief Budihardjo, Umair Hasan, "Temperature effects on the numerical modelling of flexible pavement due to Climate Change", Special Issue "Soil and Climate Change", International Journal of Ecosystem (manuscript submitted).
- Ghadimi B., Umair Hasan, "Review of Finite Element Simulation of Granular Materials", Applied Mechanics and Materials, Vol. 709, pp. 219-226, 2014.

BOOK CHAPTER

- Umair Hasan, Amin Chegenizadeh, Hamid Nikraz, "Nanotechnology Future and Present in Construction Industry: Applications in Geotechnical Engineering" submitted and approved for upcoming book, "Advanced Research on Nanotechnology for Civil Engineering Applications", 2015.

TABLE OF CONTENTS

LIST OF FIGURES

LIST OF TABLES

LIST OF ABBREVIATIONS AND SYMBOLS

The following is a list of abbreviations and symbols used within the text of this thesis. In addition, the symbols and abbreviation have also been described alongside their first usage. The list has been prepared in the logical ascending alphabetical order.

ε = Strain
θ = Angle of incident or angle of diffraction
λ = Wavelength of light
σ = Normal stress
σ' = Effective normal stress
σ_n = Normal or vertical stress
τ = Shear stress
ϕ' = Effective angle of internal friction
p_{at} = Atmospheric pressure
u_a = Pore air-pressure
u_w = Pore water pressure
τ_f = Unsaturated soil shear strength
τ_I = Shear index
τ_{us} = Suction strength
$\bar{x}$ = Mean
ΔL = Change in length
A = Soil activity
a = Soil parameter
A or A_o = Initial or original cross-sectional area of the compacted specimen
A' = Post-test altered cross-sectional area of the failed specimen
ABFS = Air-cooled blast furnace slag
ASTM = American standards for testing of materials
AVSR = Ratio of axial strain to volumetric strain
BFS = Blast furnace slag
c = Cohesion

c = Cohesion

c' = Effective cohesion

CBR = California bearing ratio

CEC = Cation exchange capacity

CFA = Class-C fly ash

CH = Clay with high plasticity

CI = Inorganic clays or lean clays of medium plasticity

CKD = Cement kiln dust

CL = Clay with low plasticity

CMCW = Crushed masonry and construction waste

CNT = Carbon nanotube

CS = Consolid system

CSH = Calcium silicate hydrate

CW = Construction waste

d = Resolution capacity of optical microscope

= Sample lattice spacing or spacing between atomic layers

d_h = Horizontal displacement of the sheared specimen in direct shear test

DSS = Direct shear strength

DST = Direct shear test

d_v = Vertical deflection of the sheared specimen in direct shear test

EBFS = Expended or pelletised blast furnace slag

E_{comp} = Energy applied by hammer

EDS = Energy dispersive spectroscopy

EP = Expended polystyrene

EPHC = Environment Protection and Heritage Council

F = Lorentz force

FA = Fly ash

FEM = Finite element method

FFA = Class-F fly ash

f_{oc} = Focal length

FSI = Free swell index

GBFS = Granulated blast furnace slag

GBFS = Granulated blast furnace slag

GGBFS = Ground granulated blast furnace slag

$H^{/}$ = Magnified image height

h_d = Falling distance of hammer

I_L = Liquidity index

I_p = PI = Plasticity index

K_α = X-rays produced as electron transitions of n = 2 → 1

K_β = X-rays produced as electron transitions of n = 3 → 1

L = Length of the failed specimen after the test

LD slag = Linz Donowitz slag

LL = Liquid limit

L_o = Initial height/length of the compacted specimen

m, n = Indices in graphene honeycombed crystalline lattice denoting unit vectors along two directions

MBV = Methylene blue value

MC = Moisture content

MDD = $(\gamma_d)_{max}$ = Maximum dry density

m_h = Mass of hammer

MI = Inorganic silts or clayey silts of medium plasticity

N_b = Number of blows

N_L = Number of compacted soil layers

OMC = Optimum moisture content

P = Normal or vertical load

PL = Plastic limit

POFA = Palm oil fuel ash

PSC = Portland slag cement

PSD = Particle size distribution

q_u = UCS = Unconfined compressive strength

RHA = Rice husk fly ash

RSD = Relative standard deviation

SD = Standard deviation

SDI = Strength development index

SEM = Scanning electron microscope

SIF = Strength improvement factor

SL = Shrinkage limit

S_t = Sensitivity

TEM = Transmission electron microscope

V = Volume of soil in mould

XRD = X-ray diffraction

CHAPTER 1
INTRODUCTION

1.1 BACKGROUND

Geotechnical engineers often encounter unsuitable or weak soils on project sites. Due to the ongoing rapid population growth it has become almost inevitable to execute construction on the grounds with weaker bearing capacities. It is common to observe volumetric deviations in some soils because of the climatic fluctuations. These soils, also termed as reactive soils, are susceptible to volumetric deviations induced by climatic variations. These changes in volume are a major big concern during the structural designing of foundations and pavements on these soils and the post-construction stability of such structures. A recent study encompassing foundation design on an expansive soil through the numerical back analysis of a residential unit damaged due to the damages by heave of expansive soil was conducted by Li, Cameron, and Ren (2014) where non-uniform moisture conditions were a result of drainage and excessive watering issues and had caused visible cracks in the walls. Further study revealed that the additional stresses have caused the beam steel reinforcement bars in the affected region to yield and revised beam dimensions had to be recommended to counter the additional stresses developed due to the swelling of soil. The study showed that a technical understanding of the expansive behaviour of soils and stabilisation efforts can go a long way in minimising the repair costs associated with the insurance claims and budgets for maintenance of residential and commercial structures built over the expansive soils.

Expansive clay like bentonite constitute of small sized reactive clay particles, such as montmorillonite. They can be categorised as plastic soils containing high cation exchange capacity with a high degree of particle dispersion. The distinguishing feature of expansive soils is their ability to swell and shrink cyclically due to changes in soil moisture content that are caused by the changing environmental conditions. These soils tend to swell when wetted, while display shrinkage upon drying. Due to the damages caused to overlaying structures because of the presence of expansive soil, identification of soil type present on the site is important and ensure that it is

safe for the intended construction purposes. There are various methods available to identify and classify the soil based upon its plastic limit, liquid limit, cation exchange capacity and swelling index.

These clays are differentiated by their property to repetitively exhibit significant swelling and shrinkage due to the variations in the soil moisture content, depending upon the changes in their environmental conditions. They tend to swell when wetted, while display shrinkage upon drying, often incurred due to climatic changes as illustrated in Figure 1.1.

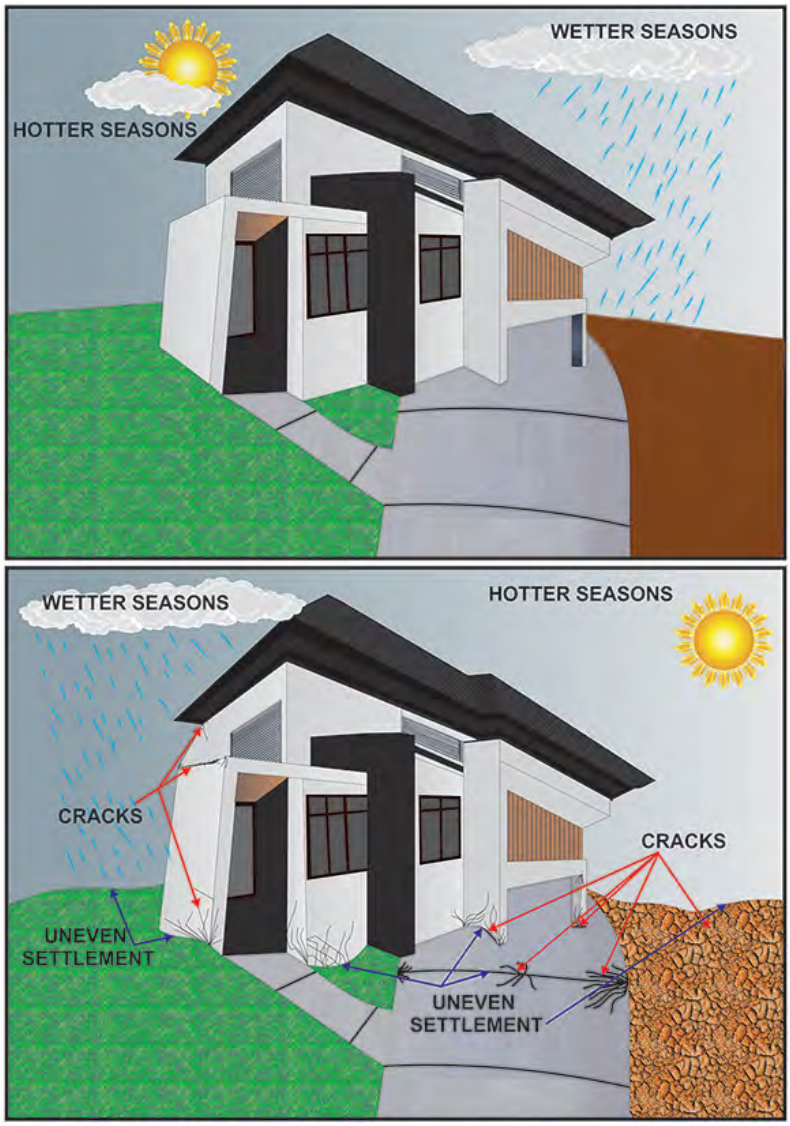

Figure 1.1 Differential/Uneven Settlement of Low Rise Structure on Expansive Clay due to Inadequate Capacity and Wetting-Drying Cycle

These types of highly dispersive and plastic soils largely having high cation exchange capacity and smaller particle size composed of reactive clay minerals such as montmorillonite and illites are found in many terrains around the world. The arid and semi-arid areas are especially prone to comparative large percentages of such soil compositions. The change in volume due to climatic changes, especially around rainfall, is a major concern in structural design and stability of foundations and pavements constructed over expansive soils. Over time, the buildings constructed upon expansive soils show noticeable signs of soil movement in terms of cracks and structural damage due to the distress caused by moisture variations. Low-rise structures are especially susceptible to failure due to their inadequate resistance capacity against ground movements (Bell and Maud 1995).

Many parts of the world, particularly the arid and the semi-arid areas, are especially prone to comparative large percentages of expansive soil compositions (Schanz and Elsawy 2015). Over the past decades, many researchers have carried out extensive amount of investigative work to understand the behaviour of expansive soils. These expansive soils constitute of small sized reactive clay particles. They can be categorised as plastic soils containing high cation exchange capacity with a high degree of particle dispersion. It is important to assess the shrink-swell potential of the expansive clays and their ability to provide adequate bearing capacity to support structures before the execution of construction work. Figure 1.1 shows that due to the inability of the clay to support the overlying house, several cracks were formed on the structural members of the residential structure. Due to the differential or uneven settlement of the soil, it was not strong enough to bear the stresses induced by the structure and thus failed. This is a typical case of crack formation in low-rise structures due to bearing capacity failure of the supporting soil.

A critical review of the economic damages caused by the lack of proper research on land development projects developed over expansive soils before the commencement of construction work produces a clear statement about the dire need of site evaluation, assessment and recommendation on each project site. Since the environmental impacts such as weather, human activities and the chemical, mineralogical and geological composition of each project site have wide variations, and the cost of investigation far exceeds that of repairs, therefore it is absolutely

imperative to investigate the unique nature of the expansive soil present on each site so that the associated huge financial losses could be avoided. The problems associated with the expansive soil hold significant position in Australia as approximately 20% of Australia is covered with expansive soil and among the eight major Australian metropolises, six remain affected by the expansive soil (Walsh and Cameron 1997).

The upper soil strata or the "active zone" is the main problematic zone in the expansive soils as most of the climate-influenced volumetric changes occur in that zone (Nelson et al., 2015). The extent or the depth of this zone may depend upon the geo-climatic conditions of the region (Jones and Jefferson, 2012). This zone is also important for providing support to the overlying structure and transference of load and stresses to the ground from the supported structure.

There are several soil stabilisation approaches to counter the hazards presented by these soils; such as chemical, electrical, mechanical and thermal stabilisation (Hausmann 1990; Nicholson 2014). The orthodox methods for the improvements of the soils' textures, plasticity and strengths incorporate mechanical stabilisation through mixing of distinctive soils, surcharge loading, compaction-controlled replacement of soil and pre-wetting. Another technique is of chemical stabilisation through the induction of particular proportions of additives such as slag, fly ash, cement, gypsum and/or lime. Every method has its merits and demerits regarding effectiveness, cost-adequacy and environmental concerns. Edil et al. (2002) specify replacement of unsuitable soil with a material having better ability to support loads, such as rock as the best approach. Conversely, the higher replacement costs of some weak soils such as expansive soils may require a more economical remedial method involving a suitable stabilisation method. The suitability of the treatment method can be determined through field examinations and laboratory experiments.

1.2 RESEARCH SCOPE AND OBJECTIVES

The purpose of this project is to perform laboratory investigation in order to assess the effect of slag and construction and demolition waste on the morphology, microstructure, elemental distribution, compressive strength and shear strength

parameters of expansive bentonite clay. The samples were prepared with different compositions of the two stabilising agents and tested after being subjected to different curing periods. Since this research assesses the feasibility of stabilising bentonite clay with slag and construction waste, inducted in different percentages, the objectives of this research are:

- To determine the optimum proportion and curing conditions of stabiliser used in stabilised expansive soil.
- To evaluate the performance of a selected stabilised soil in terms of bearing capacity, shear strength and compressive strength.
- To evaluate microscopic effects of stabilisers on the stabilised expansive bentonite clay, in terms of microstructure, appearance, elemental distribution and mineral formation or occurrence in the bentonite-stabiliser composites.

1.3 OUTLINE OF THESIS

This thesis is divided into five chapters based upon the individual aspect of the research project discussed. An introduction to the research problem and brief discussion on the inadequate bearing capacity, volumetric variations and uneven strength of expansive clays is covered in the first chapter. Chapter 1 also outlines the research scope and objectives and the overall thesis outline. The problems associated with expansive clays, stabilisation of expansive clays using additives like lime, cement, slag and fly ash etc., have been covered in the literature review and background presented in chapter. Chapter 2 also discusses the generation of construction and demolition waste around the world, in general, and specifically focuses on the Australian market. The reuse and recycling methods either currently practiced or probable recycling applications are also presented. Moreover, brief introduction, background and purpose of the geotechnical, imaging and spectroscopic laboratory experiments conducted as part of this research work, have also been provided in chapter 2.

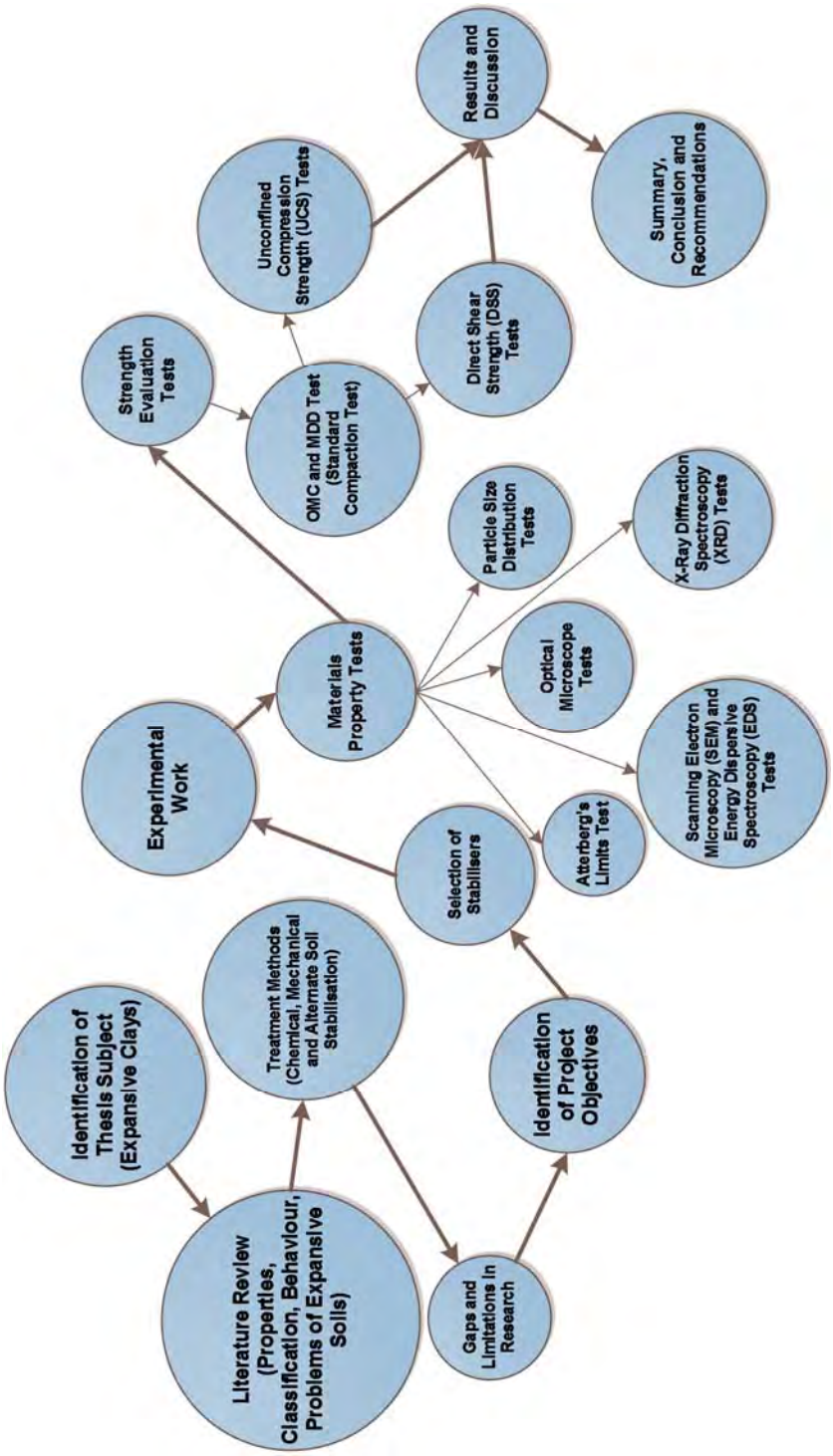

Figure 1.2 Outline of the Thesis

Chapter 3 outlines the research methodology and presents the procedure of the laboratory experiments performed on pure bentonite clay, construction and

demolition waste, GGBFS and the clay-stabiliser composite. A brief introduction to the adapted tests, including standard compaction test for optimum moisture content and maximum dry density determination, Atterberg's limits tests, particle size distribution test on construction waste, unconfined compression tests on stabilised and unstabilised specimens and direct shear tests on pure bentonite and bentonite-stabilisers composites.

The results of the experimental work have been presented in chapter 4 along with the discussion on the results. Comparative analysis of the samples prepared with different additive proportions and subjected to different curing periods and the effects of the two stabilisers as well as the curing time have been separately evaluated.

Chapter 5 presents a summary of the entire research work including expansive clay problems and stabilisation, geotechnical laboratory experiments and imaging and spectroscopy tests. Conclusions deduced from the results obtained from the experimental work have also been covered in chapter 5. Moreover, limitations of this research project and directions for future research have also been presented. The outline of the thesis project has been further illustrated in Figure 1.2.

CHAPTER 2
BACKGROUND

2.1 INTRODUCTION

These soils often have inadequate bearing capacities to support the overlying structures. There are several soil stabilisation approaches for countering the hazards presented by these soils, such as chemical, electrical, mechanical and thermal stabilisation (Hausmann 1990; Nicholson 2014). The volumetric deviations in montmorillonite-rich clays like bentonite render such soils unsuitable to support overlying pavement and foundation structures. Orthodox methods for the improvement of soil texture, plasticity and strength incorporate mechanical stabilisation through mixing of distinctive soils, surcharge loading, compaction-controlled replacement of soil and pre-wetting. Another technique is chemical stabilisation through the induction of particular proportions of additives like lime, fly ash, slag, cement and/or gypsum. Chemical or additive stabilisation is among the most popular soil stabilisation methods. Treatment can be aimed at increasing soil particle size, reducing the plasticity index, enhancing strength and decreasing the shrink-swell potential or cementation. It involves introducing one or more chemical compounds into the soil mass. Conventional compounds like cement and unconventional or recycled compounds such as slag, fly ash and lime have been effectively utilised for soil stabilisation. Moreover, green construction and sustainable waste management practices have adapted use of waste recycled materials for engineering purposes.

This study explores the feasibility of using recycled construction and demolition waste and ground granulated blast furnace slag for developing compressive and shear strength properties of expansive bentonite clay as well as study additive introduction influence on the chemical distribution and microstructure of the stabilised mixtures. This chapter is compiled to study the nature of the expansive clay in general, structure and behaviour of bentonite clay, identification of any type of expansive soil on the project site and the several treatment procedures that have been adapted so far in dealing with weak and expansive soils. Since slag and

construction waste have been used for soil stabilisation in this study, production, physical and chemical characteristics of slag and stabilisation of soil through slag has also been studied. Furthermore, the sources and generation of construction waste globally and specifically in Australia have been studied in addition to construction wastes' reuse and recycling. The last section of this chapter deals with the theoretical review, methodology and operation of the geotechnical and micro analysis tests adapted for this research work. The flowchart in Figure 2.11 further displays the outline of this chapter.

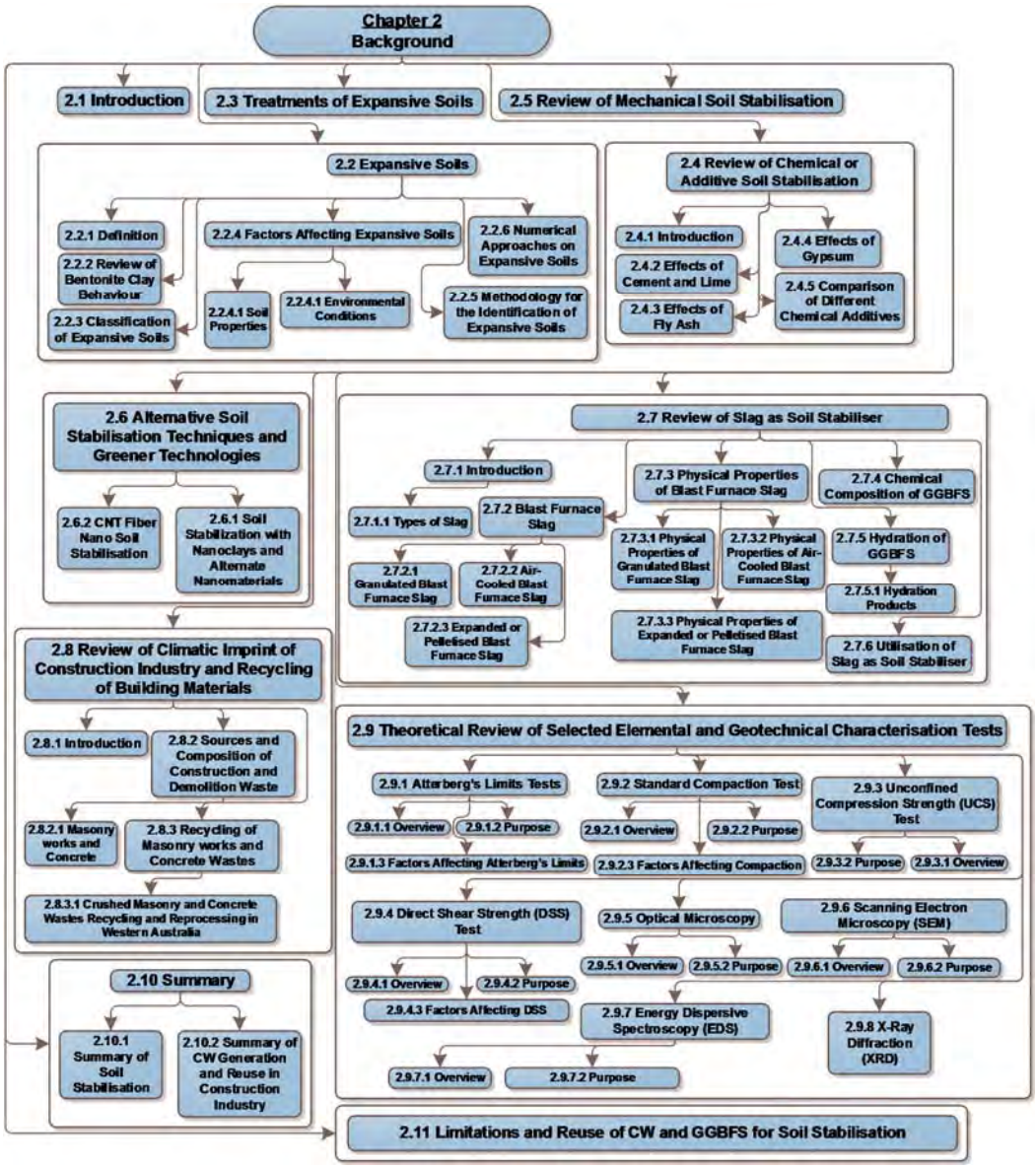

Figure 2.1 Outline of Chapter 2

2.2 EXPANSIVE SOILS

2.2.1 Definition

The soil that causes damage to the overlaying structures such as foundations and pavements is called "reactive" or "expansive" soil. It mainly consists of a specific type of clay, which swells with an increase in its water content and shrink, with the reduction. The changing seasonal conditions are usually responsible for these fluctuations in the soil moisture content. The variation in the soil's volume causes vertical or horizontal deformation of the ground. Expansive soil may result in vast damages to civil engineering structures (Karunarathne et al. 2012; Fredlund 2006).

2.2.2 Review of Bentonite Clay Behaviour

The behaviour of any clay is dictated by its mineralogical and morphological composition. The clay minerals fall in the hydrous phyllosicicates group, as significant amount of water can be found between their sheets which can be further increased or decreased due to changes in atmospheric conditions. Further addition of water increases the plastic behaviour of the clay particles and renders their remoulding significantly easier. However, the addition or absorption of water by the clay particles usually results in the expansion of the clay as the water particles penetrate the voids between the silicate layers of the micro- to submicroscopic crystals. In nature, it is quite rare to find virgin clay particles as they often found mixed with other clays and minerals like feldspar, mica, carbonates and quartz etc.

Clay minerals are structured as two-dimensional sheets of SiO_4 tetrahedrons. Each tetrahedron is linked with another through the sharing of its three corners, forming a hexagonal mesh. The fourth oxygen molecule which is perpendicular to the sheet or is at the top of each tetrahedron connects to the adjacent octahedral layer which has smaller cations as Mg^{2+} (magnesium) or Al^{3+} (aluminium). The shared oxygen atoms (O^{2-}) and the hydroxyls (OH), which are unshared, are found at the same level at the junction of the two layers. The partial substitution of the silicon atoms with aluminium has been commonly observed. However, some cases of ferric iron substitution have also been found to replace the cations. The layer arrangement of the tetra- and octahedral sheets classifies the layer.

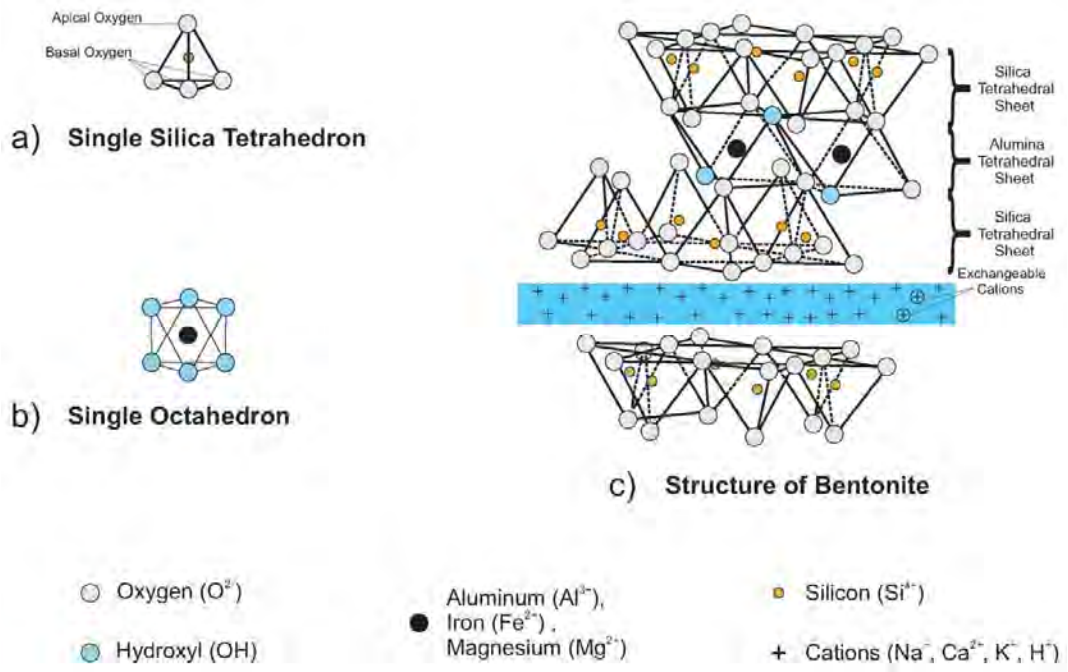

Figure 2.2 Schematic Diagram of Montmorillonite Crystal

The classification of clay minerals can be either as 1:1 or 2:1. The originating parameter behind this nomenclature is as they are formed by octahedral hydroxide and tetrahedral silicate sheets. This has been further elaborated in Figure 2.2 and the following description. Clay with 1:1 arrangement has one octa- and one tetrahedral sheet, such as serpentine and kaolinite. However, for the clay with 2:1 arrangement, two tetrahedral sheets sandwich one octahedral sheet, such as montmorillonite, talc and vermiculite. Montmorillonite is from the smectite family, which is the most dominant clay mineral found in a special category of clays called expansive soils which cause many issues for the projects on such structures, has a 2:1 layer arrangement (Figure 2.2). This implies that it has two tetrahedral sheets sandwich the octahedral sheet. Each of the two tetrahedral sheets of the layer has one unshared oxygen vertex. These vertexes from adjacent layers point towards each other but do not have a lot of attraction which provides space for the exchangeable cations and water molecules. Due to the replacement of the silicon by aluminium atoms as well as Al^{3+} by the Mg^{2+} at some parts of the octahedral sheets provides the negative charge that gives montmorillonite a high cation exchange capacity (CEC). This high

CEC value is in turns responsible for the sensitivity of the expansive soils to the climatic variations.

2.2.3 Classification of Expansive Soils

The most common and comparatively inexpensive parameter utilised for the purpose of classifying expansive soils is the degree of expansion or swelling potential of expansive soils. Site surveys supported by laboratory investigations are necessary to identify the degree of expansion of expansive soils. After the degree of expansion for a particular site has been established, it can be employed as a decisive factor to select a certain type of treatment that might be required for the specific soil present on the site. The successful application of a suitable soil treatment can help to reduce the degree of soil deformation and the damages to the overlaying structures can be kept within an acceptable range.

Clays have been categorised based on the activity as inactive, normal and active clays. The concept of clay activity, which depends upon the clay content and the plasticity index of the soil, will be discussed in detail in the Atterberg's limits section of this study. Generally, the inactive clays have the clay activity values less than 0.75, while normal clays have the clay activity values in the range of 0.75 to 1.25 and the active clays have the clay activity values higher than 1.25 (Skempton 1953). Furthermore, some of the researchers have used the liquid limit of the soil as the classifying criterion. According to Indian Standard IS: 1498 (2007) , soils with liquid limit (calculated in percent) in the range of 20-35 were classified as soils with low degree of expansiveness, medium degree of expansiveness if the liquid limit is in the range of 35-50, high for the range of 50-70 and very high degree of expansiveness if the value of the liquid limit falls in the range of 70-90. A somewhat slightly different criterion using the same percentile value of liquid limit as the classifying factor, was proposed by Chen (1975). The soil was categorised as low degree of expansive soil for the liquid limit value of less than 30; medium for a value in the range of 30-40, high degree of expansiveness with value in the range of 40-60 and a value greater than 60 implies very highly expansive soils.

2.2.4 Factors Affecting Expansive Soils

Extensive amount of research material has been published elaborating the investigations about the expansive soil and the factors responsible (Nelson and Miller 1992). These factors are postulated below:

- Clay mineralogy.
- Soil particles arrangement.
- Compaction and Atterberg limits characteristics.
- Environmental conditions such as moisture variations, water chemistry, percentage of clay fractions and confining pressure etc.

2.2.4.1 Soil Properties

Clay mineralogy produces different swelling potential index due to the valency variations. The swell potential is based upon the type and amount of specific clay minerals, composition and arrangement and soil-water chemistry. Due to the small size of particles, electron microscopy and X-Ray diffractive methods tests are conducted to identify the thickness and spacing between bonding layers and other particle features and engineering properties. Soil-water chemistry such as hydration cations such as of Na^{+}, Ca^{2+}, Mg^{2+} and K^{+} can result in the accumulation of significant amounts of water in between clay particles causing the closely packed clay particles to drift apart. The plasticity and density of soil also affects the swell-shrink potential of soil. Atterberg limits are used to describe the expansive potential of soil while quantifying the soil consistency.

2.2.4.2 Environmental Conditions

Moisture variations constitute a large share of volumetric changes that occur in an expansive soil. The ability of soil to absorb or release water depends upon initial moisture content, plastic limit and shrinkage limit. Top layer or active zone of soil in any geography is exposed to the largest amount of moisture changes exhibiting the majority of shrink-swell behaviour. They are affected by rains, altered drainage conditions, irrigation, land contours and bad or leaking plumbing works. Proper research investments before construction can go a long way to mitigate expensive damages.

2.2.5 Methodology for the Identification of Expansive Soils

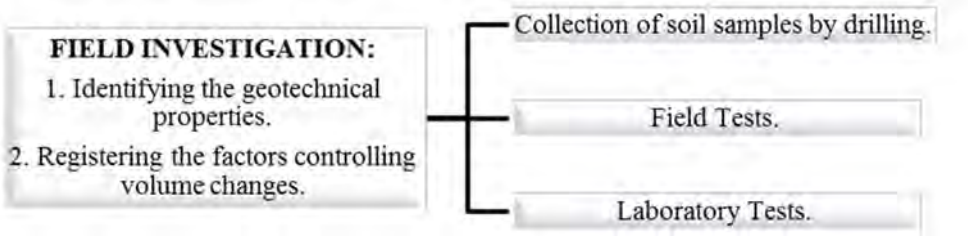

Figure 2.3 Identification Procedure of Expansive Soil

Detailed field investigation includes determining the soil profile, shrink-swell potential and the geotechnical soil properties. Samples can be excavated and carefully transported to the testing area. There are various methods available in the field for the testing of the sample to calculate the shrink-swell potential, bearing capacity and shearing strength of these soils.

In their study, Kariuki and Meer (Kariuki and van der Meer 2004) performed analysis of the different indices that are currently used to identify expansion such as cation exchange capacity (CEC), Atterberg limits and saturated MC tests for different soil samples. Their results show that the expansive behaviour of any soil relies heavily upon the clay content, type of clay present, CEC and MC. Therefore an investigation of these properties and understanding of the clay mineral type can help to identify the expansive nature of the soil.

S. G. Fityus (2004) performed field and laboratory tests on a site near Newcastle containing highly plastic expansive silty clay where field monitoring instruments have been installed as a part of their long study. Ground movement and the water content and suction data for the varying were obtained. They concluded that the suction varies linearly with depth and the data obtained from in situ has a high probability of errors whereas measurements obtained from lab tests on collected samples have shown more accurate results in comparison.

2.2.6 Numerical Approaches on Expansive Soils

In addition to the field investigations, several numerical methods have been introduced to understand the shrink-swell problem and relation of soil strength with

the soil suction, soil MC variations and the degree of saturation. One such model was developed by Miao, Liu, and Lai (2002) during their analysis of the effects of the stress state of soil and moisture changes on the soil-water characteristic curve. They developed two sets curves of expansive soil samples. Change in the specimen volume was permitted in one set and constant volume was maintained for the other set by means of applying a pre-load on the sample. The comparison between the soil-water curves obtained from both samples was made and the soil initial stress–state was deduced to affect the curve's shape. Triaxial tests were performed to obtain shear strength parameters for the expansive soils. The triaxial tests on expansive soils at different pressures with controlled suction showed independency of strength parameters from suction. They manipulated the test results to develop a hyperbola model of the suction strengths of the expansive soils which can be employed to display strength behaviour of the soils, described in the following equation.

$$\tau_{us} = \frac{au_s}{1+\frac{1-a}{p_{at}}u_s} \qquad \text{Equation (2.1)}$$

And the unsaturated soil strength equation as:

$$\tau_f = c' + (\sigma - u_a)\tan\emptyset' + \frac{au_s}{1+\frac{1-a}{p_{at}}u_s} \qquad \text{Equation (2.2)}$$

Where; τ_{us} = suction strength, u_a = pore air-pressure, u_w = pore-water pressure, a = soil parameter, $u_s = u_a - u_w$, p_{at} = atmospheric pressure, τ_f = unsaturated soil shear strength, c' = saturated soil effective cohesion; ϕ' = saturated soil effective frictional angle. Based on this model, the shear strength of these soils can be calculated. Although the parameters involved in the model can be easily obtained, it was observed that they are related to the range suction of the triaxial test for the specimen.

One of the researchers to study the slope failure on ridge tops having expansive soils were Jiang et al. (2013). They developed the soil profile for the area under study and tabulated the soils' characteristics like clay mineralogical behaviour, composition, particle texture and colour after performing X-ray diffraction, electron microscopy and chemical analysis. In addition the activity parameters such as; Atterberg limits, cohesion, expansion ratio, compaction, moisture content and angle of friction were

also reported. They reported that the soil layers show different expansive behaviour due to having different clay percentages between them and the cracked grey clay middle layer exhibited most expansive behaviour. One of their most important observations was the effect of landscape and geotechnical properties of soil on the slope failure. They also validated existing engineering practices for the mitigation of such risks like constructing retaining walls, digging drainage ditches, soil nailing and reinforcing the existing soil with addition of geotextiles.

Expanding over a previous laboratory study on the volumetric variations of unsaturated expansive soil from different sites Puppala, Manosuthikij, and Chittoori (2013), evaluated existing mathematical relations estimating displacement due to expansive nature of soils using 3D swell strain tests. Existing analytical models (potential vertical rise R. Lytton (2004)), a proposed new correlation between swell strain and plasticity index based on laboratory test results at optimum moisture content (OMC) and other modified correlations between volumetric change and MC variations from Kodikara (2006) were compared with the actual data collected through field investigations. Comparisons were also made against a pavement section model developed in Abaqus software for numerical finite element method (FEM) simulation. Abaqus software suite is widely used in the industry and academics for the purpose of finite element modelling and its customisability. Abaqus/CAE is used for both modelling and analyses as well as presenting results of FEM simulation in visual manner (Hibbitt, Karlsson and Sorensen 2005).

Puppala, Manosuthikij, and Chittoori (2013) found out that the predictions from the analytical models encompassed the upper and lower bound limits of the field measurements while the MC based relations and FEM modelling produced close predictions as of the actual field readings of expansion. However the absence of enough research on the soil shrinkage was observed and recommendations were made to conduct more research utilising a higher range of expansive soil samples. Furthermore Puppala, Manosuthikij, and Chittoori (2014) evaluated the volume changes in expansive soil due to swelling using 3D swell strain tests. They found out that the ratio of axial strain to volumetric strain (AVSR), expressed unit less is similar for tests on different soil samples. They proposed a third correlation based upon their test results obtained at optimum moisture content conditions as:

$$\varepsilon_{s,ver} = \frac{\Delta h}{h}(\%) = 0.0148 \times PI^{1.415} \quad \text{Equation (2.3)}$$

Their test results also yielded empirical relations between shrinkage strain and plasticity index of expansive soil and different moisture conditions. These relations as derived by Puppala, Manosuthikij, and Chittoori (2014) are:

For vertical shrinkage strain;

$$Wet\ of\ OMC\ \varepsilon_{sh,ver} = 0.41 \times PI^{0.83} \quad \text{Equation (2.4)}$$

$$OMC\ \varepsilon_{sh,ver} = 0.06 \times PI^{1.22} \quad \text{Equation (2.5)}$$

$$Dry\ of\ OMC\ \varepsilon_{sh,ver} = 0.001 \times PI^{2.25} \quad \text{Equation (2.6)}$$

For volumetric shrinkage strain;

$$Wet\ of\ OMC\ \varepsilon_{sh,vol} = 0.75 \times PI^{0.96} \quad \text{Equation (2.7)}$$

$$OMC\ \varepsilon_{sh,vol} = 0.19 \times PI^{1.20} \quad \text{Equation (2.8)}$$

$$Dry\ of\ OMC\ \varepsilon_{sh,vol} = 0.44 \times PI^{0.72} \quad \text{Equation (2.9)}$$

Wang and Chen (2011) coupled the set analysis of triangular fuzzy numbers based on stochastic simulation to develop and to understand the risk associated with the expansion and shrinkage of expansive soils. The model was numerically evaluated for a case study and it was deduced that the model can provide efficient evaluation to design and analyse the potential risk of the construction projects that will be executed over expansive soils.

A stability analysis of soil slope was performed by Huang and Wu (2007) on expansive after employing the unsaturated soil shear strength eq. suggested by Miao, Liu, and Lai (2002) and Mohr-Coulomb strength criterion to develop a hyperbola model of suction strength and performed analysis by Bishop's method of slices and limiting equilibrium (Bishop and Blight 1963). They employed the regressive analysis techniques to obtain the test parameters for the equations. They not only highlighted the importance of strength stratification during slope stability analysis but also their results validated the standard slope ratio of 1.75:1 recommended for construction in places containing expansive soil. Furthermore, the calculations associated with the landslide of expansive soil slopes are quite complex in nature.

Ansys is a powerful finite element analysis tool that can aid in the calculation of differential equations and has been used by researchers like Zhang (2005) for solution of coupled thermal stress equations. Another research by Tan, Zhang, and Lai (2013) adopted the approach of nonlinear elasto-plastic soil model for analysing the Nanyou expansive soil landslides based upon the FEM shear strength reduction method. Their results showed that reducing the expansive force of the soil could significantly enhance its stability. They recommended the use of expansive soil cut slope moisture impermeable and flexible support as the treatment measures.

2.3 TREATMENTS OF EXPANSIVE SOILS

The treatment method for expansive soil is also referred to as soil stabilisation defined as a mechanical or chemical treatment intended to sustain stability, reduce compressibility, improve engineering properties (i.e., shear strength) and or limit water absorption capacity of the treated soil (Harris 2005). Soil stabilisation may involve blending soils together to get a target gradation or mixing certain proportions of commercially produced materials or industrial by-products as additives that can modify gradation, texture, plasticity and strength or function as soil cementing agent (Joint Departments of the Army and Air Force 1994).

Mechanical stabilisation involves mixing of native and a different gradation soil to get a targeted gradation of the final mixture. It can be performed directly in the field or at a separate location before the mixture is returned to the job site, spread and compacted to the required density. Chemical stabilisation is performed by adding other additive materials at a certain portion of the treated soil. The choice of stabiliser depends on the treated soil. Due to the chemical reaction between the additive and soil, improvements occur in strength and stiffness and may also improve gradation, workability and plasticity of subgrade soil.

Edil et al. (2002) specify replacement of unsuitable soil with a material having better ability to support loads, such as rock as the best approach. However, due to the higher replacement costs of some unsuitable soils like expansive soil, the more economic improvement technique may involve an appropriate stabilisation method.

The most suitable treatment could be determined after initial field investigations and laboratory evaluation of expansive soil.

Miller (1997) has reported some treatments for expansive soils such as chemical additives, pre-wetting, soil substitution with control of compaction, moisture content and loading of surcharge and thermal treatment. Pre-wetting aims to increase water content of expansive foundation soils so that most of the expansion occurs pre-construction. Then shrinkage is prevented by maintaining the high water content condition. The swelling potential of soil can be reduced by modifying the soil compaction practice (Yilmaz 2006). This soil compaction treatment can be applied on highway construction or light building. The swelling pressure exerted by expansive soils with low to moderate swelling pressures can be countered by placing a heavy surcharge load on the soil surface.

2.4 REVIEW OF CHEMICAL OR ADDITIVE SOIL STABILISATION

2.4.1 Introduction

Several buildings around the world are constructed with inadequate foundations that show signs of failure with climatic changes. The main reason is that the soils under those foundations are weak and unable to provide adequate support against the imposed stresses due to low bearing capacity or changes in the strength due to climatic variations. Extensive research work has been carried out to define treatment procedures for stabilising expansive soils by different stabilisers like cement, industrial waste, fly ash, and lime.

Petry and Little (2002) have listed some cemented stabilising additives and divided them as traditional, by-product and non-traditional stabilisers. The traditional stabilisers include Portland cement, fly ash and hydrated lime while by-product stabilisers incorporate the dust from cement, lime kiln and slag. Other additives such as potassium compounds, polymers, ammonium chloride, sulphonated oils and enzymes are categorised as non-traditional stabilisers (Petry and Little 2002).

Several factors as recommended by the Texas Department of Transportation (2005) can be employed to select a suitable stabiliser namely; soil classification which includes gradation and plasticity, soil mineralogy and content (sulphates and

organics), objectives of treatment, mechanisms of additives, material properties (modulus, strength), environmental conditions (water table, drainage), design life, and desired engineering and the economic constrains (cost–effectiveness). The text that follows is an attempt at the part of the author to evaluate various additives for stabilisation of expansive soils.

2.4.2 Effects of Cement and Lime

Two of the most widely used additives for expansive soil stabilisation are cement and lime such as quicklime, lime slurry and extinct lime. The procedure is a technique used in pavement and foundation engineering and mainly involves reduction of plasticity and resulting increase in the bearing capacity. Various researchers have investigated the usage of cement and lime for expansive soils of different locations.

Al-Rawas, Hago, and Al-Sarmi (2005a) studied the stabilisation of expansive soil in the arid and desert climate of Oman using cement and lime. Their results showed the changes in different soil characteristics with variations in additives and depicted a reduction in swell percent and pressure with the usage of stabilisers. The addition of lime to expansive clayey soils triggers a number of chemical reactions including cation exchange (between cations on the surface of clay particles and calcium cations of lime), carbonation (formation of $Ca(OH)_2$ from reaction between water and quicklime), increase in pH catalysing the dissolution of silica in clay which in turn reacts with calcium oxides to form the cementing compound CSH (calcium silica hydrate) and pozzolanic reaction.

One of the recent research works investigating the stabilisation of expansive soils by use of additives was carried out by Seco et al. (2011) on expansive soil in Spain. The additives used were of two types, cement-lime and consolid system (CS). Dry samples of natural soil were mixed with powdered additives (lime, Portland cement, cereal, rice husk and steel fly ashes and gypsum). The results were evaluated through unconfined compression strength (UCS) test for soil specimen at 7, 14 and 28 days curing periods. Figure 2.4 elaborates their results:

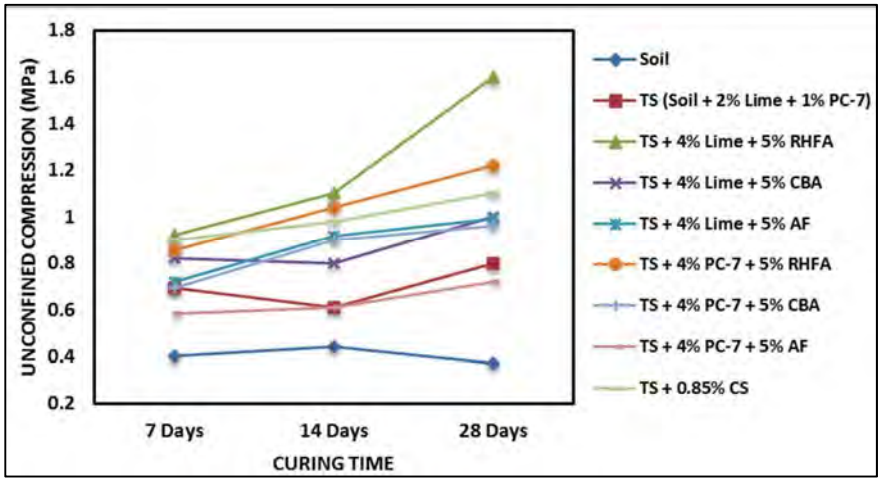

Figure 2.4 Development of UCS with Different Stabilisers Proportions and Curing Periods (after Seco et al. (2011))

These experiments indicated the utility of different additives including industrial wastes for soil treatment by reducing potential free swelling and improving the soil bearing capacity. Another recent work studying the physical, chemical and mechanical parameters of over-consolidated expansive soil stabilised by lime and Portland cement was carried out by Khemissa and Mahamedi (2014a). Their experimental programme comprised Proctor compaction, California bearing ratio (CBR), methylene blue (MBV) and undrained direct shear tests upon untreated and cement-lime treated finely crushed soil with optimum moisture content at room temperature. It was observed that test clay swell-potentials reduced with MBV > 6 to a lesser with 2 < MBV < 6, the SSA tests confirm the validity of these results and the CBR values were increased with treatment. Direct shear tests showed improvement in shear strength with stabilisation process and optimum stabiliser value is obtained with an 8% cement and 4% lime mixture in the expansive soil.

One of the important studies conducted was done on expansive organic soils by Saride, Puppala, and Chikyala (2013a). The optimum lime content of each specimen was obtained using J.L. Eades (1966) and Texas Department of Transportation (1999) for soil passing through sieve 4.75mm and lime percentage 2,4,6,8 and 10% by dry mass of soil were used for sample preparation. They observed that OMC of soils increase with increase in organic content (OC) because of high water retention capability of organic soils. It was observed that the lime treatment caused larger

reduction in plasticity than cement treatment and the improvement in unconfined compressive strength was negligible or even decreased after 28 days curing period. They also proposed a non-dimensional parameter, strength improvement factor (SIF) to understand the strength improvement in stabilised expansive soils:

$$SIF = \frac{UCS\ of\ stabilised\ specimen\ cured\ at\ n\ days}{UCS\ of\ unstabilised\ specimen\ cured\ at\ n\ days} \qquad \text{Equation (2.10)}$$

Another recent work studying the stabilisation of over-consolidated expansive soil was carried out by Khemissa and Mahamedi (2014a) with various cement-lime mixing ratios. It was noted CBR values increased with treatment and optimum results were obtained when cement and lime were added (2% and 8%) for soaked CBR. Meanwhile for the unsoaked CBR the optimum results were reached with addition of 8% cement and 4% lime. Also the direct shear tests (DST) showed that the optimum value for the improved bearing capacity of soil is obtained with an 8% cement and 4% lime mixture.

2.4.3 Effects of Fly Ash

Fly ash (FA) is a residual product or by-product generated during the thermal processing of pulverized coal in coal-fired electric and steam generating plants. In a study by Pandian and Krishna (2003), class-F FA (FFA) up to 100% was added to black cotton soil in 10% increments. They observed that the CBR values improved up to the 20% FA addition, then after initially decreasing upon further FA increments, it showed an increase to attain an optimum value with 70% FA content. Another research by Phani Kumar and Sharma (2004b) also investigated the influence of FFA addition on some geotechnical properties of expansive soil. Their study also noticed improvements in these properties with addition of FA.

Ji-ru and Xing (2002), Zha et al. (2008) and Bose (2012) were among some other researchers that examined the effects of lime and FFA adding upon the expansive soil behaviour and observed positive results. FFA and cement stabilisation of expansive soil was investigated by Amu, Fajobi, and Afekhuai (2005a). They noticed that the effect of 9% cement and 3% FA was better as compared with that of 12% cement in terms of soil stabilisation. Cokca (2001), Nalbantoglu and Gucbilmez (2001), Pandian and Krishna (2003) and Misra, Biswas, and Upadhyaya (2005)

researched influence of class-C fly ash (CFA) addition in expansive soils with different geotechnical characteristics and had found varied success. In the studies conducted by Ji-ru and Xing (2002) and Zha et al. (2008), only FA was used for expansive soil stabilisation without the addition of any other stabiliser. They observed no considerable improvement in the early UCS test; but, the UCS values showed a sudden increase after 7 days of curing. Another investigation performed by Solanki and Zaman (2010) confirmed that the increment in UCS values of their samples followed the same trend. This result was observed when they evaluated the performance of two subgrade soils (CL and CH) stabilised with three different stabilisers (hydrated lime or lime), CFA, and cement kiln dust (CKD).

2.4.4 Effects of Gypsum

An important research investigating the stabilisation of expansive clayey soils was carried out by Yilmaz and Civelekoglu (2009) on the variation of swell potential and strength.

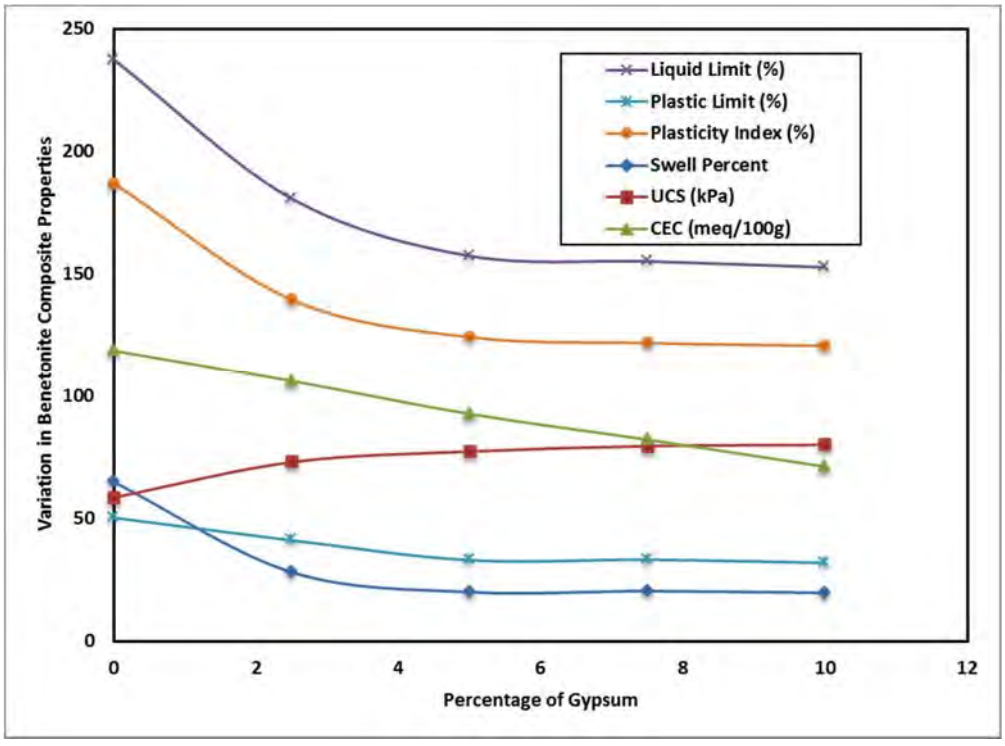

Figure 2.5 Variation in Geotechnical Characteristics of Bentonite with Addition of Gypsum

They mixed and compacted different bentonite and gypsum percentages and obtained OMC as 41%. They obtained data for Atterberg limits (British Standards 1975), CEC (Ammonium acetate method and amount of sodium in the solution through atomic absorption method), free swell (ASTM D-4546 1994) and unconfined compressive strength (ASTM D-2166 1994) tests on treated and untreated specimens tested through Standard Proctor compaction effort at determined OMC and cured for a week. The test results have been compiled in Figure 2.5. These results deduced that gypsum, which has a lower cost than lime, can be utilised for stabilisation of expansive soils by increasing bentonite UCS when used in percentages equal to or less than 5% for optimum results. Conversely the researchers also acknowledged that the usage of gypsum can result in contamination of groundwater.

2.4.5 Comparison of Different Chemical Additives

In an effort to compare the effectiveness of different additives, Seco et al. (2011) mixed expansive soil with different percentages of different combinations of additives for example cement; lime; steel, rice husk and cereal fly ashes; aluminate filler and gypsum. The free swell was determined for the one day cured test specimens and a second set of tests were carried out on the samples cured at 7, 14 and 28 days to calculate the UCS values of the treated and untreated expansive soil specimens. They observed an escalation of UCS while decline in the swelling potential. A combination of cement and lime additive mix and 4% of cement or lime addition with 5% rice husk fly ash were considered to show most notable improvements. Swelling potential reduced to 0.7% when 5% rice husk fly ash was introduced while it increased the compaction strength to two to four times in comparison to that of the untreated expansive soil.

2.5 REVIEW OF MECHANICAL SOIL STABILISATION

The mechanical techniques for soil stabilisation have been applied for many years. The most widely known practices are soil compaction, dynamic and vibro-compaction; soil replacement and blending; and soil reinforcements and installation of barriers (Shillito and Fenstermaker 2014). The effect of replacement of expansive

bentonite with blended sandy-recycled EP (expanded polystyrene) was investigated by Abdelrahman, Mohamed, and Ahmed (2013). The soil replacement reduced the volumetric expansion-reduction of the expansive soil and increased the optimum moisture content with increasing EP beads content.

Pre-wetting of the soil has also been practiced over time. The main concept is to provide moisture to the expansive soil to allow the heaving to occur before the construction execution. However, the moisture content has to be kept at the higher value to maintain the soil volumetric variation at a fixed state. Soil replacement is among the most commonly applied mechanical soil stabilisation techniques. The depth of the soil to be replaced depends upon the local soil profile, conventional practices and governing building code recommendations (Chen 2012).

2.6 Alternative Soil Stabilisation Techniques and Greener Technologies

The evolution of technology has given rise to the research in establishing alternate soil stabilisation techniques. They can be more cost effective and environment-friendly than the conventional soil stabilisation methods. The "greener" soil stabilisation methods normally induce polymers, tree resins, fibres, alkali chlorides and enzymes. Viswanadham, Phanikumar, and Mukherjee (2009) analysed the swell behaviour of an expansive soil reinforce stabilised by different fibre percentages, with varying aspect ratios. The results of oedometer swell-consolidation test showed the maximum decrement in swell pressure with lower aspect ratio at both fibre percentages. Studies have indicated that recycled fibres from random sources, such as scrap rubber tires, can be used for soil stabilisation (Belabdelouahab and Trouzine 2014). The 2% tire content has been found as optimum for UCS increment by Akbulut, Arasan, and Kalkan (2007). They also found 0.2% of polypropylene and polyethylene to be optimum for UCS. The fibre addition at these percentages also increased the shear moduli and damping ratios of treated samples.

Alternatively, waste products from industries such as the food industry have been researched as suitable soil stabilisers (Ahmad et al. 2008). Pourakbar et al. (Article In Press) investigated the effect of palm oil fuel ash (POFA) and POFA- cement mix on clay properties. They found that the addition of POFA significantly reduced the

plasticity index and optimum moisture content. The cement-POFA mix produced better improvements in the UCS than the pure POFA.

2.6.1 Soil Stabilisation with Nanoclays and Alternate Nanomaterials

Montmorillonite, sedimentary soil and kaolinite were pulverized by Taha (2009) in a ball-mill to obtain nano-sized soils termed as nanosoils. These nanosoils were mixed with the original soils and were observed to improve soil properties by increasing the specific surfaces and therefore, reducing the plasticity index.

Different nanomaterials such as nano metallic oxides (MgO and CuO) and nanoclays was used by Majeed, Taha, and Jawad (2014) to stabilise weak soils. They used two types of soils, namely organic silt (Soil 1) and highly plastic clay (Soil 2). The UCS value of treated samples improved with increasing percentage of the nanomaterials. The UCS enhancement effect of the nanomaterials for both soils showed somewhat of a bell-curve, with the Soil 2 showing comparatively sharper increase and subsequent UCS decrement with introduction of the stabilising nanomaterials. The optimum percentages of all the stabilising nanomaterials were documented to be less than 1% for both of the weak soils investigated in the laboratory experiments. Figure 2.6 shows the ratios between the strengths of unstabilised and stabilised Soils 1 and 2, as stabilised with the optimum respective nanomaterial percentage.

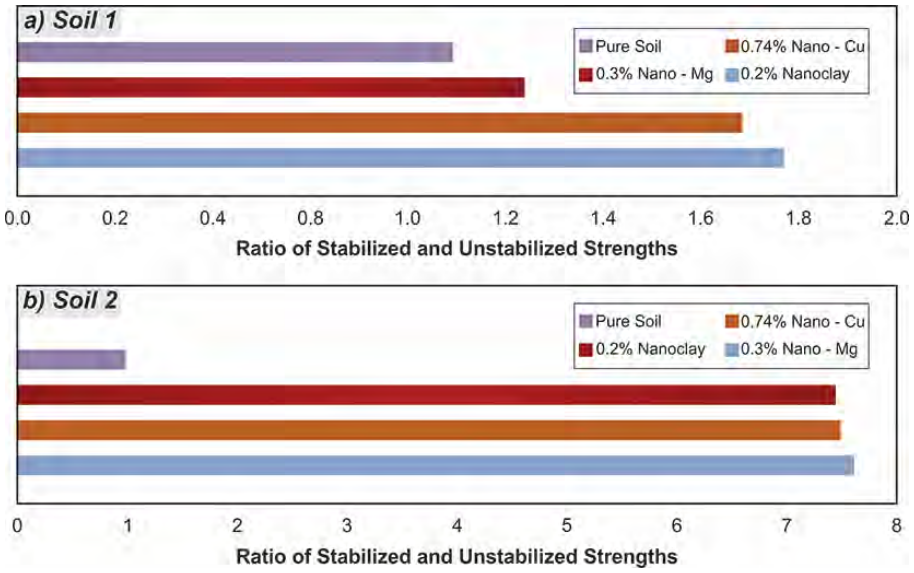

Figure 2.6 Effects of Nanomaterials on Unconfined Compressive Strength (based on results from Majeed, Taha, and Jawad (2014))

2.6.2 CNT Fiber Nano Soil Stabilisation

Fiber reinforcement has been investigated to enhance the unconfined compressive strength of weak fine grained soil. Jafari and Esna-ashari (2012) added fibre reinforcements obtained from alternate recycled sources in different percentages along with lime. They observed that by adding fibre, the samples stabilised by 4% lime produced higher compressive strength values than the unstabilised and samples with 8% of lime.

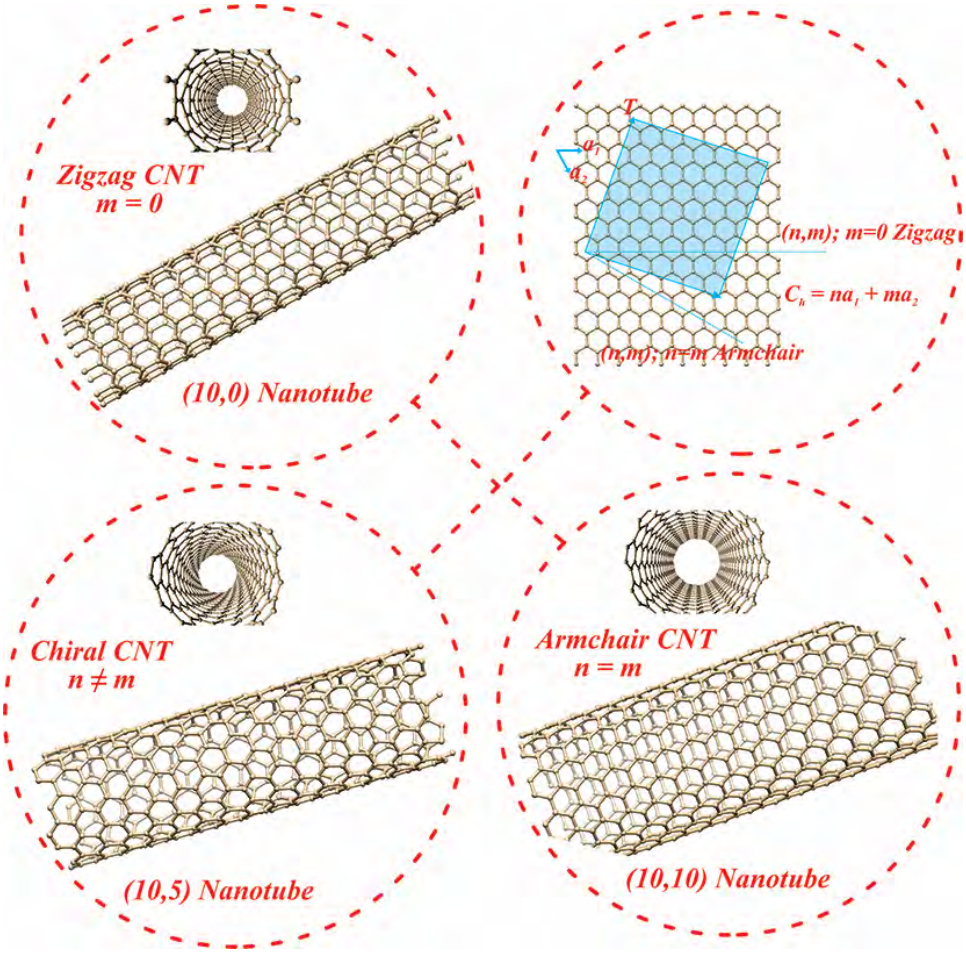

Figure 2.7 Schematic Illustration of Different CNTs

Carbon Nanotubes or CNTs are nanofibers that exhibit remarkable mechanical properties; for example higher stiffness, high strengths, high young modulus as well as high elastic stress-strain behaviour. CNTs have a much higher strength when compared with steel, prepared from carbon manipulation and modification.

Structurally they are composed of single or more graphene layers, which is a sheet shaped by carbon atoms bonded in hexagonal honeycomb shape, forming a cylinder structure which are named after a "n,m" nomenclature, based upon the rolling of the graphene sheet vector to form the tube-like nanostructure where diameters are usually ≤ 2nm (Kumar et al. 2012; NanoScienceWorks n.d.). It has been further illustrated Figure 2.7.

Those remarkable properties suggest CNTs as great materials for reinforcement of soil. Taha and Ying (2010) performed initial research work on the effect of CNTs induction on the rheological characteristics of the kaolinite clay and noted that the addition of CNTs can increase the Atterberg limits of the clay. The CNTs induction also caused the compressibility of the samples to increase while the hydraulic conductivity or permeability was decreased. Also an inclusion of 1% CNTs fibers in the soil matrix resulted in the rise in the void ratio of the treated mixture. They also observed that the CNTs addition resulted in significant enhancement in the compressive strength of the stabilised mixture Figure 2.8. CNTs can also be designed or consolidated inside a soil matrix and aid in resisting overburden stresses or help to control the porosity of the composition.

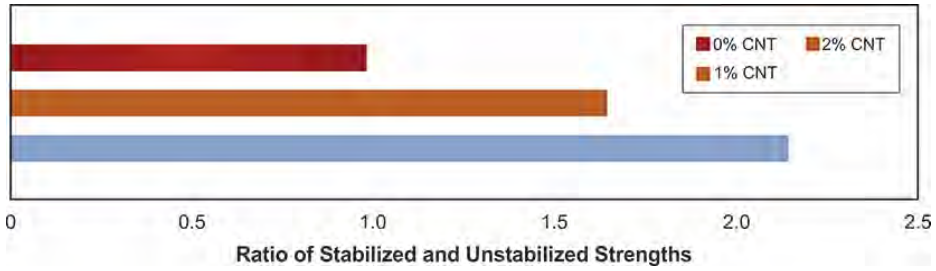

Figure 2.8 Effect of CNTs Inclusion on Compressive Strength of Clay (based on results from Taha and Ying (2010))

2.7 REVIEW OF SLAG AS SOIL STABILISER

2.7.1 Introduction

Slags are the by-product of the steel and iron production industries and have similar characteristics to the rocks produced from volcanic eruptions such as granites and basalts, with some hydraulic and cementitious properties. In the wake of green constructions and utilisation of industrial wastes, slag has gained wide attention due

to its comparatively lower cost and ease of replacing at least part of Portland cement in building and road constructions.

2.7.1.1 Types of Slag

There are two principal types of slag called blast furnace slag and metallurgical slags. Blast furnace slags are formed in the blast furnace when pig iron or crude iron is produced by reduction or removal of oxygen and other contaminants from the iron ore using reducing agents like carbon and flux at high temperatures. The impurities then infuse with the reduction agents to give a molten glassy-looking substance that primarily contains metallic silicates. Metallurgical slags are produced during smelting of nonferrous metals like copper, zinc and lead as well as in the production of ferro- alloys with silicon, chromium and manganese (Rai et al. 2002). Linz–Donawitz slag or LD slag is among the most common examples of metallurgical slags that is generated during the manufacturing of crude steel from pig iron and contains metallic oxides like calcium oxide and iron oxide as well as silicon dioxide as the primary constituents (Panda 2013). It is mainly employed in the pavement engineering during road construction. The primary focus of this research is on the blast furnace slag, which is discussed in detail in the succeeding text.

2.7.2 Blast Furnace Slag (BFS)

During the purification process that involves reduction of iron ore, aluminous and siliceous residue infuses with coke ash and flux of limestone to produce iron BFS. The primary constituents of iron BFS are therefore, lime and other bases silicates and alumino-silicates (Barnett et al. 2006; McGrath, White and Downey 2014). The molten alkali-metallic residue has 1300^{o}C to 1600^{o}C temperature which is then cooled to produce BFS. The appearance of BFS is mainly glassy with a crystalline structure that corresponds to the development of cementing behaviour in slag composites. It is further classified into three types depending upon the method which is used for the cooling of molten slag (Oss 2003; Ouf 2001a).

2.7.2.1 Granulated Blast Furnace Slag (GBFS)

GBFS is produced by rapidly cooling with water to avoid crystallisation, which causes the slag to solidify as glassy particles with particle sizes similar to sand

grains, producing a granulated textured material. This disordered morphology produces hydraulic cementitious characteristics and when GBFS is fine-ground, it is called ground granulated blast furnace slag (GGBFS) (Nidzam and Kinuthia 2010; Chen 2006). GGBFS is widely used in industry, when activated with lime, in ready-mix concrete or blended cement. The GGBFS-cement concrete has higher impermeability, lower hydration heat, higher resistance against sulphate attack and improved long-term strength (Oss 2003; Ouf 2001a).

2.7.2.2 Air-Cooled Blast Furnace Slag (ABFS)

Unlike GBFS, molten slag is cooled at a comparatively slower rate under ambient or open-air conditions and sometimes sprayed with water to form the ABFS. It has a harder and denser appearance with vesicular texture. ABFS is then crushed and screened to be employed in the pavement industry as road fill and bases, railway ballast, concrete and asphalt pavement aggregate (Oss 2003; Ouf 2001a). The crushed ABFS has a cubical shape with rougher edges providing better frictional resistance. It is also highly permeable and resistant against fire as well as being reactive at room temperature.

2.7.2.3 Expanded or Pelletised Blast Furnace Slag (EBFS)

Similar to the GGBFS, EBFS is cooled using a jet of water which produces steam and expanded foamy formation along with vesicles in slag. Expanded slag has relatively lower density and higher mechanical binding with cement mortar. Ouf (2001a) and Oss (2003) have stated that due to the lower water-slag ratio, expanded slag is utilised in building industry for lightweight masonry works and concrete aggregates. It is also used as a cementing hydraulic material in cement pastes like GGBFS.

2.7.3 Physical Properties of Blast Furnace Slag

Although different types of blast furnace slag are obtained from the metallurgy industry, the physical properties, i.e., the appearance, composition, specific gravities, absorption capacity, particle sizes and unit weights etc. widely vary between the different types.

2.7.3.1 Physical Properties of GBFS

GBFS has a granular glassy appearance which shows variation is physical appearance depending upon the nature of the parent materials, production method and cooling technique. The particle size can range from sand grain sizes (< 4.75mm) to coarser structure that exceeds 4.75mm. It has a similar appearance as to the river sands with comparatively lower density (60% – 70%) of the natural sand (Australasian (iron & steel) Slag Association 2013). The size can be reduced further to the cement fineness and blain sizes to be used as a cementation agent in cement-slag mixtures.

2.7.3.2 Physical Properties of ABFS

ABFS has an approximately cubical and angular particle range that has glassy and versicular surfaces. The specific gravity of ABFS varies from 2 – 2.5 and the unit weight lies in the range of 1120kg/m^3 – 1360kg/m^3, although it may largely vary based upon the production process of the crude iron. The absorption capacity ranges from 1% – 6 %.

2.7.3.3 Physical Properties of EBFS

EBFS has similar appearance as the air-cooled blast furnace slag but with a comparatively rougher texture and therefore, higher porosity. The unit weight of expanded blast furnace slag varies in the range of 800kg/m^3 – 1040kg/m^3 (National Slag Association 1971).

2.7.4 Chemical Composition of GGBFS

The focus of this research is on the chemical stabilisation of the selected expansive clay with GGBFS and therefore, its chemical composition is of significant importance. The physical and chemical characteristics of GGBFS are roughly comparable to Portland cement. As GBFS is formed through speedy water quenching by high pressure water sprays, the matrix normally consists of a disordered array of aluminium, silicon and calcium ions bonded with oxygen with other metals also present inside the slag matrix (Australasian (iron & steel) Slag Association 2013; Ouf 2001b). The nature of the contributing materials; i.e.; fluxes,

carbon and the originating iron ore dictate the chemistry and chemical composition of the resulting GGBFS. It is primarily composed of metallic oxides such as alumina (Al_2O_3), magnesium oxide (MgO), calcium oxide (CaO), iron oxides (Fe_2O_3 or FeO), manganese oxide (MnO) and silica (SiO_2) and sulphur (Proctor et al. 2000). Table 1, reproduced from (Australasian (iron & steel) Slag Association 2013), outlines the typical BFS chemical composition produced in the Australasian region.

Table 1 Typical chemical composition of BFS manufactured in Australasian region

Constituent	Symbol	Percentage (%)
Calcium Oxide	CaO	41
Silicon Dioxide	SiO_2	35
Aluminium Oxide	Al_2O_3	14
Magnesium Oxide	MgO	6.5
Titanium Oxide	TiO_2	1.0
Iron Oxide	Fe_2O_3	0.7
Sulphur	S	0.6
Manganese Oxide	MnO	0.5
Potassium Oxide	K_2O	0.3
Vanadium Oxide	V_2O_5	<0.05
Chromium Oxide	Cr_2O_3	<0.005

Researchers have found that the reactive potential of GBFS is comparatively lower than Portland cement and is mainly dependent upon the morphological characteristics and particle size distributions, glass phase content and chemical composition (Song and Jennings 1999; ACI Committee 226 1989). Furthermore, Ouf (2001b) has stated that alkalis and sulphates can be used for the activation of GBFS. The hydration of Portland cement releases these compounds which then react and disintegrate the slag matrix forming cementitious aluminate hydrate and calcium silicate chains. Although GGBFS does exhibit hydraulic properties without the use of any activators but the initial gain in strength is comparatively slower which can be accelerated by increasing the fineness of GGBFS.

2.7.5 Hydration of GGBFS

The hydration of slag is a comparatively slower process and takes long time to yield binding properties. Therefore, an activator is employed for accelerating the hydration reactions. Several researchers have proposed hydroxides and silicate compounds as activators. Portland cement and sulphates as well as hydroxides of alkali metals; like sodium hydroxide, calcium hydroxide; silicates of alkali metals such as sodium silicate, sodium metasilicate (Na_2SiO_3) and sodium carbonate have been documented to act as slag activators (Puertas, Fernández-Jiménez and Blanco-Varela 2004; Živica 2007; Chen 2006; Haha et al. 2011). The hydration reactions result in calcium–silicate–hydrates (C–S–H) production in presence of activators. However, hydration of pure slag shows some pozzolanic behaviour by occurrence of cementitious products like portlandite (Kolani et al. 2012).

The microscopic structure of GGBFS has a crystalline and glassy disordered appearance that contributes to the cementitious nature of slag, giving it a hydraulic nature as it hardens upon exposure to water over extended time period (Song et al. 2000a). Furthermore, slag-cement concretes have higher sulphate-resistant (Gruyaert et al. 2012). The GGBFS hydration products in Portland cement and hydrated lime are primarily calcium aluminate silicate hydrates, calcium silicate hydrates (C–S–H) and calcium aluminate hydrates (C–A–H) gel-like formations in the mixture matrix. Ouf (2001b) has identified that the degree of hydration of GGBFS depend upon several factors such as the alkali characteristics of the reaction system, chemical composition, fineness, glassy content and temperature of the GGBFS. Moreover, exposure to water causes a thin silicon–aluminium–oxygen (aluminosilicate) layer to form upon the surfaces of the GGBFS grains. The absorption of hydrogen ions by the surface layer increases the basicity of the slag-water solution but render the grains to be water impermeable barring further hydration (Brough and Atkinson 2002), even though some calcium silicate hydrates are formed with extended curing.

2.7.5.1 Hydration Products

In hydration of GGFS, a thin layer is formed over the grains of slag and the hydration products are comparatively more crystalline than the Portland cement hydration products (Chen and Brouwers 2007; Ouf 2001b). As discussed earlier, the

hydration products of GGBFS are dependent upon the chemical composition of the composite material. GGBFS is often used to reduce the heat of hydration, increase resistance against chemicals such as sulphate, provide long-term durability and reduce the carbon imprint of Portland cement concrete. In addition, the hydration products are mainly dependent upon the nature of the alkaline activators (Kim et al. 2011). Generally; alkali-based silicic salts, $R_2O•nSiO_2$; nonsilicic salts like $R2CO_3$, R_2S, RF; and alkali hydroxides, ROH; where the letter "R" is the representative of alkali metals like sodium, potassium and lithium; can be used for the activation of the GGBFS (Yang, Sim and Nam 2010).

Song et al. (2000a) have identified that hydration reaction that involves the GGBFS activation with sodium hydroxide (NaOH), the reaction rates are dependent upon the pH of the reaction system. In their study, calcium silicate hydrate was found to be the primary hydration product, but at higher pH values and later hydration stages, hydrotalcite denoted by chemical formula $Mg_6Al_2CO_3(OH)•4(H_2O)$ was also found. Moreover, in a study by Regourd (1980), the hydration products between calcium and sodium hydroxide as GGBFS activators were found to be varied. C–S–H (calcium silicate hydrate), C_2ASH_8 (strätlingite) and C_4AH_{13} (tetracalcium aluminate hydrate) were found to be the main products of the hydration reaction. However, strätlingite was not found to be present when calcium hydroxide was used as activator. But aluminium hydroxide, ettringite and calcium silicate hydrates were found as hydration production of slag in presence of gypsum.

Ettringite or calcium sulpho-aluminate ($3CaO•Al_2O_3•3CaSO_4•32H_2O$) is also common production of Portland cement and GGBFS-Portland cement blend hydration (Kim et al. 2011; PCA 2001). Researchers (Fernández et al. 2014; Ouf 2001b) have shown that portlandite or $Ca(OH)_2$ and other alkali hydroxides are a common product of the hydration of Portland cement that reacts with alumina and silica constituents of GGBFS to produce ettringite compounds. The mechanism of slag hydration with $Ca(OH)_2$ as the activator was also investigated by Biernacki et al. (2002). They observed that the hydration of slag was significantly accelerated by calcium hydroxide and hydration kinetics is influenced by the slag-activator ratio.

2.7.6 Utilisation of Slag as Soil Stabiliser

The ability of GGBFS to increase the durability, sulphate-resistance and strength has widely been established. Therefore, researchers have investigated the possibility of using GGBFS to produce similar properties in weak or unsuitable clays in order to stabilise such soils under laboratory conditions (Ouf 2001b; Higgins 2005). Veith (2000) has suggested that environmental consideration should be regarded during the selection of an appropriate stabiliser for soils. Due to this reason, the utilisation of slag (a by-product and waste material) in soil stabilisation has emerged as a popular choice for engineers in comparison with lime and cement which may cause large amount of carbon dioxide (CO_2) emissions during their production phase. Since CO_2 is a greenhouse gas, it may cause warming of the Earth's surface by reducing outward radiation. Moreover, slag is cheaper as compared to many other cementing agents, rendering the economic feasibility of highway projects possible.

Similar to concrete applications, the use of GGBFS in soil stabilisation has been researched using alkali activators such as hydrate lime. In a study on expansive clay native to Egypt, lime and GGBFS were use as soil stabilisers by Ouf (2001b). The study incorporated the use of both hydrated and unhydrated (without lime) GGBFS additive in soil with different compositions. The maximum percentage of GGBFS when only pure slag was used was kept at 10% by dry unit weight of soil, followed by replacement of GGBFS with hydrated lime by up to 30%. Results showed that the maximum dry density (MDD) of the expansive soil only slightly reduced due to the inclusion of GGBFS in the soil matrix whereas a minor rise in the optimum moisture content (OMC) was also observed. In addition, he also observed that due to the slow hydraulic nature of GGBFS, the pozzolanic reaction between GGBFS and expansive soil required some time to occur when GGBFS was used as the soil stabiliser.

Moreover, the effect of curing time on the development of unconfined compressive strengths was investigated by considering curing periods of 1, 4 and 12 weeks. In samples using unhydrated GGBFS, optimum strength was observed for 6% of slag with 7 and 28 days of curing. Further curing yielded 4% slag as the optimum strength producing slag percentage. Remarkable improvement in the strength of stabilised specimens was observed with mixtures containing 6% GGBFS and 30% hydrated lime by dry unit weight of soil. He noted that contrary to the relatively

faster rate of pozzolanic reaction between cement-soil mixtures, slag stabilisation provides sufficient time for the finalisation of site engineering works such as excavation, removal or compacting and construction of foundations and subgrades. Generally, a curing period of 28 days was identified as the curing time required for the generation of optimum strength in GGBFS-stabilised expansive soil specimens.

Induction of lime in the GGBFS-soil system results in variations in the stabilised soil reaction products. The clay-slag-lime hydration reactions have been widely researched in literature and have been established as the primary reactions incurring in clays stabilised with lime-hydrated GGBFS. Several phases and variations of alkali silicate hydrates like tetracalcium aluminate hydrates and/or tricalcium aluminate hydrates, calcium–silicate–hydrates and strätlingite have been observed to be the primary hydration products of such reactions (Ouf 2001b). The additional phases of calcium silicate hydrates are contributed by the calcium, silica and alumina constituents of GGBFS and lime that also accelerates the hydration reaction. This study showed that there are primarily two reactions that occur when soil is stabilised with lime-hydrated GGBFS. The first reaction occurs between soil and lime within the soil-lime system and second reaction is the hydration reaction of GGBFS with lime. Wild et al. (1996) proposed that the slag-lime ratio is specifically critical considering the observation that the hydration reaction of GGBFS with lime is faster than the reaction between lime and soil.

Furthermore, soil characteristics such as the type of soil, clay content, organic content, inter-particle interactions, surface chemistry, particle morphology, and curing configurations dictate the optimum GGBFS-lime ratio (Yi, Gu and Liu 2015; Rogoff and Williams 2012; Lenssen and Roodman 1995; Tam and Tam 2008). However, these researches have shown that the enhancement in strength of GGBFS stabilised samples was more pronounced as the quantity of lime increased. This observation could have been developed due to the availability of more lime for the hydration of GGBFS. In another study on lime activated slag, Higgins (2005) stated that the stabilisation of soil with GGBFS-lime system involves two tasks where both additives are separately introduced in the soil system, commonly is a 15% hydrated lime and 85% slag ratio. However, he identified that the actual slag-lime ratio depends upon the type of the native soil.

Kavak, Bilgen, and Capar (2011) also investigated the effect of lime-GGBFS system on strength characteristics and swelling behaviour of clayey soil with low plasticity. Such soils are highly susceptible to failure due to their lower bearing capacity and high swelling behaviour due to water exposure. In this study, seawater was used for achieving hydration or curing in the stabilised soil specimens. Different additive percentages we used and curing periods of 1, 7 and 28 days were used for specimen testing and monitoring. CBR and UCS tests were performed for comparative analysis to identify the stabiliser effect and results showed that soaked CBR values increased by almost 10 times from the initial untreated benchmark sample due to stabilisation. In addition, optimum enhancement in UCS was obtained for samples treated with 33.3% GGBFS, 5% lime and curing period of 28 days to 2500kPa by using seawater. This increment was attributed to produce approximately eight times UCS value in the treated sample as compared with the untreated specimen.

Other cementitious compounds, specifically Portland cement have been used to cause the activation of GGBFS. In a soil-cement-GGBFS system where cement is primarily used for the stabilisation of weak soils and GGBFS is used for partial substitution of cement, the strength is primary developed through cement pozzolanic reaction while cement-hydrated GGBFS also contributes to the overall strength. A recent study conducted by Ashango and Patra (2014) studied the effect of Portland slag cement (PSC) and rice husk fly ash (RHA) on the strength characteristics of clayey soils. Different percentages of the additives were used under different curing periods of 0, 7, 14 and 30 days. The test study comprised of four stages of laboratory experiments with the establishment of geotechnical characteristics of the soil and stabilisers in the first stage, determination of optimum additive proportions for different curing periods in the second stage and UCS, durability and CBR tests constituting the third stage. Cyclic triaxial tests (strain-controlled) were then performed in the fourth stage to identify the damping ratio, shear modulus and degradation index for the identified optimum mixture employing 0.4%, 0.6%, 0.8% and 1.0% strain amplitudes at 0.2Hz and 1.0Hz frequencies. Results showed that the maximum dry density decreased with increasing stabiliser proportions while the optimum moisture content increased. Moreover, the optimum RHA, PSC and soil proportions were respectively determined as 10%, 7.5% and 82.5% with UCS value

showing a 76.8% increment, rising to 835kN/m^3 from 193kN/m^3 and the strength increment was more pronounced with each curing day. Similarly, approximately 91.75% increment in soaked CBR was observed for the sample stabilised with the optimum stabiliser proportions. Also, the optimum mixture exhibited a durability value of 0.91 after 12 wet-dry cycles compared with the unsoaked CBR value. Cyclic tests showed that both damping ratio and shear modulus declined with escalating cycles while the degradation index only declined during initial 25 – 50 cycles at a relatively faster rate and thereafter remained approximately unchanged.

In another study conducted by Cokca, Yazici, and Ozaydin (2009) investigated the effect on expansive clays using GGBFS and GGBFS-cement. The expansive soil used was artificially prepared by adding kaolin and sodium bentonite in the ratio of 85% for kaolin and 15% bentonite by dry unit weight. Cement and GGBFS were introduced in the soil matrix in 25% and 5% proportions by dry unit weight of soil, respectively. Their results showed variations in particle size distribution of the expansive soil samples by exhibiting an increase in silt fractions and reduction in clay fractions after the addition of the two stabilisers. Also, reduction in plasticity index and increase in specific gravity was observed after additive introduction. Furthermore, both additives showed a decrease in swelling percentage of the expansive soil and the effects were more pronounced with extending curing periods for the total swelling readings or t_{50} readings of test samples. Generally, GGBFS displayed promising results for controlling the swelling potential of expansive soil while also being environment-friendly.

In their study on soft soil stabilisation using ground granulated blast furnace slag (GGBFS), Yadu and Tripathi (2013b) used soft inorganic intermediately compressible fine soil, classified as CI-MI based on the Indian Standard Classification System (ISCS), native to the Chhattisgarh region of India. The soil was stabilised with different percentages of GGBFS as 3%, 6%, 9% and 12%; and Atterberg's limits, UCS and California bearing ratio (CBR) values were calculated. It was observed that both plastic and liquid limits displayed a tendency to decline with increasing GGBFS percentages with the plasticity index decreasing to 13% for 9% addition of GGBFS by dry unit weight of the soft soil. Further increment of GGBFS proportion however, did not produce any significant reductions in the

plasticity index values. Similar results were obtained by Akinmusuru (1991) in an investigation incorporating stabilisation of lateritic soil by different percentages of slag from 0% to 15%.

Moreover, Yadu and Tripathi (2013b) reported that the increment of slag in stabilised specimens resulted in increased UCS values. The increase was as high as 28% from the UCS value of untreated soil when 9% of slag was introduced. Furthermore, swelling pressure of soft soil also reduced from 42kPa to 34kPa when 9% of GGBFS was employed for stabilisation. However, further addition of GGBFS, beyond 9%, resulted in reduction of UCS value. Similar results were obtained for both soaked and unsoaked CBR values with 6% and 9% exhibiting the optimum results as 10% on 9% and 20% on 6% respectively. These trends in reduction of strength characteristics of GGBFS-stabilised soft soil specimens depict that even though GGBFS can be used for stabilisation of unsuitable soils, a theoretical optimum GGBFS percentage exists and further increments beyond such GGBFS proportion may not produce significant enhancement in the strength of weak soils.

The influence of GGBFS on reducing the swelling potential of expansive clay was also investigated in a laboratory study conducted by Veith (2000). In this study, lime-hydrated GGBFS was introduced within the expansive soil system and swelling magnitudes were noted. Results showed that swelling potential of soil decreased with increasing percentage of GGBFS and reduction in swelling percentage from 28% to up to 4% was observed. This decline in the swelling potential can be attributed to the formation of cementitious gels within soil matrix when lime-hydrated GGBFS was inducted. He proposed that the swelling could have been reduced as more cementitious gels were available to bind the soil particles together. This binding force might have suppressed the swelling pressure produced by particle expansion upon water exposure and thereby reducing the overall specimen swelling.

Another recent study on the effect of slag on the swelling, strength and volumetric stability of clayey soils was conducted by Ortega-López et al. (2014). They performed the stabilisation of clayey soils using five different types of ladle furnace slag at a proportion of 5% as recommended by Manso et al. (2013). They observed

positive results such as reduction in the swelling potential of soil, strength and volumetric stability and higher CBR indices as compared with the untreated soils.

2.8 Review of Climatic Imprint of Construction Industry and Recycling of Building Materials

2.8.1 Introduction

The modernisation of architectural practices and industrialisation has fashioned large quantities of debris from demolition of structures. The term construction and demolition waste is generally very broad that may constitute of waste materials such as glass, contaminated soils, asbestos, metals, papers and cardboards, plastics, bricks, asphalt, concrete, rubber and tyres etc. from several types of construction activities.

2.8.2 Sources and Composition of Construction and Demolition Waste

Following the huge impact of construction activities on the environment and the vast amount of construction wastes being annually generated globally, compositional characterisation and quantification of construction wastes (CW) have garnered global attention. The variety in construction activities such as piling, tiling, masonry works, offshore structures, reinforced concrete structures, roads and bridge works, site excavation, repacking and landscaping activities renders the recycling of these wastes to be difficult as the composition is also varied. Even though, rectification of construction techniques reduce the volume of generated construction and demolition wastes, recycling and redisposition is economical for the various stakeholders like clients, contractors and consultants involved in the construction projects.

It should be noted that the extent of CW recovery, market demand for recycled products and the willingness to apply recovered resources for industrial or commercial scale applications largely depend upon the industry practices, location, reuse feasibility and price of new or virgin materials. Moreover, large landfill disposal costs of CWs may also contribute to the decision for recycling of such materials specifically if a levy is associated. Hyder Consulting (2011) have highlighted in their report that these factor contribute to generation of special interest in some materials such as masonry works and metals because of their physical

characteristics like weight for metals and generation volumes for masonry, soil and concrete from civil-works, demolition and earthwork activities.

2.8.2.1 Masonry works and Concrete

Building demolishing sites and residential and commercial projects commonly produce large volumes of masonry wastes, either as rubble or leftover/rejected building materials. Composition of bricks is largely varied depending upon constituent materials but primarily consist of feldspars, illites, smectites and other earth-forming mineral groups commonly found in clay and natural sand that are the main ingredients for bricks around the world. Moreover, building rubble or discarded masonry often consists of large amount of concrete mixed in the waste volume. The reuse and recycling of demolished and leftover or discarded concrete and/or masonry from construction projects is a comparatively easier practice. Concrete and bricks rubble can easily be crushed and employed for filling excavation sites and as road base material. Moreover, as demolition projects involve large volumes of crushed concrete and/or masonry and disposal of these large amounts in landfills may incur additional costs on projects, it is usually more economical to reemploy the rubble or leftover bricks and concrete for new construction projects, primarily as reprocessing plants in metropolitans are well-established and may produce qualitative aggregate products.

2.8.3 Recycling of Masonry works and Concrete Wastes

Processing of materials that have already been utilised either for similar or different applications falls in the category of material recycling. In the process of recycling of masonry and concrete wastes, the generic construction waste deposits are screened to remove plastics, metals, timber, cardboard, gypsum board, glass and other waste products. The screened masonry and concrete wastes are then further processed by being crushed into smaller fragments employing different crushing techniques like manual/hammer crushing, cone crushers, impact crushers and jaw crushers etc. (Li 2008). Derek Chisholm (2011) in a report on reuse of recycled aggregates in concrete identified that the following steps may be involved during recycling of masonry and concrete wastes for production of high quality aggregates:

- Stock piling
- Pre-sizing
- Pre-crushing sorting/Screening
- Crushing
- Post-crushing sorting

2.8.3.1 Crushed Masonry and Concrete Wastes (CMCWs) Recycling and Reprocessing in Western Australia

Matias et al. (2013) have proposed that the mechanical and physical characteristics of recycled aggregates are affected by the type and efficiency of the crushing process. The crushers' selection during the crushing and processing stages is dependent upon the elements such as particles fineness, shape and sizes; output volume, consistency, quality and efficiency; and feed size. The quality and consistency of the processed CWs cannot be completely guaranteed as the input consistency cannot be maintained. However, this should only marginally hinder the reuse of recycled construction waste as the mobility and portability of recycling and crushing plants means that the reprocessing facility can be established near project sites to reduce the freight distance (Mehta and Meryman 2009).

Nonetheless, traditionally reprocessing is done in specific plants and in cities like Melbourne, Brisbane and Perth with the recycled and quarry products equidistant from market outlets and thereby relying mainly on landfilling costs and local waste disposal laws rather than competitive prices and proximity to construction sites. Inert landfill costs around Western Australia are significantly lower and pose difficulty for reprocessing facilities to compete for CMCW. Furthermore, in far WA regions like Kimberley and Pilbara, the number and access to recycling facilities is primarily limited as landfills are comparatively closer while recovering and reprocessing may incur cartage costs (Hyder Consulting 2011). On the other hand, materials like clays and timber are still being somewhat recycled. The main hindrance for reprocessing and recycling of CMCWs in Perth is that the site operators absorb landfill levy costs sometimes but increases in landfill levy have been recently introduced which resulted in a rise in recycling activity as reported by some reprocesses around recycling facilities in Western Australia but is still

comparatively lower at 29%, from other Commonwealth states although most recycling plants reported 90% processing capacity (Pogson and Mountjoy 2013; Hyder Consulting 2011). Although other states have introduced legislations for gradually reducing the waste disposal including concrete and masonry works by 2020, Victoria setting a 80% CWs recovery rate, NSW introducing legislature to 76% CWs recovery rate, SA to have increased CWs recovery rate by 50% whereas ACT aims to have a waste-free society; WA is still in the procedure of introducing and implementing such regulations.

2.9 Theoretical Review of Selected Elemental and Geotechnical Characterisation Tests

The study has employed the techniques of both mechanical and chemical stabilisation, through the induction of recycled CW and GGBFS, in controlled proportions. Several elemental and geotechnical characterisation tests were performed to study the morphology, microstructure, unconfined compressive and direct shear strengths of stabilised and unstabilised samples. This section presents the theoretical background of the adapted laboratory tests for this research study.

2.9.1 Atterberg's Limits Tests

2.9.1.1 Overview

Generally, clays and silts can be found in many states dependent upon the volume and percentage of water within the soil system. The properties and characteristics of both types of soils are dependent upon the water content in the system. The addition of water to dry clay or silt mass introduces a thin film of water molecules over the soil particles, which thickens as more voids and particle surfaces are covered by water molecules upon further addition of water. Induction of water content incurs adhesive and cohesive properties within the clay or silt soil system. Water molecules exhibit attractive behaviour towards each other which is produced because of the hydrogen bonding. Also, the water molecules are attracted towards clay or silt particles, creating adhesion or water-soil bonding (Das 2013). The degree of the soil consistency is the representative of the adhesive and cohesive forces in the soil-water system. Albert Atterberg defined consistency limits that have been used over the

years as plastic soil classification parameters; namely plastic limit, liquid limit and shrinkage limit. Figure 2.9 illustrates the Atterberg's limits and moisture content relationship in accordance with the soil states.

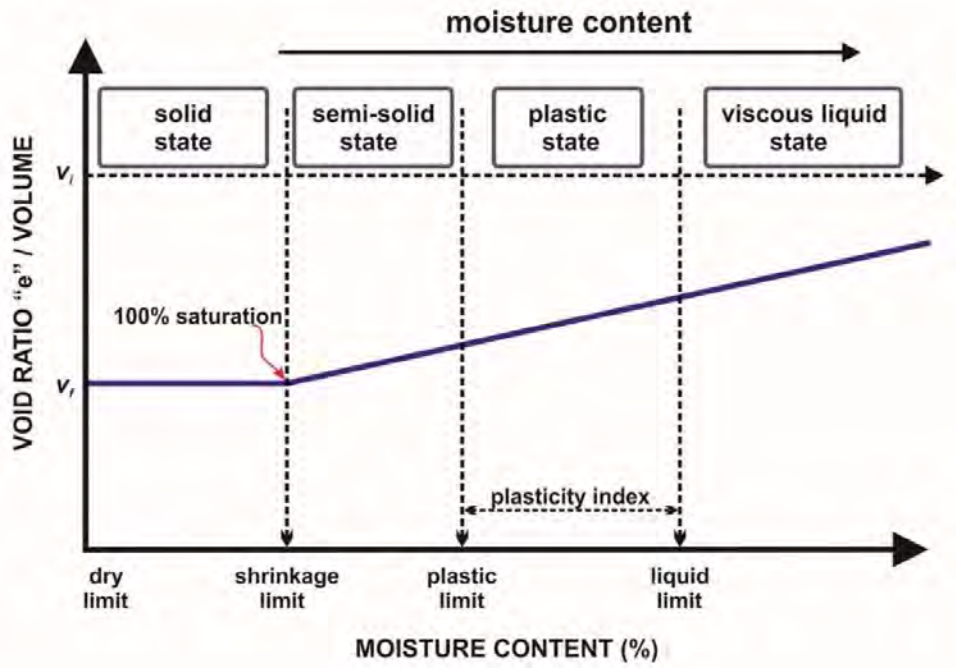

Figure 2.9 Moisture Content-Atterberg's Limits Relationship (based on Das and Sobhan (2014))

Plastic limit represents the boundary between the semi-solid and plastic states. In other words, it is the moisture content at which the soil changes from semi-solid to flexible or plastic state and behaves like a plastic material. The boundary between plastic and liquid states is represented by the *liquid limit* (LL). It means that soil has changed from plastic or flexible material to a viscous-fluid state. At this state, application of a very small force shear force causes the soil to flow. The third Atterberg's limit is referred to as *shrinkage limit* and represents the boundary between the solid and semi-solid states and is the moisture content that is required for saturating the soil completely, i.e. 100% saturation.

2.9.1.2 Purpose

If soil consistency or Atterberg's limits are established for the soil present on a project site, the performance of the soil and its long-term post-construction

behaviour can be predicted as the Atterberg's limits are a comparatively quicker and easier way of distinguishing between various types of clays and silts. They are utilised for interpreting clays and silts for swelling potential, compressibility, bearing capacity and shear strength characteristics (Jacob and Clarke 2002), but the most common use of Atterberg's limits to predict the expansive behaviour of the fine-grained soils. Two indices are most commonly used for this purpose, referred to as *plasticity index* (PI) and *liquidity index* (LI). Plasticity index represents the moisture content range where the soils display plastic behaviour and it is represented by "I_p". The specifications outlined in Standards Australia AS: 1289.3.3.1 (2009) define the plasticity index by the following equation:

$$I_p = Liquid\ limit\ (\%) - Plastic\ limit(\%) \qquad \text{Equation (2.11)}$$

Liquidity index is a quantitative method used to identify the moisture content present at a certain state in the soil system with regards to the Atterberg's limits. Empirically, it is the ratio of difference between natural moisture content and PL and the PI, written as:

$$Liquidity\ index = I_L = \frac{[Water\ content\ (\%) - Plastic\ limit(\%)]}{I_p} \qquad \text{Equation (2.12)}$$

Another parameter that is used in conjunction with the Atterberg's limits is clay content. The soil clay content can be identified as the proportion of soil particles with a diameter less than 2µm. Clay content is specifically significant as the specific surface area of clay particles determine the volume of water necessary for causing the soil-water system to change phases, from plastic to liquid phase. The clay content can then be used along with the PI to define a single parameter called clay activity, which is used to classify clays. Muntohar (2006) concluded that LL, PI and clay fractions are the factors that contribute to the swelling of the soil. These properties have been employed for the estimation of the degree of swelling of expansive soil. Skempton (1953) developed a relationship between the PI and the clay content of the soil, in terms of clay activity. The criteria used for the classification of expansive clays based upon the parameters that have been elaborated in the preceding paragraphs have been tabulated in Table 2.

Table 2 Classification of Expansive Clays based on Atterberg's Limits

Degree of Expansion	Chen (2012)	Chen (1965)		Raman (1967)		Holtz and Gibbs (1954)
	Plasticity Index	Liquid Limit (%)	Plasticity Index	Shrinkage Index	Plasticity Index	Shrinkage Limit
Low	0 – 15	< 30	< 12	< 15	< 18	> 15
Medium	10 – 35	30 – 40	12 – 23	15 – 30	15 – 28	10 – 16
High	20 – 55	40 – 60	23 – 32	30 – 40	25 – 41	7 – 12
Very High	≥ 35	> 60	> 32	> 40	> 35	< 11

The estimation of the activity (A) of soil is another important application of determining Atterberg's limits, determined based on the following empirical relation:

$$Activity = \frac{Plasticity\ index}{Clay\ content\ (<2\mu m)}$$ Equation (2.13)

The dominant clay type present in a soil sample can be proposed based upon activity value and predict swelling potential and degree of expansion of soil. Highly active clays show high chemical reactivity in addition to exhibiting high swelling upon wetting and significant shrinkage upon drying. The criteria used for the classification of expansive clays based upon the activity have been outlined in Table 3.

Table 3 Classification of Clays based upon Activity (Skempton 1953)

Activity Classification	Activity Value
Inactive	< 0.75
Normal	0.75 – 1.25
Active	> 1.25

2.9.1.3 Factors Affecting Atterberg's Limits

Atterberg's limits are essentially parametric representations of soil consistency and response of soil system to moisture content. Therefore, the primary factor that should

affect the Atterberg's limits is the clay content and size of the clay particles. Seybold, Elrashidi, and Engel (2008) have noted that several researchers have used the clay content to predict the LL and PL of specific soils using statistical relationships like least squares estimates, however, these relationships were generally limited in application and can only employed for specific types of clays such as kaolin and sodium bentonite etc. or regionally native clays.

NRCS (2012) have identified several soil characteristics such as clay content, type, particle sizes and shapes to affect the Atterberg's limits and developed prediction models based upon the interaction relationships between these parameters. Generally, the shrink-swell potential and plasticity of the soil increases with an increase in the clay content (Mitchell and Soga 1993). Odell, Thornburn, and McKenzie (1960) performed a study on soil samples obtained from several sites in Illinois. They observed that the percentage of the expansive montmorillonite mineral in the clay fraction influences the Atterberg's limits and correlation between both may be established. Moreover, in total the factors such as montmorillonite percentage in clay, total clay and organic content can describe liquid limit and plastic limit variability respectively by 86% and 94% in the soil system, which may show great diversity for any specific type of clay mineral.

2.9.2 Standard Compaction Test

2.9.2.1 Overview

The standard compaction test is a commonly performed laboratory experiment for determining the maximum dry density (MDD) and moisture content (MC) relationship for a particular soil sample and is based upon the principle of applying standard compaction effort. It is performed by mixing dry soil with different moisture content variations, compacted in a cylindrical mould, referred to as Proctor compaction mould, with an inner diameter of 105mm and volume of approximately $9.44\times10^{-4}m^3$ in three layers of approximately equal thicknesses (Standards Australia AS 1289.5.1.1 2003; ASTM D1140 2014; ASTM D1557 2012). The details of the rammer and mould have been illustrated in Figure 2.10.

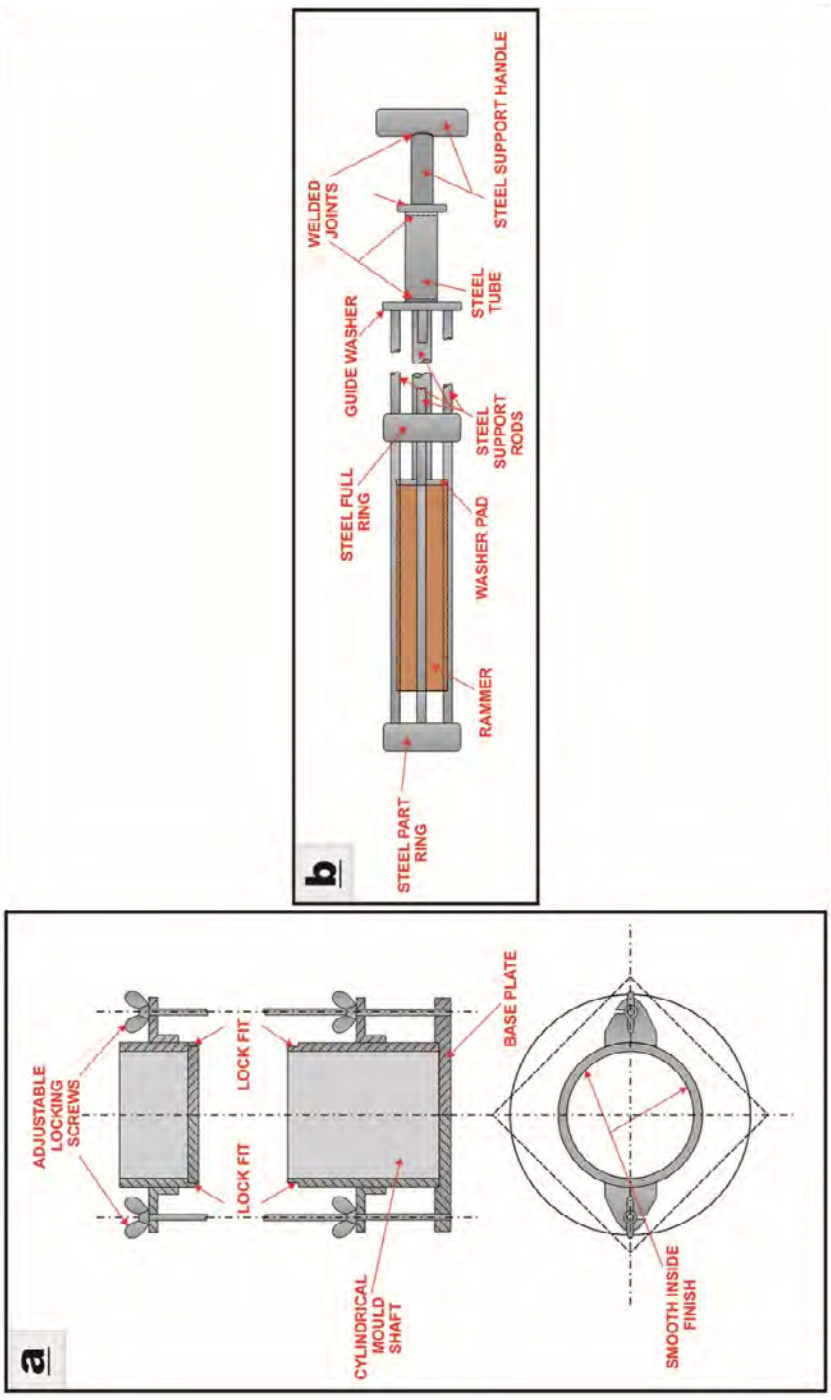

Figure 2.10 Standard Compaction (a) Mould and (b) Rammer (based on Standards Australia AS 1289.5.1.1 (2003))

Each layer is compacted using a 2.5kg weight hammer dropping a distance of 305mm in a rammer, therefore, the energy being applied by the rammer for each

compaction layer is predetermined which can be calculated using the following empirical relationship as per (Budhu 2011b), for a mould containing soil volume of V that is compacted in N_l layers using a hammer of m_h weight falling a distance of h_d in N_b number of blows, the energy applied by hammer is E_{comp} calculated as:

$$E_{comp} = m_h g \frac{h_d}{V} N_b N_l \qquad \text{Equation (2.14)}$$

As for the standard Proctor test, the hammer has a 2.5kg mass, the fall height is 305mm and three layers are compacted using 25 blows for a soil volume of $9.44\times10^{-4}m^3$, the energy can be calculated as:

$$E_{comp} = 2.5 \times 9.8 \frac{0.305}{9.44\times10^{-4}} \times 25 \times 3 \times 10^{-3} = 594 kJ/m^3 \qquad \text{Equation (2.15)}$$

Generally, the standard compaction test is performed in at least five or more iterations with different moisture contents used each time for the soil-water system. The compaction degree is measured in terms of dry unit weight. The repetition of the test is stopped once the bulk unit weight of the wet compacted sample starts decreasing with increasing moisture content (MC).

The test results are then plotted in a dry unit weight versus MC graph with dry unit weight on the ordinate and MC at abscissa. Normally, humps are found in the dry unit weight-moisture content curves of coarse grained soils such as sands. Uniformly graded sand exhibits a decline in the dry unit weight caused by restraining of soil particles movement due to capillary tension; it is then succeeded by a rise in the dry unit weight generating a hump. However, for fine poorly graded sands, more humps may be produced. On the other hand, the typical dry unit weight-moisture content curves for clays form a bell-shaped curve.

A typically desired compaction curve that is commonly obtained for most soils is shown in Figure 2.11 (Budhu 2011b). The optimum moisture content (OMC) corresponds to the moisture content at which the maximum dry unit weight $(\gamma_d)_{max}$ of the soil is achieved. The region of graph at the left hand side of the bell curve corresponds to the moisture content that is below the optimum moisture content. This moisture content, dubbed as “dry of optimum”, is attributed to the readjustment of soil particles into comparatively denser arrangements due to expelling of air and facilitated by water molecules.

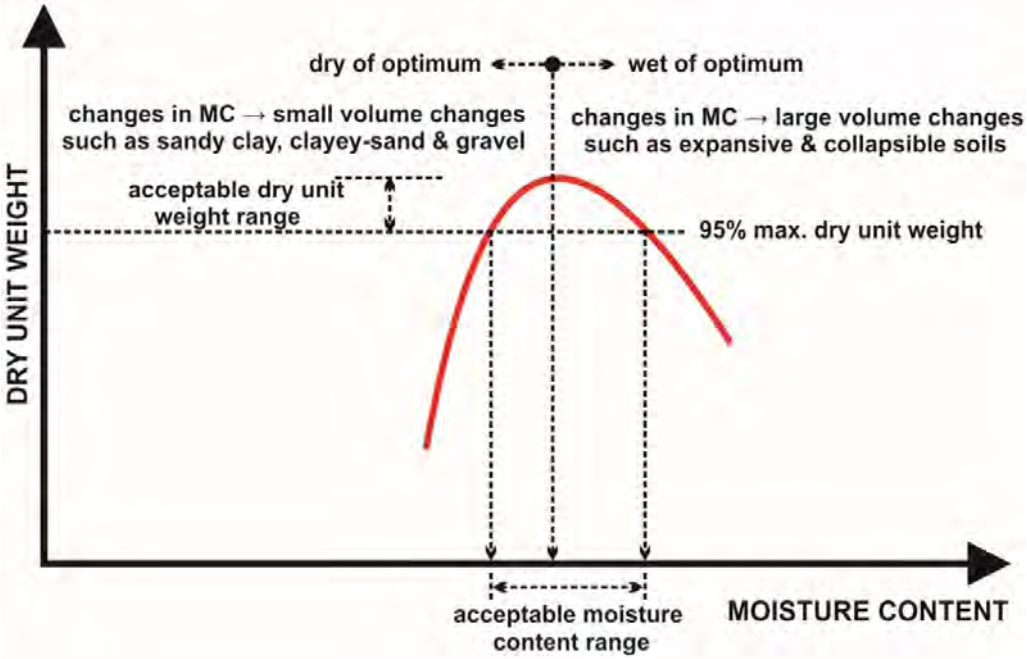

Figure 2.11 Typical Compaction Curve (illustrated after Muni Budhu, 2011)

Conversely, the region at the right hand side of the bell curve corresponds to moisture content above the optimum moisture content termed as "wet of optimum". At this stage, air can no longer be expelled from the sample and any addition of moisture will displace the soil particles, therefore, reducing the soil grains present for specific soil volume and in turns decreasing the dry unit weight (Budhu 2011b).

2.9.2.2 Purpose

The determination of both OMC and $(\gamma_d)_{max}$ through standard compaction test is significant in the prospect of soil improvement through compaction. Soil compaction is important for bearing capacity enhancements and slope stability as well as controlling any detrimental volume changes, as is the case with expansive soils. Practically, for footing, embankments and other earth structures, at least 95% of $(\gamma_d)_{max}$ as obtained by Proctor compaction, is specified. Budhu (2011b) has also noted that this compaction level can be achieved at two moisture contents, namely the dry and wet of optimum.

The dry of optimum is reached before the maximum dry unit weight whereas the wet of optimum is reached after the maximum dry unit weight. Dry of optimum usually

corresponds to sandy clays, clayey-sand and granular soils. i.e., soils that exhibit insignificant volume variations with moisture content deviations. Conversely, wet of optimum is usually used for compaction of expansive soils and clays, for example bentonite clay. Normally upon shearing, if the soil is heavily compacted, it will exhibit a sudden failure as compared to a soil which is not compacted closer to the maximum dry unit weight. Sudden failure of soil is not recommended in engineering practice and therefore a more ductile behaviour is desired. This implies that the soil should practically be compacted to a factored dry unit weight, usually 80% – 90% of the determined maximum dry density (Budhu 2011b).

The test is usually regarded as satisfactory for most types of soils in the common construction projects, however, for aviation projects that involve application of heavy air-traffic loads on runways etc., the test is modified by using a 4.54kg hammer free-falling an extended height of 457mm. Soil compaction is done is 5 layers instead of 3 by imparting a modified compaction energy of 2695kJ/m^3.

2.9.2.3 Factors Affecting Compaction

The compaction of soil mass depends upon several factors, some of which are explained in the following text. *Type of soil* has a significant impact upon its compaction behaviour and the observed MDD and OMC reading. In general, coarser grained soils like gravel and sand are more responsive to the compaction process and can attain higher dry densities compared with the finer soils like clay and silt, which have higher air voids and require more water for compaction. Furthermore, addition of certain proportions of finer soils to coarser soils increases the MDD values, as long as the amount of finer particles in the resultant mixture do not exceed the volume required to fill in the inter-particle voids of the coarser soil. In other words, a well-graded soil has higher MDD than poorly or uniformly graded soil.

The soil *moisture content* also affects its compaction behaviour as the soil shows lesser resistance to compaction at higher moisture content due to lubrication of the soil particles. This increases the workability of the mixture and allows the particles to pack more closely. Initially, the dry density increases with increase in the moisture content until the OMC value is reached, after which the volume of air voids becomes

constant and any further increase in the moisture content only increases the total void ratio, thereby decreasing the dry density.

The *compaction effort* and the *compaction method* like static or dynamic action, vibratory or kneading type equipment also influence the compaction of soil as the degree of compaction increases with the increase in the compaction effort. The choice of compaction method and effort is selected based upon the type of soil.

2.9.3 Unconfined Compression Strength (UCS) Test

2.9.3.1 Overview

As stated earlier, many engineering projects have problems with the presence of weak soils on the construction sites. These soils are often incapable of resisting the imposed stresses from the overlying structures such as foundations and road works and fail or subside, triggering cracks and damages to the structural members of the supported structures. The ability of a soil mass to resist the imposed stresses is termed as the strength of the material. For geotechnical engineering purposes, the strength of the material is often expressed in terms of the maximum stress that can be sustained by the soil provided the boundary and loading conditions are maintained. In case of clays and other types of soils, the compressive and shearing strengths are the most critical parameters.

The compressive strength of any type of soil can be defined as the maximum normal stress sustained by the soil mass subjected to crushing load (Figure 2.12). It is empirically defined as the maximum load imposed upon the soil sample divided by the sample cross-sectional area.

$$Unconfined\ compressive\ strength =$$

$$q_u = \frac{Normal/Vertical\ load(P)}{Cross-sectional\ area(A)} \quad \text{Equation (2.16)}$$

The cross-section area "A" is corrected for the changes in the area as with the progression of the test, the sample undergoes strain "ε". The sample bulges from the middle of the specimen which renders the assumption of uniform stress throughout the specimen incorrect. If the original cross-sectional are of the specimen is "A_o", the area correction can be expressed as:

$$A = \frac{A_o}{1-\varepsilon}$$ Equation (2.17)

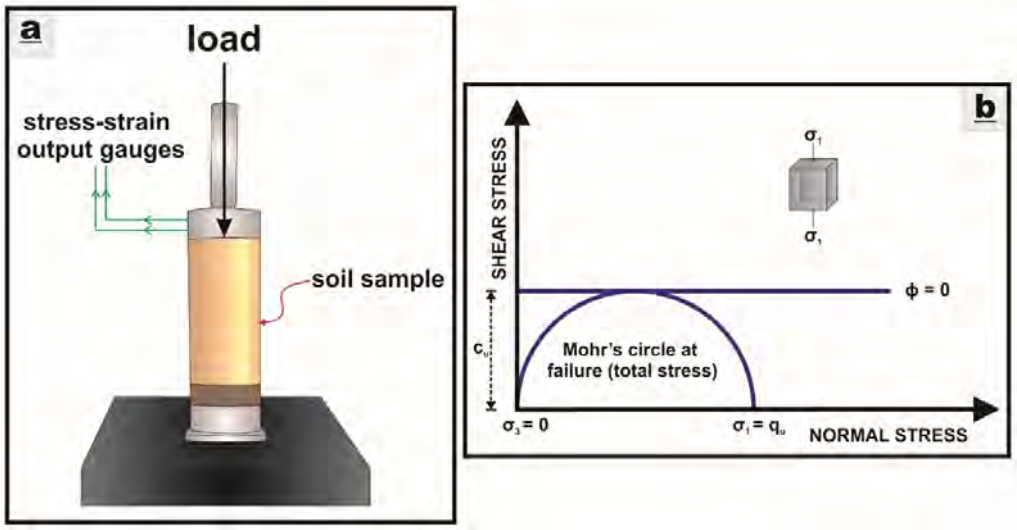

Figure 2.12 UCS Test on Soil Sample (a) Under Load, and (b) Stress Profile

ASTM D-2166 (1994) defines the unconfined compressive strength (UCS) of cohesive soil as the peak compressive stress that can fail an unconfined cylindrical soil specimen under compression testing. UCS value is obtained as either the maximum load sustained by the specimen per unit are or load per unit area at axial strain of 15%.

2.9.3.2 Purpose

The compressive strength of an undisturbed or remoulded soil sample is the measure of its ability to sustain imposed stresses. UCS tests are conducted for assessing the mechanical properties of the soil mass and empirical data about the soil relative consistency, sensitivity and undrained strength can be obtained in addition to the stress-strain characteristic relationship of soil. A compacted cylindrical sample of soil is placed between two plates in the loading device so as the upper plate is just in contact with the surface of the sample and all applied vertical load and deformation values are set as zero. The test can be performed either under stress-controlled on strain-controlled conditions. The end of the test is marked by the observance of visible deformations in the sample and a drop in the normal stress value. The UCS test is one of the most comply conducted tests performed for designing and assessing

the stability of foundations and slopes as wells as of earth-supporting structures like embankments and retaining walls. In this way, a rough estimate of the soil's strength can be calculated. However, the UCS test cannot be applied to gravels or cohesionless coarser soils and is only used for the cohesive soils. Moreover, the UCS tests are often used to quantify the consistency and sensitivity of clays, as outlined in Table 4 (Das and Sobhan 2014).

$$\text{Sensitivity} = S_t = \frac{q_{u_{undisturbed}}}{q_{u_{remoulded}}} \qquad \text{Equation (2.18)}$$

Table 4 Clay Consistency – UCS Relationship

Shear Strength (q_u) kN/m^2	Consistency
0 – 25	Very soft
25 – 50	Soft
50 – 100	Medium
100 – 200	Stiff
200 – 400	Very stiff
> 400	Hard

2.9.4 Direct Shear Strength (DSS) Test

2.9.4.1 Overview

One of the commonly encountered parameters in the study of soil stability is the shearing resistance or shear strength of soil. Several geotechnical engineering problems such as lateral pressures on an earth retaining structure, slope stability for clay slopes under rainy season or soil erosion and bearing capacity have failure imparted by critical arrangement of both shear and normal stresses and not the individual stress (Mohr 1900). Therefore, there must be a functional relationship between the two parameters acting along a failure plane. Based on the functional relationship, a graph or failure envelope may be plotted (Figure 2.13) that is actually a curved line. However, it may be represented through linearly related function. The actual shear – normal stresses function can be written as (Das and Sobhan 2014):

$$\tau_f = f(\sigma) \qquad \text{Equation (2.19)}$$

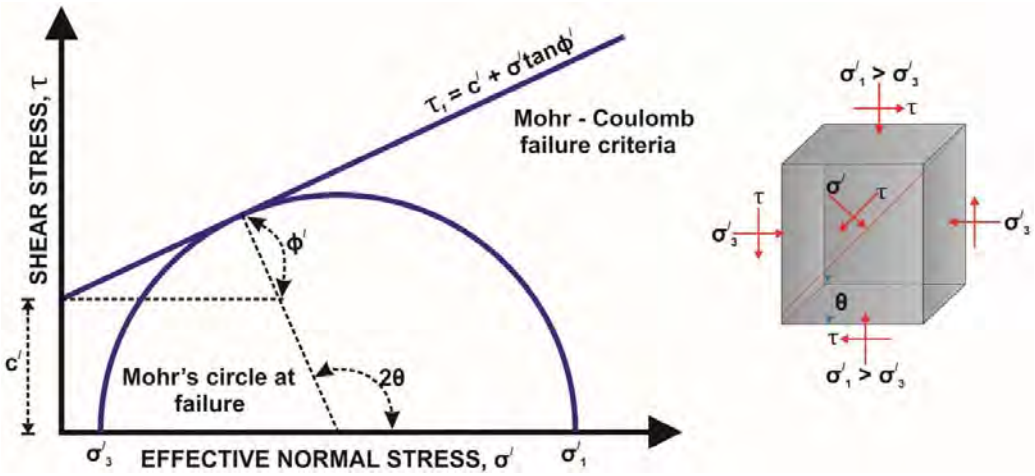

Figure 2.13 Mohr – Coulomb Failure Criterion

Furthermore, the approximated linear shear – normal function as proposed by Coulomb is represented by the following equation. The overall relationship is famously known as Mohr – Coulomb failure criterion. If the cohesion of soil is represented by "c", normal stress along failure plane is "σ", internal friction angle is "ϕ" and the shear strength is "τ_f", the Mohr – Coulomb failure criterion is:

$$\tau_f = c + \sigma \tan \phi \qquad \text{Equation (2.20)}$$

The relationship holds true for saturated soils with an additional component of pore water pressure. However, instead of representing the normal stress, it utilises the effective stress, as displayed in (Figure 2.13) and the following equation.

$$\tau_f = c' + \sigma' \tan \phi' \qquad \text{Equation (2.21)}$$

2.9.4.2 Purpose

One of the critical engineering parameters of any soil mass is the shear strength that governs its failure resistance ability. DSS test is specifically important if the planar strain failure is likely to occur in the soil mass. It is used for the calculation of soil shear strength under consolidated drained/undrained conditions. The DSS test output data has been summarised in the flowchart provided in Figure 2.14.

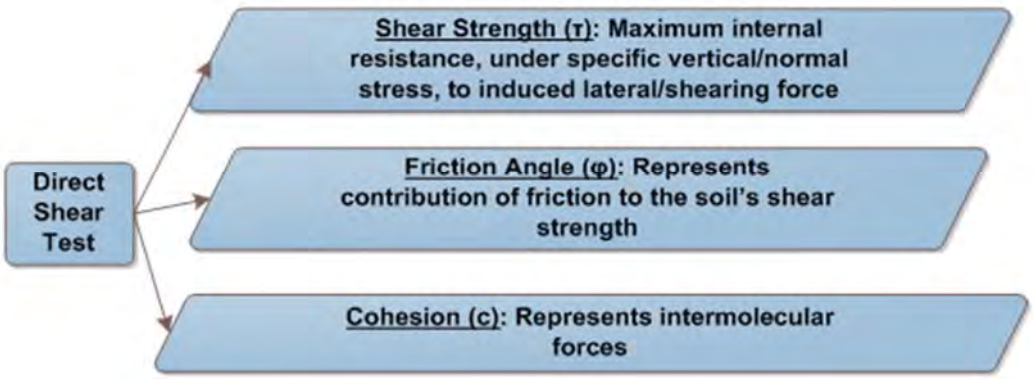

Figure 2.14 Typical Parametric Outcomes of Direct Shear Test

Direct shear test (DST) is employed for the calculation of several soil strength parameters such as the shear stress, normal confining stress, internal frictional angle and cohesion. The shearing strength parameters namely cohesion, c or c' and ϕ or ϕ' depending upon the stress configuration are significant due to the susceptibility of soil masses to erosion or slope failure which is critical in the case of earth-supporting structures like retaining walls; earth-fill damns, dikes, tunnels etc. These parameters can be determined from any of the tests in Figure 2.15 (Das and Sobhan 2014).

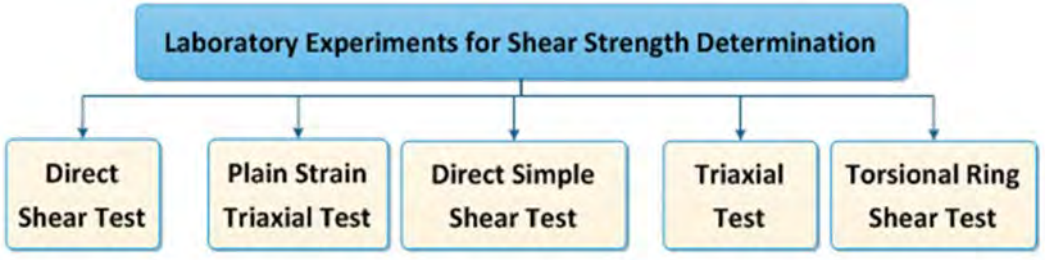

Figure 2.15 Typical Laboratory Experiments for Determination of Shear Strength Parameters

Triaxial and direct shear tests are the most commonly practiced shear strength tests for most types of soils and rocks. For the purpose of this research study, direct shear test was employed. Direct shear test (DST) is performed for soil shear strength determination with regards to the effective stress. Due to the popularity of the test, several standards are practiced throughout the world that govern the test procedure

such as Standards Australia AS 1289.6.2.2 (1998), British Standards BS 1377-7 (1990), AASHTO T236-08 (2013) and ASTM D3080/D3080M (2011).

It should be noted at this stage that in a standard direct shear apparatus, moisture drainage from the shear box cannot be completely prevented. However, Budhu (2011a) and Kalinski (2011) have noted that cohesive soils undrained shear strength can be estimated by running DST at faster loading rate. Furthermore, using the data obtained from DST as specified earlier, Coulomb failure criterion can be used for determining the shear strength, cohesion and friction angle as specified in figure (Figure 2.13) above. Based on the data obtained, a shear stress versus increase in the specimen shear or horizontal displacement can be plotted.

2.9.4.3 Factors Affecting DSS

The shear strength of clay is the magnitude representation of its resistance against soil subsidence triggered by shear stresses. As stated earlier, shear stress is a function of the normal stress and is dependent upon the cohesion of soil particles and its interlocking mechanism, which provides frictional resistance. Therefore, it depends upon several soil-system characteristics, some of which are discussed below.

Mineralogy of soil has a significant effect upon the shear strength of soil as the type of mineral present may dictate soil cohesion. In a study conducted by Namdar (2010), it was found that the presence of minerals like saponite and illite may increase the cohesion of soil mass whereas it may be reduced by carbonation. Furthermore, Hebib and Farrell (2003) and Prabakar, Dendorkar, and Morchhale (2004) have found that the inclusion of hydraulic chemicals like fly ash may increase the cohesive properties of the resulting mixture.

Particle size distribution of soil has also been found to influence the shear strength. As explained in the review of clay behaviour conducted earlier, the inter-particle forces at the nanoscale level are significantly important for providing soil cohesion, which are in turn dependent upon the shape and size of the individual particles and their interaction. The sizes of the particles also affect the internal friction angle as it depends upon the interlocking mechanism. Stark et al. (2014) and Ghazavi, Hosseini,

and Mollanouri (2008) have identified that the particle arrangement is affected by the shape of the individual grains which can influence the internal frictional angle.

Effective normal stress and void ratio largely influence the shear strength of the soil mass as the packing or particle arrangement is influence by these factors. A soil system subjected to higher normal stress may have denser particle configuration and therefore, may generate higher shear strength in terms of the peak shear stress displayed by the sample upon failure.

2.9.5 Optical Microscopy

2.9.5.1 Overview

Light or optical microscopes have been used for centuries for magnifying smaller objects. These microscopes use a combination of visible light wavelength range and lenses-system for achieving this purpose. The design and complexity of the microscope depends upon the intended use and may range from a system of two lenses to a complex lenses, mirrors and prism system. Normal photographic cameras are often included within the microscope system to obtain pictures of the magnified objects as the images projected by the optical microscope system can be captured by the light-sensitive films or charge-couple devices. In this way, output of optical microscopy can be directly obtained in form of coloured micrographs. Optical microscopes are fairly limited in scope as under extremely high magnifications; the focus of the lens is disturbed, resulting in a blurred or distorted image with fuzzy disks often visible (airy disks), which fairly limits the resolution capacity of optical microscopes. The resolution capacity is empirically expressed as:

$$d = \frac{1}{2} \times \frac{Wavelength\ of\ light(\lambda)}{Numerical\ aperture\ of\ lens} \qquad \text{Equation (2.22)}$$

Several attempts have been made to surpass the resolution limits imposed by the operating principle of optical microscopes; such as near-field scanning optical microscopes, spectral-precision distant microscopes and spatially-modulated illumination microscopes etc. Alternative methods include Fourier transform infrared spectroscopy, atomic force microscopy, scanning electron microscopy, transmission

electron microscopy, nanoindentation and micro- and nano-electro-mechanical sensor systems.

2.9.5.2 Purpose

Optical microscopes are employed for the purpose of creating magnified images of samples in order to analyse them with clearer, sharper and more focused conditions. The system collects natural or artificial visible light, such as from a light bulb, to illuminate the object to be analysed. Optical microscopes are often limited by their power of magnification or resolution, normally expressed as power of 10, ranging from 10^2–10^3. Nonetheless, several fields of science and engineering like pharmaceutical industry, nano-science, microelectronics, microbiology, mineralogy and geology utilise several variants of optical microscope for research, production and development.

In the field of mineralogy, geology and geotechnical engineering, the appearance, shape and apparent sizes of the soil and rock particles can be studied by the optical microscope and results can be documented in form of digital images. In order to achieve the magnification of a smaller sample, a typical optical microscope consists of some arrangement of lenses, as illustrated in Figure 2.16.

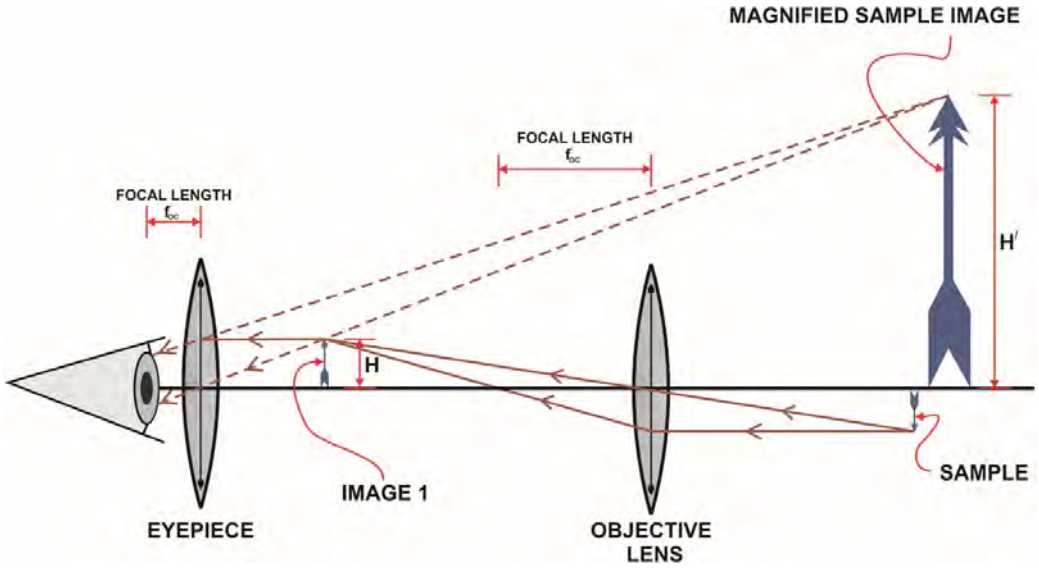

Figure 2.16 Typical Optical Microscope Schematic Diagram

2.9.6 Scanning Electron Microscopy (SEM)

2.9.6.1 Overview

Optical microscopes are fairly limited in scope to study smaller particles, on the nanometric scale, as these microscopes work on the principle of light microscopy. This problem is resolution and magnificent in overcome by using an electron microscope. The electron microscopes bombard the surfaces of the test specimen with concentrated beam of high energy electrons, the detectors are furnished with the devices to scan the electron signals from the atoms and provide information about the morphology and mineralogy of the specimen. Electrostatic and electromagnetic lenses are used in electron microscopes for the purpose of directing the electrons. The electromagnetism is achieved by using a solenoid which is then subjected to the passage of an electron beam. The degree of magnification an electron microscope depends upon the wavelength of the electrons, higher wavelengths result in lower resolving power of the microscope. The electrons are often accelerated in electron microscopes to increase the magnification power as higher speeds of electrons correspond to shorter wavelengths. The degree of acceleration may range from 1keV to greater than 1MeV. Moreover, at this range, the electron velocities become closer to the speed of light, the wavelengths (λ) are treated accordingly as described from the empirical relationship provided below (Tarrant 2010):

$$\lambda = \frac{Planck's\ constant\ (h)}{[2(electron\ rest\ mass)\times(electron\ charge)\times(accelerating\ voltage)]^{0.5}} \times \frac{1}{\left[\left\{1+\frac{(electron\ charge)\times(accelerating\ voltage)}{2\times(rest\ mass\ of\ electron)\times(speed\ of\ light)}\right\}\right]^{0.5}} \quad \text{Equation (2.23)}$$

In general, the electron microscopes can be classified as:

1. Scanning electron microscope (SEM); voltage ranges of 1kV – 30kV.
2. Transmission electron microscope (TEM); voltage ranges usually exceeding 100kV.

2.9.6.2 Purpose

After their initial development in the mid-20th century, scanning electron microscopes have been largely employed for the purposes of soil analyses and

detection in the field of geology and geotechnical engineering. These microscopes use scattered electrons to give images of the samples and are capable of providing particle surface imagery, in addition to the sizes and shapes of the particles.

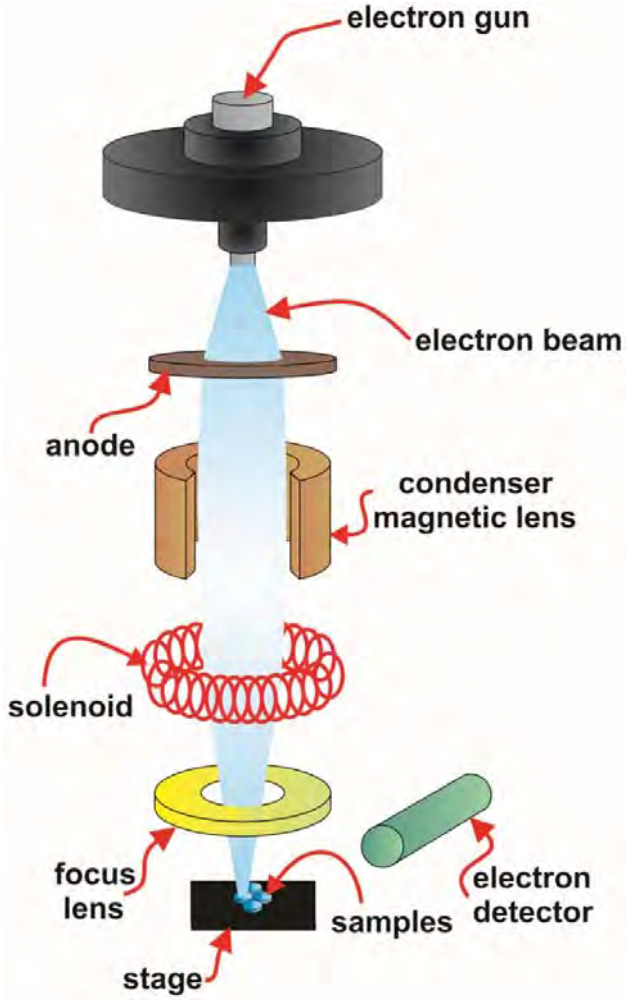

Figure 2.17 Schematic Representation of SEM Device Mechanism

The operation of a typical scanning electron microscope is shown in Figure 2.17. The primary benefit of using SEMs over optical or light microscopes is the ability to focus smaller samples at higher levels of magnification. Furthermore, as apertures and electromagnetism are used in such microscopes instead of lenses to focus the electron beam, better control over the resolving power can be achieved at the user-end. The electromagnetic lenses normally comprise of hollow cylindrical iron cases, with the hole in the middle serving the purpose of a path for the electron beam.

Solenoid coils are provided with these cases to generate magnetic field between the two piles. Vacuum is maintained within this main component of the device so as to prevent any disturbances in the path of the electron beam. Acceleration is maintained through anode-attraction forces, whereas the focus is obtained by a solenoid. The force "F" applied by the lenses is defined as Lorentz force, which is the force applied on an electric charge in motion by surrounding magnetic field, mathematically:

$$F = electron\ charge \times (net\ velocity\ \perp magnetic\ field) \times magnetic\ field$$

Another solenoid coil is used for steering the electron beam to the point of interest on the sample being analysed. The electrons are then transmitted back from sample surface and detected by an electron detector while a secondary detector is often added. The number of transmitted back electrons are largely high and for practical micrograph purposes only two types of electron emissions are used, referred to as secondary electrons and back-scattered electrons, as illustrated in Figure 2.18 (Tarrant 2010). Secondary electrons are low energy electrons (≤ 50eV) ejected from outer electron shells due to collision with high energy electrons and are used for illustrating the topographical features of the test specimen whereas back-scattered electrons have comparatively high energies used for the purpose of EDS systems.

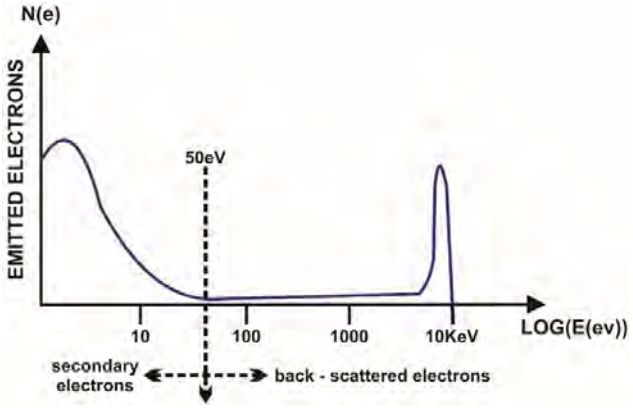

Figure 2.18 Emitted Electrons Spectrum (prepared after Tarrant (2010))

In general, SEMs are capable of giving accurate live images of the particle surface with 0.4nm resolution and the analysis speed is significantly high. The data produced has a high accuracy rate and can pick up minute details on the particle surface as it uses the electro-diffraction techniques. However, due to nonconductive nature of most clay particles and geomaterials, the charged bombarded by the electron beam

tends to segregate and provides imagery that is difficult to interpret. Nonetheless, this "particle-charging effect" can be rectified through the use of conductive coatings such as of platinum or carbon, as thin as 5nm. This technique is commonly known as sputter coating which means that ultra-thin electricity conducting material coating is applied on sample surface to prevent charging of the specimens. The SEM devices can only provide data about the particle surface whereas the procurement, operation and maintenance of the devices are very expensive. Moreover, they limited in their scope of operation as SEMs cannot produce atomic scale imagery.

2.9.7 Energy Dispersive Spectroscopy (EDS)

2.9.7.1 Overview

Energy dispersive spectrometers are normally assimilated within the SEM devices. The backscattered electrons from the sample exhibits compositional contrast due the variation in the atomic numbers of the elements and the proportion of the element within the specimen. The typical components of an EDS device include an X-ray detector, a liquid nitrogen flask to act as coolant and computer with dedicated software for data analysis and collection.

2.9.7.2 Purpose

The variety of X-rays emitted by the different element of the specimen are distinguished by the EDS system into an energy spectrum that can be read and analysed through interactive software systems to identify the elemental distribution of the specimen and then elemental compositional maps can be obtained in terms of atomic or weight percentage. In contrast with the SEM system, EDS system is used for studying the chemistry and elemental composition of the test specimens. The back-scattered electrons undergo relatively higher elastic collisions with atomic nuclei and therefore, maintain significant portion of the imparted electron beam's energy (1kV – 30kV) and provides information regarding the composition of the sample. Due to this additional component of an energy dispersive spectrometer, SEMs are therefore, also able to determine the elemental composition of the test specimens. The output data is usually interpreted in terms of quantitative analysis data, which is graphically plotted in an X-Y graph with the energy level of electron

counts on the X-axis whereas the counts detected by the X-ray detector on the Y-axis. In the fields of geology, mineralogy and geotechnical engineering, the elemental distribution of a specimen and therefore the effect of introducing a foreign mineral in the soil or rock system can be quantified.

2.9.8 X-Ray Diffraction (XRD)

The XRD analysis is employed for the purpose of identifying mineralogy of test specimens. It is a comparatively accurate and quicker analytical method of mineral crystallisation phase identification. The basic operational principle of XRD is the constructive interference of monochromatic X-rays produced through a cathode ray tube in form of parallel beam geometrics and concentrated to the sample's centre through collimation, travelling. The test specimens are normally grounded to fine powdered form and may range from organic, inorganic, synthetic, polymer, metallic and composite materials. Figure 2.19 presents the schematic illustration of an XRD.

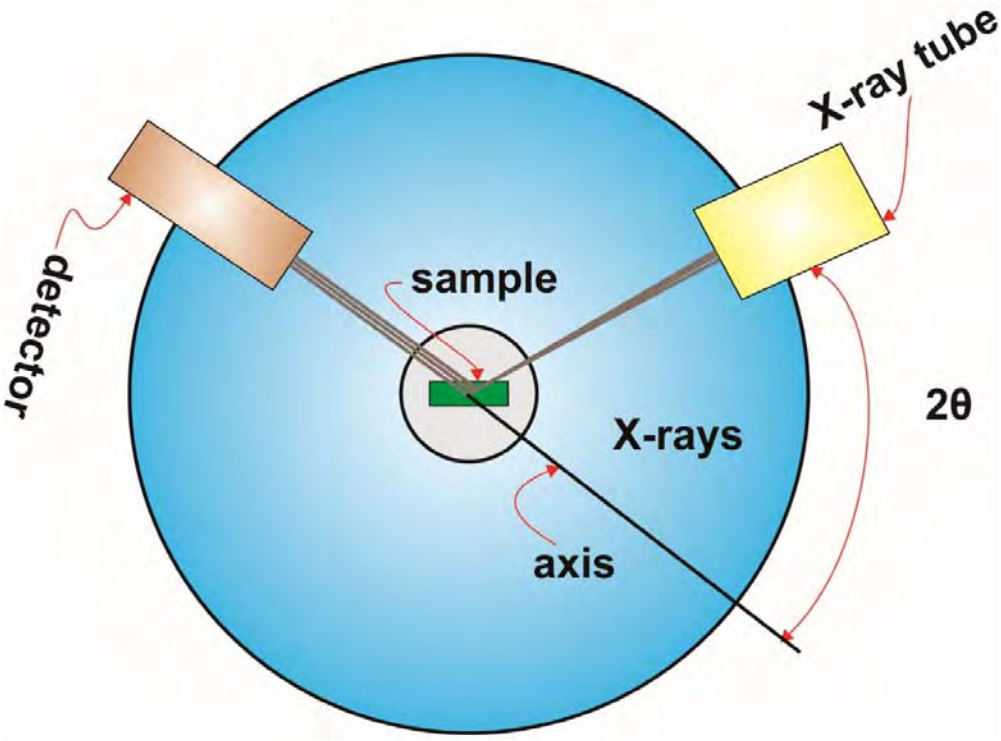

Figure 2.19 Schematic Representation of XRD Device Mechanism

As the rays interact with the sample, diffracted rays and constructive interference are produced, working on the principle of Bragg's law, empirically expressed as:

$$n\lambda = 2d \sin\theta \qquad \text{Equation (2.24)}$$

Where; n = any integer, λ = beam wavelength, d = sample lattice spacing or spacing between the atomic layers, θ = angle of diffraction/incident and is used in terms of a range of 2θ to account for all probable directions of X-rays diffractions.

The X-rays diffracted by the sample are detected, counted and processed. The two most common spectra components are K_α and K_β, which is further comprised of $K_{\alpha 1}$ and $K_{\alpha 2}$ depending upon the magnitude of the wavelength. The most commonly used crystal diffraction material is copper and XRD spectral images are usually recorded with CuK_α radiation. The diffracted X-rays are used to give information about the mineralogy and crystallography of the specimens through the peaks and angle (2-theta) of the reflection spectra. As each type of mineral has unique lattice spacing, the minerals can be easily identified by assessing against a mineral peak and diffraction angle database. The sample does not need to be polished or prepared with specific coatings. The crystallography, sample chemical composition, and mineralogical data obtained are highly accurate. In the field of geology and geotechnical engineering, the identification of clay minerals and layers and the presence of each element can be quantified. Furthermore, the phase of a mineral and any changes in the crystallography and mineralogy of the soil and rock samples due to introduction of a foreign agent like a stabiliser can be identified. However, the quality and accuracy of the data is limited by the size of the specimens. In addition, as non-crystalline samples give weak signals, the technique is more suitable for the crystalline samples

2.10 SUMMARY

2.10.1 Summary of Soil Stabilisation

The successful application of a suitable soil treatment, commonly termed as soil stabilisation, can help to reduce the degree of soil deformation and the damages to the overlaying structures can be kept within an acceptable range. Many remedial methods exist for the treatment of such soils and the selection of any particular

treatment method is largely dictated by its ability to enhance the strength of the soil. Soil stabilisation is classified based upon the mode of application such as thermal stabilisation by heating to decrease repulsive forces between clay particles and/or temperatures exceeding 100^{o}C reduced the absorbed moisture volume, either can cause an increase in the soil's strength (Venkatramaiah 2006); mechanical; electrical and stabilisation through nanomaterials such as adding carbon nanotubes. Among other methods, mechanical and chemical stabilisation methods are the most common techniques.

Soil is "mechanically stabilised" by changing soil's texture or gradation by mixing different soils, compaction or densification, pre-wetting, surcharge loading, electro-osmosis and drainage. Conversely, additives or stabilisers may be added to the soil for additive or chemical stabilisation. Moreover, additives such as alkali salts, lime, bitumen, fly ash and cement can be added to the soil to decrease its shrink-swell potential and enhance shear and compressive strength through cementation, hydration or formation of stronger particle matrices. The selection of the stabiliser(s) depends upon the soil mineralogy, treatment objectives, plasticity, gradation, additive-mechanism, material rheology, soil profile; and design constraints of time, cost and quality (Texas Department of Transportation 2005). Furthermore, economic factors such as the cost of manufacturing and transportation as well as climatic factors like environmental impact of stabiliser production also play a significant role in selecting any stabiliser.

Chemical or additive stabilisation is among the most commonly applied soil stabilisation methods. The treatment can be aimed to increase the soil particle size, reduce the plasticity index, enhance the strength, and decrease the shrink-swell potential or cementation. It is attained through the introduction of one or more chemical compounds in the soil mass. Compounds like cement, fly ash and lime have been effectively utilised for soil stabilisation (Neeraja and Rao Narsimha 2010).

The selection of the stabiliser(s) depends upon the soil mineralogy, treatment objectives, plasticity, gradation, additive-mechanism, material rheology, soil profile; and design constraints of time, cost and quality (Texas Department of Transportation 2005).

Many researchers have investigated the stabilisation of expansive soil through the use of additives (Cokca 2001) (Nalbantoğlu 2004) (Pandian and Krishna 2003) (Misra, Biswas and Upadhyaya 2005) (Veith 2000). The following table (Table 5) reviews some of the studies presented in the preceding pages on enhancing the strength of the expansive soil through addition of chemical additives:

Table 5 Review of Research on Chemical Soil Stabilisation

Reference	Scope		Results of Remedial Procedure
	Base Material	**Remedial Procedure**	
<u>Fly Ash Stabilisation</u>			
Phani Kumar and Sharma (2004a)	Inorganic expansive soil containing sandy fat clay with a free swell index (FSI) of 250%.	Adding different percentages of fly ash (FA).	• ↑FA content ⇒ ↑PL. • ↑FA content ⇒ ↓Permeability. • ↑FA content ⇒ ↓FSI (by 50% for FA content 0f 20%). • ↑FA content ⇒ ↑UCS (by 27% for 20% FA).
Zha et al. (2008)	Overconsolidated and highly plastic expansive soil and free swell of 55.5 %.	Different percentages of FA. Different percentages of FA and lime mix. Samples had two curing days 0 days and 7 days.	• ↑FA content ⇒ ↑UCS (Optimum results for 9-12% FA and 2-3% lime, 7 days curing).
Amu,	Expansive	Different	• UCS; 9% C + 3% FA > 12%

Fajobi, and Afekhuai (2005b)	greyish clayey soil.	percentages of cement (C). Different percentages of FA. Different percentages of cement and FA mix.	C. The UCS increased to 1756.13 kN/m^2.
Solanki and Zaman (2010)	Two subgrade soils; clay with high plasticity (CH) and clay with low plasticity (CL) with respective activity of 0.69 and 0.47.	Different percentages of lime. Different percentages of Class C FA and cement kiln dust.	• 9% lime (K) ⇒ ↑UCS (by 1,638%). • 9% lime (K) ⇒ ↑UCS (by 2,033%).
Cement and Lime Stabilisation			
Al-Rawas, Hago, and Al-Sarmi (2005b)	Expansive soil	Different percentages and combinations of pozzolan cement and lime.	• ↑Lime% ⇒ ↓Swell Potential. • ↑Pozzolan% ⇒ ↑Swell Potential.
Saride, Puppala, and Chikyala (2013b)	Organic expansive soils	Different percentages of lime (L). Different percentages of cement.	• ↓Plasticity by L > ↓Plasticity by C. • After 28 days: ↑UCS = negligible (for L), UCS = decreased (for C). • Optimum results: 3% - 6.5%

			(based on soil type), 7 days curing ⇒ 1035kPa UCS.
Thyagaraj and Zodinsanga (2014)	High plasticity expansive soil with LL=76%, PL=28%.	Compacted expansive soil permeated by $CaCl_2$ and NaOH to simulate in-situ precipitated lime stabilisation.	• Sequential alkali solution permeation ⇒ Lime precipitation, ↑pH and pozzolanic reactions and ↑UCS.
Khemissa and Mahamedi (2014b)	Over consolidated expansive soil	Various cement-lime mixing ratios.	• ↑Stabilisers ⇒ ↓Swell Potential (methylene blue value > 6 reduced to ~ 2). • ↑Stabilisers ⇒ ↑CBR. • Optimum results: 2% C + 8% L, for soaked CBR. 8% C + 4% L, for un-soaked CBR. • Optimum direct shear test values: 8% C + 4% L.
Slag Stabilisation			
Yadu and Tripathi (2013a)	Soft inorganic fine soil with the Atterberg limits as LL = 46 %, PL = 29 % and PI = 17 %	Different percentages of granulated blast furnace slag.	• Optimum UCS and CBR: ~↑28% (for 9% slag).
Akinmusuru (1991)	Lateritic soil.	Slag percentages	• ↑Slag% ⇒ ↑PI, cohesion and MDD (up to 10% of slag).

		from 0 % to 15 %.	• ↑Slag% ⇒ ↓LL and PL.
Ortega-López et al. (2014)	Clayey soils.	Five different types of ladle furnace slag at a proportion of 5%.	Reduction in the swelling potential of soil, strength and volumetric stability and higher CBR indices as compared with the untreated soils.
Ashango and Patra (2014)	Clayey soils.	Different percentages of Portland slag cement (PSC) and rice husk fly ash (RHA) under different curing days.	• ↑RHA and PSC ⇒ ↑OMC, ↓MDD. • Optimum UCS and CBR: ~ ↑76.8% UCS, ↑91.75% soaked CBR (for 10%RHA and 7.5%PSC).

These researchers have utilised different techniques and approaches to counter the problems of soft or reactive expansive soils. The majority of the studies have focused on either increasing the overall strength or decreasing the swelling potential by adding a cementing material; such as slag, cement and/or their mixture. Although cement has been used as a binder in most cases, (Wong 1992) have found that fine granulated blast furnace slag produces similar effects as Portland cement as a cementitious material.

2.10.2 Summary of Construction and Demolition Waste Generation and Reuse in Construction Industry

Several countries have commissioned studies on the identification of the scope and mitigation of this issue. The environmental impacts of construction related activities were studies by (Hill and Bowen 1997) (Association 1993) and (Ofori 1992). These construction wastes or CWs form a major component of the solid waste in many countries and only marginal quantities are utilised in backfilling on construction sites. The major chunk of the CW is still mostly dumped on already scarcer landfill

sites. Therefore, the construction waste causes land, resource and material depletion and deterioration (Wang, Li and Tam 2014) (Behera et al. 2014b). The problems associated with the generation and management of construction and demolition waste is a global issue. In United States alone, approximately 29% of solid waste dumped in landfills originates from construction and demolition activities (Rogoff and Williams 2012). However, around 50% of the solid waste disposed in United Kingdom landfills originate from the construction industry while construction and demolition activities contribute to 70 million tonnes of waste (Lenssen and Roodman 1995; Tam and Tam 2008). Also, it was documented that annually generated construction and demolition waste volumes in Germany almost exceeded 44 million tonnes for the year 1993 (Kohler and Kircher 1993) whereas 26% of wastes generated in The Netherlands were from construction activities that corresponded to approximately 14 million tonnes (Bossink and Brouwers 1996).

Australian construction industry alone produces approximately 38% waste for landfills each year (Li and Du 2015). In a report prepared by Hyder Consulting (2011), comprising of largely consistent data across Commonwealth states jurisdictions, it was stated that in Australia during the 2008-2009 period 55% of CW was recovered, i.e., approximately 10,468,186 tonnes of CW were being annually recycled while 8,529,374 tonnes of it were being disposed. Furthermore, more than 8 million tonnes of construction and demolition wastes were being deposited in landfills and other solid waste management processes while approximately 10 million tonnes were being annually recycled. Even though, the data presented above is based upon the statistics compiled by Hyder Consulting (2011), utilising industrial and Commonwealth government figures, firm conclusions cannot be drawn from these reports. Therefore, the actual amount and composition of CWs may deviate as complete data regarding these two factors has not yet been compiled for all Commonwealth jurisdictions as Victoria, Western Australia and South Australia data had been used to draw out the data for Australian Capital Territory, Tasmania, Queensland and New South Wales. The most significant constituents of CWs include bricks, concrete and asphalt etc., approximately more than 31% in New South Wales alone and are also among the most recycled of the CW constituents with around 97% recycling rate in Western Australia (Environment Protection and

Heritage Council (EPHC) 2010). Furthermore, approximately 56% of bricks wastes were reported to have disposed in landfill sites in Australia for the year 2005. However, EPHC acknowledges that the techniques and applicable process for reuse of concrete and bricks CWs can still be diverted to enhance the recycling practice and reduce construction project costs due to high cost of virgin materials, especially that after recycling around 69.8% of these wastes by recycling 6.73 million tonnes and only disposing 2.92 million tonnes for the 2006-07 financial year. The following pages review the composition and type of the commonly produced waste, i.e., concrete and brick works, from the construction and demolition activities, followed by current and potential recycling activities.

2.11 LIMITATIONS AND REUSE OF CW AND GGBFS FOR SOIL STABILISATION

Over the years, the global concern over the climatic imprint of construction activities has gathered interest in recycling of masonry and concrete wastes. Apart from research institutes, commercial vendors have also stepped in recycling these wastes to produce aggregates for new projects. Crushed masonry and concrete wastes (CMCWs) can be used as recycled aggregates in preparation of new concrete mixes. Another important market for CMCWs includes pavement subgrades, road fills and road bases. One market report recognises that the employment of recycled CMCWs actually holds advantage over virgin materials at the consumer end as it can provide 10% – 15% additional volume/tonne (Hyder Consulting 2011), thereby, proposing a major benefit of using recycled aggregates.

Furthermore, the huge demand of orthodox construction materials has caused a depletion of high quality virgin aggregates due to the increased consumptions resulting from exponential investments and growth in the construction sector. The costs are further escalated due to the expenses associated with the haulage and transportation of materials. Furthermore, many countries have problems with illegal or environmentally unsafe disposal of industrial by-products such as blast furnace slag. The globally growing concern over environmental safety has made researchers worldwide find more sustainable solutions to these problems and reuse the waste materials. Similarly, different researchers have worked to find alternative materials for achieving soil stabilisation using industrial by-products such as fly ash, slag and

lime (Al-Malack et al. 2014; Amu, Fajobi and Afekhuai 2005a; McCarthy et al. 2014).

CHAPTER 3
MATERIALS AND METHODOLOGY

3.1 INTRODUCTION

Previous chapter identified that several world regions, especially arid and semi-arid regions, are prone to comparatively large percentages of expansive and weak soil compositions (Schanz and Elsawy 2015). Considering the huge imprint of construction activities on the environment (Horvath 2004), this research work is focused on the use of recycled materials for soil stabilisation. The techniques of both chemical/additive stabilisation and mechanical composite stabilisation have been employed with GGBFS and construction waste as the soil stabilisers. Recycled construction waste (CW) has been preferred as the production of new aggregates increases CO_2 imprint (Limbachiya, Meddah and Ouchagour 2012). These materials have already been used for reinforcement in various developed countries around Europe (Kasai 1989; Hansen 1986; Khalaf and DeVenny 2004; Poon and Chan 2007; Chakradhara Rao, Bhattacharyya and Barai 2011).

The materials used for the purpose of this study and the methodology adapted to achieve the goals of the experimental programme have been outlined in this chapter. It has been divided into two principal sections; respectively explaining the testing materials and the test methodology. Details and specifications of the laboratory equipment used to perform the experimental work have also been subsequently provided. The first section is further subdivided into two subsections. The first subsection discusses the specifications of the expansive bentonite clay that was used as the base material for the experimental procedure. Second subsection outlines the two types of stabilisers used for the purpose of soil stabilisation, construction and demolition waste obtained from a commercial recycled material supplier, and ground granulated blast furnace slag procured from BGC Australia. In addition, due to the significance of specimen curing period during soil stabilisation, six different curing periods were utilised. The experimental works were performed at geomechanics and pavement laboratory and physical imaging laboratories of Curtin University (Bentley

Campus). The flowchart in Figure 3.11 further illustrates the organisation of chapter 3.

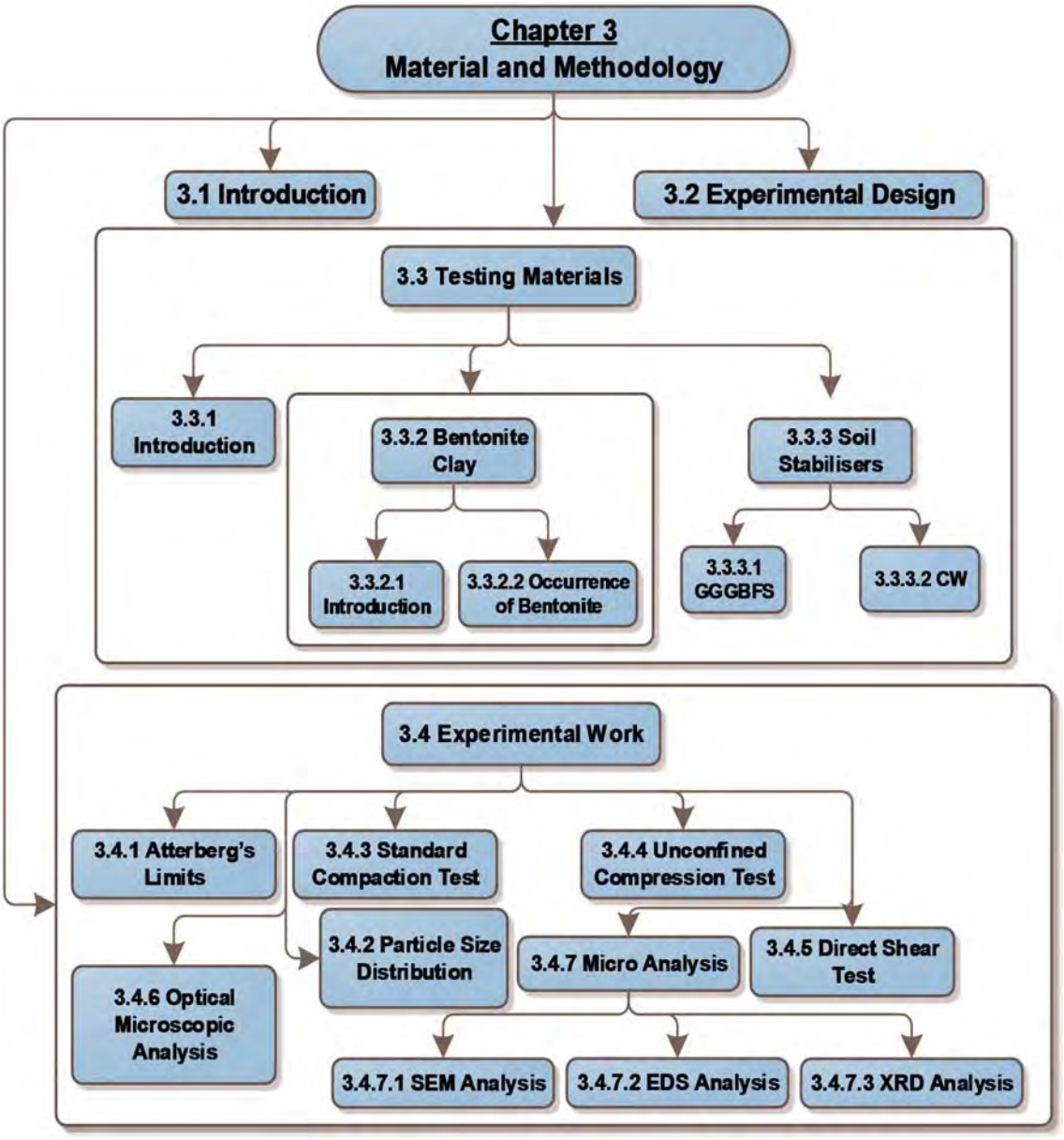

Figure 3.1 Outline of Chapter 3

The second principal section elaborates the experimental procedure and was sectioned into three parts. The first portion of the second section explains the laboratory work conducted for the establishment of Atterberg's limits and determination of the moisture content and maximum dry density of bentonite

clay. In order to gain insight on the physical appearance including colour and texture of the materials, optical microscopic analysis was conducted, as has also been explained in the first subsection of the second principal section. Moreover, the bearing capacity of the stabilised and unstabilised specimens was also determined in terms of the unconfined compressive strength, and the experimental procedure performed for this purpose has also been explained in this section.

The second portion of the second principal section outlines the testing method employed for estimating the effect of stabilisation process in terms of the shear strength enhancement by conducting direct shear strength tests on pure bentonite and bentonite-stabiliser composite specimens. The last subsection deals with the explanation of the microstructural analysis methodology. Scanning electron microscope (SEM) and energy dispersive spectroscopic (EDS) spectra analyses were performed to identify the morphology and microstructure of the stabilised and unstabilised specimens. The changes in the elemental composition of the stabilised specimens after addition of different volumes of both stabilisers and passage of sample curing period were explored through X-ray diffraction (XRD) spectroscopy to identify the effects of the stabilisation process on bentonite clay and stabiliser composite specimens, the methodology for which has also been presented in this section.

3.2 EXPERIMENTAL DESIGN

This study had, therefore, been conducted to investigate the feasibility of utilising construction waste and GGBFS for the stabilisation of clay. For this purpose, the material properties including texture, appearance, particle sizes, elemental distribution and Atterberg's limits were to be determined initially. The two principle strength parameters that have been identified in the literature review conducted in chapter 2 are unconfined compressive strength and shear strength. The experimental design was devised to identify both properties separately. The experimental design of the research methodology for calculating the evolution of UCS values of bentonite clay with additive percentages and sample curing periods has been illustrated in Figure 3.2.

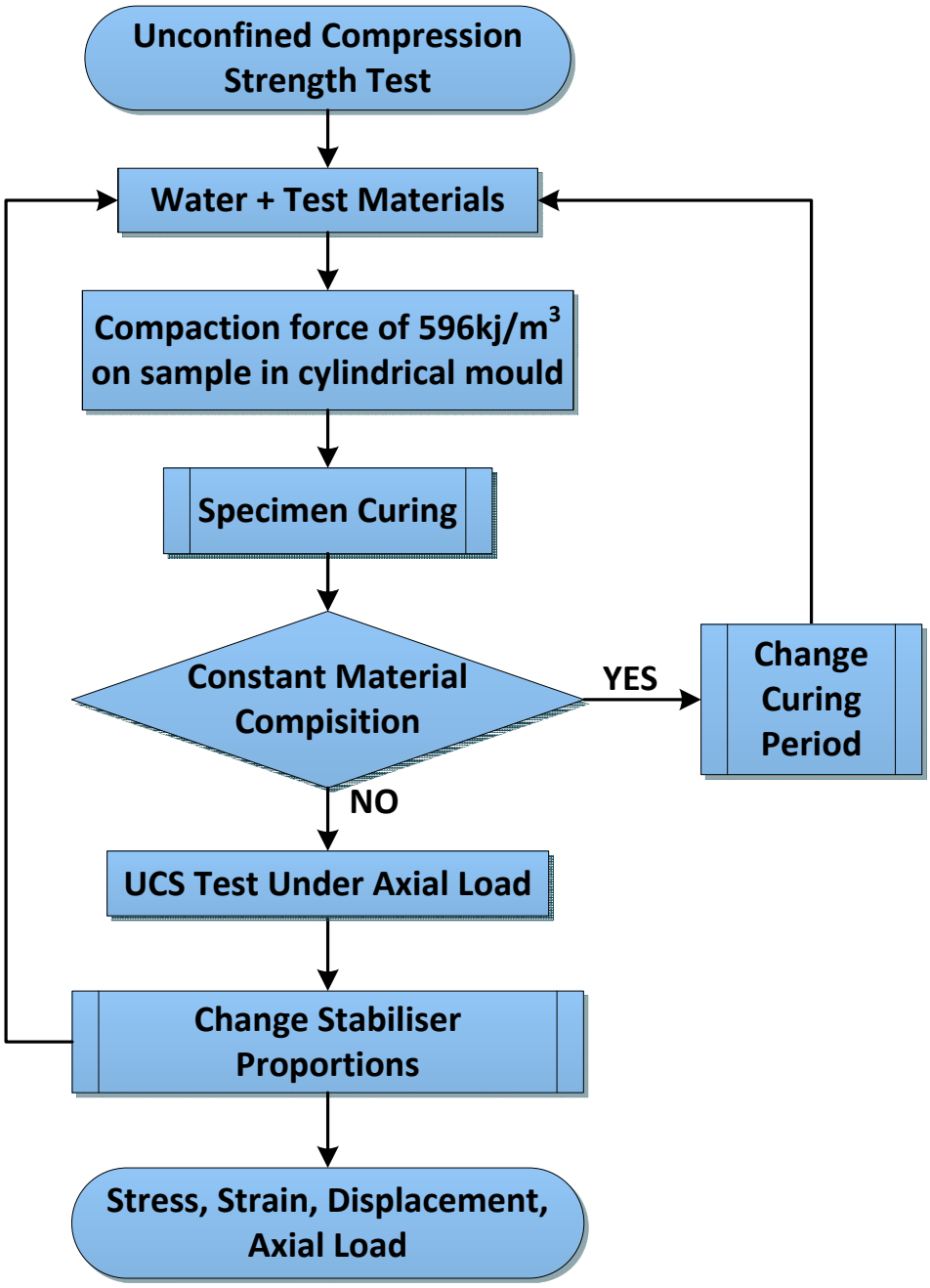

Figure 3.2 Experimental Design of UCS Test Methodology and Outputs

Similar to UCS tests, the efficiency of the adapted two additive materials; namely construction waste (CW and ground granulated blast furnace slag (GGBFS) in enhancing the mechanical characteristics of the reactive soil was evaluated through laboratory experiments. The outline of laboratory experiment, controlling parameters and outputs has been summarised in Figure 3.3.

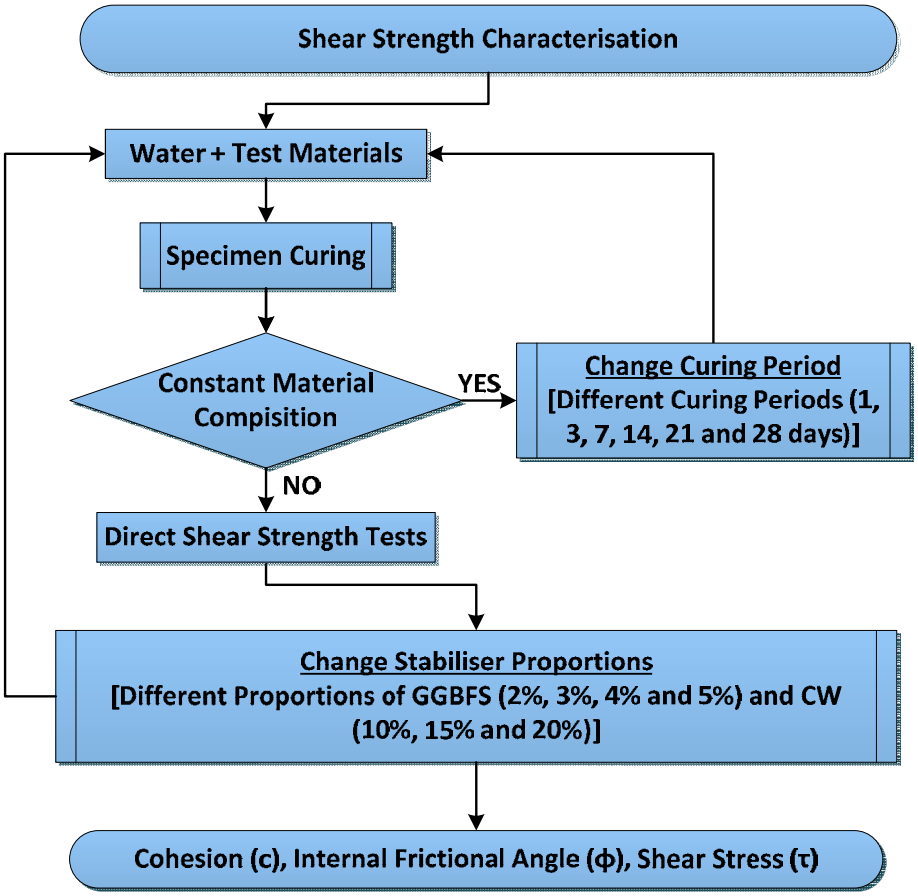

Figure 3.3 Experimental Design of the DSS Test Methodology and Outputs

3.3 TESTING MATERIALS

3.3.1 Introduction

The descriptions of the materials used in the experimental study have been presented in this section. The section is divided into two main sections, bentonite clay and the stabilisers. The purpose of the study was to identify the effect of the two stabilising agents, construction and demolition waste and ground granulated blast furnace slag on bentonite clay containing montmorillonite as the expansive mineral.

3.3.2 Bentonite Clay

3.3.2.1 Introduction

The expansive soil that was selected for the purpose of this test was commercially manufactured bentonite procured from Sibelco Australia Limited. Other researchers

have also used sodium bentonite in their investigation on expansive soils (Abdelrahman, Mohamed and Ahmed 2013). It is absorbent aluminium phyllosilicate clay that primarily consists of montmorillonite mineral (Hosterman and Patterson 1992). The generic formula for the expandable di–octahedral montmorillonite can be expressed as $\left(\frac{1}{2}\mathrm{Ca, Na}\right)_{0.7}\,(\mathrm{Al, Mg, Fe})_4[(\mathrm{Si, Al})_8\mathrm{O}_{20}](\mathrm{OH})_4 \cdot \mathrm{nH_2O}$. The nomenclature of bentonite derives from the element donating the primary exchangeable cation to the clay. The most commonly observed bentonites as sodium bentonite and calcium bentonite, whereas metabentonite or potassium bentonite; saponite or magnesium bentonite, found in volcanic material and mineral cavities; rare form of hectorite or lithium bentonite; are also found. Due to its swelling nature, bentonite in general and sodium bentonite in particular is used for several purposes such as applications in landfill systems as clay liner, in mud-drilling and in foundry as bonding clays etc. and for these industrial and large-scale applications, two main types of bentonite namely; Na-bentonite and Ca-bentonite are commercially produced.

3.3.2.2 Occurrence of Bentonite

The term "Fuller's earth" or bentonite is used to represent any clay of the smectites clay group with higher absorptive capacity and contains montmorillonite as the most dominant clay mineral. Bentonite naturally occurs in volcanic or sedimentary formations and is also found in the seabed strata. The chemistry and elemental distribution of the occurring bentonite is dictated by the nature of the parent rock and the surrounding environment. In Australia, it most commonly found in New South Wales and Queensland and the commercial production of bentonite in both regions exceeds 25,000tonnes/annum and 100,000tonnes/annum, respectively. There are also several sites in the eastern state of Victoria where bentonite has been discovered. It is also commercially mined from Moora mines approximately 300km from Perth (Whitehouse J. et al. 2007) and has also been discovered near Watheroo area (EPA 1992) as shown in the map produced in Figure 3.4.

Figure 3.4 Location of Bentonite Mines in Australia (based on reports and data generated by EPA (1992); Huleatt and Jaques (2008); Whitehouse J. et al. (2007))

3.3.2.3 Test Bentonite Clay

Bentonite is a cohesive soil with the smectite clay group minerals constituting the primary portion, approximately 74%, of the clay composition. It was supplied by Sibelco Australia Limited and contained finely powdered eggshell shade of white as illustrated in Figure 3.3(b).

Figure 3.5(a) shows the bentonite bags of 25kg each that were provided by the commercial supplier. Bentonite was supplied in paper sacks of multiple layers of high quality and weight Kraft paper with plastic films acting as inner layers to prevent excessive moisture exposure of the sacked bentonite. The bentonite bags were stacked and stored in the geomechanics and pavement laboratory of Department of Civil Engineering at Curtin University (Bentley campus) as displayed in Figure 3.3 (a).

Figure 3.5 (a) Storage of Bentonite Paper Sacks, (b) Bentonite Clay

Bentonite has a specific gravity of 3.30 and as stated earlier, it is predominately composed of smectite group of clay minerals. In addition, small percentages of impurities in the form of other clay minerals such as quartz and cristobalite (less than 18%), and plagioclase, feldspar and kaolinite mixtures (less than 8%) are also present. Bentonite primarily contains fine Na-montmorillonite particles (surface area of 800m^2/kg) (NRC 2006). The smaller size causes bentonite particles to have high adsorption ability and have more sensitive to reactions. The higher tendency of the bentonite to swell upon hydration is due to the predominant presence of Na-montmorillonite, making it a suitable representative of the actual expansive clay present in site conditions as it is also the major component of expansive clay (Fadl 1971). Montmorillonite rich clays often form deep honeycombed crack after drying and water can readily penetrate through the cracks during a wetter season. The typical chemical composition of bentonite clay has been reproduced in in Table 6.

Table 6 Chemical Composition of Bentonite (Karnland 2010)

Compound	Content
Silica; SiO_2	65.9–69.0%
Aluminium Oxide; Al_2O_3	20.4–21.7%
Ferric Oxide; Fe_2O_3	3.95–4.46%
Magnesium Oxide; MgO	2.48–2.82%
Calcium Oxide; CaO	1.31–1.63%
Sodium Oxide; Na_2O	1.95–2.69%
Potassium Oxide; K_2O	0.5–0.61%
Titanium Oxide; TiO_2	0.15–0.24%

3.3.3 Soil Stabilisers

The soil stabilisers that were used for this study were of two types. Firstly, granulated blast furnace slag has been employed both as a cementing agent and a stabiliser. Secondly, the construction and demolition waste has been used to enhance the bearing capacity of the expansive soil.

3.3.3.1 Ground Granulated Blast Furnace Slag (GGBFS)

Blast furnace slag is produced by steel industry in the molten form as a by-product of purification of iron ore. It is then rapidly cooled to prevent crystallisation, producing a granulated material. The cementitious nature of slag essentially develops because of the silicates and aluminium-silicates of lime and other bases (Lee 1974). It has become an increasing practice to use greener stabilising agents such as slag due to the environmental considerations (Veith 2000). Slag is a cheaper alternate to other stabilisers such as lime and cement, rendering the economic feasibility of highway projects possible. Moreover, with lime and cement, large amount of carbon dioxide (CO_2) emissions may occur during their production phase. Since CO_2 is a greenhouse gas, it may cause warming of the Earth's surface by reducing outward radiation which can be reduced by using alternate stabilisers like slag. The slag that was used for the purpose of this study was Ground Granulated Blast Furnace Slag (GGBFS) provided commercially by Cement Australia Pty Limited.

GGBFS contains fine particles with a glassy crystalline texture and cementitious nature that enables it to show hydration upon addition of water. The texture and appearance of the GGBFS employed for the purpose of this research has been illustrated in Figure 3.6(c). Similar to bentonite, it was supplied in heavy-duty multilayered Kraft paper bags of 20kg each as shown in Figure 3.6(a). Moreover, as Figure 3.6(b) illustrates, GGBFS was properly weighed in percentages of dry unit volume of bentonite and sealed in plastic bags. The plastic bags were then placed in moisture-controlled container to minimise contamination from the surrounding environment and was also stored in geomechanics and pavement laboratory, as displaced in Figure 3.6(d).

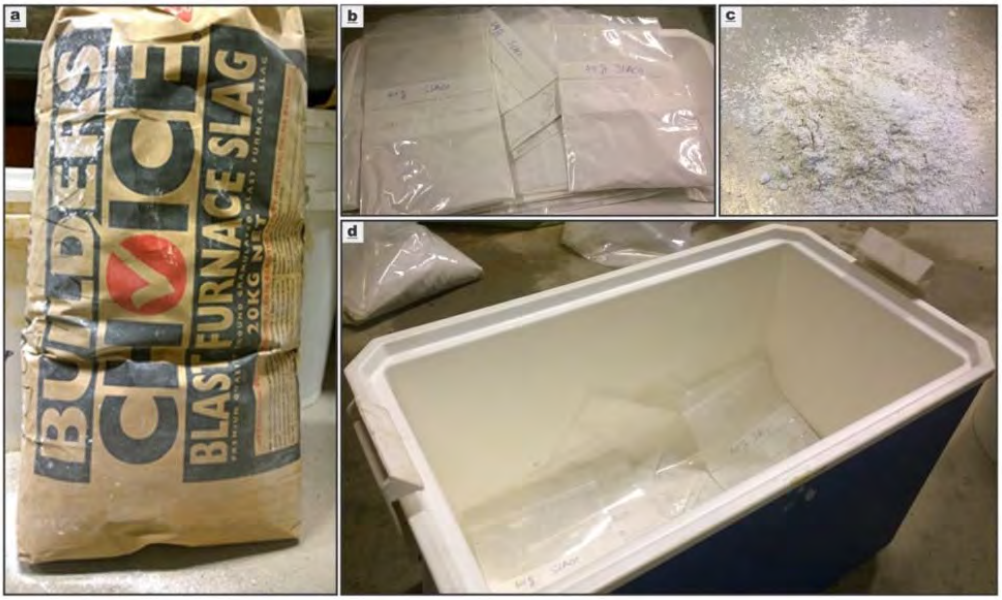

Figure 3.6 Test Material Images (a) GGBFS Paper Sack, (b) GGBFS Weighed and Sealed Plastic Bags, (c) GGBFS Particles, and (d) Storage of Plastic Bags

GGBFS has mildly cementitious properties that enable it to show hydration upon addition of water. and is used with cement or lime (D.D. Higgins 2005). However, due to the hydraulic nature of the slag, considerable presence of calcium, it may harden and hydrate without any additional material in presence of water, even though the hydration process is considerably slower and may take considerable time to complete (Song et al. 2000b). The chemical composition of the GBFS is provided in the Table 7 and Figure 3.7.

Table 7 Chemical Composition of GGBFS (BGC Australia)

Compound	Content
Calcium Oxide; CaO	30–50%
Amorphous Silica; SiO_2	35–40%
Aluminium Oxide; Al_2O_3	5–15%
Sulphur; S	< 5%

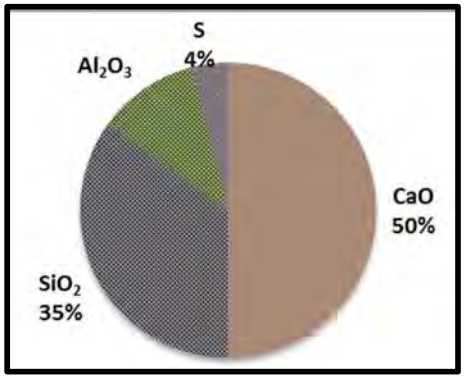

Figure 3.7 Chemical Composition of GGBFS

GGBFS hardens in presence of water through hydration process to produce volumetrically stable compounds and increased strength over long period of time. The silica content of GGBFS is more than the Portland cement. It produces comparatively higher calcium silicate hydrates, which in turn gives lower hydraulic conductivity, porosity and enhanced structural formation which can be more resistant against weather variations (Ouf 2001b).

3.3.3.2 Construction and Demolition Waste

Construction waste (CW) was obtained from Capital Recycling Australia and mainly consisted of crushed concrete, tiles and masonry works that had been sieved at the storage facility by the supplier to remove the wood and glass residues (Figure 3.8).

Figure 3.8 Storage and Sieving Facility for Construction and Demolition Waste

Initially, the procured construction waste was stored in a reinforced plastic container as displayed in Figure 3.9(a) to achieve air-drying of the wet material. After considerable reduction in the moisture content of the construction waste was noticed from visual inspection, it was collected in small buckets and stored in the storage area of the geomechanics laboratory as Figure 3.9(b) shows. As can be seen from Figure 3.9(c), the particle size range of construction waste was widely distributed. It is intended for the purpose of usage as a road base material (19mm) and is produced based upon the standard specification of Main Roads Western Australia (2010) consisting of general clean rubble from construction projects.

Figure 3.9 Construction Waste Container, (b) Storage of CW in Plastic Buckets, and (c) Un-sieved Construction Waste Particles

As the procured construction waste primarily consisted of crushed masonry, tiles and concrete, which produced a widely varied texture, appearance, colour and composition of the CW, it was screened to remove glass and wood impurities and was dried in the oven at the temperature of 105 ± 2^{o}C for a 24 hours period. The appearance and texture of the construction waste particles post-screening has been displayed in Figure 3.10(a). The wide variations in the shapes and colours of the particles can be observed from this image, which illustrates the particles passing through sieve 4.75mm and retained on sieve 2.36mm that were selected for the purpose of this study.

As the procured construction waste was oven-dried, followed by sieving and the construction waste particles that fall in the range of particle sizes smaller than

4.75mm sieve and larger than 2.36mm sieve were separated, precautions were taken to maintain the moisture conditions of the sieved particles, as much as possible. The separated CW particles were then stored in plastic bags for reducing interactions of the construction waste grains with outside moisture and environmental conditions as shown in Figure 3.10(b). These bags were then placed in moisture-controlled containers and were stored to be later used for soil stabilisation process, as exhibited in Figure 3.10(c) and Figure 3.10(d).

Figure 3.10 Test Material Images (a) Construction Waste Particles, (b) Construction Waste Weighed and Sealed Plastic Bags, (c), and (d) Storage of Sieved Construction Waste Plastic Bags

3.4 EXPERIMENTAL WORK

The study has employed the techniques of both mechanical stabilisation, through the induction of the recycled construction waste and chemical stabilisation, by introducing GGBFS; in controlled proportions. The experimental programme was divided in five stages. The flowchart of the research work as presented in Figure 3.11, illustrates the outline of the soil treatment process. The stages were classified based upon the nature of the work conducted and encompassed procurement or collection of the test materials; namely bentonite and the two additives, construction waste and ground granulated blast furnace slag (GGBFS) in the first stage followed

by screening of construction waste and characterisation of bentonite and GGBFS in the second stage.

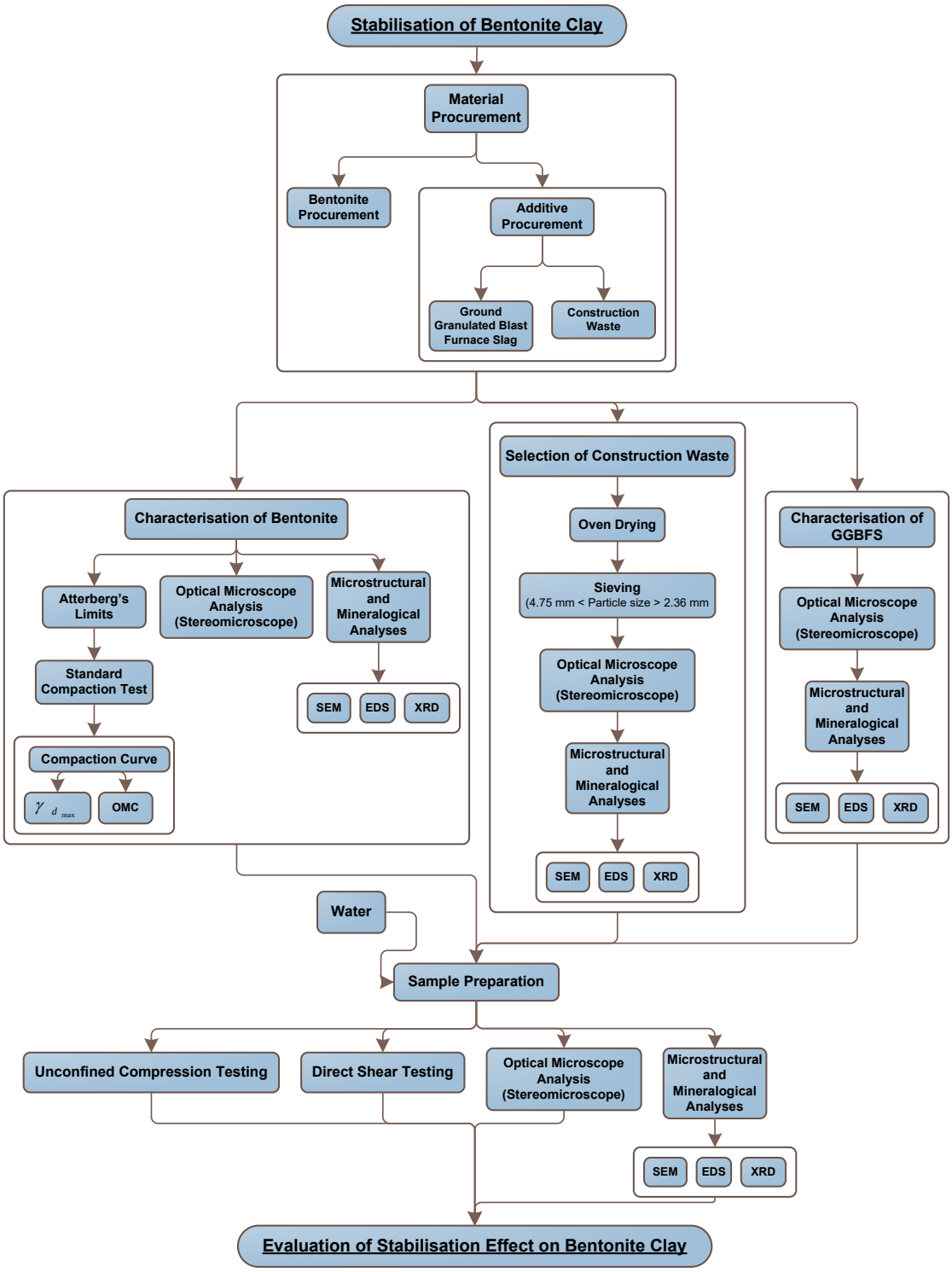

Figure 3.11 Flowchart of Research

The material screening and characterisation was then succeeded by preparation of material by adding water in controlled proportions and series of geotechnical, imaging, mineralogical and microstructural tests were then performed to evaluate the effect of both stabilisers on the compressive and shear strength as well as microstructure, elemental distribution and mineralogical composition of bentonite clay. GGBFS hydration is a primarily time-dependent process and may behave differently under different curing periods depending upon its proportion in the bentonite-stabiliser system. Construction waste grains have a comparatively different size than bentonite and GGBFS and may change the gradation of the mixture in increasing number of volumes. Therefore, both parameters of stabiliser percentages and curing time were investigated.

3.4.1 Atterberg's Limits

The degree of expansion of an expansive soil is interpreted through the Atterberg's limits or plastic and liquid limits. The Bureau of Indian Standards 1498 (Indian Standard IS:2720-40 1977) has also specified plastic limit as another criteria for soil classification. The soils are classified as soils with low degree of expansion (PL < 12), medium (12 < PL < 23), high (23 < PL < 32) and very high (PL > 32). These criteria have been assessed by Sridharan and Prakash (2000). They reported that the LL and PL cannot provide authentic estimations of the swelling potential of the soil as these criteria do not acknowledge the type and composition of the clay. The oedometer test was recommended as a better classifier of the expansive soils to determine the free swell index of the soil based upon their degree of expansion.

Cone penetrometer apparatus was employed to determine the liquid limit (LL) of the used bentonite based on the Standards Australia AS 1289.3.9.1 (2002) as illustrated in Figure 3.12. This method is normally used for determining the liquid limit of fine soil (< 425μm). Using this method, bentonite clay was placed in a container and increasing amount of water was added. The sample was thoroughly mixed with a palette knife to achieve homogeneity in the mixture, as displayed in Figure 3.12(b). The soil paste was then cured for 12 hours and placed inside a metallic cup. The surface of the bentonite clay mixture in cup was levelled and smoothened with a palette knife and placed under the cone as shown in Figure 3.12(a). The cone was

lowered so that the tip was just in contact with the surface of bentonite in the metal cup and then clamped. It was then followed by releasing of clamps so that the cone freely penetrated the clay sample, as can be seen from Figure 3.12(c).

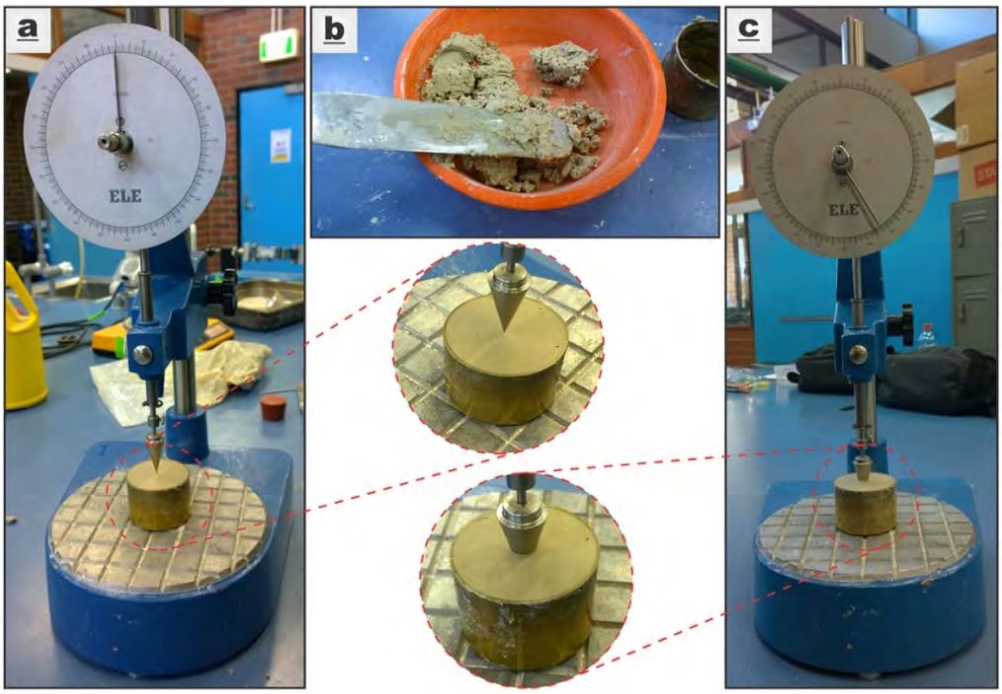

Figure 3.12 Cone Liquid Limit of Bentonite (a) Setup of Bentonite Specimen Cup in Cone Penetrometer, (b) Preparation of Bentonite Specimen, and (c) Cone Penetration in Bentonite Specimen

The plastic limit (PL) was then calculated based on Standards Australia AS: 1289.3.2.1 (2009) by adding water and rolling into threads of decreasing thicknesses as illustrated in Figure 3.13. Initially, small amount of bentonite was moulded between the palms and fingers into the shape of a small ball. The ball was then further rolled to ensure sufficient drying of bentonite by continuing rolling, as shown in Figure 3.13(a), until cracks were observed on the surface of the rolled-out bentonite thread, as can be seen from Figure 3.13(b). This was followed by rolling it out on a flat glass plate. The principle of the standard plastic limit calculation method is that the bentonite clay thread should theoretically continue to retain its shape if it has a plastic nature and water was added when the bentonite clay thread crumbled before reaching the 3mm diameter mark. Figure 3.13(c) shows the

comparison of bentonite thread thickness against the metal rod used for assessing if the thread has reached the 3mm mark. Plastic limit was recorded when the bentonite tread crumbled at the standard specified diameter of 3mm. Figure 3.13(d) illustrates the rolled-out thread samples that were then placed in a metal container and placed in oven for determination of the moisture content (MC). The plasticity index of the bentonite was then calculated in association with the Standards Australia AS: 1289.3.3.1 (2009) specifications as,

$$PI = LL - PL \qquad \text{Equation (3.1)}$$

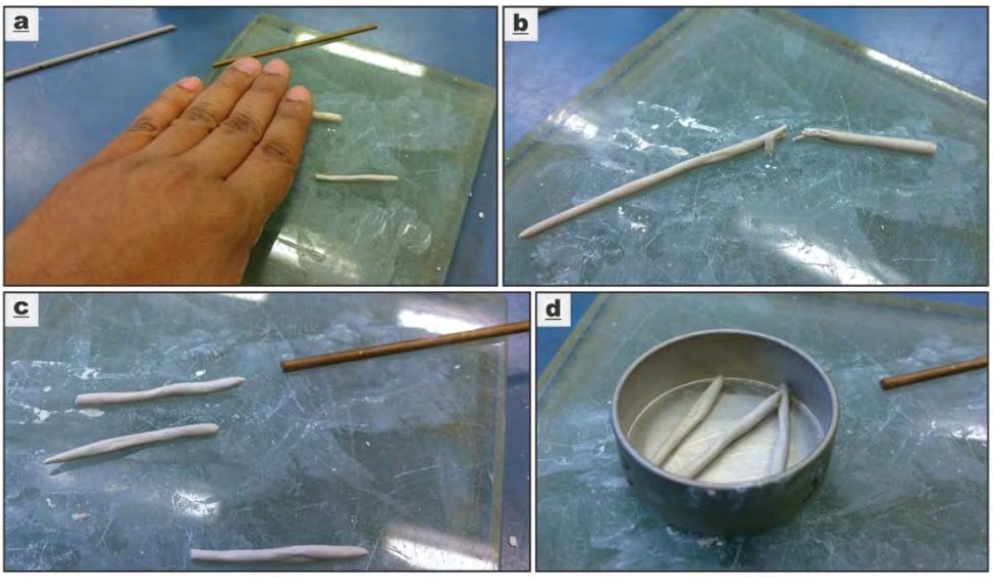

Figure 3.13 Plastic Limit Test of Bentonite Clay (a) Rolling of Clay in Threads, (b) Crumbling of Thread, (c) Comparison of Thread Thickness against 3mm Rod, and (d) Storage of Rolled-out Threads in Container for MC Determination

3.4.2 Particle Size Distribution

The construction and demolition waste selected for this study contained a wide range of particles. After the first stage of material procurement, the next phase was the characterisation of the procured bentonite and GGBFS. The construction waste was sieved to select the particles that passed through sieve with aperture of 4.75mm but retained on sieve aperture of 2.36mm. As more than 1 tonne of material was initially procured, representative samples were drawn from the whole mass for the purpose of laboratory experiments. Figure 3.14(a) shows the wet samples in metal trays that were used to place the construction in the oven for drying. Oven temperature of 105

± 2ºC was used, as shown in Figure 3.14(b). Therefore, as illustrated in Figure 3.14(d), the samples were initially oven-dried before being sorted for the purpose of sieve analysis. The particle size distribution curve of the construction waste particles was plotted after conducting sieve analysis based upon the specifications of Standards Australia AS 1289.3.6.1 (2003) using automated sieving device as shown in Figure 3.14(c).

Figure 3.14 Drying and Sieving of CW (a) Trays of Wet Samples, (b) Drying Oven, (c) Sample Placement in Oven, and (d) Automatic Sieving of CW

3.4.3 Standard Compaction Test

Bentonite was subjected to the standard compaction effort of 596kJ/m^3 as per the Standards Australia AS 1289.5.1.1 (2003) to determine the optimum moisture content (OMC) and the corresponding maximum dry density ($\gamma_{d_{max}}$). This standard was used as it is applicable to soils passing sieve 37.5mm and clays. The bentonite clay sample was initially dried in the oven under 105^{o}C for 24 hours to remove any pre-existing moisture. Later the dried sample was compacted in the standard cylindrical mould of 10cm diameter and 20cm height in three layers by addition of specific water content and compacting with the same number of blows through the standard rammer (Figure 3.15).

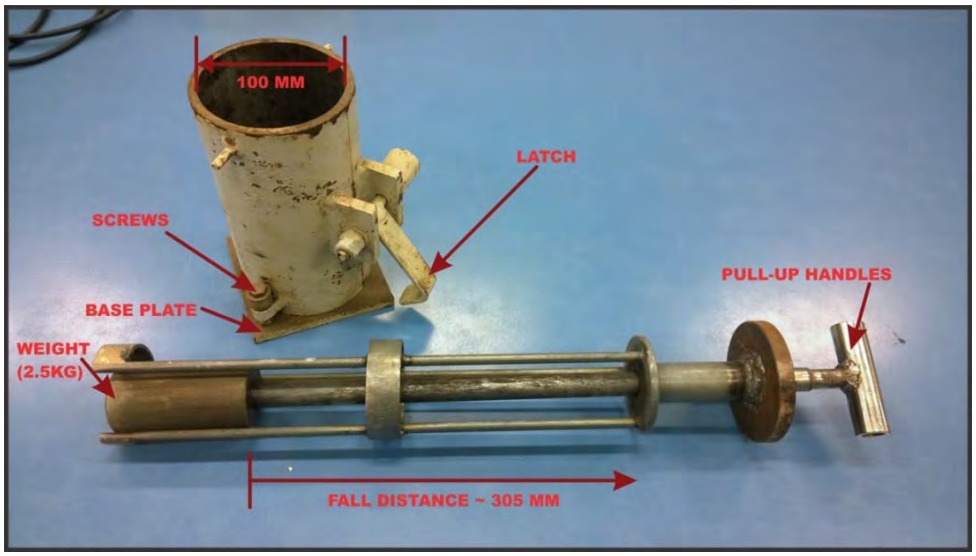

Figure 3.15 Standard Compaction Mould and Rammer

Compaction was performed using different moisture contents as a range of moisture contents produce different dry densities, in general producing the data required for plotting the moisture content – dry density curve. In order to achieve this, representative volume of bentonite clay was drawn from the oven-dried mass and mixed with certain volume of water. It was then compacted in the mould, as stated earlier. The surfaces were trimmed and levelled to obtain as flat surface as possible (Figure 3.16(a)) and the samples were then extruded using a hydraulic jack (Figure 3.16(b)). As the standard compaction mould contains a latch for easy extraction of the sample, the control of jack is gradually pressed by foot to extrude the sample out

of the mould without causing any disturbances to the compacted sample and maintain its form and shape as shown in Figure 3.16(c). The mass of the mould, base-plate and extruded sample was recorded. The sample was then dried in oven as per the standard to achieve complete drying of the compacted bentonite specimen. The process was repeated several times with increasing volume of water in the mixture, calculated against the dry unit weigh of pure bentonite clay, for each iteration and the optimum moisture content was then calculated based upon the oven-drying method to plot the moisture content – dry density curve. Similar technique was adapted for the purpose of preparing samples under different curing periods. Figure 3.16(d) illustrates an extracted specimen, which was then tightly wrapped in plastic, carefully tied by elastic bands to minimise moisture entrance and properly tagged, as displayed in Figure 3.16(e).

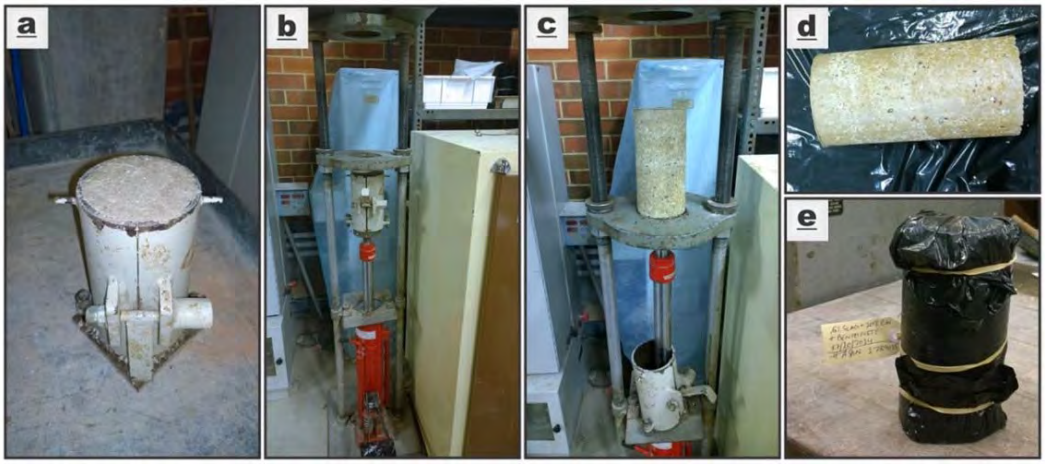

Figure 3.16 Standard Compaction (a) Levelled Specimen in Mould, (b) Extraction through Hydraulic Jack, (c) Extracted Specimen, (d) Wrapping of Specimen, and (e) Wrapped Specimen

3.4.4 Unconfined Compression Test

The laboratory tests involved the investigation of the effects of stabilisers, GGBFS and construction waste, on the engineering behaviour of stabilised bentonite clay, for example, the unconfined compressive strength (UCS). Different percentages of the two additives, GGBFS and CW were used to separately investigate the influence of each additive on the UCS over a number of different curing periods. The sample combinations and the identified curing period are listed in detail in Table 8.

Table 8 Test specimen matrix

Curing Periods (Days)	1	3	7	14	21	28
Sample ID		**Composition**				
Group 1	S1G1	100% Bentonite				
Group 2	S1G2	2% Slag + 10% CW + 88% Bentonite				
	S2G2	2% Slag + 15% CW + 83% Bentonite				
	S3G2	2% Slag + 20% CW + 78% Bentonite				
Group 3	S1G3	3% Slag + 10% CW + 87% Bentonite				
	S2G3	3% Slag + 15% CW + 82% Bentonite				
	S3G3	3% Slag + 20% CW + 77% Bentonite				
Group 4	S1G4	4% Slag + 10% CW + 86% Bentonite				
	S2G4	4% Slag + 15% CW + 81% Bentonite				
	S3G4	4% Slag + 20% CW + 76% Bentonite				
Group 5	S1G5	5% Slag + 10% CW + 85% Bentonite				
	S2G5	5% Slag + 15% CW + 80% Bentonite				
	S3G5	5% Slag + 20% CW + 75% Bentonite				

The optimum moisture content (OMC) by weight of the dry sample was used for all the samples to deduce comparative data for assessing the effects of the aforementioned two controlling factors. A manual mixing technique was adapted to mix the additives into the soil mass. The mixtures were then prepared in a large tray by constantly spraying water at amounts calculated for the OMC through a spray bottle and mixing with the help of spatula till a homogeneous appearance was attained, as illustrated in Figure 3.18 (a). Then the stabilised clay mixes were compacted in standard cylindrical steel moulds to produce specimens with dimensions of $10cm \times 20cm$ under the standard compaction effort following Standards Australia AS 5101.4 (2008) as Figure 3.18 (b) and Figure 3.18 (c) illustrate. The extracted samples were then wrapped with thick plastic sheets, labelled accordingly to indicate the mixing ratios for the proportions of base material, i.e., bentonite and the two additives as well as the intended sample curing period and then placed in a storage room for the respective curing periods to limit the effects of any external factors on the samples (see Figure 3.17).

Figure 3.17 Storage of Compacted and Plastic-wrapped Labelled Samples

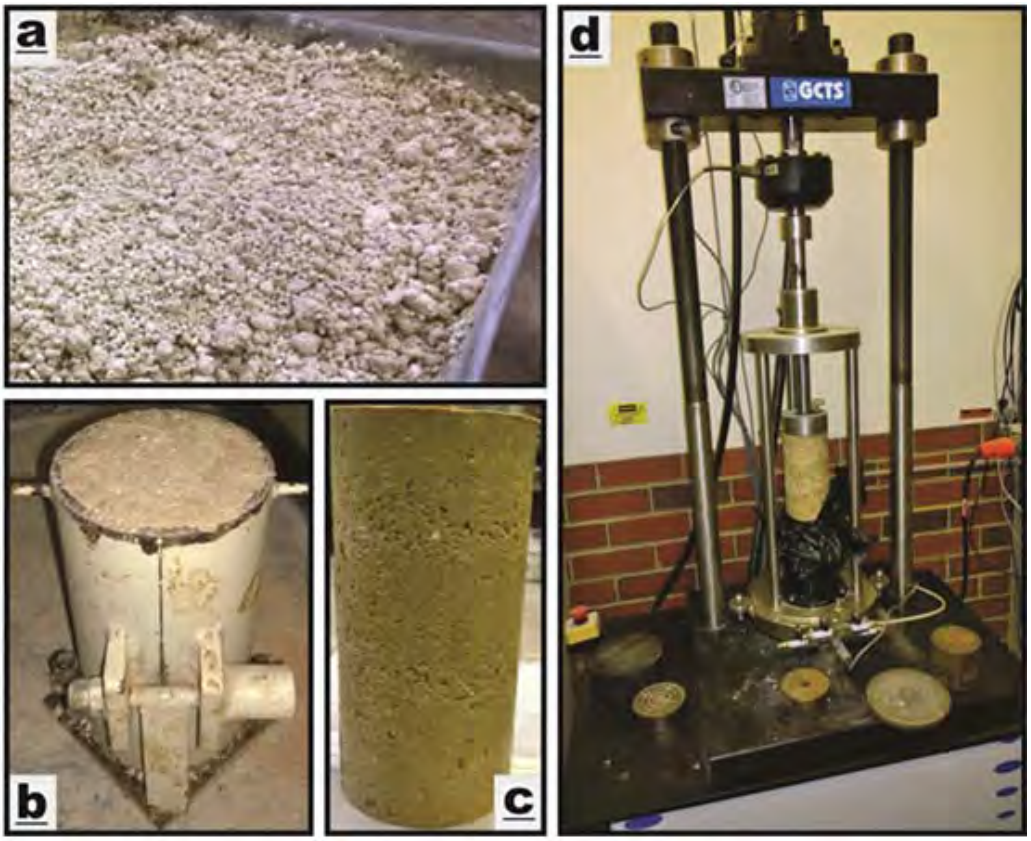

Figure 3.18 UCS testing (a) prepared stabilised mixture, (b) specimen compaction, (c) stabilised specimen, and (d) STX-300 UCS test device

The UCS tests were performed as per the Standards Australia AS 5101.4 (2008) specifications. The device used for this purpose is the GCTS Stress-Path Soil Triaxial System (STX-300) as shown in Figure 3.18 (d). It has dedicated software in the attached computer interface, enabling control of the test parameters and results generation. An axial load was applied at the constant rate of 1.0 ± 0.1mm/min and the testing was stopped once the deformation had been recorded.

Figure 3.19 illustrates the unconfined compression of a typical test sample. Once the load was applied, the sample underwent deformation. A reduction in the length of the specimen was observed, whereas the cross-sectional area increased from 'A' to 'A/' under the influence of the applied compressive loading and the length changes from 'L' to 'L_o' after the ΔL change. The compressive strength of the sample is associated with two parameters; the applied normal or axial compressive loading, 'P', and the surface area of the sample where the load is being applied, which is dependent upon the diameter of the sample. The strain "ε" is given as

$$\varepsilon = \frac{\Delta L}{L} \times 100 \qquad \text{Equation (3.2)}$$

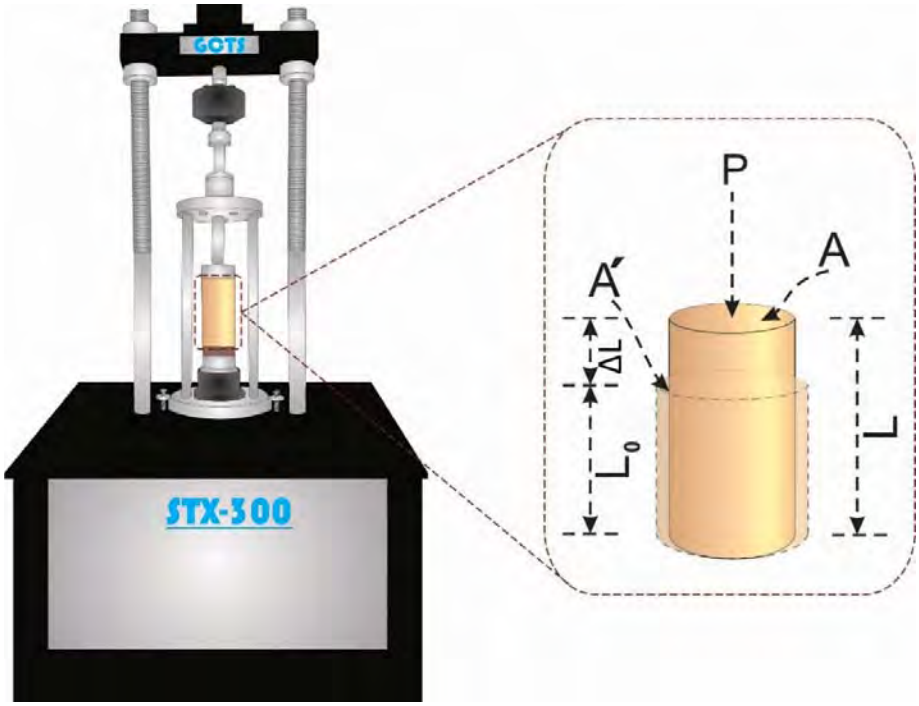

Figure 3.19 Unconfined compression testing of soil specimen

The deformation was mainly observed through the formation of deformation bands in tested specimen after being subjected to axial compressive load as the sample tried to maintain the initial cylindrical shape as it underwent deformation. Such behaviour resulted in the formation of roughly "X-shaped" deformation bands and bulge on the outer shell of the specimen. The formation of the deformation bands started even before the complete failure of the samples. Initially, only minor fractures were observed on the sample surface. The cracks started to widen and nominal bulge

could be witnessed on the outer shell of the specimen until the complete failure occurred in the form of chunks detaching from the specimen. Figure 3.20(b) shows the development of localised shear bands and bulge around the middle of a partially deformed/failed test soil specimen. This phenomenon is a common failure mechanism of ductile materials during unconfined compression.

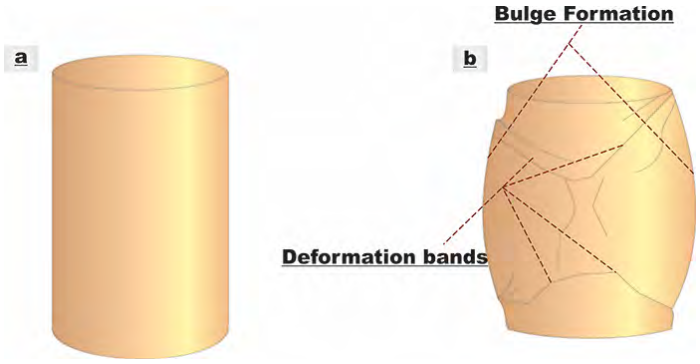

Figure 3.20 Formation of Deformation Bands (a) Undeformed Typical Soil Sample (b) Partially Deformed Typical Soil Sample

3.4.5 Direct Shear Test

Shear strength of bentonite – stabiliser composites were investigated using direct shear technique as specified by Standards Australia AS 1289.6.2.2 (1998). Direct shear tests were conducted using Geocomp ShearTrac-II automated direct shear device. The device uses a horizontal and a vertical displacement transducer to assist in control of the horizontal and vertical loading system. Dedicated software is provided in the computer interface attached to the sensors and controls the micro-stepper motoring system for maintaining control of the constant displacement rate.

In order to maintain consistency of the mixture containing same proportion of construction waste and slag, both additives were mixed with bentonite in a large tray and water was carefully added in controlled proportions and the mixture was thoroughly mixed using manual mixing technique to produce and uniform granular texture, as illustrated in Figure 3.21(a). After assembling the shear box shown in Figure 3.21(b) and Figure 3.21(c), samples were placed inside the shear box and saturated with water (Figure 3.21(f)). The shear box employed for the study has an

internal size of 63.5mm × 63.5mm × 24mm. Normal stress was then applied on each sample to consolidate the samples for a 24 hours period.

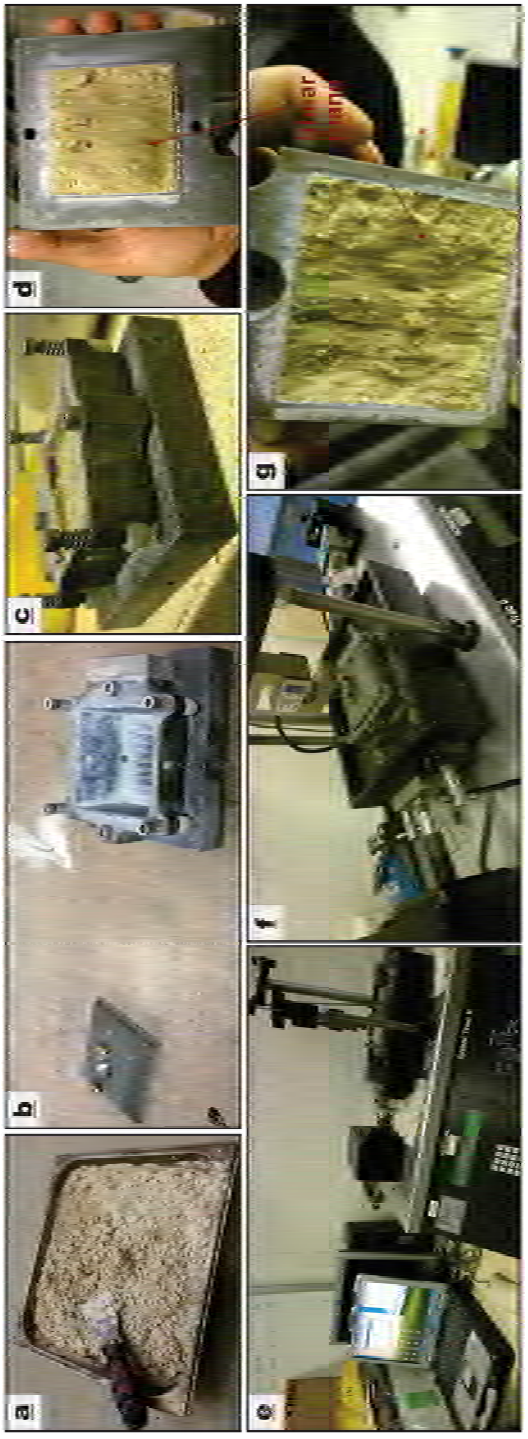

Figure 3.21 (a) Stabilised Mixture, (b) Shear Box, (c) Compacted Specimen, (d), (g) Failed Specimen, (e) DST Device, (f) Water-submerged Specimen

Five groups of samples, each with different additive percentages as specified in Table 9 were cured for 1, 3, 7, 14, 21 and 28 days of curing period, saturated and consolidated under the normal stress. Three levels of normal stresses; i.e. 50kPa, 100kPa and 200kPa; were used for testing each composition and curing day combination. The failure of sample was marked by shearing or splitting of the sample along the shearing plane, as highlighted in Figure 3.21(d) and Figure 3.21(g). Initially, the shear strength of pure bentonite was explored under increasing curing periods to obtain the benchmark results to assess the effect of both controlling parameters.

Table 9 Soil-Stabiliser Composite Proportion Scheme

Curing Periods (Days)	1	3	7	14	21	28
Sample ID		**Composition**				
Group 1	S1G1	100% Bentonite				
Group 2	S1G2	2% Slag + 10% CW + 88% Bentonite				
	S2G2	2% Slag + 15% CW + 83% Bentonite				
	S3G2	2% Slag + 20% CW + 78% Bentonite				
Group 3	S1G3	3% Slag + 10% CW + 87% Bentonite				
	S2G3	3% Slag + 15% CW + 82% Bentonite				
	S3G3	3% Slag + 20% CW + 77% Bentonite				
Group 4	S1G4	4% Slag + 10% CW + 86% Bentonite				
	S2G4	4% Slag + 15% CW + 81% Bentonite				
	S3G4	4% Slag + 20% CW + 76% Bentonite				
Group 5	S1G5	5% Slag + 10% CW + 85% Bentonite				
	S2G5	5% Slag + 15% CW + 80% Bentonite				
	S3G5	5% Slag + 20% CW + 75% Bentonite				

The shear strength of soil was evaluated in terms of the shear strength parameters, soil cohesion (c), angle of internal friction (ϕ), horizontal displacement (d_h), vertical deflection (d_v), shear stress (τ) and normal stress (σ_n). Generally, failure of any engineering material is imparted by critical arrangement of both shear and normal stresses and not the individual stress (Mohr 1900). The actual approximated linear

shear – normal function as proposed by Coulomb is represented by the following equation. The overall relationship is famously known as Mohr – Coulomb failure criterion. If the cohesion of soil is represented by "c", normal stress along failure plane is "σ", internal friction angle is "ϕ" and the shear strength is "τ_f", the Mohr – Coulomb failure criterion for saturated soil is:

$$\tau_f = c + \sigma \tan \phi \qquad \text{Equation (3.3)}$$

Therefore, there two parameters namely cohesion, c and ϕ depend upon the normal stress configuration and was then used to plot the Mohr – Coulomb failure envelopes by plotting shear stress versus normal stress results.

3.4.6 Optical Microscopic Analysis

The optical microscopic analysis was also performed through a stereomicroscope, a Nikon SMZ800 (Figure 3.22) furnished with the computer display and image processing software called Image Pro Plus. The sieved construction waste was also oven dried and stored in sealed moisture controlled conditions. Optical microscopic analysis was performed to identify the physical attributes of the various particles in the selected construction and demolition debris. The physical characteristics of the GGBFS such as texture, colour and appearance, were also analysed through the stereomicroscope analysis.

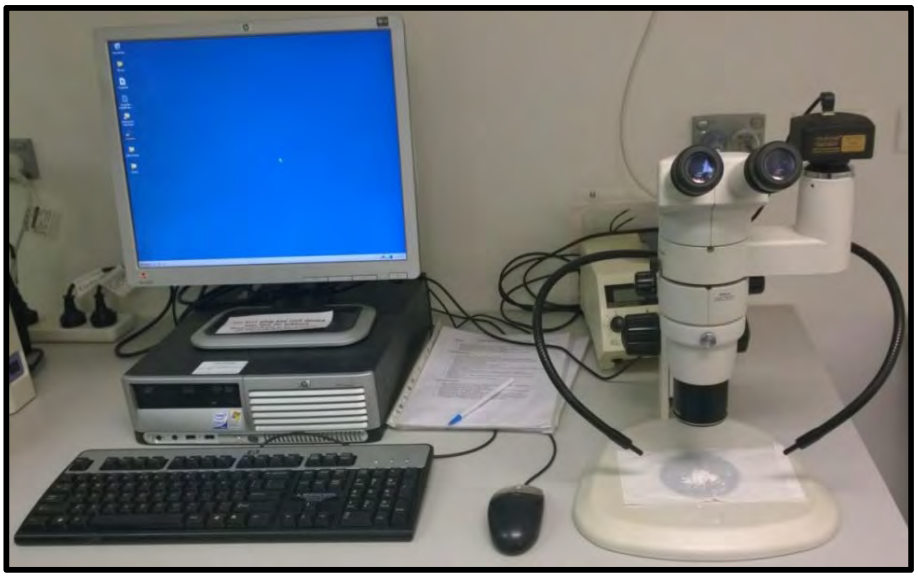

Figure 3.22 Optical Microscopy/Stereomicroscopy Device

3.4.7 Micro Analysis

Microanalysis was performed to identify any changes in the elemental composition and physical appearance of the bentonite after the action of the stabilisers. Optical microscopy photographs, X-ray diffraction (XRD) graphs and scanning electron microscope (SEM) images were developed for the pure bentonite, GGBFS and construction waste. The analyses were also performed for the hydrated bentonite, slag and construction waste mixes to perform comparison between the test results.

3.4.7.1 Scanning Electron Microscope (SEM) Analysis

Unpolished samples were coated with the standard carbon coating, thickness of 8.0nm and 2.25g/cm^3. The samples were placed on specifically designed aluminium stubs with surface area of 12.7mm and pin size of 6mm. The stubs were then mounted in a plastic container, as exhibited in Figure 3.23(b) and then stored in vacuum to maintain moisture control and prevent environmental contaminations as displayed in Figure 3.23(a).

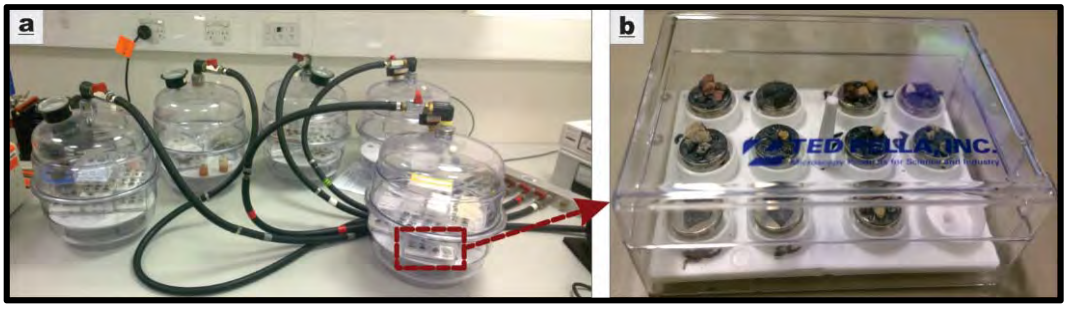

Figure 3.23 (a) Vacuum Transducers for SEM Storage, (b) SEM Stubs and Mounting Box

The elemental distribution, morphology and arrangement at the microscale were analysed through Zeiss Evo 40XVP SEM analysis device, as illustrated in Figure 3.24. It is also capable of performing energy dispersive spectrometer (EDS) analysis among other functions. It is provided with a dedicated computer and Oxford X-ray system controlled through the software INCA. An electron beam with acceleration voltage of 20kV and 100µA beam current was used with a 450nm spot size and 8.5mm working distance.

Figure 3.24 Zeiss Evo 40XVP SEM Analysis Device and Computing Setup

3.4.7.2 Energy Dispersive X-ray Spectroscopy (EDS) Analysis

Zeiss Evo 40XVP SEM analysis equipment, picture above in Figure 3.24, was also employed for the analysis of the particle elemental distribution. The device is assisted by Oxford x-ray system that is controlled through INCA data acquisition and analysis software on the attached computer and utilises an electron beam for collection of micrographs. It was operated at beam current of 100μA and 20kV as acceleration voltage at working distance of 8.5mm with 450nm as the spot size. The EDS spectra and SEM monographs were obtained at different points of interests on the test samples to obtain the elemental and chemical distribution and the arrangement and structure of the different compounds within the sample matrixes.

3.4.7.3 X-ray Diffraction (XRD) Analysis

Further reliable data on the elemental composition and the mineralogy of the stabilised and unstabilised samples was collected through XRD quantitative analysis. X-ray diffraction quantitative analyses were performed to determine the mineralogical characteristics of the test specimens using a Bruker-AXS D8 Advance Powder Diffractometer with Cu-Ka X-ray radiation beam (λ = 0.15404nm, voltage =

40kV, current = 40mA). 0.02°/s was set as the scanning rate whereas the 2-theta data was collected in the 7.5°- 90° area (Figure 3.25).

Figure 3.25 Bruker-AXS D8 Advance Powder Diffractometer

CHAPTER 4
RESULTS AND DISCUSSION

4.1 INTRODUCTION

The principal objective of this study was to identify the effect of stabilisation process on the geotechnical behaviour and physical and chemical characteristics of bentonite clay stabilised with different percentages of construction waste and ground granulated blast furnace slag under different curing conditions and subjected to various geotechnical, imaging and spectroscopic tests. This study employed both chemical and mechanical soil stabilisation methods. Chemical additive stabilisation was performed by adding controlled volumes of GGBFS, whereas mechanical stabilisation was performed through adding CW. Several elemental and geotechnical characterisation tests were performed to study the morphology, microstructure, and direct shear strengths of the stabilised and unstabilised samples. The summary of each test and its results have been separately provided in the following sections.

After the initial characterisation of bentonite through the determination of Atterberg's limits and calculation of maximum dry density and optimum moisture content using standard compaction test, series of geotechnical, microstructural and imaging tests were conducted. Initially, the physical characteristics such as appearances, colour and textures of the test materials; namely bentonite clay, GGBFS and construction waste was studied through optical microscopy or stereomicroscopy. Moreover, microanalyses were also separately performed on the stabilised and unstabilised specimens. The materials were analysed through SEM, EDS and XRD analysis techniques before proceeding with the geotechnical tests exploring the strength parameters of the test samples.

The two primary parameters evaluated for exploring the effect of stabilisers upon bentonite clay were the compressive and shear strengths of the stabilised and unstabilised specimens under different curing periods. This chapter presents the results of the experimental works on the bentonite and bentonite-stabiliser composite

specimens. Analyses and discussion on the results have also been provided. The flowchart in Figure 4.1 further illustrates the organisation of chapter 4.

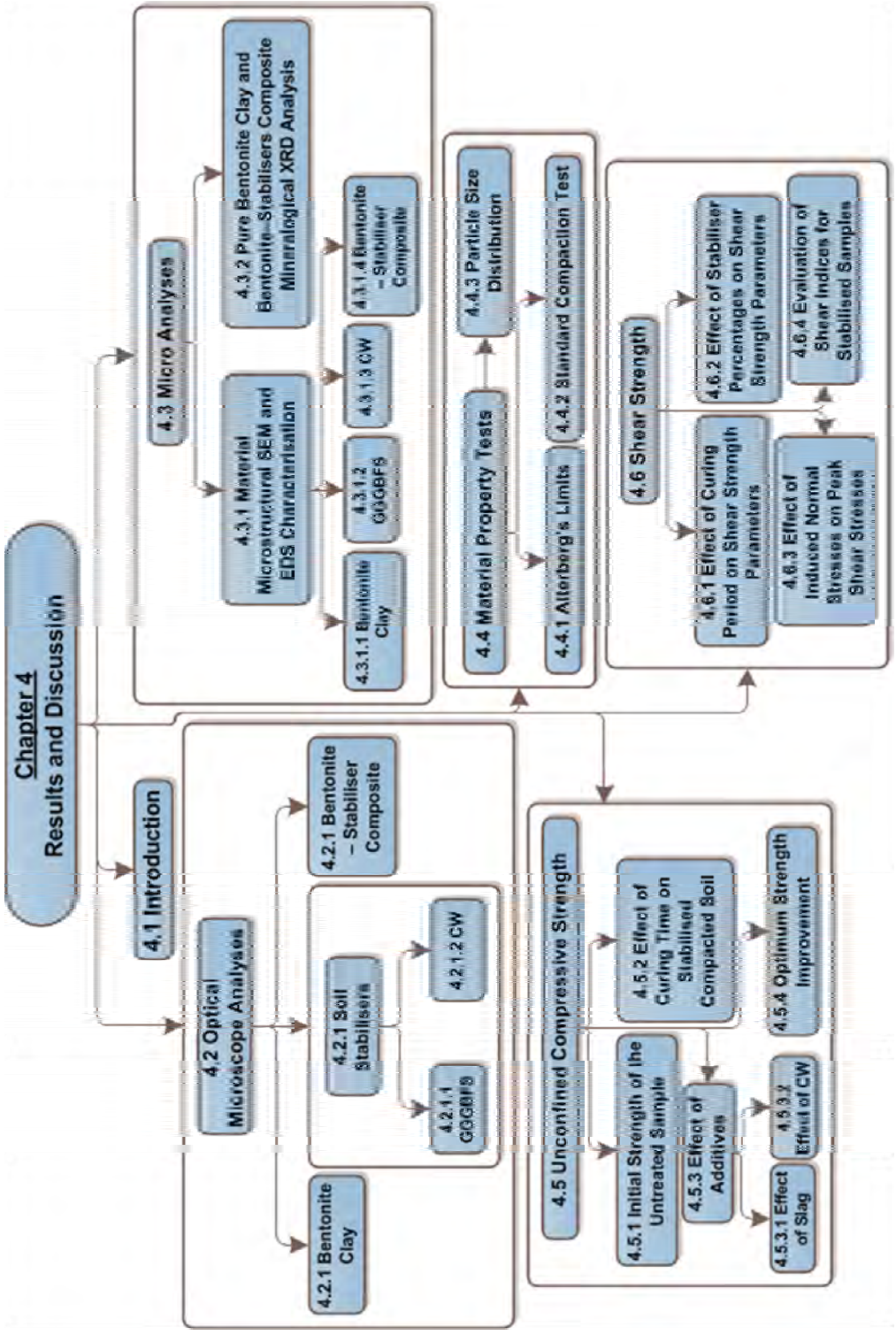

Figure 4.1 Outline of Chapter 4

This chapter has been divided into five primary sections, specifically aimed at covering the experimental works conducted for studying the physical characteristics, strength parameters and elemental distribution of the stabilised and unstabilised specimens. The first section outlines optical microscopic analyses performed on the test materials, illustrating the physical appearance, colour and texture of bentonite and the two stabilisers as well as bentonite-stabiliser composite mixture. This is followed by micro analyses; SEM, EDS and XRD tests on the contributing materials and composite mixtures to highlight the effect of stabiliser and curing on the sample morphology, microstructure and elemental composition in the second section. This section is further subdivided into two subsections; first subsection illustrates the SEM micrographs of pure bentonite clay, construction waste and GGBFS and discusses the microstructure and elemental distribution of these materials. In addition, the SEM micrographs of bentonite-stabiliser composite are also presented along with EDS spectra and quantitative analysis results to identify the effect of stabilisers on the microstructure and elemental distribution of bentonite clay. The second subsection highlights the results of X-ray diffraction spectroscopic analysis for pure bentonite clay and bentonite with additives.

The third section presents the results and discussion of geotechnical experiments conducted to establish the material properties. Two types of property tests were conducted on pure bentonite clay; namely Atterberg's limits tests to identify the plastic and liquid limit of bentonite clay, and standard compaction test to calculate the maximum dry density and optimum moisture content for pure bentonite clay. The particle sizes of construction waste hugely varied and therefore, particle size distribution test was performed on the procured construction test before limiting the particle sizes to certain sizes (passing sieve 4.75mm and retained on sieve 2.36mm) to be used for the purpose of bentonite stabilisation.

Fourth section covers the series of unconfined compression testing conducted on pure bentonite and bentonite-stabiliser composite specimens cured for different curing periods; 1, 3, 7, 14, 21 and 28; containing different proportions of additives; 2%, 3%, 4% and 5% of GGBFS; and 10%, 15% and 20% of CW. The section is subdivided into four subsections based upon the evaluated parameters. The first subsection presents the initial strength of the untreated samples before the addition of

stabilisers. The second subsection discusses effect of curing time on stabilised samples followed by effect of the two additives and the optimum strength improvement discusses in terms of a dimensionless shear development parameters, introduced as part of this study. Direct shear strength (DSS) tests were also conducted based upon the same controlling parameters of additive percentages and sample curing times and discussion of the results of DSS tests have been presented in the last section.

4.2 Optical Microscope Analyses

The physical attributes of bentonite clay, CW and GGBFS were explored through a series of stereomicroscopic or optical microscopic analyses to identify the appearance, colour and texture of these materials. In addition, the effect of stabiliser and water addition for preparation of composite specimens was also studied.

4.2.1 Bentonite Clay

The bentonite used was of off-white colour and fine powdered composition as can be seen from the stereomicroscopic images of the bentonite used as provided in Figure 4.2. Bentonite is a reactive clay with montmorillonite as the central mineral and traces of accessorial minerals such as calcites, different classes of feldspar, iron oxides, quartz and other clay minerals (Karnland 2010). The physical and chemical characteristics of bentonite clay play a significant role in its mechanical behaviour and have been summarised in Table 10.

Table 10 Properties of Bentonite Clay

Properties	Value
Chemical name	Hydrated aluminium silicate
Molecular formula	$Al_2O_3.4SiO_2H_2O$
Physical appearance	Eggshell white granules
Specific gravity	3.3
pH	7 – 9
Odour	None
Flammability	Inflammable

Density	593 kg/m^3
Surface Area	0.09 – 1.8 m^2/cc

Figure 4.2 Stereomicroscope image of bentonite

4.2.2 Soil Stabilisers

Granulated blast furnace slag and construction and demolition waste were used as the stabilising agents in this study. The results of optical microscopic analyses on both stabilisers have been presented in the following two subsections.

4.2.2.1 Ground Granulated Blast Furnace Slag (GGBFS)

The nature of the contributing materials i.e. fluxes, carbon and the originating iron ore, dictate the appearance, colour and chemical composition of the resulting GGBFS. It generally has a glassy, fine and crystal-like texture as can be seen from the stereomicroscope photos provided in Figure 4.3. The surface area of GGBFS is typically greater than 350kg/m^2 (Siddique and Khan 2011).

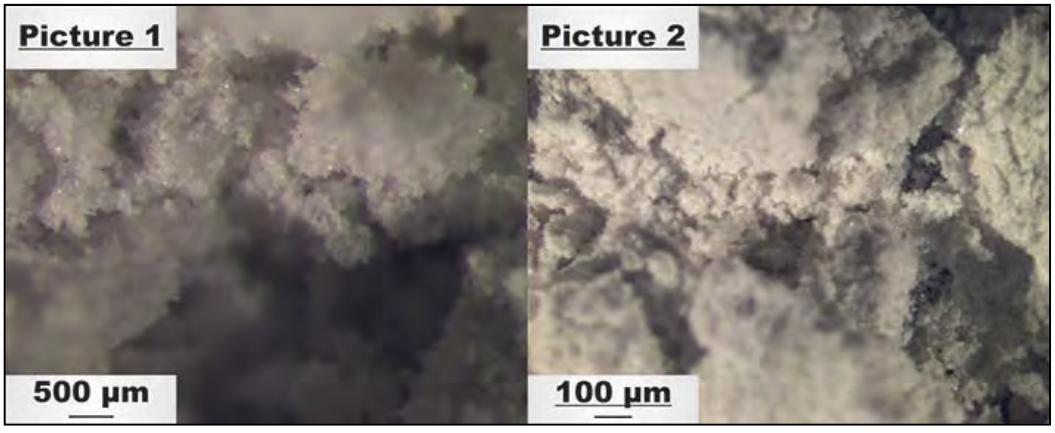

Figure 4.3 Stereomicroscope images of GGBFS

4.2.2.2 Construction Waste (CW)

The construction and demolition waste (CW) employed in this study was collected from a commercial recycling organisation and had originated from variety of construction projects including rubble, crushed masonry and concrete from residential and infrastructural projects. The texture, appearance and colour of CW grains largely varied due to the variation in the source and might have also caused variation in the elemental distribution of the CW particles. The composition and texture of the construction waste varied widely due to the variations is the source materials as shown in Figure 4.4.

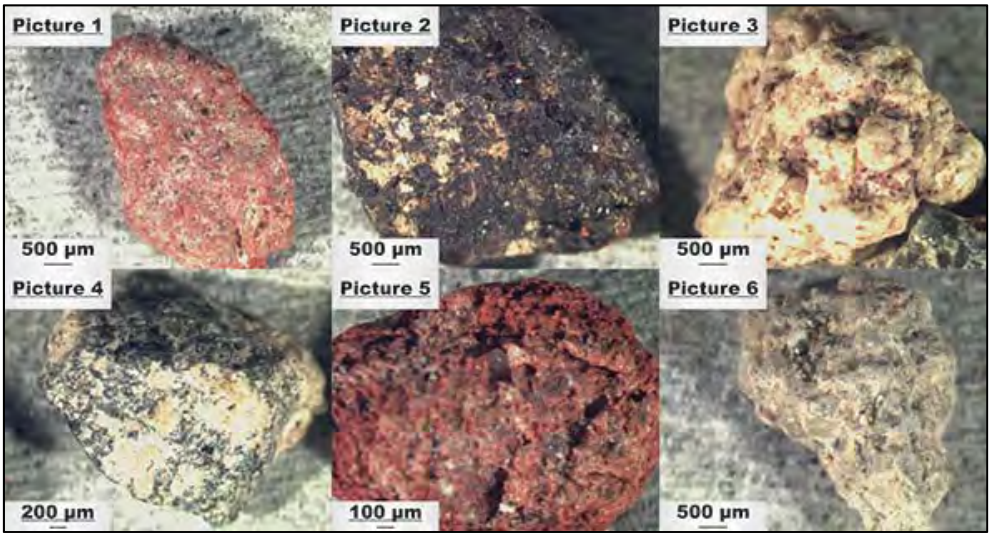

Figure 4.4 Stereomicroscope image of Construction Waste

4.2.3 Bentonite – Stabiliser Composite

The results of the optical microscopic analysis on the bentonite stabilised with slag and construction waste are presented in Figure 4.5. It shows that during the mixing, the bentonite and slag particles clung to the construction waste grains. This phenomenon was also observed during the manual mixing as the mixture attained a granular appearance. Moreover, it was also observed during sample preparation that a construction waste particle was found at the crux of every grain formed. It was also noted that the percentage of slag in the mixture affected the adherence of the mixture to the construction waste particles. Figure 4.5 shows that with the inclusion of slag and construction waste within the bentonite-water matrix, the construction waste

grains were mostly surrounded by slag and bentonite particles, causing the formation of a stronger structural bond. Although, similar appearances were observed for all samples on visual inspection, sample S3G5 was used for the purpose of this test. Moreover, small cracks and fissures were also sometimes observed on the surface; however, in general the surfaces of the construction waste grains were mostly covered by cohesive bentonite and slag particles and were also found to cover the cracks found on the surfaces of the construction waste particles.

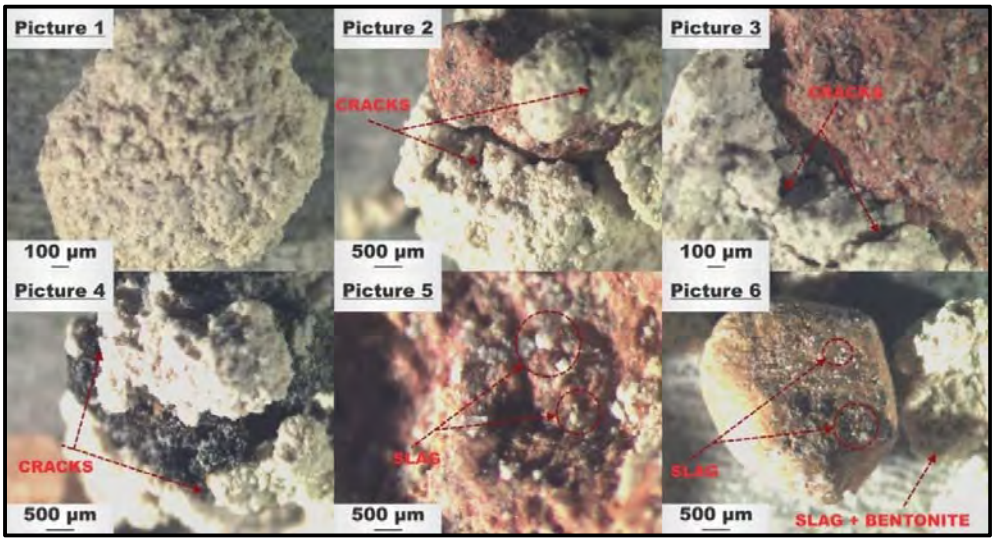

Figure 4.5 Stereomicroscopic images of stabilised soil mix S3G5

4.3 MICRO ANALYSES

Microanalysis was performed to identify any changes in the morphology, microstructure and elemental composition of bentonite after the induction of the stabilisers. X-ray diffraction (XRD) graphs, energy dispersive spectra (EDS) and scanning electron microscope (SEM) images were developed for the pure bentonite, GGBFS and construction waste. The analyses were also performed for bentonite, slag and construction waste mixes to perform comparison between the test results.

4.3.1 Material Microstructural SEM and EDS Characterisation

The SEM micrographs and EDS analytical elemental or chemical characterisation on the samples generated comparatively precise information on the elemental composition of each of the specimens.

4.3.1.1 Bentonite Clay

Bentonite clay primarily contains sodium or calcium as the natural exchange cation with a higher absorptive capacity. It has a chemical formula of $Al_2O_3.4SiO_2H_2O$ and chemically named as hydrated aluminium silicate. SEM and EDS microstructural and mineralogical characterisation analyses were performed to yield further data regarding the material composition and structure of pure bentonite clay. Figure 4.6 shows the SEM micromorphology of pure bentonite clay.

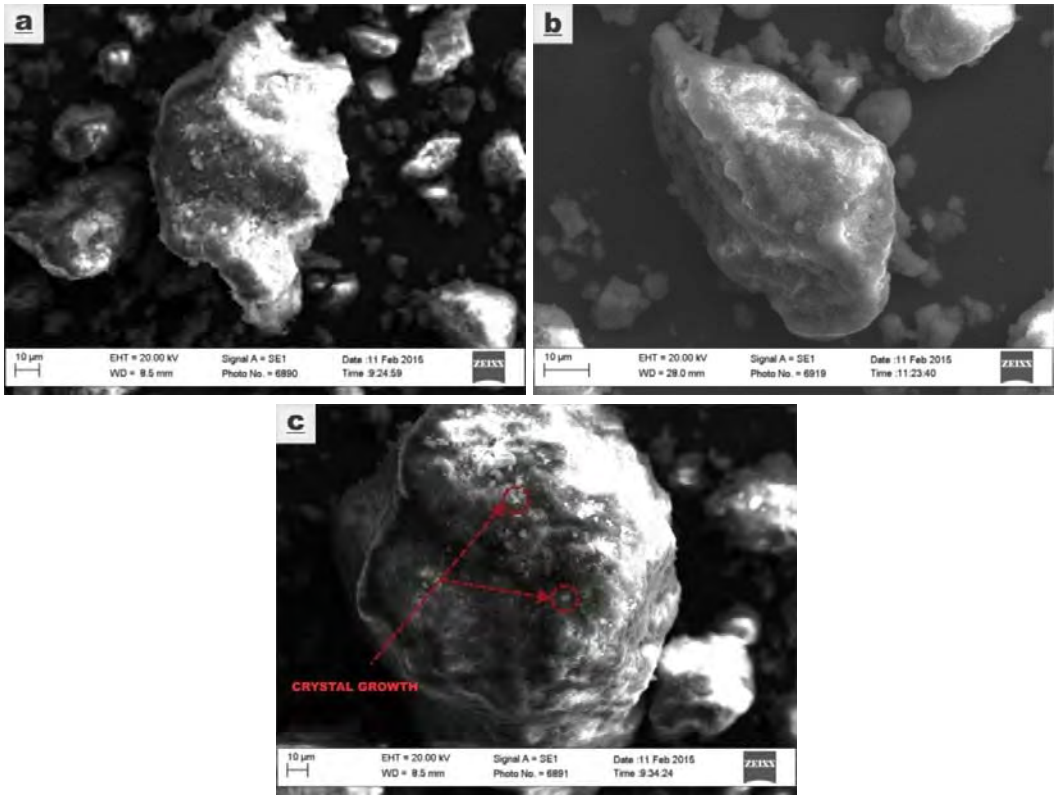

Figure 4.6 SEM Micrographs of Bentonite Clay at (a) Working Distance of 8.5mm, (b) Working Distance of 28.0mm, and (c) Crystal Growth on Bentonite Particles

The bentonite particles have amorphous crystallography as illustrated in Figure 4.6. In general, as can be observed from Figure 4.6(a) and Figure 4.6(b), the bentonite particle sizes approximately ranged between 10-30µm. Therefore, it can be stated that the particle crystallography appeared to be amorphous with significant deviations in the particle shapes and sizes. Furthermore, crystal growth was also

identified on the surfaces of some of the bentonite particles as has been highlighted in Figure 4.6(c).

In addition to obtaining a series of SEM micrographs for bentonite samples, several EDS spectral images and quantitative chemical composition data was calculated. Figure 4.7 presents two of the EDS spectra results of the bentonite particles.

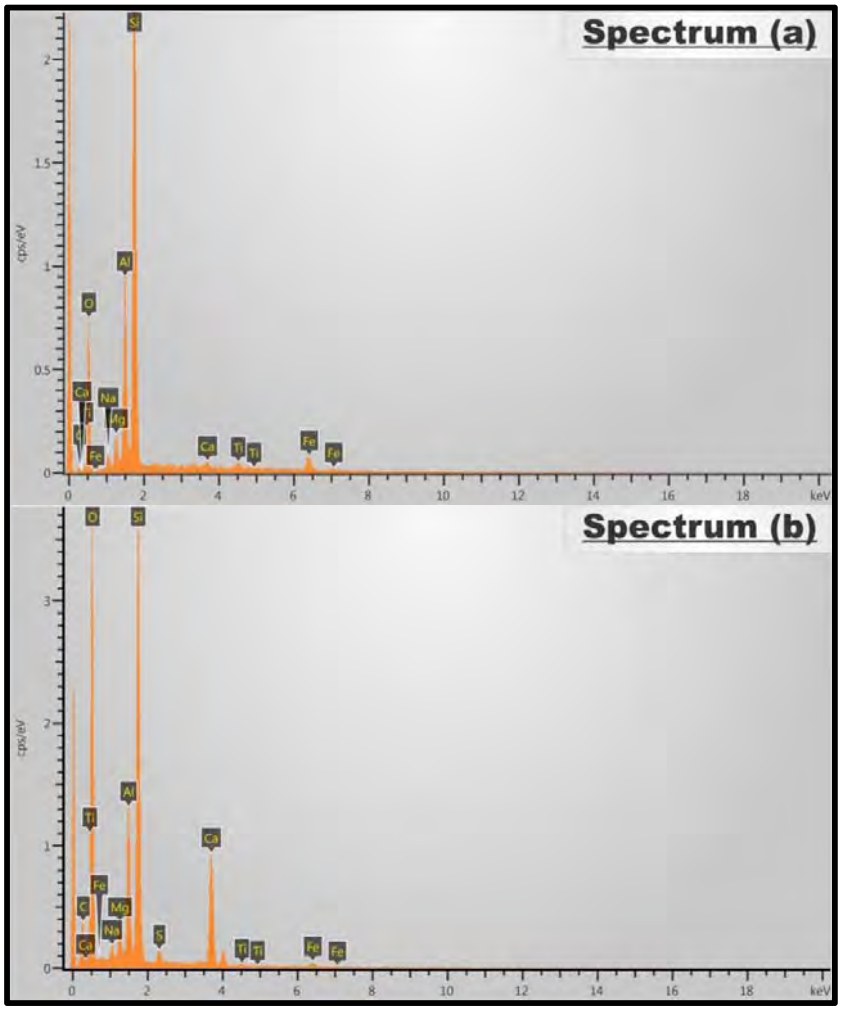

Figure 4.7 Bentonite clay EDS spectra for (a) Sample 1, and (b) Sample 2

The most dominant peak in the line spectrum is for silicon, followed by oxygen and aluminium. The results of the quantitative analysis of the bentonite particles are shown in Table 11. In case of sample 1, silicon and oxygen were observed to be the most dominant elements, followed by aluminium, sodium, titanium, magnesium, iron and calcium. The results indicate the presence of the montmorillonite-beidellite

series. Furthermore, similar results were obtained for quantitative analysis of sample 2 which showed that silica and metallic oxides were normally found in the sample as the other dominant elements were calcium, aluminium, magnesium, sodium, sulphur and iron followed by titanium. These results support the elemental distribution of montmorillonite-smectites (Hasan et al. 2015; Deer, Howie and Zussman 2013).

Table 11 Quantitative chemical composition of bentonite clay

Element	Weight%	Atomic%	k Ratio	Standard
Sample 1				
O	62.07	75.21	0.34248	SiO_2
Na	1.02	0.86	0.00604	Na_2O
Mg	1.7	1.35	0.01468	MgO
Al	6.35	4.56	0.0664	Al_2O_3
Si	19.71	13.61	0.23039	SiO_2
Ca	0.73	0.44	0.0089	CaO
Ti	7.51	3.63	0.11461	TiO_2
Fe	0.26	0.11	0.00367	Fe_2O_3
Total	100.00	100.00		
Sample 2				
O	55.91	70.25	0.34248	SiO_2
Na	1.12	0.98	0.00604	Na_2O
Mg	1.93	1.60	0.01458	MgO
Al	7.65	5.70	0.0664	Al_2O_3
Si	22.26	15.94	0.23039	SiO_2
S	0.78	0.49	0.0089	FeS_2
Ca	9.19	4.61	0.11461	CaO
Ti	0.32	0.13	0.00367	TiO_2
Fe	0.84	0.30	0.00936	Fe_2O_3
Totals	100.00	100.00		

4.3.1.2 Ground Granulated Blast Furnace Slag

As stated earlier, the chemistry of GGBFS is influenced by the chemical characteristics of the parent compounds including iron ores, cokes and carbon fluxes

etc. It is primarily composed of metallic oxides such as aluminium oxide (Al_2O_3), magnesium oxide (MgO), calcium oxide (CaO), iron oxides (Fe_2O_3 or FeO), manganese oxide (MnO) and silica (SiO_2) and sulphur (Proctor et al. 2000; Nidzam and Kinuthia 2010). Figure 4.8 illustrates the SEM micrographs of the GGBFS used in this study at scales of 20 µm, 10 µm and 1 µm.

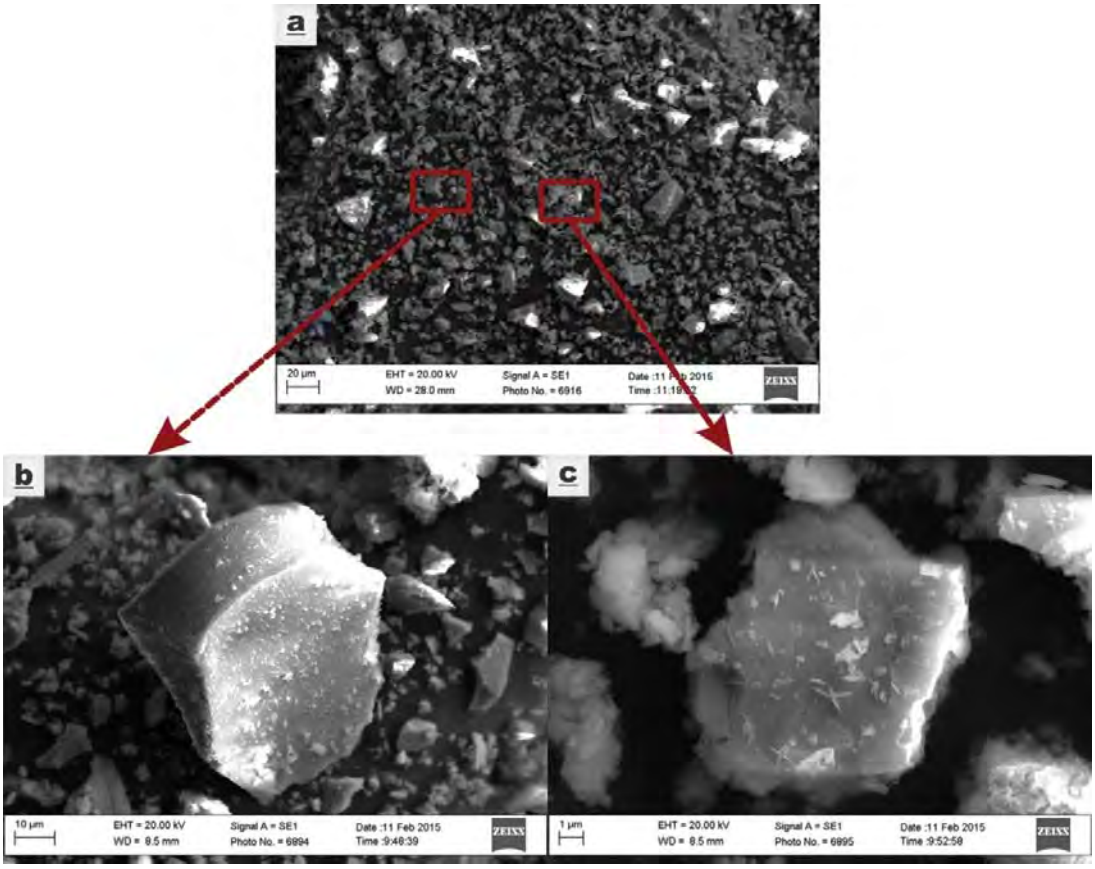

Figure 4.8 GGBFS SEM Micrograph at (a) 20µm, (b) 10µm, and (c) 1µm scales

Figure 4.8(a) shows that the GGBFS particles appeared to possess particle morphology that is dissimilar from bentonite particles as the particle sizes and shapes exhibited wide variations and random size distribution can be postulated for slag particles even though the appearance of the slag granules appeared to nominal variance in terms of particle texture. Moreover, the slag crystals generally displayed a glassy crystalline structure with particle sizes in the range of 11µm – 40µm as highlighted in Figure 4.8(b), with slag granules generally demonstrating straight-edged rougher texture. Although, there was little uniformity in the shapes of the

crystals, as can be seen from Figure 4.8(c), random crystal growth was found on most of the crystal surfaces similar to bentonite particles.

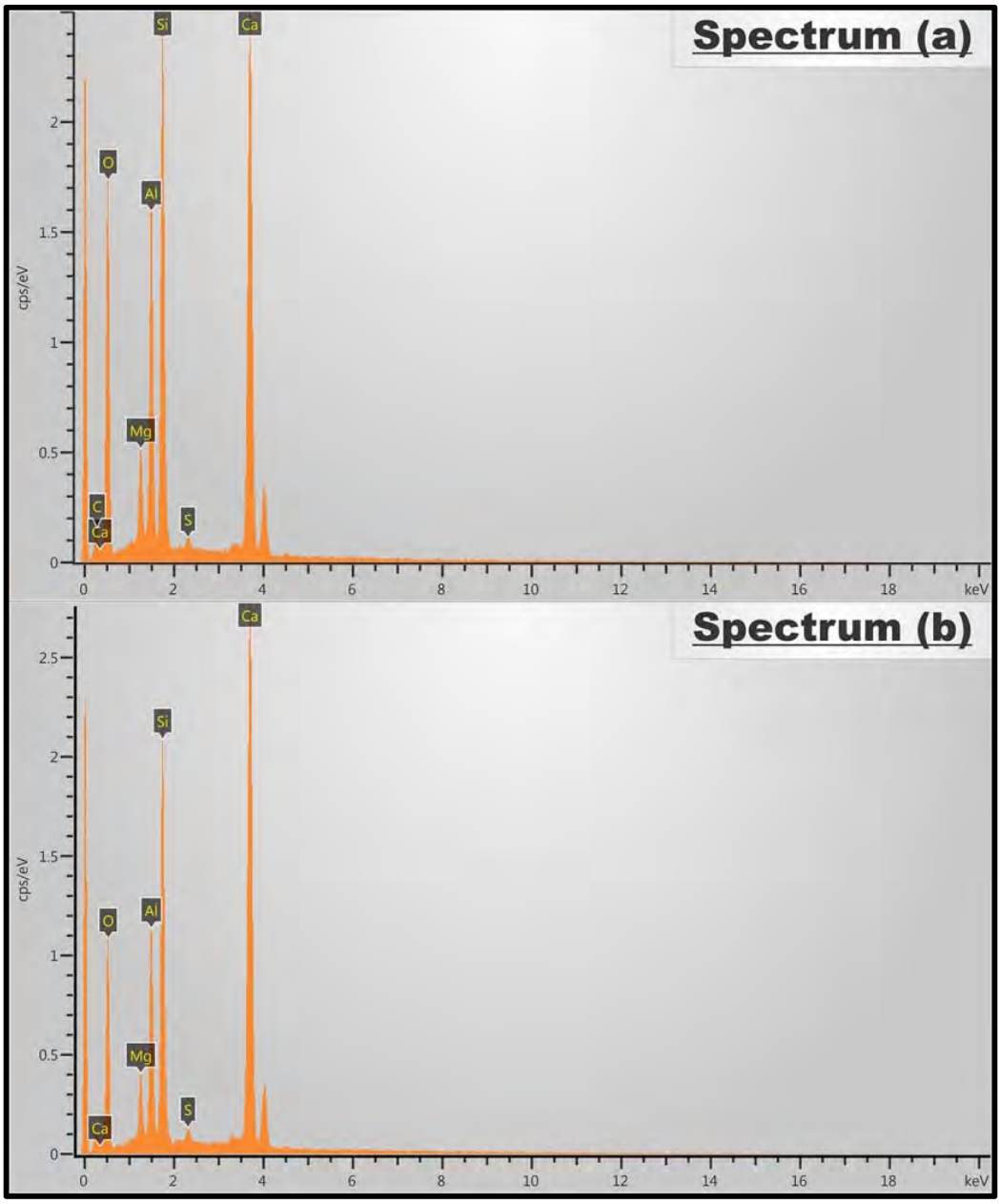

Figure 4.9 GGBFS EDS Spectra for (a) Sample 1, and (b) Sample 2

The elemental distribution of the GGBFS employed in this study was also explored through EDS testing and the EDS spectra of two sample spots on the test material are illustrated in Figure 4.9. The results of the quantitative analysis of the GGBFS

particles are outlined in Table 12 for two different samples presented in the micrographs above. The results of sample indicate a strong presence of oxygen, with SiO_2 and MgO as the leading chemical compounds followed by aluminium, ferric and calcium oxides. Similarly, for sample 2, oxygen was observed as the most dominant element which was followed by calcium and sulphur. Silicon and metals like aluminium and magnesium succeeded as the most common elements which confirms the presence of silica and metallic oxides in GGBFS as has been found by other researchers (Gardner et al. 2015; Murthy, Babu and Rao 2014; Fredericci, Zanotto and Ziemath 2000), whereas the presence of sulphur can be attributed to the supplier signature as the exact chemical composition might vary between different commercial suppliers as suggested by Snellings, Mertens, and Elsen (2012).

Table 12 Quantitative Chemical Composition of GGBFS

Element	Weight%	Atomic%	k Ratio	Standard
Sample 1				
O	47.41	64.39	0.17233	SiO_2
Mg	3.03	2.71	0.02271	MgO
Al	9.68	7.80	0.08227	Al_2O_3
Si	14.78	11.43	0.14747	SiO_2
S	0.44	0.30	0.0051	FeS_2
Ca	24.67	13.38	0.31293	CaO
Total	100.00	100.00		
Sample 2				
O	41.64	61.43	0.04488	SiO_2
Mg	0.96	0.94	0.00395	MgO
Al	3.97	3.47	0.02032	Al_2O_3
Si	9.89	8.31	0.05941	SiO_2
S	1.36	1	0.00938	FeS_2
Ca	42.18	24.84	0.3362	CaO
Total	100.00	100.00		

4.3.1.3 Construction Waste

The construction and demolition waste (CW) employed in this study was collected from a commercial recycling organisation and had originated from variety of construction projects including rubble, crushed masonry and concrete from residential and infrastructural projects. The texture, appearance and colour of CW grains largely varied due to the variation in the source and might have also caused variation in the elemental distribution of the CW particles.

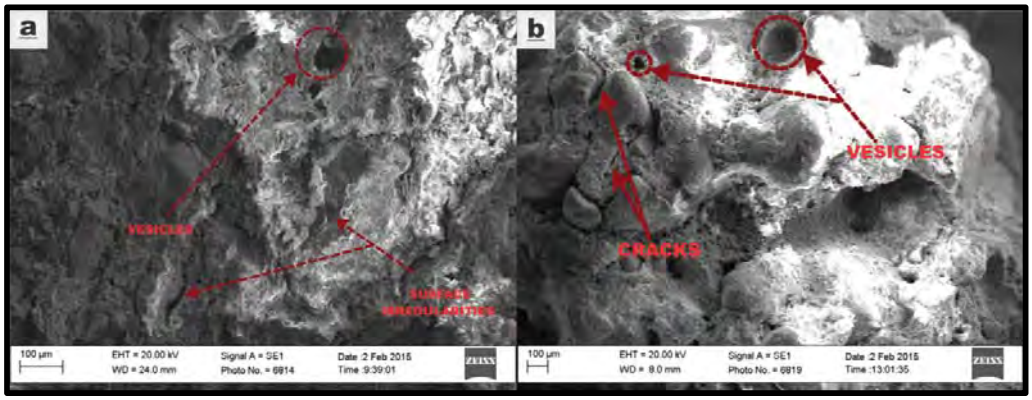

Figure 4.10 (a) and (b) Construction Waste SEM Micrographs

Figure 4.10 illustrates the micromorphology of the construction waste particles. As can be seen, the construction waste particles have irregular or lenticular shapes Figure 4.10(a). Even though the sources, texture and appearance of construction waste particles widely varied, fissures or vesicles and cracks were often found on the surfaces regardless of the appearance as Figure 4.10(b) shows similar cracks and voids on the surface of a construction waste grain with a different shape.

The fissures and voids are quite common with gravels and building aggregates, and this may have aided in the interlocking mechanism between the bentonite and construction waste particles. In addition, it can be speculated that the formation of surface cracks and voids, due to bearing similarity with aggregates and gravels, may aid in generation of a higher angle of internal friction of the composite particles as the particles might interlock upon compaction.

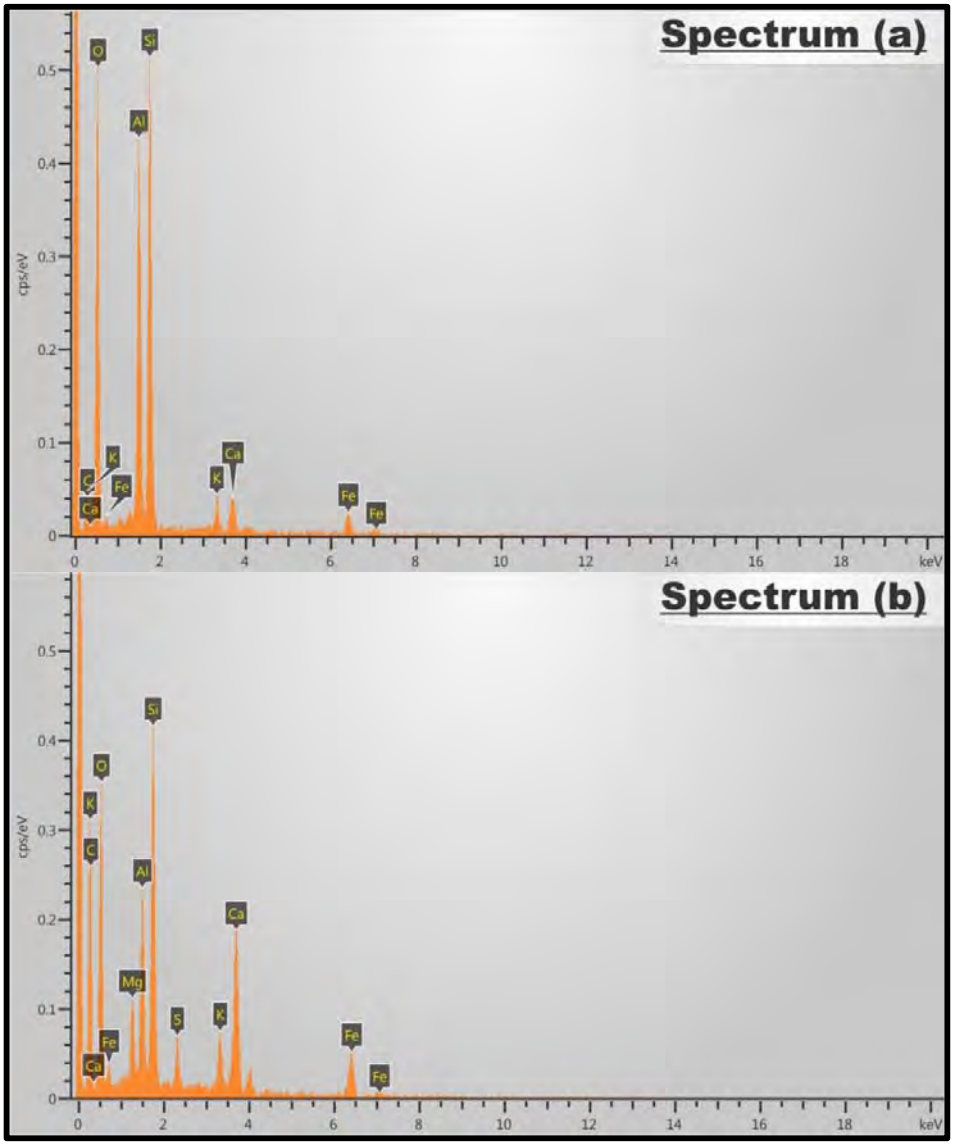

Figure 4.11 Construction Waste EDS Spectra for (a) Sample 1, and (b) Sample 2

The EDS spectra and quantitative data of the selected construction waste grains are displayed in Figure 4.11. Since the construction waste contains a variety of materials such as crushed bricks, rubble, mortar etc., the elemental distribution may vary between the grains. The results of quantitative analysis on construction waste grains have been tabulated in Table 13 for two different samples. As the source of the grain is most likely crushed bricks, the quantitative chemical distribution indicates that these grains may belong to the large mineral family of plagioclase feldspars. It can be observed from both Table 13 and Figure 4.11 that silica, metallic and alkali

oxides were found to be the most common compounds as is common with the plagioclase feldspars (Hasan et al. 2015; Deer, Howie and Zussman 2013).

Table 13 Quantitative Chemical Composition of Construction Waste

Element	Weight%	Atomic%	k Ratio	Standard
Sample 1				
O	51.75	66.80	0.32205	SiO_2
Al	16.40	12.55	0.14126	Al_2O_3
Si	22.23	16.35	0.20074	SiO_2
K	2.18	1.15	0.02482	K_2O
Ca	2.70	1.39	0.03121	CaO
Fe	4.74	1.75	0.05127	Fe_2O_3
Total	100.00	100.00		
Sample 2				
O	45.12	62.76	0.17139	SiO_2
Mg	4.37	4.00	0.0249	MgO
Al	8.82	7.27	0.05653	Al_2O_3
Si	15.74	12.47	0.12137	SiO_2
S	2.52	1.75	0.02298	FeS_2
K	3.58	2.04	0.03518	K_2O
Ca	11.43	6.35	0.11292	CaO
Fe	8.43	3.36	0.07549	Fe_2O_3
Totals	100	100.00		

4.3.1.4 Bentonite – Stabiliser Composite

The effects of stabilisation process on the microscopic scale were studied through SEM and EDS tests on bentonite-stabiliser composites after 28 days of curing period, as has been presented in micrographs illustrated Figure 4.12. The results of SEM analysis on bentonite-stabiliser composites reveal that the cavities and cracks on the surface of construction waste grains as well as the inter-particle voids were filled in by slag and bentonite particles as highlighted in Figure 4.12(b). This might

have aided in the improving the interlocking mechanism between the particles and therefore developing the internal frictional angle.

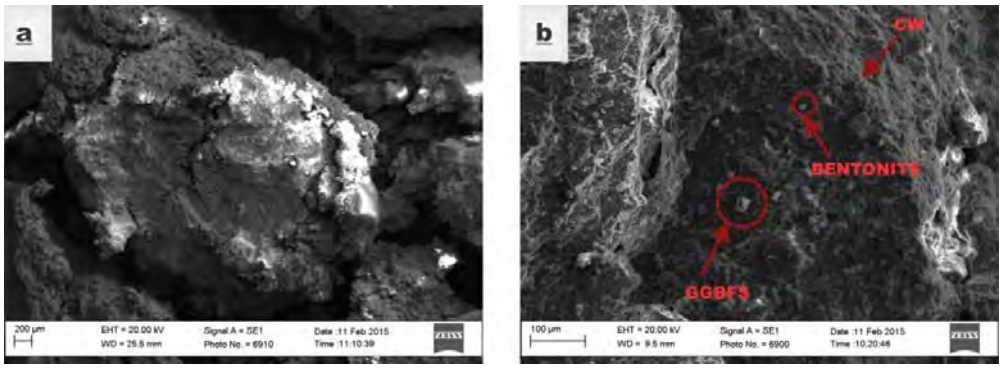

Figure 4.12 SEM micrograph of bentonite-stabiliser composite specimen after 28 Days of Curing at (a) 200µm, and (b) 100µm scales

The results of EDS spectra and quantitative analysis further show the presence of bentonite and slag particles clung to construction waste grains and have been presented in Figure 4.13 and Table 14. Oxygen and silicon were the most common elements in the bentonite-stabiliser specimen matrix.

The peaks illustrated in Figure 4.13(a) and quantitative data presented in Table 14(a) indicate that silicon and oxygen formed the major composition of the sample mineralogy. Other elements included aluminium, iron, magnesium, sodium, titanium and calcium while silica and oxides of the dominant metals were the most dominant compounds. Overall, the results exhibited consistency with the findings from SEM and EDS tests on pure bentonite clay. Figure 4.13(b) spectra peaks and quantitative analysis results from Table 14(b) display similar peaks of silica and metallic oxides and those observed for GGBFS, whereas the quantitate analysis results of Table 14(c) and spectra peaks from Figure 4.13(c) resembled the mineralogy results of EDS quantitative analysis for the construction waste particles.

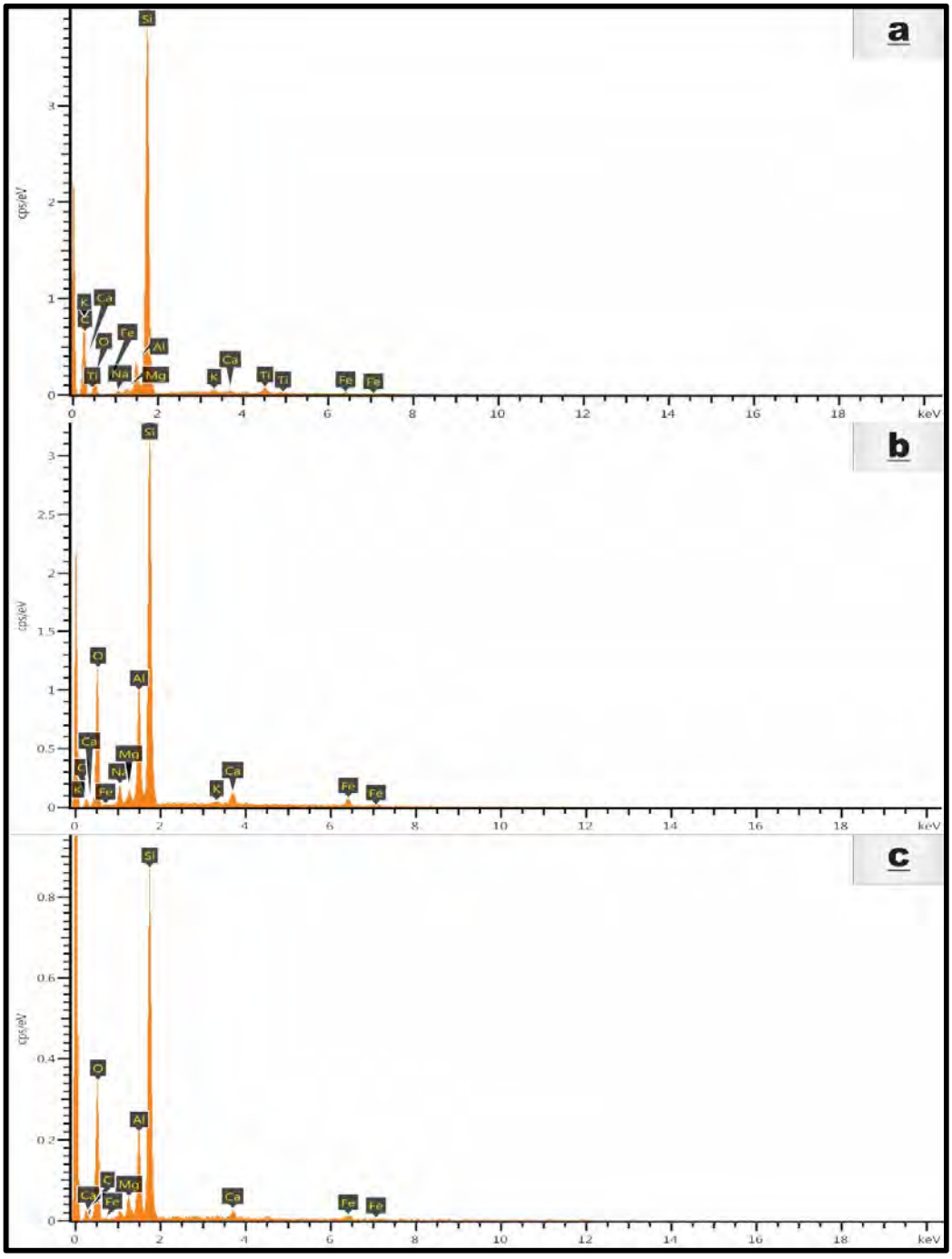

Figure 4.13 EDS Spectra and Quantitative Data of S3G5 after 28 Days of Curing with (a) Bentonite, (b) GGBFS, and (c) Construction Waste Grains

Table 14 Quantitative Data of S3G5 after 28 Days of Curing

Element	Weight%	Atomic%	k Ratio	Standard
Table 14(a) – Quantitative Data for Figure 4.13(a)				
O	17.71	27.95	0.04014	SiO_2
Na	0.57	0.63	0.00222	Na_2O
Mg	0.54	0.56	0.0028	MgO
Al	4.56	4.27	0.02556	Al_2O_3
Si	70.19	63.10	0.44365	SiO_2
K	1.01	0.65	0.00526	K_2O
Ca	0.96	0.61	0.00554	CaO
Ti	3.01	1.59	0.01649	TiO_2
Fe	1.43	0.65	0.0082	Fe_2O_3
Totals	100	100.00		
Element	Weight%	Atomic%	k Ratio	Standard
Table 14(b) – Quantitative Data for Figure 4.13(b)				
O	39.80	54.24	0.19039	SiO_2
Na	2.76	2.62	0.01417	Na_2O
Mg	1.25	1.12	0.00851	MgO
Al	10.67	8.62	0.08185	Al_2O_3
Si	39.55	30.70	0.33768	SiO_2
K	0.46	0.26	0.00435	K_2O
Ca	1.88	1.03	0.01854	CaO
Fe	3.61	1.41	0.03354	Fe_2O_3
Total	100.00	100.00		
Element	Weight%	Atomic%	k Ratio	Standard
Table 14(c) – Quantitative Data for Figure 4.13(c)				
O	43.67	58.06	0.20219	SiO_2
Mg	2.36	2.07	0.01541	MgO
Al	9.47	7.47	0.06808	Al_2O_3
Si	40.43	30.62	0.32617	SiO_2
Ca	1.54	0.81	0.01404	CaO

Fe	2.54	0.97	0.02194	Fe_2O_3
Total	100.00	100.00		

4.3.2 Pure Bentonite Clay and Bentonite–Stabilisers Composite Mineralogical XRD Analysis

In addition to the SEM and EDS analyses on the material morphology and mineralogy, the diffraction bands of the untreated bentonite clay were used to understand the presence of different minerals and to obtain benchmark data for comparing the effects of the two stabilising agents on the virgin clay. The EDS spectra and SEM images indicated the presence of bentonite and GGBFS particles in the cavities and cracks found on the surface of construction waste grains. A series of XRD tests were conducted to obtain insight into the mixture mineralogy and elemental distribution. The test results have been presented in Figure 4.14 and provide the diffraction bands for the benchmark pure bentonite clay sample (S1G1) and bentonite-stabiliser composite specimen S3G5 that displayed the maximum improvement in shear strength under the imposed normal stresses and after 28 days of curing period. The improvement in shear strength after 28 days of curing was primarily due to the formation of $Ca(OH)_2$ from pozzolanic reaction of GGBFS which is a time-dependent process.

Figure 4.14 illustrates the X-ray diffraction (XRD) spectrum for the stabilised soil specimen S3G5 after 28 days of curing alongside the XRD for untreated bentonite clay, so as to gain further insight into the crystallography and mineralogy of the treated and untreated specimens. The sample was selected based upon the SDI criterion as it showed a maximum SDI value (SDI_{28} = 3.09) and the shear index criteria and the lowest shear index of 0.71 among the tested specimens (these points are further elaborated in the respective compressive and shear strength sections succeeding this section), indicating that the maximum strength had been achieved for this sample.

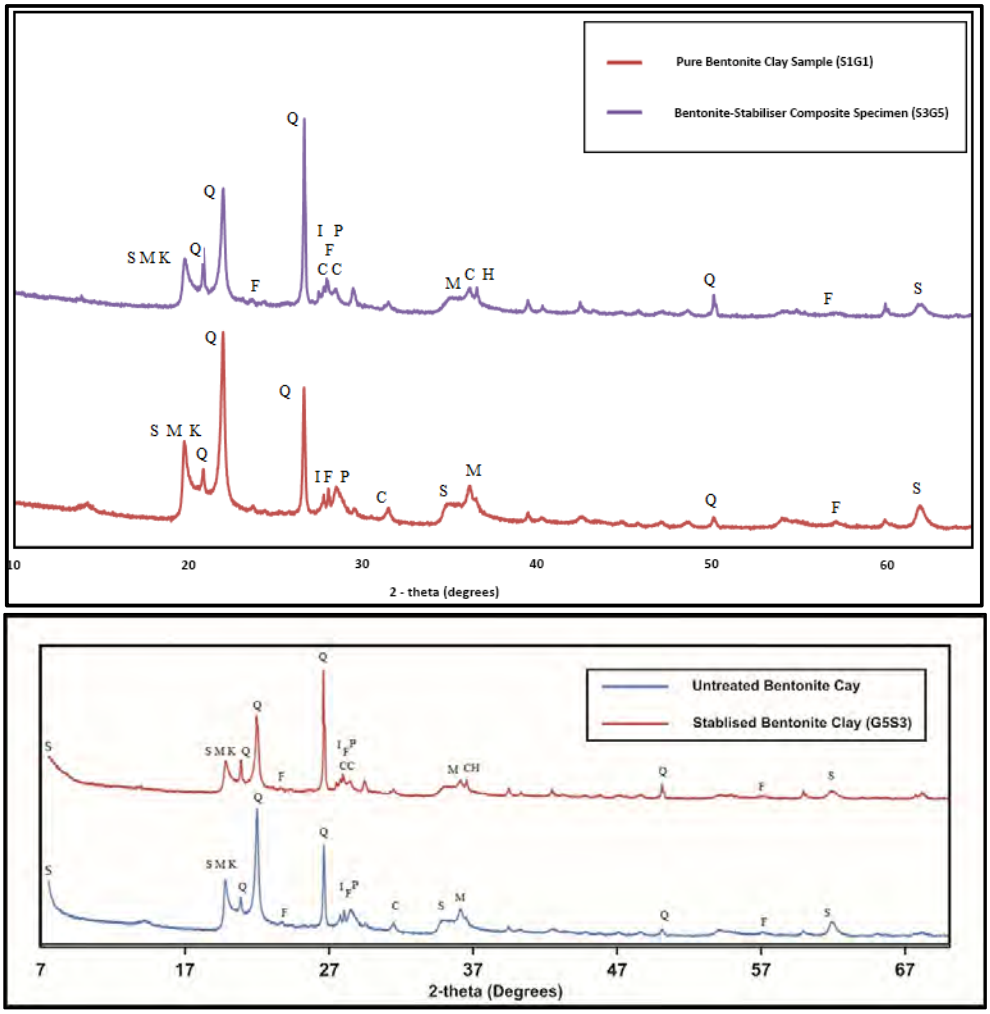

Figure 4.14 X-ray Diffraction Spectrum of Pure Bentonite Clay and Bentonite – Stabiliser Composite Specimens after 28 Days of Curing (S: Smectite, M: Mica, K: Kaolinite, Q: Quartz, F: Feldspar, I: Illite, CC: Calcium Carbonate, P: Plagioclase, CH: Calcium Hydroxide, C: Calcite)

The peaks of the XRD diffraction bands indicate that the tested stabilised mixture showed similar peaks overall, with slight variation resulting from the formation of cementitious compounds (Figure 4.14). Comparative analysis of the two samples shows the effect of the clay stabilisation process using the two additives. Similar to the EDS results for both pure bentonite and bentonite-stabiliser composite specimens, quartz [SiO_2] was associated with the most dominant peaks for both stabilised and unstabilised samples, followed by other clay minerals like kaolinites

$[Al_4[Si_4O_{10}](OH)_8]$, illites $[K_{0.65}Al_2[Al_{0.65}Si_{3.35}O_{10}](OH)_2]$, mica and alkali feldspars.

Furthermore, the diffraction spectrum of bentonite-stabiliser composite specimen shows that in addition to the peaks observed for the pure bentonite clay sample, the stabilised sample exhibited peaks associated with calcium hydroxide $[Ca(OH)_2]$. This may be indicative of the hydration of the stabilised mixture to produce $Ca(OH)_2$ (Birss and Thorvaldson 1955) from hydration of calcium oxide that was also found in the test material EDS spectra.

4.4 MATERIAL PROPERTY TESTS

Several property tests including determination of Atterberg's limits, i.e., plastic limit (PL) and liquid limit (LL) of pure bentonite clay; calculation of maximum dry density (MDD) and optimum moisture content (OMC) of pure bentonite clay; and particle size distribution (PSD) of the unscreened construction and demolition waste. The results of these tests have been produced in the following subsections.

4.4.1 Atterberg's limits

Some of the most common parameters evaluating the critical moisture content of clays and other fine soils are collectively labelled as Atterberg's limits. The term encompasses the plastic limit and liquid limit of clayey soils which are also used for the calculation of the plasticity index of such soils. As this study investigates the effect of stabilisers and curing periods on bentonite – stabilisers composites prepared by adding controlled amount of water, the moisture content of pure bentonite clay were studied through laboratory experiments.

The results of plastic and liquid limit tests and the calculation for the plasticity index of pure bentonite clay have been presented below.

$$Liquid\ Limit\ of\ pure\ bentonite = LL_{bentonite} = 440\% \qquad \text{Equation (4.1)}$$

$$Plastic\ Limit\ of\ pure\ bentonite = PL_{bentonite} = 38\% \qquad \text{Equation (4.2)}$$

$Plasticity\ Index\ of\ pure\ bentonite;$

$$\Rightarrow PI_{bentonite} = 440 - 38 = 402 \qquad \text{Equation (4.3)}$$

The plasticity index of the tested pure bentonite clay is very high as is common for sodium montmorillonite clays. These results are also similar to the Atterberg's limits tests studied by (Bain 1971; Inglethorpe, Morgan and Highley 1993), where the plasticity indices of Na-montmorillonite clay were found to be in the range of approximately 300 – 600.

4.4.2 Standard Compaction Test

Bentonite was subjected to a standard compaction effort of 596kJ/m^3 as per Standards Australia AS 1289.5.1.1 (2003) to calculate the optimum moisture content (OMC) and the corresponding maximum dry density ($\gamma_{d_{max}}$). Bentonite clay was mixed with water and compacted in the standard mould and oven-dried to obtain the moisture content and increasing percentages of water were used for each repetition of the test. As further moisture is added to the dry bentonite mass, more volume of air is expelled from the inter-particle voids and cavities. In addition, as the sample was being compacted, the relocating and repositioning of bentonite particles further triggered expulsion of air molecules and thereby causing densification of the bentonite particles. As the clay sample becomes wetter, it also becomes further densified due to compaction under stress and reaches a point where maximum dry density (MDD) is achieved. The moisture content associated with the MDD is called optimum moisture content or OMC.

For the purpose of this study, a compaction curve was plotted based on the data obtained after a series of compaction tests performed on bentonite clay with increasing water content and the OMC and MDD were obtained. The results of the compaction tests, in terms of compaction curve are plotted in Figure 4.15. Based on this curve, the OMC and $\gamma_{d_{max}}$ calculated for the pure bentonite clay used in this study were respectively obtained as 43% and 1.08gr/cm^3. This moisture content value was also used for bentonite-stabiliser composites.

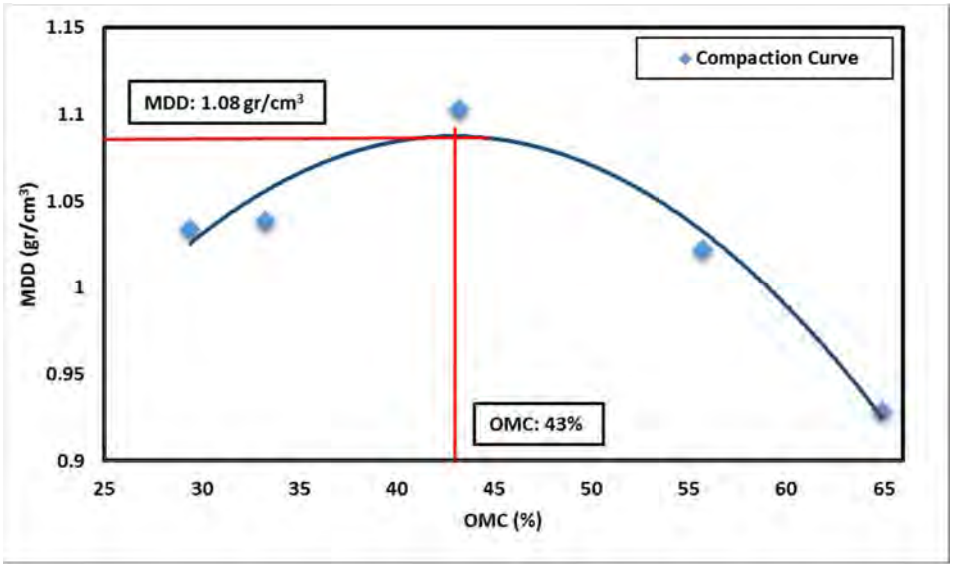

Figure 4.15 Standard Compaction Curve of Pure Bentonite Clay

4.4.3 Particle Size Distribution

After the mechanical sieving was done, the dry mass of the construction waste particles retained on each sieve was noted and plotted against the sieve opening size to produce the particle size distribution curve illustrated in Figure 4.16.

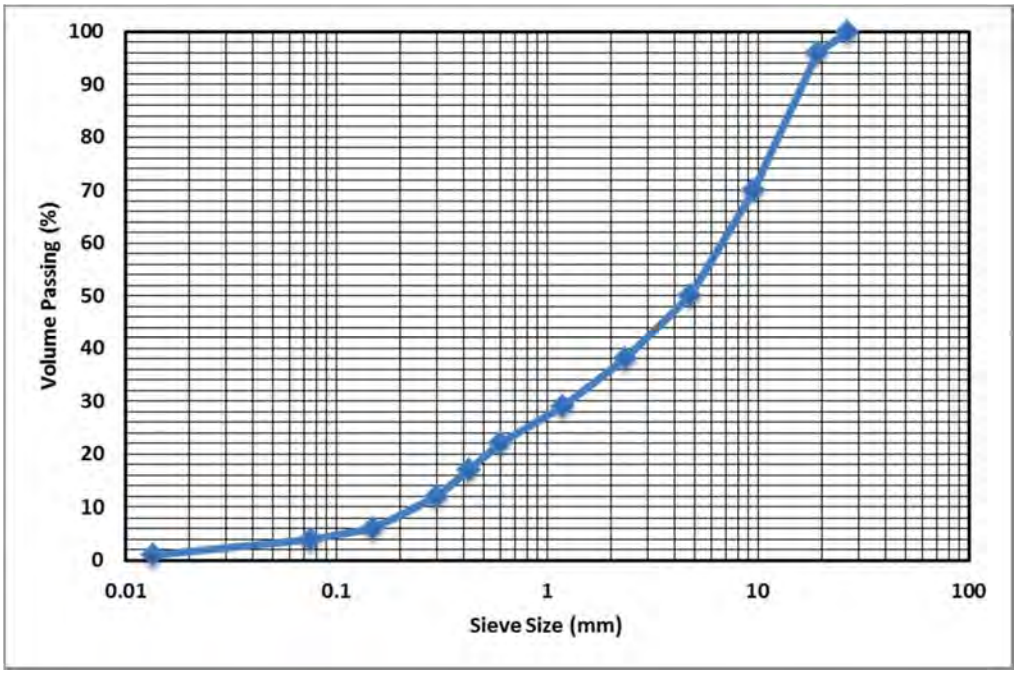

Figure 4.16 Particle Size Distribution of Selected Construction and Demolition Waste

The particle sizes of the selected construction and demolition waste largely varied but mostly remained lower than 19mm as it was already screened by the supplier to remove particles with size ranges exceeding 19mm. Furthermore, a small fraction of particles, approximately 4%, were found to have particle sizes more than 19mm as can be seen from Figure 4.17. The majority of particles retained on sieve opening 0f 4.75mm as the proportion of construction waste particles retained on this sieve, was approximately 47%. However, only a small fraction of particles retained on sieve opening of 2.36mm after passing through sieve 4.75mm, as these particles only formed 12% of the sieved construction and demolition waste particles. These particles were then separately stored in plastic bucket to be used for the purpose of soil stabilisation.

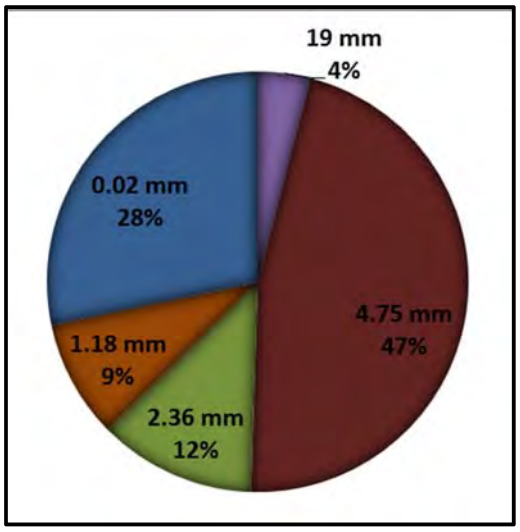

Figure 4.17 Percentages of Particles Retained on Standardised Mesh Sizes

4.5 UNCONFINED COMPRESSIVE STRENGTH

Unconfined compressive strength (UCS) is essentially a parameter of stabilisation process efficiency which is defined as the maximum unit stress calculated after subjecting the stabilised samples to a monotonic axial load. The deformation was mainly observed through the formation of minor cracks on the outer shell of the specimen which widened until specimen failure was observed. Figure 4.18 shows the failure mechanism of the test specimens. This phenomenon is a common failure mechanism of ductile materials during unconfined compression.

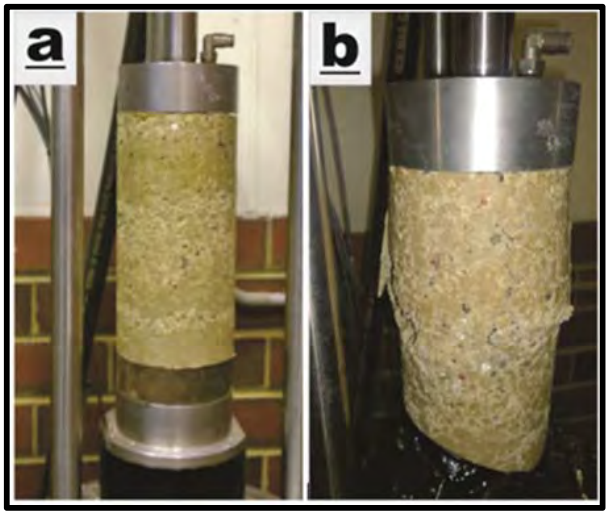

Figure 4.18 Sample failure mechanism (a) undeformed sample, (b) deformed sample

A strength development index (SDI) was introduced as a non-dimensional parameter to easily quantify the effect of each of the controlling factors, i.e. the effect of the percentage of each additive and the curing time on the UCS of the stabilised soil. It is defined as:

$$SDI_{n_{curing,\%\ of\ additives}} = \frac{UCS\ of\ the\ stabilised\ soil\ specimen}{UCS\ of\ the\ unstabilised\ soil\ specimen} \geq 1 \qquad \text{Equation (4.4)}$$

Where 'n' corresponds to either of the controlling factors, representing either the percentage of the two stabilising additives in the mixture or the number of days the sample has been subjected to the curing conditions. The lower limit of '1' indicates that the addition of any admixture should not result in a decrement in the UCS. A similar parameter has also been proposed by Saride, Puppala, and Chikyala (2013a).

4.5.1 Initial Strength of the Untreated Sample

The stress-strain relationship of pure bentonite is illustrated in Figure 4.19 for the different curing periods investigated in this research. Test results suggest that although all pure bentonite samples showed a slight variation in the failure strain, little or no strength development was observed for the unstabilised soil samples for different curing periods. The maximum compressive strength of the untreated bentonite was found to be 76.71kPa.

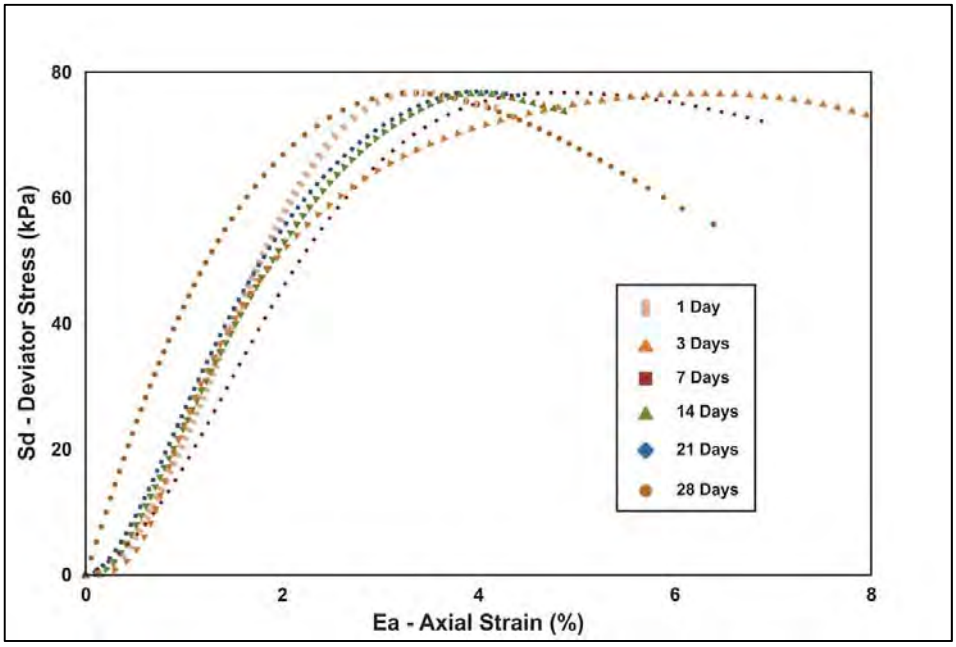

Figure 4.19 Stress-strain curves of pure bentonite for 7 and 28 day curing periods

The value of the standard deviation (SD) and relative standard deviation of the tested samples are given as:

$$SD = \sqrt{\frac{1}{n-1}\sum_{i=1}^{n}(x-\bar{x})^2} = 0.02738 \ll 1 \qquad \text{Equation (4.5)}$$

$$RSD = \frac{SD}{\bar{x}} \times 100 = 0.04\% \qquad \text{Equation (4.6)}$$

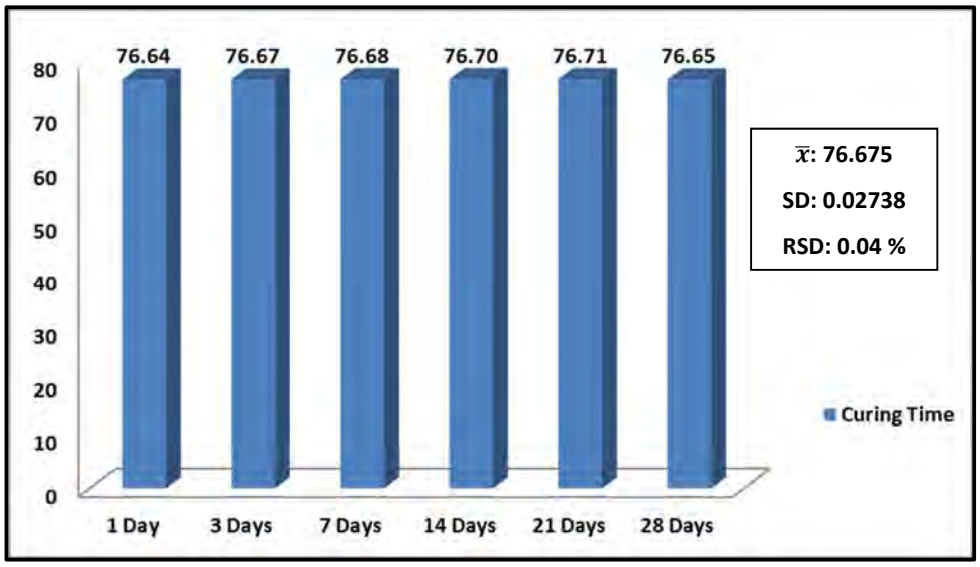

Figure 4.20 UCS of unstabilised soil specimens

The lower SD and RSD values show that the tested specimens showed similar UCS values. Figure 4.20 illustrates the development of unconfined compressive strength with curing periods of the compacted bentonite samples. It shows that the compressive strength of the expansive bentonite is unaffected by the curing period, provided the curing is performed under moisture control conditions, preventing the escape of moisture from the soil specimens (Figure 4.20).

4.5.2 Effect of Curing Time on Stabilised Compacted Soil

The curing time of the additive-stabilised bentonite specimens was among one of the primary control factors. The evolution of the unconfined strength of the stabilised specimens throughout the final curing period of 28 days is illustrated in Figure 4.21 to Figure 4.23.

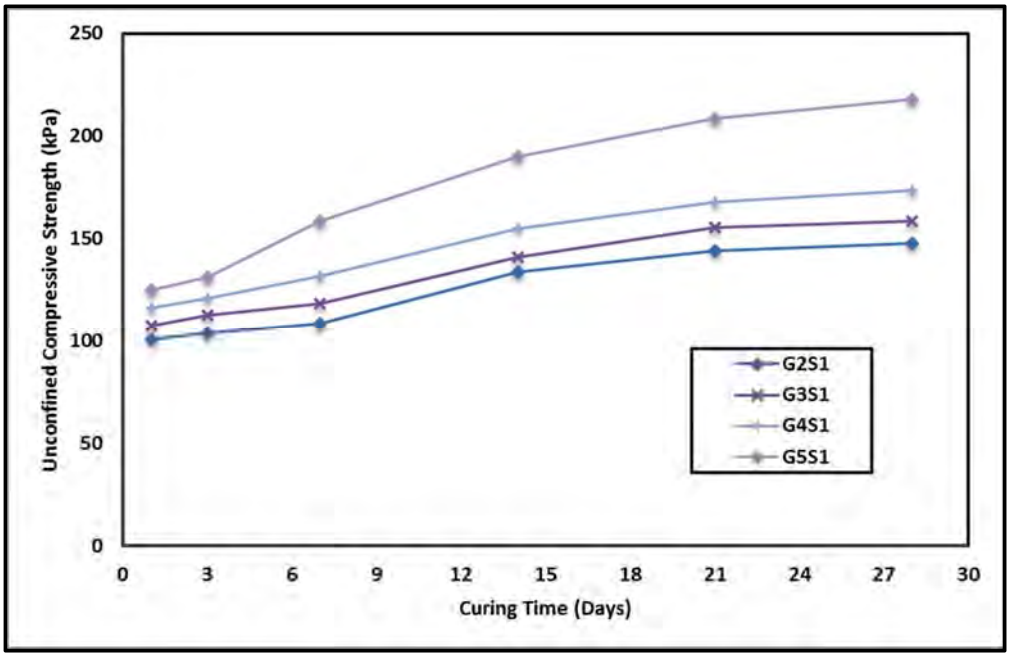

Figure 4.21 Evolution of UCS with curing time for 2%, 3%, 4% and 5% slag and 10% construction waste

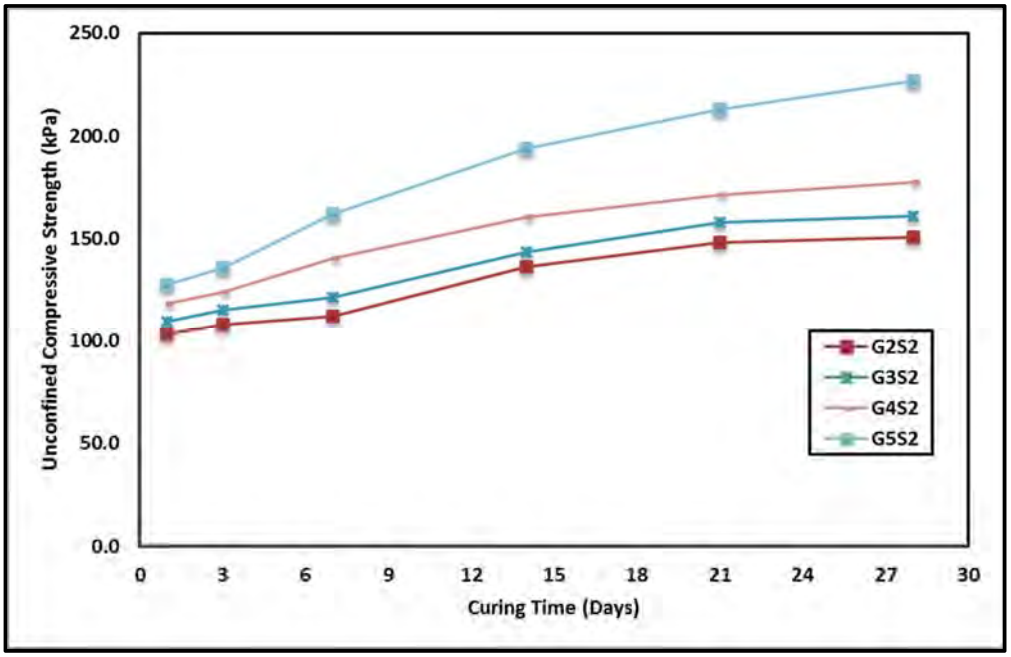

Figure 4.22 Evolution of UCS with curing time for 2%, 3%, 4% and 5% slag and 15% construction waste

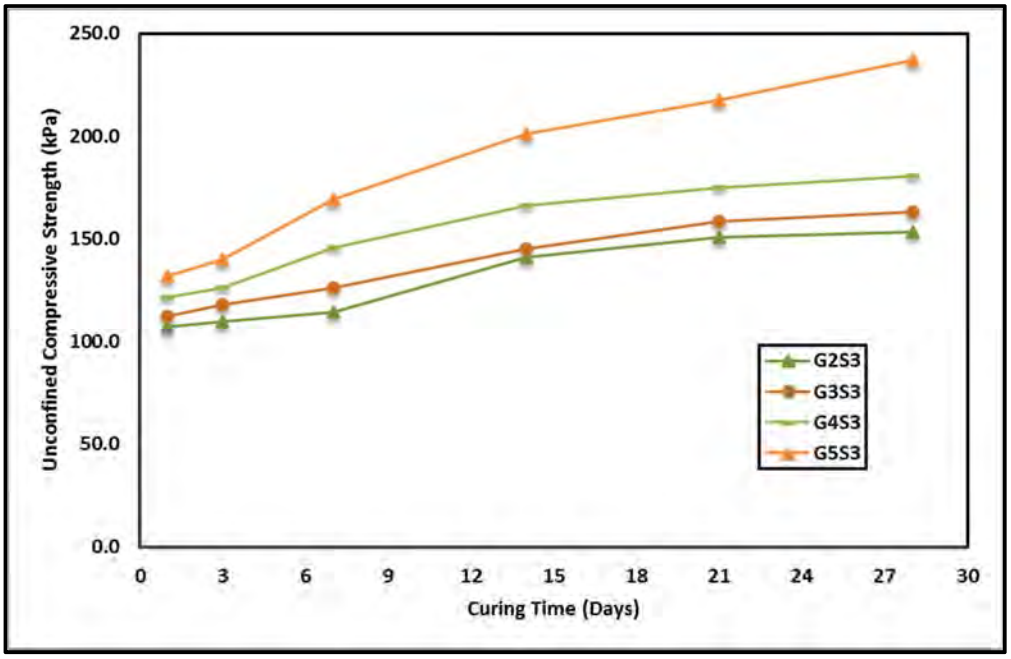

Figure 4.23 Evolution of UCS with curing time for 2%, 3%, 4% and 5% slag and 20% construction waste

The UCS results for the construction waste and bentonite blended samples with increasing percentages of slag show the development of strength with curing. The

effect was more noticeable in the initial periods of curing with all of the specimens gaining at least 75% of the strength increment by the 14th day of curing. Although further curing resulted in an increase in strength values, the effect was not as prominent as for the 14 day curing period. The effect of curing became more noticeable as the percentage of additives, specifically GGBFS, was increased. This might have been due to the cementitious nature of the slag and its slower hydration reaction. Although the hydration reaction of the stabilising GGBFS might have continued after the 28th day of curing (Kim et al. 2011), the construction waste grains tend to produce little effect with each successive curing day, and may have showed a negligible increase in the compressive strength of the stabilised mixture over time.

4.5.3 Effect of Additives

Each of the additives produced different effects on the UCS of the stabilised mix for the same curing period. The effect of each additive is discussed separately.

4.5.3.1 Effect of Slag

It was observed that for all combinations of additives, the maximum strength was achieved in the 28 day curing period (Figure 4.24). This finding shows that the cementitious nature of GGBFS plays a vital role in the development of compressive strength. It was observed that the increase in UCS value with the increment in the proportion of GGBFS only grew by 15% when the percentage of GGBFS was increased from 2% to 3% for 28 days of curing, SDI_{28} of 1.92 to SDI_{28} of 2.07 respectively for the 10% proportion of the construction waste. Conversely, a higher increment in the strength was observed when the percentage of slag was further increased. The SDI_{28} value rose by a factor of 0.19, corresponding to a 19.27% rise when the GGBFS percentage was increased from 3% to 4% for a construction waste content of 10%. Furthermore, an increase of 0.58 was documented in SDI_{28}, being a sharp 58.16% rise when the GGBFS proportion was further increased to 5% for the same percentage of construction waste. The maximum increase after one day of curing was observed for the sample G5S3 which had an SDI_1 of 1.71. However,

further curing resulted in a sharper increase in the compressive strength, where a maximum strength of 236.93kPa was observed for the sample G5S3 (SDI_{28} = 3.09).

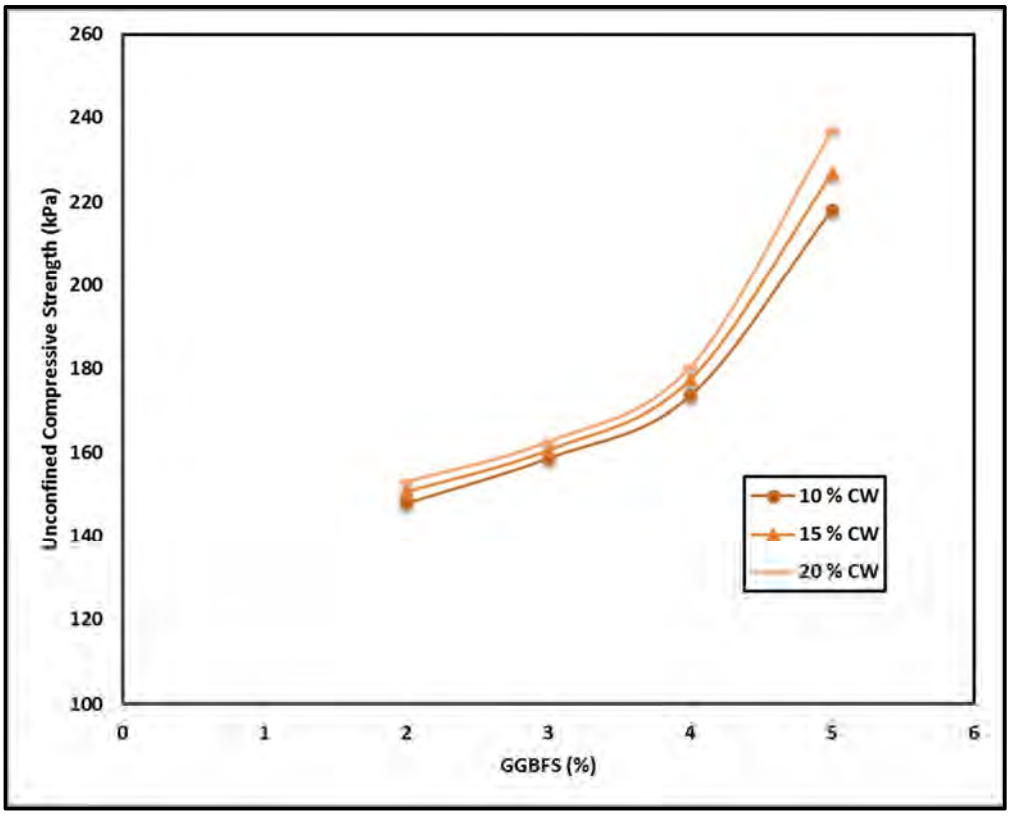

Figure 4.24 Evolution of UCS with GGBFS over a 28 day curing period

4.5.3.2 Effect of Construction Waste

Figure 4.25 shows the development of compressive strength with increasing percentages of the selected gradation of construction waste over a 28 day curing period. The increase in the UCS of the stabilised bentonite clay samples was observed to be directly correlated with the proportion of the construction and demolition waste in the mixture. After the first day of curing (Figure 4.21), the UCS of the stabilised sample with the least amount of slag, i.e. 2%, was seen to grow by an SDI factor of 0.03 from $SDI_{2\%\ GGBFS\ +\ 10\%\ CW}$ = 1.31, corresponding to a strength of 100.82kPa, to $SDI_{2\%\ GGBFS\ +\ 15\%\ CW}$ = 1.34 (UCS = 103.07kPa), with a 5% increment in the amount of inducted construction waste. A further increase of 5% yielded an increase in the SDI by a factor of 0.04 which produced a UCS value of 106kPa. Further strength increment was observed with the lengthening curing

periods, because of the GGBFS cementitious nature, and the effects of the increased percentage of construction waste in the stabilised mixture were more pronounced with the high percentages of GGBFS in the treated samples.

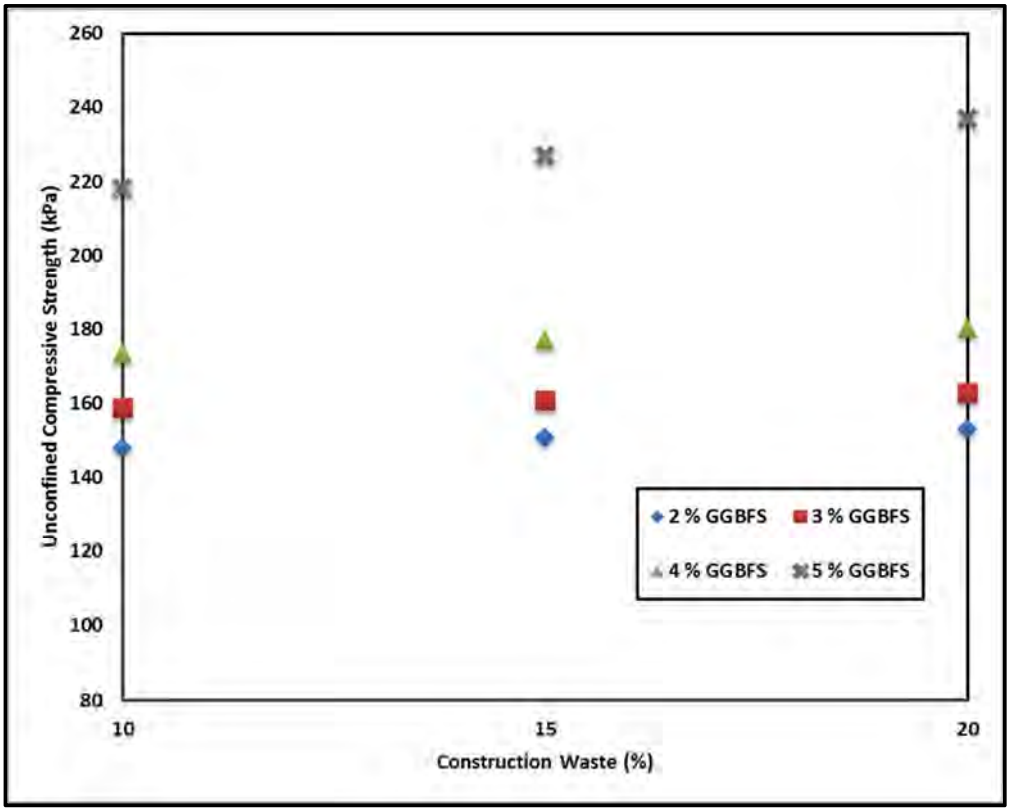

Figure 4.25 Evolution of the UCS of construction waste for different GGBFS concentrations after 28 days of curing

This statement was reconfirmed, as after the curing of the stabilised samples for 28 days (Figure 4.25), the UCS value was found to have increased from 147.93kPa to 150.67kPa, which shows an SDI increment from $SDI_{2\%\ GGBFS\ +\ 10\%\ CW} = 1.93$ to $SDI_{2\%\ GGBFS\ +\ 15\%\ CW} = 1.96$. Upon addition of another 5% of construction waste, the UCS value rose to 153.09kPa, corresponding to $SDI_{2\%\ GGBFS\ +\ 20\%\ CW} = 1.99$. The development of strength with increasing proportion of construction waste could be attributed to change in the texture of the soil-stabiliser composite. The process is fairly common with mechanical soil stabilisation technique where the gradation and particle size distribution of the soil are changed to increase the strength of the resulting material.

4.5.4 Optimum Strength Improvement

Figure 4.26 shows the strength development indices of all of the treated specimens for the 28 day curing period, as the maximum strength for all admixture-stabilised bentonite samples was observed after the samples had been cured for 28 days. The maximum strength after the 28 day curing period was observed for sample G5S3, which contained 5% slag and 20% construction waste, being $SDI_{5\%\ GGBFS\ +\ 20\%\ CW} = 3.09$. This shows that stabilised soil strength grew by almost 209%, while the least strength development was observed for sample G2S1 which contained the lowest percentages of additives.

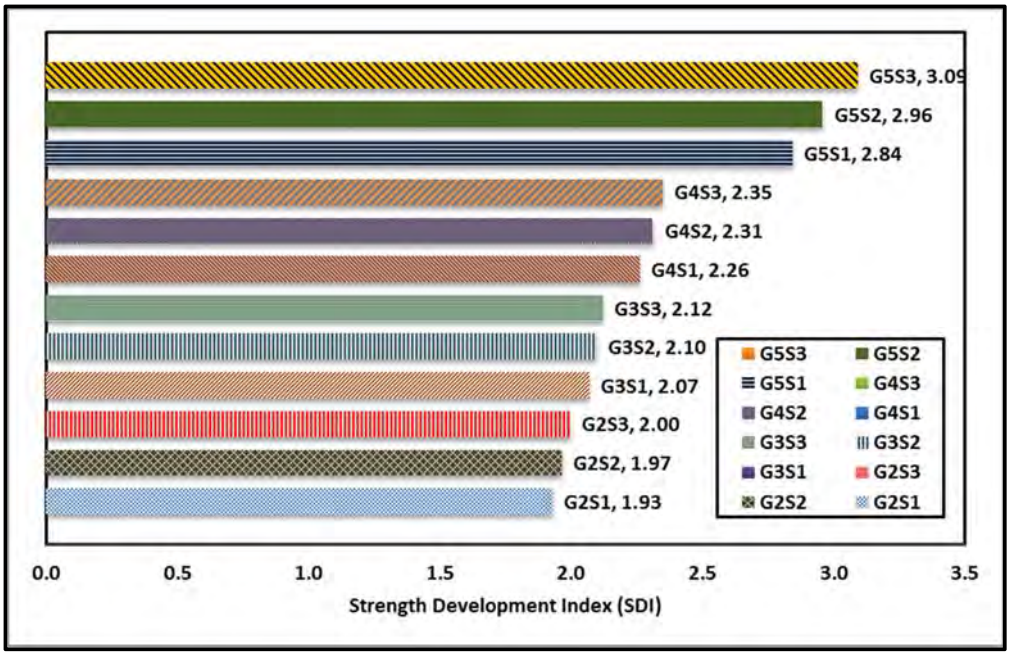

Figure 4.26 SDI for 28 days curing (SDI_{28})

4.6 SHEAR STRENGTH

Shear strength of soil is primarily used to evaluate the efficiency of stabilisation process in enhancing the ability of the material to resist a lateral load that tends to trigger shear failure in the material. It is usually generated through the particle interlocking mechanism which depends upon the type, morphology, cementitious nature and texture of the particles represented through internal frictional angle "ϕ" and soil cohesion "c". Generally, DST is conducted under strain/displacement

controlled condition by specifying a certain rate of strain depending upon the test apparatus, soil characteristics such as cohesive or non-cohesive soil and standard specifications. Displacement controls enables the user to calculate both critical and peak shear forces unlike load/stress controlled tests that cannot generate data once the peak shear value has been recorded.

Usually several iterations of test are performed using differed normal stress values. Soil failure is marked by the inability of the sample to resist further load. Once the vertical and horizontal displacements and horizontal and vertical loads are noted, along with the peak shear force, critical state shear strength, peak and critical state friction angles are tabulated (Budhu 2011b). In this study, specimens prepared from bentonite and bentonite-stabilisers were subjected to normal stresses of 50kPa, 100kPa and 200kPa after different curing periods and changes in the shear strength parameters including the shear stress (τ), internal frictional angle and cohesion. DST is a particularly important test if the planar strain failure is likely to occur in the soil mass. It is used for the calculation of soil shear strength under consolidated drained/undrained conditions. For the purpose of this study, it was performed by using a shear box that shears the sample under a specified shearing rate (Figure 4.27).

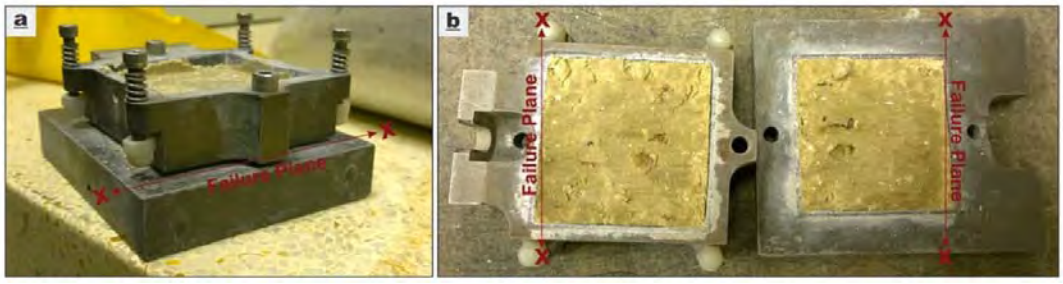

Figure 4.27 Direct Shear sample Assembly (a) Compacted Specimen in Shear Box, and (b) Sheared/Failed Specimen

As can be observed from the above picture, the apparatus mainly consisted of a cubical shear box which contained an open metals box that could be split horizontally. Grooved or serrated metal plates were placed on the top and bottom of the soil specimen, along with porous stones. Figure 4.27(a) illustrates one of the bentonite-stabiliser samples, placed and compacted inside the metal box. The two

halves of the metal box, referred to as upper and lower boxes, were approximately of equal dimensions and during shearing of sample under controlled normal stress, lateral load was applied to push the upper part under controlled strain. This induced a sample shear failure along the horizontal plane "XX", causing the specimen to split along that plane, as exhibited by Figure 4.27(b).

In order to quantify the effects of increasing curing periods or stabiliser proportions in the bentonite-stabiliser composites, a non-dimensional parameter based upon the strength development index introduced by Hasan et al. (2015) was adapted. The shear stress index "τ_I" employed in this study is empirically defined as:

$$\tau_I = \frac{Shear\ stress\ of\ pure\ bentonite\ sample}{Shear\ stress\ of\ bentonite{-}stabiliser\ composite\ sample} \leq 1 \qquad \text{Equation (4.7)}$$

The value of shear stress index indicates the efficiency of the stabilisation process and is directly correlated with the peak shear stress sustained by the specimen before failure. Higher τ_I values are attributed to lower shear strength of the stabilised composite and on the other hand, lower τ_I values are indicative of an enhancement effect in the shear strength. The upper limit of "1" indicates that the addition of stabilisers cannot generate reduction in the shear strength. The shear stress index has been extensively used in this research for identifying the effect of stabilisers which became more significant as the curing of the samples was continued.

4.6.1 Effect of Curing Period on Shear Strength Parameters

Similar to the laboratory investigations performed for evaluating the development of compressive strength of pure bentonite clay and bentonite – stabiliser composites with sample curing time, the shear strength parameters were evaluated against the curing period. The parameters of cohesion, angle of internal friction and sample shear strength were determined for the sample curing periods of 1, 3, 7, 14, 21 and 28 days to identify the effects on sample shear properties.

Shear strength of bentonite clay appeared to be largely unaffected by curing period, provided the normal stress has been kept constant as the increase in the induced vertical stress triggered an increase in the shear strength (Figure 4.28). At normal stress of 50kPa, pure bentonite sample S1G1 had a shear strength of 79.90kPa when

the sample curing time was kept at 1 day, which further developed to 80.50kPa and 81.20kPa as the sample curing period had reached 3 days and 7 days, respectively. Further sample curing caused the shear strength to further develop to 81.80kPa and 81.90kPa for 14 days and 21 days of sample curing. Even though these variations in the shear strength did not exceed 2.5% from 1 to 21 days of curing, the sample curing period of 28 days failed to further increase the shear strength as sample peak shear stress value of 81.90kPa was observed for the sample S1G1. However, generally the results of pure bentonite clay samples exhibited same cohesion and similar internal frictional angle values.

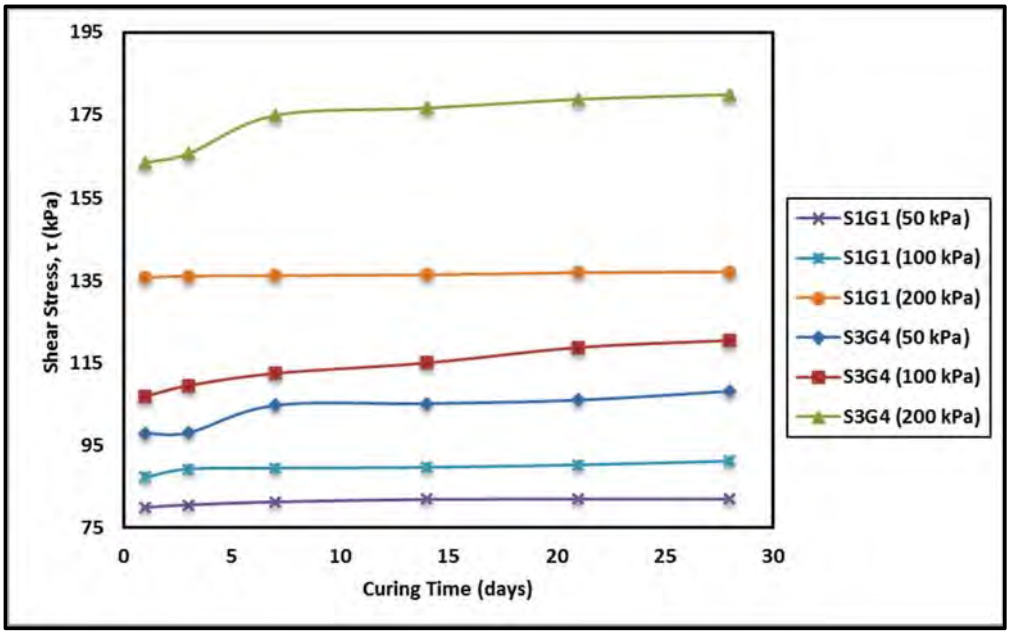

Figure 4.28 Shear stress – curing time relationships for pure bentonite (S1G1); and 76% bentonite, 4% GGBFS and 20% CW (S3G4) bentonite-stabiliser composite for 50kPa, 100kPa and 200kPa normal stresses

The effects of curing time become more pronounced with the addition of stabilisers. For all bentonite-stabiliser composites, the shear strength generally tended to increase with an increase in the curing period irrespective of the normal stress applied to the specimens. Optimum increase in shear strength was observed for the sample S3G5, which displayed a τ_I value of 0.71 corresponding to a shear stress of 193.05kPa at 0.51mm for the bentonite-stabiliser composite and shear stress of 137.10kPa at 0.91mm for the pure bentonite clay specimen, when subjected to

normal stress of 200kPa and a curing period of 28 days as illustrated by shear values displayed in Figure 4.28. This also shows that for the specimens S3G5 subjected to 200kPa of normal stress, 28 days of curing produced an increase of 17.58kPa in the shear stress compared to the 175.47kPa of S3G5 specimen after 1 day of curing to a corresponding horizontal displacement of 0.61mm (Figure 4.29). Therefore, slight reduction in the horizontal displacement observed upon peak shear stress was also observed.

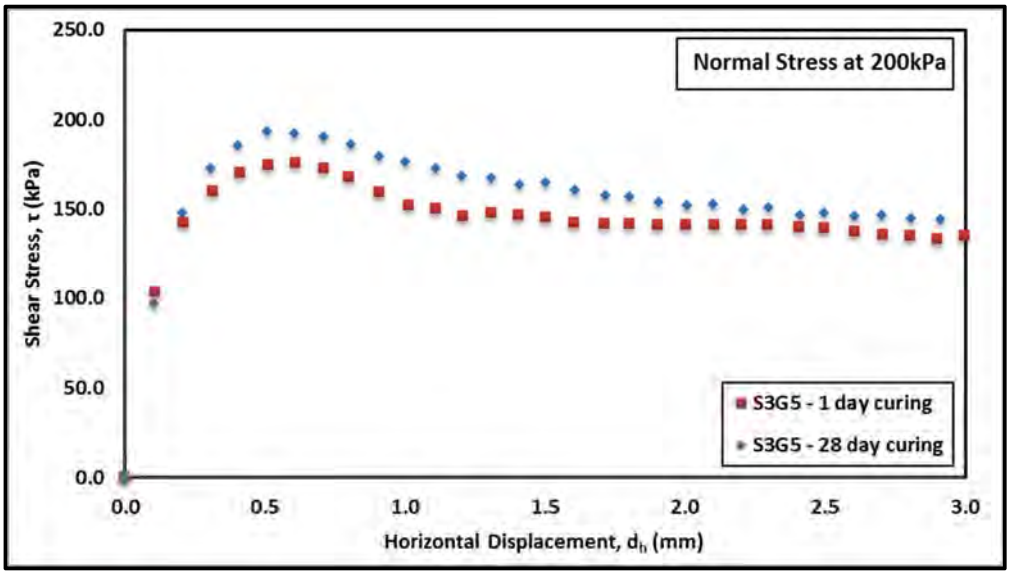

Figure 4.29 Shear stress – horizontal displacement curves for S3G5 at 200kPa normal stress after 1 day and 28 days of curing

The development of shear strength was observed for all stabiliser-bentonite composite specimens; however, the strength development was gradual and indicated that the curing of specimens produced increase in the shear strength under all normal stress conditions. On the individual parametric scale, sample cohesion tended to exhibit a uniform trend of increasing values with escalating curing period regardless of the stabiliser dosage in the composite. The trend was steeper during the initial period of curing and normally tended to gradually rise after 7 days of curing, whereas the highest cohesion values were observed at 28 days curing period as shown in Figure 4.30. The cohesion value of pure bentonite sample ranged from 55.60kPa for 1 day curing to 58.90kPa after the sample had been cured for 28 days. Similar to the trend observed for shear stress values, the cohesion values showed

more development with the increasing proportion of the stabilisers as the cohesion value for sample S3G2 ranged from 56.84kPa to 59.76kPa for the curing periods of 1 day and 28 days, respectively. Sample falling under the S3G5 category exhibited the most prominent development in the cohesion value as 28 days of curing produced cohesion of 67.26kPa compared to cohesion value of 61.9kPa after the sample was cured for only one day.

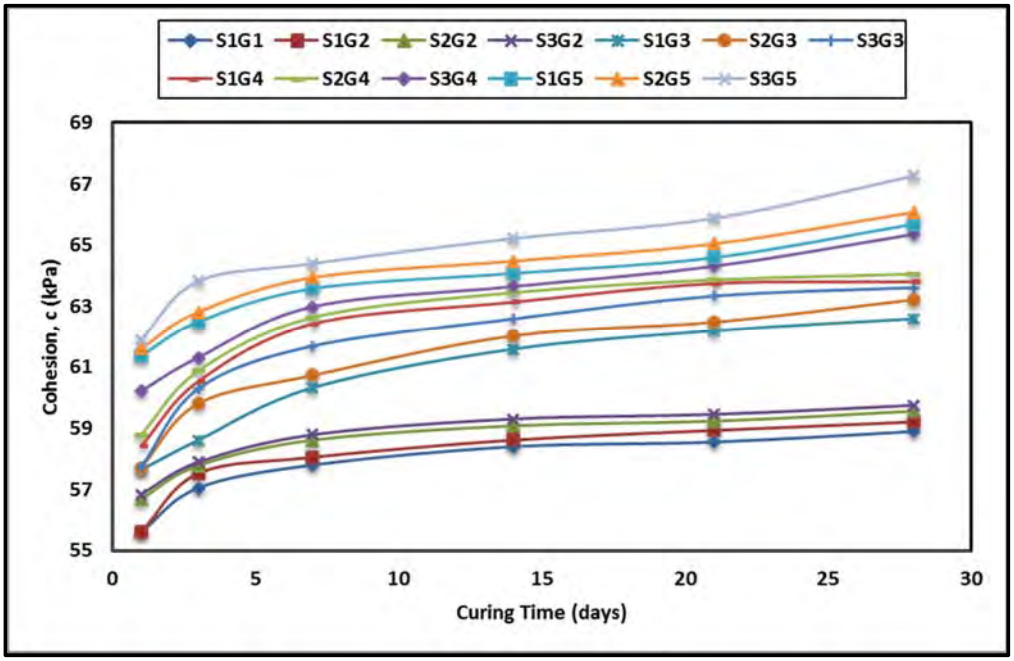

Figure 4.30 Cohesion – curing time relationships for pure bentonite and all tested bentonite-stabiliser composite specimens

Similar to the trends observed for cohesion, the internal frictional angle values increased with the increasing curing period. Even though the variations in the frictional angle with curing period inclined to be higher with further curing, the rise was gradual for majority of the samples and exhibited an arbitrary increase in succeeding frictional angle values for most of the test composite specimens as Figure 4.31 shows. It can be observed that all bentonite-stabiliser composites exhibited increased angles of internal friction as the curing of specimens progressed. Pure bentonite clay specimens displayed an internal friction angle value of 20.43° ± 0.5°, a variation of approximately 2% between all the investigated curing periods. For bentonite-stabiliser composites, a direct correlation was observed between the

gradual increase in the internal friction angle and the sample curing period. Curing period of 28 days generated the maximum internal friction angle for all sample groups. Although the results showed that the growth in the value of internal friction angle became more pronounced as the proportion of the stabilisers increased in the bentonite-stabiliser composite, interestingly, as the proportion of slag was lower in the bentonite-stabiliser composites, increasing volume of construction waste produced a lower frictional angle value.

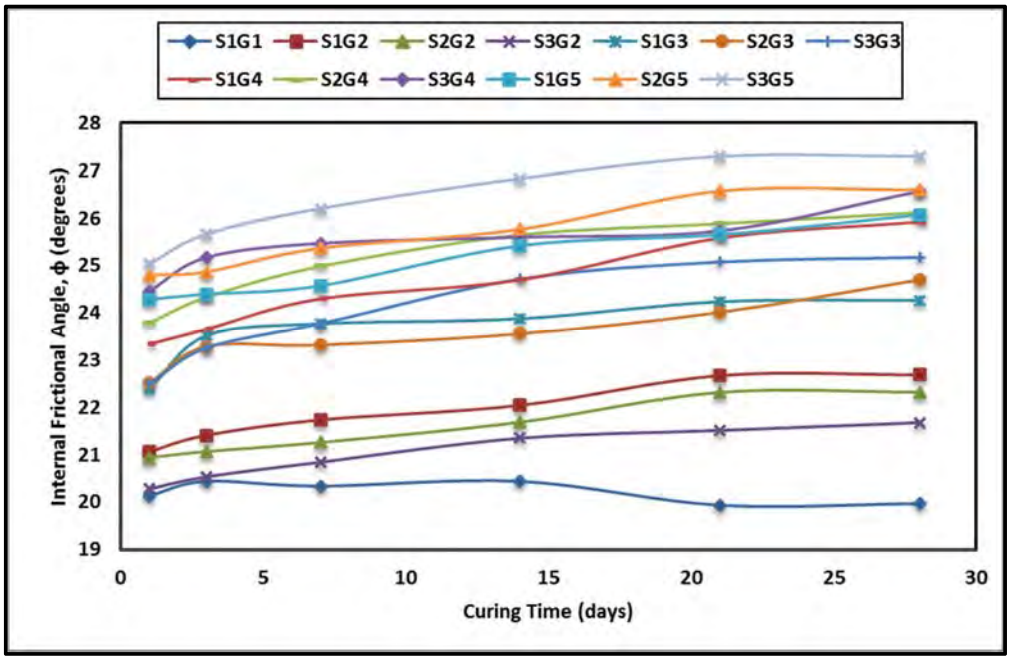

Figure 4.31 Internal frictional angle – curing time relationships for pure bentonite and all tested bentonite-stabiliser composite specimens

Approximately all of the bentonite-stabiliser composite samples had gained maximum degree of internal friction angle by 21 days of curing and further curing only produced nominal increase in the frictional angle value, with the value remaining within the range of 0.001° – 0.836°. The maximum increase in the internal friction angle due to curing was observed for specimens in the S3G5 category where the internal friction angle showed an increase of 2.3° after curing of 28 days attributed to a post-28 days' internal frictional angle value of 27.3° compared to the frictional angle value of 25.0° after 1 day of curing. The angle of internal friction increased due to changes in the soil gradation which increased with increasing

proportion of stabilisers. After 28 days curing, the cementation effect of GGBFS was also more pronounced, resulting in better bonding between the composite components.

4.6.2 Effect of Stabiliser Percentages on Shear Strength Parameters

The results of comparative analysis on sample shear strength parameters; namely cohesion, internal frictional angle and shear strength with sample curing time showed a regular correlation between the proportions of the stabilisers in the bentonite-stabiliser composites and the development of frictional angle similar to sample shear stresses and cohesion values. Evaluation of the calculated shear strength parameters showed that the introduction of stabilisers produced significant improvements in the shear strength and the effect of each additive was also evaluated. Figure 4.32 shows the relationship between the percentage of GGBFS in the bentonite-stabiliser composite specimens, prepared with different percentages of construction waste (10%, 15% and 20%), and the internal angle of friction (ϕ). Moreover, the effect of increasing the volume of construction waste in the bentonite-stabiliser composite for a specific proportion of GGBFS has been illustrated in Figure 4.33.

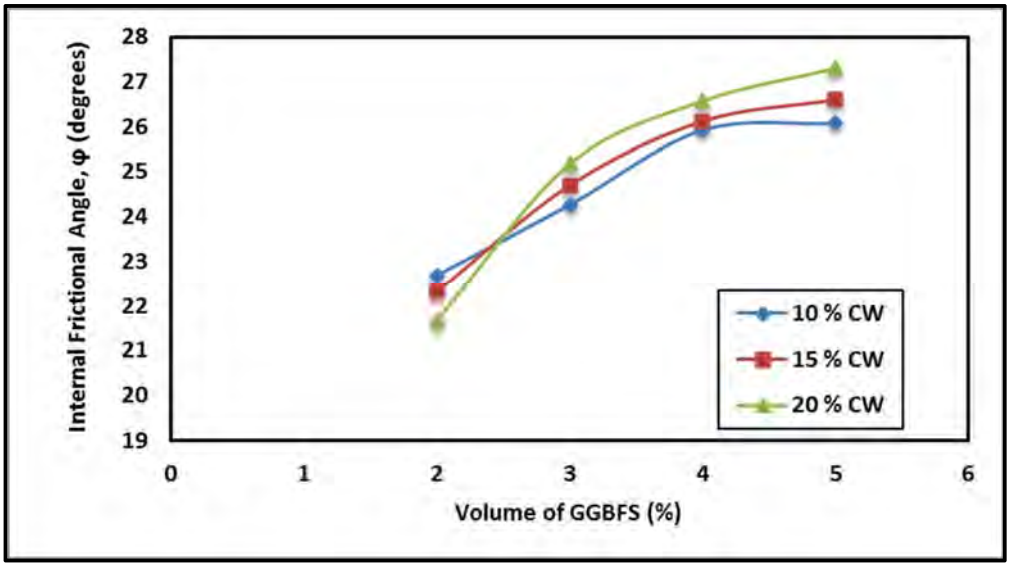

Figure 4.32 Development of internal frictional angle with volume of GGBFS for 28 days curing period

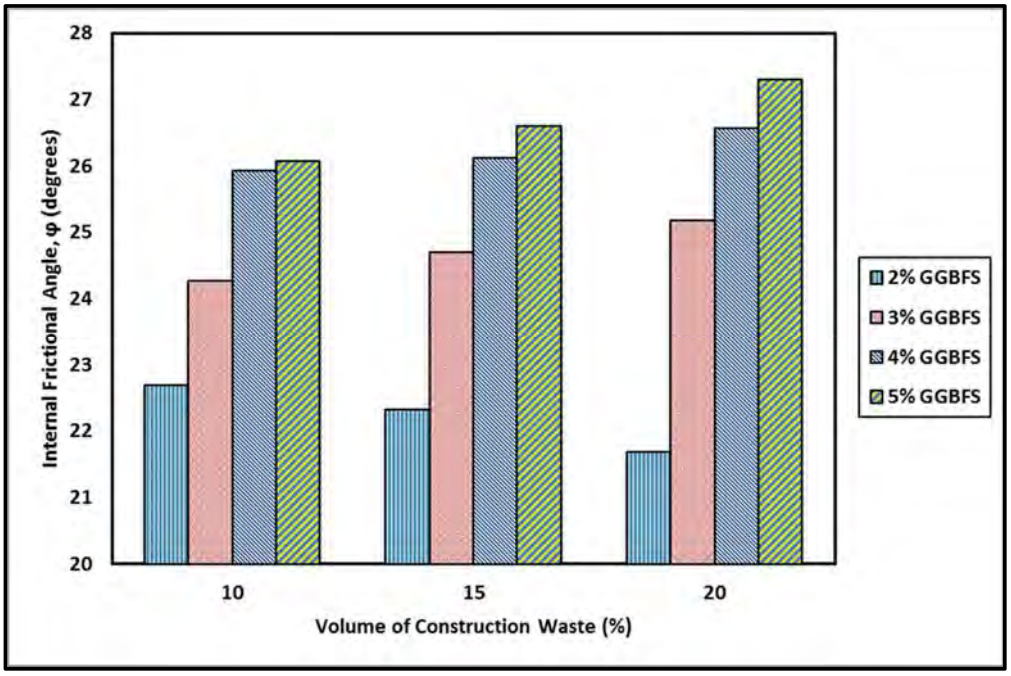

Figure 4.33 Development of internal frictional angle with volume of CW for 28 days curing period

Introduction of smaller amount of GGBFS at 2% caused the internal friction to increase by 2.7° when the percentage of construction waste was kept at 10% to generate a value of 22.7°, but the progression of frictional angle became more prominent after the volume of slag was further increased as for 3% proportion of GGBFS in the bentonite-stabiliser composite also containing 10% CW, the frictional angle further developed to be 24.3° showing increase of 4.3° in the S1G3 category samples compared to pure bentonite samples at 28 days curing period. Moreover, addition of construction waste reduced the internal friction angle when the proportion of slag was lower in the composite mixture.

For sample group 2, the frictional angle value dropped by 0.4° and further plummeted by 0.6° attributed to frictional angle values of 22.3° and 21.7° for the respective CW proportion of 15% and 20% in the mixture after curing period of 28 days. However, this decrement in frictional angle with increasing construction waste volume was limited to lower proportion of slag as for sample group 3 which contained 3% of GGBFS, the frictional angle value developed by 0.43° to 24.7° as the CW volume was increased from 10% to 15% and then 25.2° as amount of CW

was set at 20%, for 28 days of curing period. Similar trends were observed for samples containing 4% and 5% GGBFS cured for 28 days with the enhancement effect of GGBFS more prominent as the curing progressed. In general, variations in internal friction angle for 3% GGBFS sample group remained < 4% due to changes in CW quantities, whereas increments in percentage of slag to 4% caused a rise of more than 6%. Furthermore, the ϕ value developed to 26.1° when the slag content was increased to 5% for constant volume of CW at 10%. The optimum GGBFS dosage for increasing the ϕ value was found to be 5% which produced an increase of approximately 6° with sample S1G5 displaying a ϕ value of 26.1° after 28 days of curing and 10% CW, however, introduction of further construction waste caused the angle to increase up to 27.3° as the CW percentage increased to 20%. Similarly, the cohesion values of test specimens exhibited the tendency to increase as the stabiliser percentages were increased, as can be seen in Figure 4.34 and Figure 4.35. The trend continued in sample groups regardless of the type of stabiliser that was increased in the composite. As the cohesion values remained affected by the sample curing time, the increment in the cohesion value was similar for all samples with the same proportion of both additives in the bentonite-stabiliser composite.

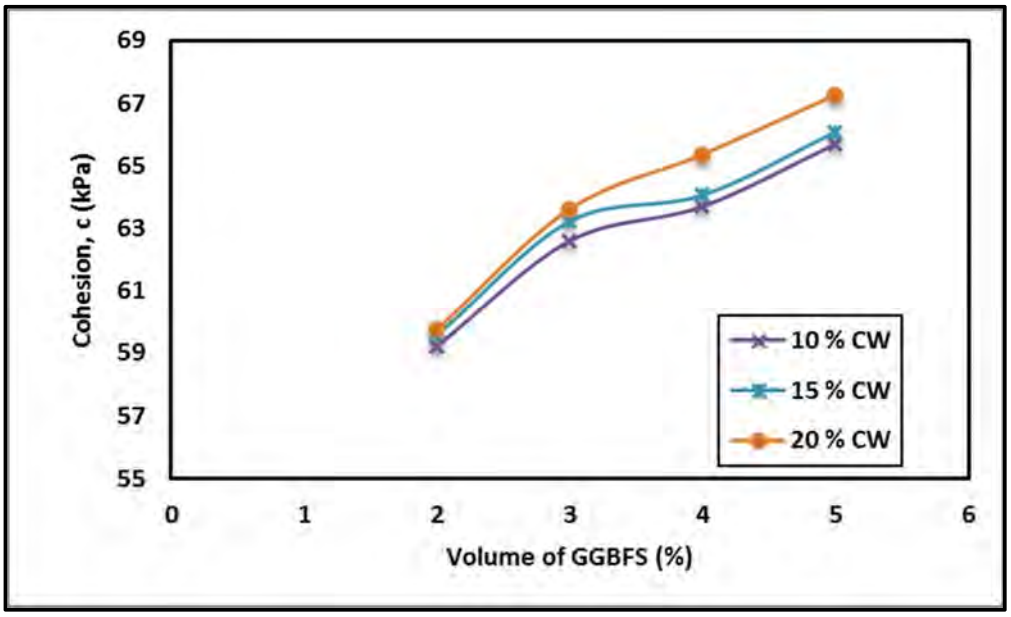

Figure 4.34 Development of cohesion with volume of GGBFS for 28 days curing period

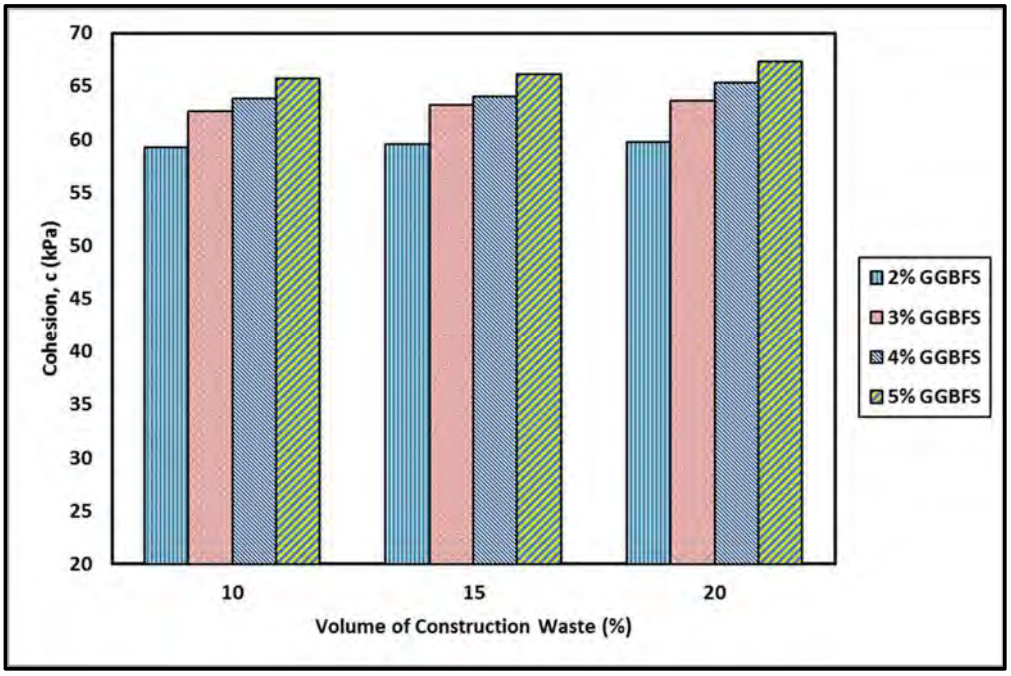

Figure 4.35 Development of cohesion with volume of CW for 28 days curing period

Cohesion value obtained for pure bentonite clay was 58.90kPa which was only nominally enhanced by 0.5% to give a cohesion value of 59.21kPa when 2% of GGBFS and 10% CW were added to bentonite in the sample mixture. Nonetheless, further increment was observed as the cohesion value increased to 59.57kPa when the volume of CW was increased to 15% while the GGBFS proportion remained unchanged and increased to 59.76kPa as the amount of CW in the mixture grew to be 20%. Similar trend was observed upon further increment of the additives as the cohesion value increased to 62.60kPa for 3% of GGBFS and 10% CW and 64.06kPa for the CW content of 15% and GGBFS volume of 4% in the bentonite-stabiliser composites. The highest development in the cohesion value was observed for the sample S3G5 with around 14.2% increase compared to the pure bentonite sample as the cohesion value increased to be 67.26kPa when the volumes of GGBFS and CW were 5% and 20% respectively. This observation can be attributed to the variations in the physical characteristics such gradation and hydraulic nature of the bentonite-stabiliser composites triggered by the increasing proportion of the two additives in the sample mixture.

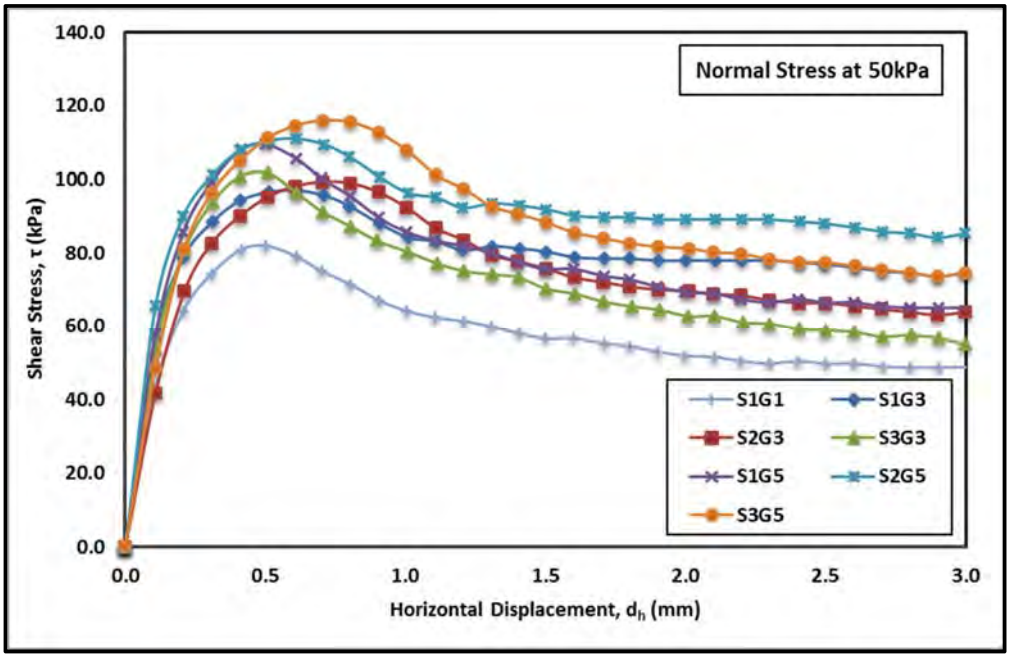

Figure 4.36 Shear stress – horizontal displacement curves for samples S1G1, S1G3, S2G3, S3G3, S1G5, S2G5 and S3G5 at 50kPa normal stress after 28 days of curing

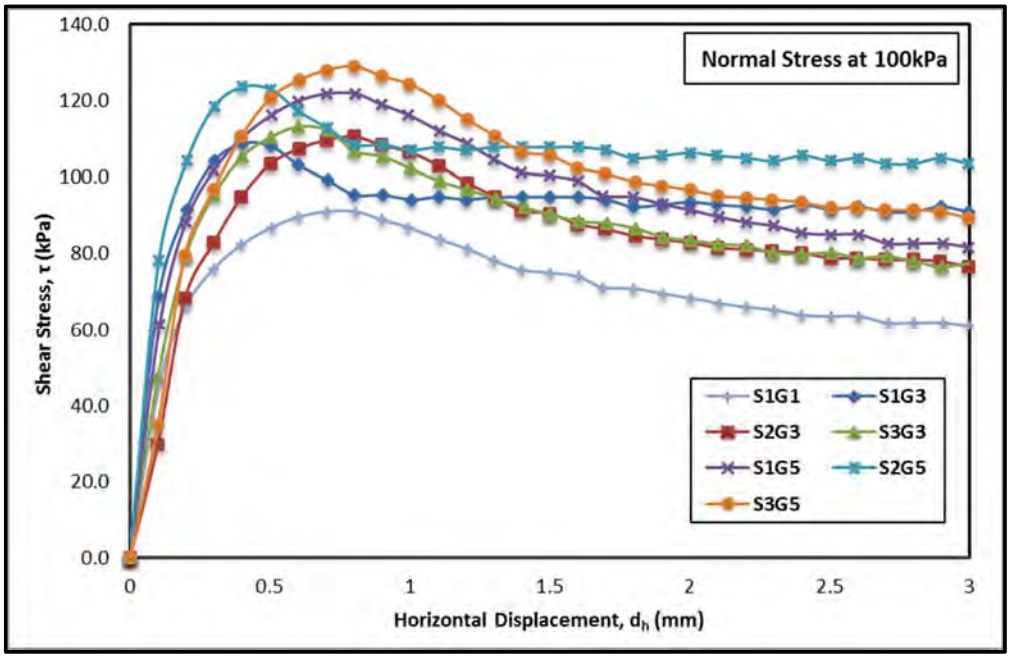

Figure 4.37 Shear stress – horizontal displacement curves for samples S1G1, S1G3, S2G3, S3G3, S1G5, S2G5 and S3G5 at100 kPa normal stress after 28 days of curing

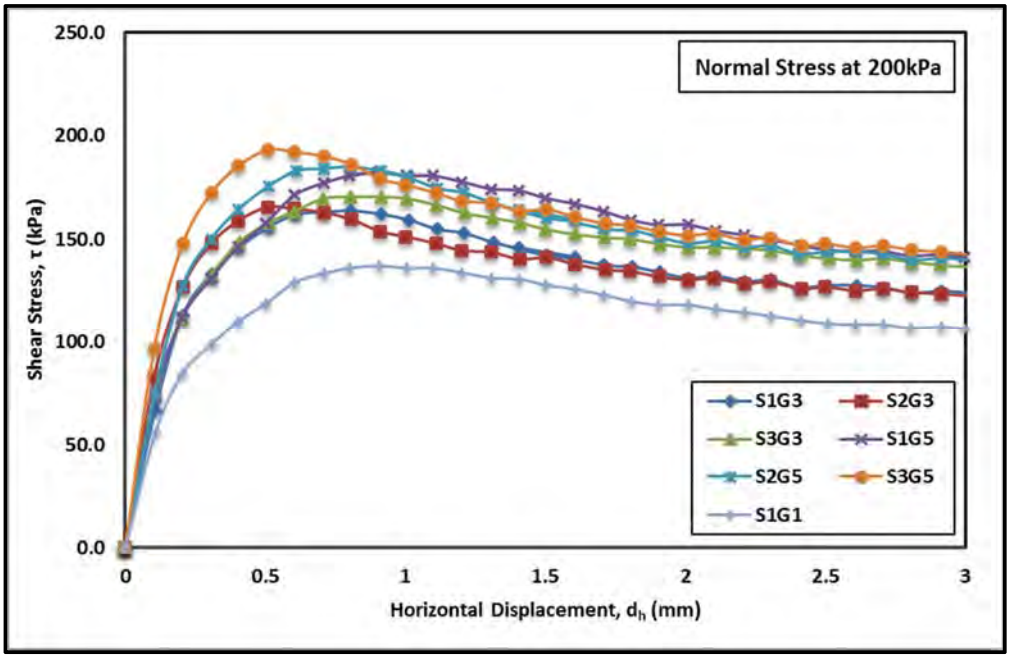

Figure 4.38 Shear stress – horizontal displacement curves for samples S1G1, S1G3, S2G3, S3G3, S1G5, S2G5 and S3G5 at 200kPa normal stress after 28 days of curing

Some of the typical shear stress-horizontal displacement curves for pure bentonite clay and bentonite-stabilisers composites after 28 days of curing have been illustrated in Figure 4.36 –Figure 4.38. These sample groups have been selected to represent the general trend that was observed for the entire specimen matrix, and therefore, the graphs were drawn based upon the minimum, moderate and maximum additive percentages. The initial slopes of the $\tau - d_h$ curves for all samples exhibited similarities provided the normal stress had been kept constant.

At a normal stress of 50kPa, pure bentonite clay sample showed a peak shear stress value of 81.90kPa occurring at displacement of 0.50mm and was improved upon introduction of 3% GGBFS and 10% CW to 97.06kPa, corresponding to a τ_I value of 0.84. The τ_I further reduced to 0.82 as the volume of CW increased to 15%, resulting in failure at shear stress of 99.35kPa and 0.70mm displacement, and at shear stress of 101.68kPa when the CW proportion became 20% for the constant GGBFS proportion of 3%, as demonstrated in Figure 4.36. It also shows that as the volume of GGBFS was raised to 5%, the peak shear stress exhibited by the sample prior to failure reached 109.44kPa occurring with horizontal displacement of

0.50mm. The specimens with 5% GGBFS and vertical stress of 50kPa showed a similar trend of increasing peak shear stress value upon increments of the CW content in the mixture as the samples from group 3 that contained 3% of GGBFS as the peak shear stress upon failure which developed as the quantity of CW in sample escalated to 15%, corresponding to peak shear stress of 111.02kPa and then 115.95kPa for 20% CW.

Figure 4.37 displays that when the normal stress was increased to 100kPa, pure bentonite clay sample S1G1 demonstrated failure when the horizontal displacement had reached 0.7mm for a shear stress value of 91.10kPa. After adding 3% GGBFS and CW volume of 10%, the shear resistance of the sample was improved as it failed at peak shear stress of 108.76kPa, this corresponds to failure at a horizontal displacement that is 0.3mm less than the pure bentonite sample.

Similar to the trend observed for samples subjected to 50kPa of normal stress, peak shear stress value further increased to 110.64kPa as the proportion of construction waste increased for sample S2G3, which contained 3% GGBFS and 15% CW corresponding to a failure strain of 0.80mm. The tendency for shear stress increment in case of 100kPa normal stress samples with addition of further amount of GGBFS was also similar to the samples exposed to a normal stress of 50kPa.

The peak shear stress increased to 121.88kPa for a displacement of 0.81mm for sample S1G5 which constituted of 5% GGBFS and 10% CW in the bentonite-stabiliser composite. Furthermore, the shear strain also exhibited a similar trend as the sample had failed a displacement value that is 0.3mm higher than sample S1G3. In addition, the maximum shear stress was again associated with sample S3G5 that exhibited a peak shear stress value of 129.13kPa and the pure bentonite clay sample yielded the lowest shear stress value of 91.10kPa.

The shear stress-horizontal displacement relationships for the direct shear strength tests on pure bentonite and bentonite-stabiliser composite samples that were subjected to 200kPa of normal stress are illustrated in Figure 4.38 which also displayed similar shear strength trends as the 50kPa and 100kPa samples. The shear stress shown by pure bentonite clay sample at failure was 55.2kPa higher than that

exhibited by the same sample at 50kPa, corresponding to respective peak shear stresses of 137.1kPa for strain value of 0.91mm.

Development in shear strength was observed for the bentonite-stabiliser composite sample compared with the pure bentonite clay sample as the inclusion of 3% slag and 10% construction waste yielded a shear stress value of 163.88kPa whereas the strain value had approximately reached 0.80mm, which was 0.11mm lower than the pure bentonite clay sample. Moreover, the peak shear stress generated by sample containing additional 5% of construction waste, i.e., sample S2G3, was approximately 1.74kPa higher than sample S1G3, failing at 165.62kPa at displacement of 0.51mm.

These results correspond to the observation from the earlier samples that indicated a correlation between evolution of shear stress in the samples and the increasing percentages of the stabilisers. This hypothesis was further supported by the increment of peak shear stress for sample S1G5 that had 10% construction waste with 5% slag exhibiting failure at maximum shear stress of 182.22kPa, corresponding to τ_I of 0.75. The lowest value of τ_I at 0.71 was observed for sample S3G5, which shows the maximum improvement in the shear strength, as the sample displayed peak shear stress of 193.05kPa showing an enhancement effect of 55.95kPa for the bentonite-stabiliser composite as compared with the pure bentonite clay sample.

4.6.3 Effect of Induced Normal Stresses on Peak Shear Stresses

The evaluation of peak shear stresses demonstrated by the test samples upon failure were closely related with the magnitude of the normal stress induced on the samples. The value of the peak shear stress for all samples increased directly with the increase the normal stress value. For pure bentonite sample S1G1 cured for 28 days, the peak shear stress value increased from 81.90kPa to 91.10kPa as the normal stress amplified from 50kPa to 100kPa and further growth of 46kPa as the peak shear stress value became 137.10kPa for normal stress value of 200kPa. Figure 4.39 shows the plot of shear-net normal stresses of pure bentonite and bentonite-stabiliser composite samples obtained after a series of direct shear tests to study the sample responses under normal stresses of 50kPa, 100kPa and 200kPa.

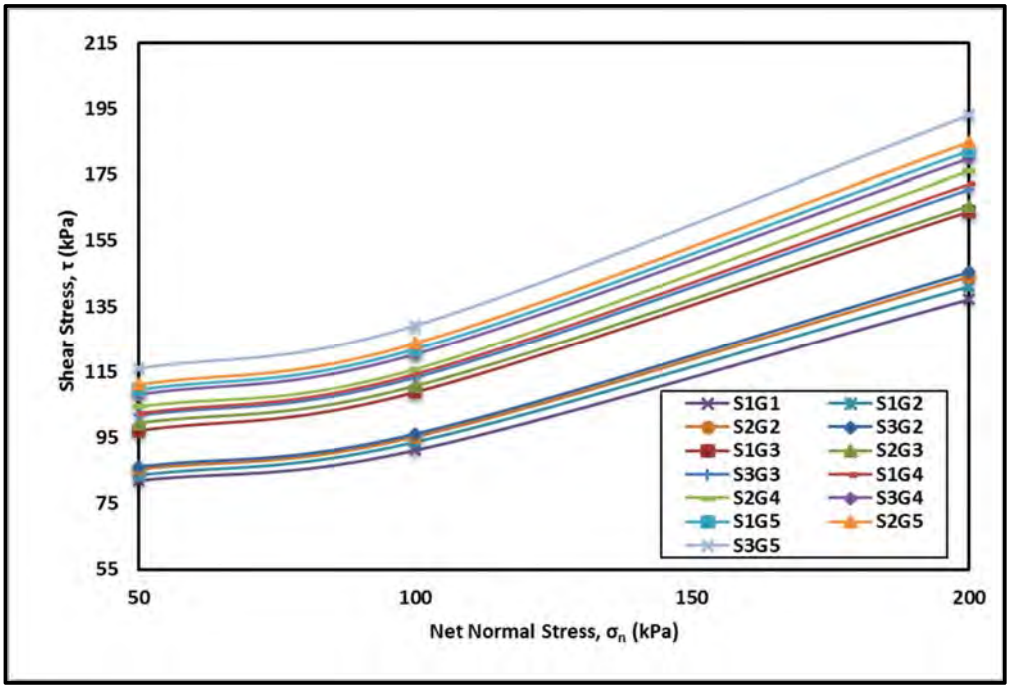

Figure 4.39 Development of shear stresses under different normal stresses for pure bentonite and bentonite-stabilisers composites after 28 days of curing

Comparative analysis of sample failures for pure bentonite sample and 2% slag and 10% construction waste content sample shows that even though the sample failure for the later occurred at a higher shear stress than the pure bentonite specimen, the difference in peak shear stresses was not significant and ranged between 1.65kPa – 3.97kPa for different normal stresses. The gap between the peak shear stresses of pure bentonite and bentonite-stabiliser composite samples widened with the increment of the normal stress as the same sample S1G2 showed a peak shear stress value of 95.22kPa at 100kPa whereas sample S1G1 failed at 91.10kPa. Notable development of shear stress was observed when the slag content was doubled for sample S1G4 which contained 4% slag and 10% CW, as the maximum shear stress value before failure had reached 102.24kPa for normal stress of 50kPa. Moreover, the variation between the unstabilised and stabilised samples became more noticeable as the sample was subjected to a normal stress of 100kPa when the sample S1G4 displayed a shear stress value of 114.24kPa which was 23.14kPa higher than the pure bentonite clay sample. Overall, as illustrated in Figure 4.39, tested samples exhibited maximum improvement in the shear strength under normal stress of

200kPa when the specimen curing time had reached 28 days. In general, direct correlation was observed between the net normal stress imposed upon the sample and the maximum shear stress exhibited by sample prior to failure.

4.6.4 Evaluation of Shear Indices for Stabilised Samples

Shear index "τ_I" values were also calculated to evaluated the variation in the shear strength of bentonite clay after stabilisation with the two additives. Since the maximum development in shear stress was observed for the sample curing period of 28 days and normal stress of 200kPa, the shear indices were also calculated for the samples subjected to 200kPa of vertical stress and after the sample curing time had approached 28 days. Moreover, the value of τ_I generally tended to reduce with increasing stabiliser percentages as illustrated in Figure 4.40.

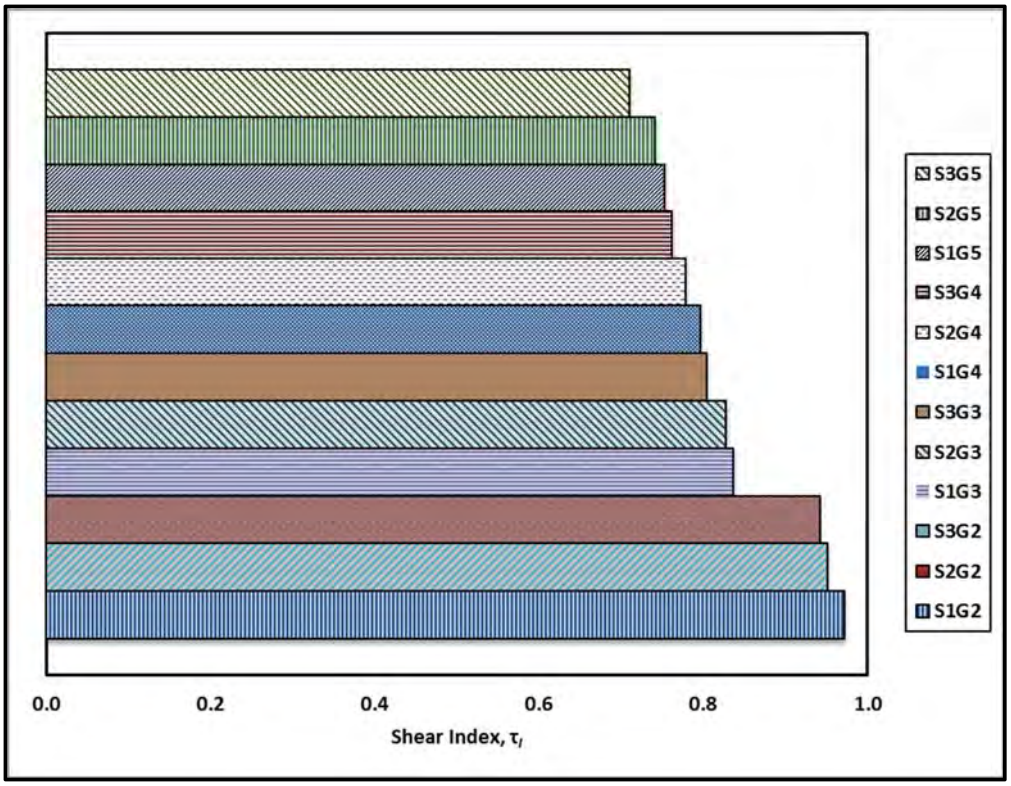

Figure 4.40 Shear indices for test specimens under 200kPa of normal stress and 28 days curing period

For the minimum stabiliser dosage, i.e., 2% of GGBFS with CW proportion of 10%, the shear index value was observed as 0.97. This value continued to reduce as the

additive proportions increased, as for sample S2G2, shear index dropped to 0.95 and further reduced to 0.83 for sample S1G3. Overall, sample group 2 showed the highest values of shear indices which ranged from 0.971 to 0.94. As the GGBFS content in the sample increased to 3%, the median values of shear indices were observed for the sample group 3, ranging from 0.83 for S1G3 on the higher side to the lowest value of 0.8 for S3G3. However, the lowest shear indices among all sample groups were observed for the sample group 5 with 5% GGBFS content with 0.71 as the lowest shear index value, overall.

The development of shear stress with additives shows that both recycled aggregates and slag have positive effects on the shear strength behaviour of the bentonite clay tested in this research, for the studied curing and additive controlled conditions. Although the addition of construction waste had initially resulted in reduction of the cohesion value, as can be observed for adding gravely soil in clay, increase in the internal friction angle was noted followed by increase in cohesion after the passage of significant periods of sample curing time, which corresponded to higher shear value and lower τ_1 value for specimens after 28 days of curing. The results displayed similarity with those observed for the UCS test where the change is soil particle size distribution, due to increment in the proportion of construction waste, resulted in higher strength values. Similarly, CW was observed to mechanically stabilise the soil by changing gradation of the composite soil. Since well-graded soil has higher strength, the shear strength increased with increasing proportion of CW. As stated earlier, some pozzolanic reactions have been observed by past researches when slag was added to the clayey soil in presence of water. The hydration of GGBFS is highly dependent on water and requires more time to occur in absence of an alkali activator. This resulted in the generation of higher strength after 28 days of curing when 5% of GGBFS, the maximum in the test specimen matrix, was introduced.

CHAPTER 5
SUMMARY, CONCLUSION AND RECOMMENDATION

5.1 INTRODUCTION

The modernisation of architectural practices and industrialisation has led to large quantities of debris generated from the demolition of structures. This construction waste (CW) forms a major component of the solid waste in many countries, with only marginal quantities being utilised in backfilling on construction sites and the rest being mostly dumped on already scarce landfill sites. Therefore, construction waste causes land, resource and material depletion and deterioration (Behera et al. 2014a; Wang, Li and Tam 2014). The Australian construction industry alone produces approximately 38% waste for landfills each year (Li and Du 2015).

Furthermore, many countries have problems with illegal or environmentally unsafe disposal of industrial by-products, for instance blast furnace slag. Globally growing concern over environmental safety has driven researchers worldwide to find more sustainable solutions to these problems and reuse waste materials. Similarly, researchers have also worked to find alternative materials for achieving soil stabilisation utilising several industrial by-products (Al-Malack et al. 2014; Amu, Fajobi and Afekhuai 2005a; McCarthy et al. 2014).

This study employed the techniques of both mechanical stabilisation through the induction of recycled construction waste, and chemical stabilisation by introducing GGBFS, in controlled proportions. Furthermore, the curing time of stabilised samples was also investigated as due to the hydraulic nature of GGBFS, the potential pozzolanic reactions occurring within the bentonite-stabilisers composite specimens are a time-dependent process. As the research study comprised of experimental investigations, a series of geotechnical, microstructural, imaging and spectroscopic tests were conducted for the purpose of achieving the goals of this study. The summary of the experimental results presented in the previous chapters and the conclusions drawn from these results have been presented in this chapter. In addition, directions for prospective future research to build and improve upon this

research project. This chapter is therefore, divided into three primary sections as illustrated in the flowchart of the chapter outline in Figure 5.1.

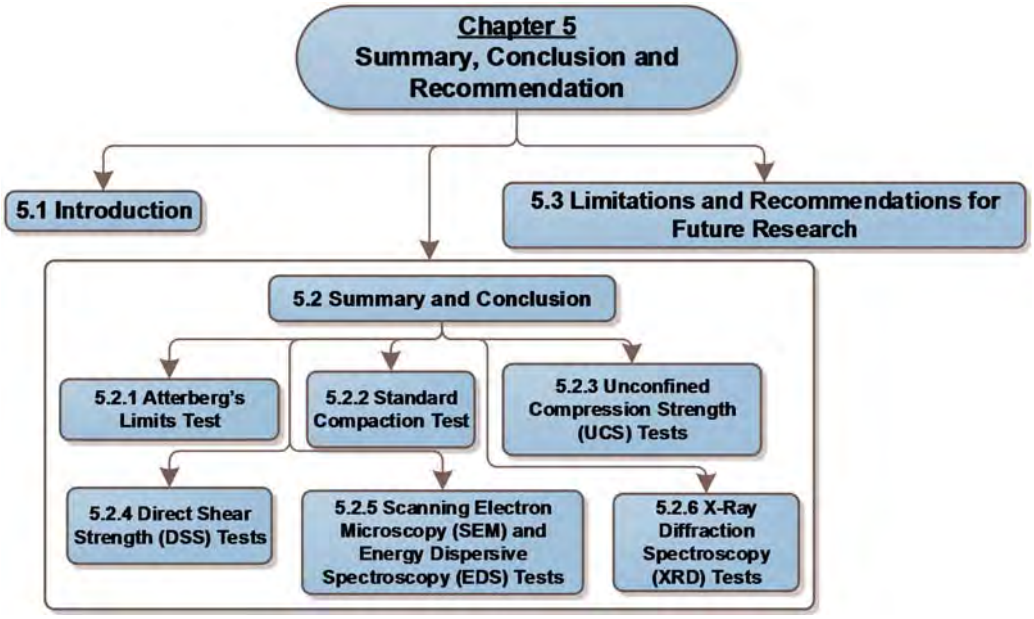

Figure 5.1 Outline of Chapter 5

5.2 SUMMARY AND CONCLUSION

Feasibility evaluation of using recycled CW and GGBFS for bentonite clay stabilisation was performed in this research by conducting optical microscopy imaging tests, scanning electron microscopic imaging tests, energy dispersive spectroscopy, X-ray diffractive spectroscopy, Atterberg's limits tests, standard compaction test, unconfined compressive strength tests and direct shear tests on the test materials and composite specimens. The geotechnical laboratory experiments employed two controlling parameters to assess the efficiency of the stabilisation process. These parameters were of sample curing time; namely 1, 3, 7, 14, 21 and 28 days; and stabiliser percentages; 2%, 3%, 4% and 5% for GGBFS and 10%, 15% and 20% for CW. The results showed that both additives can be used effectively for stabilisation purposes. The XRD results indicated that the presence of moisture in the mixture resulted in changes in the mineralogical composition of the stabilised mixtures with $Ca(OH)_2$ formation due to the hydration of CaO. The microstructural SEM analysis of the treated specimens showed that the bentonite and slag particles

adhered to the construction waste and occupied the voids and vesicles. This phenomenon was also observable during the manual mixing as the mixture attained a granular appearance and a construction waste particle was found at the crux of many grains formed. As the ratio of the admixtures grew in the samples, more slag crystals and construction waste grains were available to be surrounded, causing the formation of a stronger structural bond.

5.2.1 Atterberg's Limits Test

In the study of fine-grained soils, i.e., clays and silts, the concept of soil consistency is used which is roughly a parameter for expressing the volume of water contained within soil system. Consistency is usually described in terms of Atterberg's limits. These limits are used for the identification of soil behaviour and are specifically utilised for the purpose of cohesive soil classification. One of these, the plastic limit (PL) of the soil, calculated in percent, can be used to classify the soil in various degrees of expansiveness. Holtz and Gibbs (Holtz and Gibbs 1954) have recommended a percent free swell test and categorised the soil based on plastic limit values as low (PL < 20), medium (12 < PL < 34), high (23 < PL < 45) and very high (PL > 32). Another criteria has been released by Austroads (Austroads 2007) to identify and classify the expansive soils which is based on liquid limit, plasticity index, expansive nature and the potential swell. This study employed cone penetrometer test for the calculation of liquid limit of pure bentonite clay, whereas controlled amount of water was added to bentonite clay and it was then rolled-off into thin threads to determine the plastic limit. The results have been presented in the following table (Table 15).

Table 15 Results of Atterberg's Limits Tests

Plastic Limit	Liquid Limit	Plasticity Index
38%	440%	402%

5.2.2 Standard Compaction Test

The standard compaction test or Proctor compaction is one of the most commonly performed tests in geotechnical engineering. It is conducted for the determination of optimum moisture content and maximum dry density of soil sample through

compaction of sample into a denser configuration by moisture addition and utilisation of mechanical rammers and/or compactors. The test procedure is summarised in the chart illustrated in Figure 5.2.

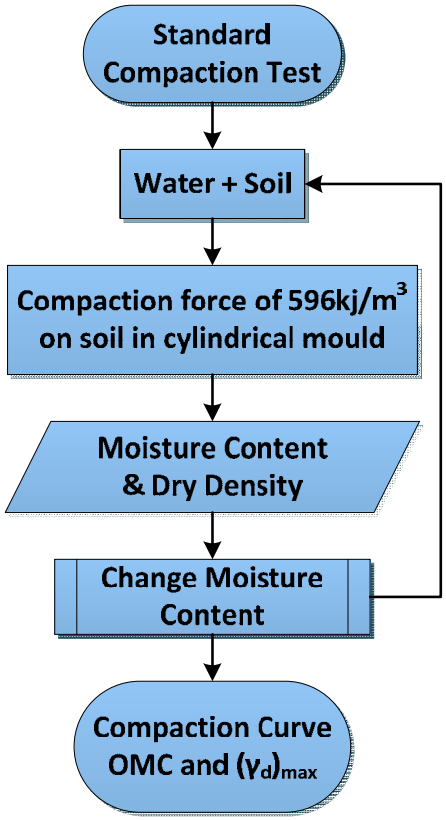

Figure 5.2 Standard Compaction Test Methodology and Outputs

The volume of water to be added was established in terms of the dry unit weight of the samples. Maximum dry density (MDD) and optimum moisture content (OMC) were obtained by performing standard compaction test (Standards Australia AS 1289.5.1.1 2003) and although the optimum moisture content may vary with variation in the additive proportion, this research has focused on analysing the effect of the stabiliser proportions and curing time on shear strength development and the OMC value was kept constant irrespective of the specimen composition. Standard compaction test was performed on bentonite clay in accordance with the Standards Australia AS 1289.5.1.1 (2003) by subjecting clay samples to 596kJ/m^3 compaction effort. After plotting the compaction curve, the $\gamma_{d_{max}}$ value was obtained as 1.08 gr/cm^3 for an optimum moisture content of 43%.

5.2.3 Unconfined Compression Strength (UCS) Tests

Unconfined compression strength tests were performed as per the Standards Australia AS 5101.4 (2008) specifications using GCTS Stress-Path Soil Triaxial System (STX-300). An axial load was applied at the constant rate of 1.0 ± 0.1mm/min and the testing was stopped once the deformation had been recorded. Two different parameter, stabiliser proportions and curing periods were used, as stated earlier.

The UCS test on pure bentonite specimen revealed that the compressive strength of bentonite clay remained unaffected by specimen curing time as the compressive strength was calculated to be approximately 76.675 ± 0.035kPa, for sample curing periods of 1, 3, 7, 14, 21 and 28 days. After introduction of additives, the UCS developed with increasing proportion of additive and curing period, probably attributed to the hydraulic nature of GGBFS and change in gradation and physical attributes of stabilised bentonite due to the induction of CW. A dimensionless parameter, called strength development index (SDI) was introduced to better quantify this effect, with higher SDI values attributed to better enhancement of compressive strength. For the median GGBFS proportion of 3% and CW proportion of 15%, UCS value increased by 32.663kPa to be 109.299kPa for the sample curing period of 1 day, corresponding to SDI value of 1.426. This variation in UCS further developed to 66.646kPa as sample curing period of 14 days caused UCS value to reach 143.343kPa, with SDI value of 1.869. Overall, both additives, GGBFS and CW produced positive results in improving the UCS values of the bentonite clay. The effects were more noticeable as the sample curing periods escalated. The maximum value of SDI, which shows the maximum improvement in the UCS value, was observed for bentonite sample containing 5% of GGBFS and 20% of CW. The SDI value was calculated to be 3.09 with UCS value of 236.93kPa for this sample, compared to UCS value of 76.65kPa for the pure bentonite sample, while both specimens were cured for 28 days under controlled conditions. The evolution of the UCS with increasing stabiliser proportions was influenced by the curing periods. The optimum results for all combinations were obtained after the curing period of 28 days. It was observed that the UCS value for the bentonite clay sample stabilised with 5% slag and 20% construction waste grew from 131.42kPa after one day of

curing, to 236.93kPa after 28 days of curing. This corresponds to the maximum strength improvement observed in the treated samples and showed a 209.09% increase from the initial untreated sample strength or an SDI improved value of 3.09. The findings from the UCS tests on the stabilised specimens can be concluded as follows:

- The initial increment in the UCS with the increased percentage of the GGBFS was comparatively lower than the increase in the UCS when the existing slag percentage was higher in the mixture (4% and 5%).
- The hydration of calcium oxide in the mixture resulted in the formation of the calcium hydroxide $Ca(OH)_2$, which is a time-dependent phenomenon. Therefore, the effect was comparatively smaller after the first day of curing.
- The effects of increasing the percentages of construction waste in the stabilised mixture were more pronounced with the high percentages of GGBFS in the treated samples. The UCS value for the treated specimens increased from 124.77kPa to 127kPa when the CW proportion was increased from 10% to 15% for the one day curing period. This gave an SDI increase of 0.033, and another 5% addition of the construction waste led to an SDI increment of 0.055 with a UCS value of 131.42kPa.

5.2.4 Direct Shear Strength (DSS) Tests

Direct shear strengths of the stabilised and unstabilised specimens were calculated and the possibility of cohesion and angle of internal frictional angle improvements within the soil matrices was also explored, using different additive proportions and specimen curing periods. Moreover, normal stresses of 50kPa, 100kPa and 200kPa were used. A shear index (τ_I) was introduced for quantifying the effects of the stabilisation process, with lower τ_I values attributed to higher peak shear stress values.

The cohesion and internal frictional angle values of pure bentonite clay specimen remained unaffected by the curing period and remained in the range of 20.15° ± 0.25°. Similarly, cohesion values of 57.25kPa ± 1.65kPa were observed for the pure bentonite clay specimen. Furthermore, similar trend of approximately equal values with escalating specimen curing periods, was observed for shear strength values of

pure bentonite clay, irrespective of the induced normal stress, although, higher peak shear stress values were noted for higher normal stresses. The shear stress remained in the range of 80.90kPa ± 1.0kPa, 89.15kPa ± 1.95kPa and 136.45kPa ± 0.65kPa for normal stresses of 50kPa, 100kPa and 200kPa, respectively. The effects of curing period were noticeably higher as the proportion of both stabilisers increased in the bentonite-stabiliser composites. For GGBFS proportion of 2% and 10% of CW, the cohesion value remained same as that of pure bentonite clay at 55.60kPa when the sample was cured for 1 day. This immediately changed to a difference of approximately 1.92kPa between both sample categories, when sample curing period had reached 3 days, as the later sample displayed a cohesion value of 57.52kPa which further developed to 59.21kPa for 28 days curing period. The angle of internal frictional angle showed a similar trend with ϕ value of 21.7° for 2% GGBFS and 10% CW bentonite-stabiliser sample compared to pure bentonite sample ϕ value of 20.3°, for specimen curing period of 7 days and further developed to be 22.7° when 28 days curing period was achieved for the stabilised specimen of same stabiliser composition.

In addition, 28 days sample curing period also showed maximum improvement in the peak shear stress value for the 2% GGBFS and 10% CW samples, as τ_I values of 0.980, 0.973 and 0.971 corresponding to peak shear stresses of 83.55kPa, 93.62kPa and 141.07kPa for normal stresses of 50kPa, 100kPa and 200kPa, respectively. Increase in proportion of CW to 15% triggered further reduction in τ_I value as it degraded to 0.95, corresponding to shear stress of 144.05kPa for normal stress of 200kPa. In general, the sample cohesion and angle of internal friction angle tended to increase with the increasing percentages of both stabilisers and escalating specimen curing time. Furthermore, peak shear stresses values also increased with increasing curing period and stabiliser percentages, with higher values observed at higher normal stresses. Maximum cohesion value of 67.26kPa was observed for sample containing 20% CW and 5% GGBFS, cured for 28 days. This sample category also exhibited the maximum angle of internal friction at 27.3°, which interestingly remained same for both 21 days and 28 days of specimen curing. The lowest shear indices and therefore, the highest peak shear stress values were also observed for this sample at 28 days of curing. The shear index values were

calculated to be 0.706 (shear stress = 115.95kPa), 0.705 (shear stress = 129.13kPa) and 0.71 (shear stress = 193.05kPa) for the respective normal stresses of 50kPa, 100kPa and 200kPa. In general, the findings of the direct shear tests can be concluded as:

- Results exhibited the potential of both stabilisers in enhancing the shear strength parameters of bentonite clay. As the curing period escalated, development in both cohesion and internal frictional angle was observed for the bentonite-stabiliser composite specimens as sample S1G2 with 2% slag and 10% construction waste showed higher frictional angle of 22.7° compared to pure bentonite with ϕ value of 20.0° for curing period of 28 days. Initially, increment of construction waste volume decreased the frictional angle as sample S2G2 with an additional 5% CW content had a lower ϕ value of 22.3° for 28 days of curing.
- The trend reversed as for higher proportions of slag, at 3%, increments in construction waste volume resulted in occurrence of higher frictional angle values.
- Similar trends were observed for cohesion values as at lower proportions of GGBFS, nominal variations in the cohesion values were observed upon introduction of more construction waste particles as sample S1G2 and S2G2 showed respective cohesion values of 59.21kPa and 59.57kPa.
- The shear strength of specimens also tended to increase with an increase in the dosage of both stabilisers and specimen curing period. The development in the peak shear stress exhibited by the specimen upon failure was more noticeable at higher proportions of the stabilisers as sample S3G5 displayed shear stress of 104.97kPa compared to the 79.90kPa shear stress of pure bentonite sample subjected to 50kPa of normal stress and 1 day of sample curing period, corresponding to shear index value of 0.76.
- Further curing of specimens under constant normal stress resulted in widening of the gap between the respective peak shear stress values as the sample S1G1 had shear stress of 81.90kPa compared to 115.95kPa shear stress value of sample S3G5 cured for 28 days.

- Moreover, higher peak shear stress values were estimated for samples subjected to higher normal stresses, triggering higher variations between the shear stress values of stabilised and unstabilised specimens as the differences between peak shear stresses of samples S1G1 and S3G5 cured for 28 days were observed as 38.03kPa and 55.95kPa for normal stresses of 100kPa and 200kPa, respectively.
- Sample S3G5 also corresponded to the lowest shear index of 0.71 among the tested specimens which corresponds to the maximum development in shear stress to 193.05kPa, for 28 days of curing period and normal stress of 200kPa.

In general, similar to the UCS results, these results of direct shear strength tests are also supported by SEM micrographs and EDS spectra of stabilised specimen which showed bentonite and slag particles occupying voids and cracks in construction waste particles, which may contribute to better interlocking mechanism in the specimen particle matrix. Alkali oxides (Na_2O, MgO, CaO and K_2O), silica (SiO_2) and metallic oxides (TiO_2, Fe_2O_3 and Al_2O_3) were commonly found the composite specimens inducted by both bentonite and the two stabilisers. X-ray diffraction spectra suggested that the specimen curing might have resulted in hydration of CaO to produce $Ca(OH)_2$ from pozzolanic reaction of GGBFS. This can be attributed to the occurrence of higher cohesion and shear stress values of the stabilised samples with the progression of the stabiliser proportions and curing periods.

5.2.5 Scanning Electron Microscopy (SEM) and Energy Dispersive Spectroscopy (EDS) Tests

SEM and EDS tests were conducted on both contributing materials, bentonite clay, construction waste and ground granulated blast furnace slag and the bentonite-stabiliser composite mixture that exhibited the maximum shear and compressive strengths after the highest curing period of 28 days.

The SEM micrographs of bentonite clay showed that the bentonite particles somewhat lacked uniform crystalline shapes with sizes ranging from 10µm–30µm. The EDS peaks showed oxygen and silicon associated with the highest peaks whereas aluminium, calcium, iron, magnesium, sodium and titanium were also

found. This implied the presence of metal oxides and silica, normally found in montmorillonite category minerals of smectite clay group. Conversely, the SEM micrographs of GGBFS showed a definitive crystalline morphology, with particle sizes ranging from 30–45μm. The EDS spectra of GGBFS showed oxides of magnesium and silicon along with alumina, calcium oxide and ferric oxide. Moreover, lenticular shapes and surface cracks and cavities were observed in case of construction waste SEM micrographs images. EDS spectra showed variation in the peaks of each element between the particles as the sources of CW were largely diverse. In general, silica, alumina, iron sulphide, ferric oxide, calcium oxide and potassium oxide were found.

The SEM micrographs of stabilised bentonite clay, containing construction waste and GGBFS, showed that the finer bentonite and GGBFS particles occupied voids within the CW matrix. This could have resulted in generation of better inter-particle cohesion and interlocking, due to irregular shape of CW grains, causing higher shear and compressive strengths. The EDS spectra also confirmed the results of SEM micrographs as bentonite and GGBFS particles were found on the surfaces of CW grains.

5.2.6 X-Ray Diffraction Spectroscopy (XRD) Tests

SEM micrographs and EDS spectra peaks of contributing materials and bentonite-stabiliser composite mixture showed the presence of inter-locking and cohesiveness between particles. XRD analysis tests were conducted on pure bentonite and stabilised bentonite samples to further understand the existence of different materials on the stabilised mixture, using virgin clay mixture as a benchmark. The XRD characterisation results of pure bentonite clay illustrated the dominance of clay minerals such as quartz $[SiO_2]$, illites $[K_{1.5-1.0}Al_4[Si_{6.5-7.0}Al_{1.5-1.0}O_{20}](OH)_4]$, alkali feldspars $[(\mathrm{K,Na})[\mathrm{AlSi_3O_8}]]$, mica $[\mathrm{AlSi_2O_6(OH)_2}]$ and kaolinites $[\mathrm{Al_4[Si_4O_{10}](OH)_8}]$ (Deer, Howie and Zussman 2013). This confirms the findings from the EDS tests which also showed SiO_2 as the major component of the bentonite clay.

The stabilised sample subjected to XRD analysis was selected based upon the strength development index and shear index. The sample with 5% GGBFS and 20%

CW, cured for 28 days was associated with the highest SDI of 3.09 and the lowest τ_I of 0.71. In general, the X-ray diffraction bands on this sample showed similar peaks as those for the pure bentonite clay, with slight variation resulting from the formation of cementitious compounds. The dissimilarity from pure bentonite clay XRD peaks was the presence of calcium hydroxide or $Ca(OH)_2$, which might have formed as a result of the hydration of calcium oxide.

5.3 LIMITATIONS AND RECOMMENDATIONS FOR FUTURE RESEARCH

The results of this research showed that the two additives, recycled construction waste and GGBFS, have shown promising compressive and shear strength improvement results. All of the samples were prepared based upon the optimum moisture content condition, which is difficult to maintain in actual construction projects. Normally, during soil stabilisation at the larger scale of real-life situations, homogenous distribution of water cannot be achieved and actual field conditions usually have some parts of the site containing more moisture than other for any particular soil stabilisation project. This variation in the moisture content distribution can be both along the surface and along the depth of the strata.

The uneven moisture distribution is further critical for areas with wide climatic variations, such as Western Australia, which normally experiences heavy rains, cold winters and sunny summers. Furthermore, the optimum moisture content used for sample preparation was based upon the pure bentonite clay and addition of construction waste and/or GGBFS may cause some change in the optimum moisture content and maximum dry density values. The optimum moisture content value may be critical over the project lifecycle as the climatic changes may further accelerate the ground deterioration or in adverse cases, land subsidence.

The distinguishing feature of expansive clays like bentonite is their ability to swell and shrink cyclically due to changes in the soil's moisture content caused by changing environmental conditions. This behaviour is often due to the presence of an expansive mineral like montmorillonite, common in clays such as bentonite from the smectite clay group. Research on the effect of the two additives on swelling potential

of bentonite clay can be conducted to further investigate the practicability of these stabilisers as effective expansive soil stabilisers.

The large quantities of construction and demolition waste generated globally, and specifically in Australia, render the cost of obtaining it at an extremely low price, with some supplier providing 19mm base course at the rate of 8 – 10 AUD/month. In addition, GGBFS also has a low cost, which enables large scale utilisation of both stabilisers for commercial soil stabilisation projects. Therefore, further research can be conducted to explore the scale effect of both stabilisers for bentonite clay stabilisation to get data for large scale use and further establish commercial applications of the two additives.

REFERENCES

AASHTO T236-08. 2013. *Standard Method of Test for Direct Shear Test of Soils under Consolidated Drained Conditions*. American Association of State Highway and Transportation Officials

Abdelrahman, GE, HK Mohamed, and HM Ahmed. 2013. "New Replacement Formations on Expansive Soils Using Recycled Eps Beads." *Proc. 18th ICSMGE*.

ACI Committee 226. 1989. *Ground Granulated Blast Furnace Slag as a Cementitious Constituent in Concrete*. American Concrete Institute

Ahmad, MH, RC Omar, MA Malek, N Noor, and S Thiruselvam. 2008. "Compressive Strength of Palm Oil Fuel Ash Concrete" *Proceedings of the International Conference on Construction and Building Technology*, *Kuala Lumpur, Malaysia,*

Akbulut, Suat, Seracettin Arasan, and Ekrem Kalkan. 2007. "Modification of Clayey Soils Using Scrap Tire Rubber and Synthetic Fibers." *Applied Clay Science* 38 (1–2): 23-32. doi: http://dx.doi.org/10.1016/j.clay.2007.02.001.

Akinmusuru, Joseph O. 1991. "Potential Beneficial Uses of Steel Slag Wastes for Civil Engineering Purposes." *Resources, Conservation and Recycling* 5 (1): 73-80. doi: http://dx.doi.org/10.1016/0921-3449(91)90041-L.

Al-Malack, MH, GM Abdullah, OS Baghabra Al-Amoudi, and AA Bukhari. 2014. "Stabilization of Indigenous Saudi Arabian Soils Using Fuel Oil Flyash." *Journal of King Saud University - Engineering Sciences*. doi: http://dx.doi.org/10.1016/j.jksues.2014.04.005.

Al-Rawas, AA, AW Hago, and H Al-Sarmi. 2005a. "Effect of Lime, Cement and Sarooj (Artificial Pozzolan) on the Swelling Potential of an Expansive Soil from Oman." *Building and Environment* 40 (5): 681-687. doi: http://dx.doi.org/10.1016/j.buildenv.2004.08.028.

Al-Rawas, Amer Ali, A. W. Hago, and Hilal Al-Sarmi. 2005b. "Effect of Lime, Cement and Sarooj (Artificial Pozzolan) on the Swelling Potential of an Expansive Soil from Oman." *Building and environment* 40 (5): 681-687. doi: 10.1016/j.buildenv.2004.08.028.

Amu, OO, AB Fajobi, and SO Afekhuai. 2005a. "Stabilizing Potential of Cement and Fly Ash Mixture on Expansive Clay Soil." *Journal of applied sciences* 5 (9): 1669-1673.

———. 2005b. "Stabilizing Potential of Cement and Fly Ash Mixture on Expansive Clay Soil. J." *Journal of applied sciences* 5 (9): 1669-1673.

Ashango, Argaw Asha, and Nihar Ranjan Patra. 2014. "Static and Cyclic Properties of Clay Subgrade Stabilised with Rice Husk Ash and Portland Slag Cement." *International Journal of Pavement Engineering* 15 (10): 906-916. doi: 10.1080/10298436.2014.893323.

Association, Construction Industry Research Information. 1993. *Environmental Issues in Construction: A Review of Issues and Initiatives Relevant to the Building, Construction and Related Industries; Volume 1-Overview Including Executive and Technical Summaries*: Construction Industry Research and Information Association London.

ASTM D1140. 2014. *Annual Book of Astm Standards, Soil and Rock*. American Society for Testing and Materials

ASTM D1557. 2012. *Annual Book of Astm Standards, Soil and Rock*. American Society for Testing and Materials

ASTM D3080/D3080M. 2011. *Annual Book of Astm Standards, Soil and Rock*. American Society for Testing and Materials

ASTM D-2166. 1994. *Annual Book of Astm Standards, Soil and Rock*. American Society for Testing and Materials

ASTM D-4546. 1994. *Annual Book of Astm Standards, Soil and Rock*. American Society for Testing and Materials

Australasian (iron & steel) Slag Association. 2013. "Quick Reference Guide 1 " In *Roads Guide Supplement on General Applications*, Wollongong: Australasian (iron & steel) Slag Association.

Austroads. 2007. *Determination of Permanent Deformation and Resilient Modulus Characteristics of Unbound Granular Materials under Drained Conditions*. Austroads

Bain, JA. 1971. "A Plasticity Chart as an Aid to the Identification and Assessment of Industrial Clays." *Clay Minerals* 9 (1): 1-17.

Barnett, S. J., M. N. Soutsos, S. G. Millard, and J. H. Bungey. 2006. "Strength Development of Mortars Containing Ground Granulated Blast-Furnace Slag: Effect of Curing Temperature and Determination of Apparent Activation Energies." *Cement and Concrete Research* 36 (3): 434-440. doi: http://dx.doi.org/10.1016/j.cemconres.2005.11.002.

Behera, M, SK Bhattacharyya, AK Minocha, R Deoliya, and S Maiti. 2014a. "Recycled Aggregate from C&Amp;D Waste &Amp; Its Use in Concrete – a Breakthrough Towards Sustainability in Construction Sector: A Review." *Construction and Building Materials* 68 (In Press): 501-516. doi: http://dx.doi.org/10.1016/j.conbuildmat.2014.07.003.

Behera, Monalisa, S. K. Bhattacharyya, A. K. Minocha, R. Deoliya, and S. Maiti. 2014b. "Recycled Aggregate from C&Amp;D Waste &Amp; Its Use in Concrete – a Breakthrough Towards Sustainability in Construction Sector: A Review." *Construction and Building Materials* 68 (0): 501-516. doi: http://dx.doi.org/10.1016/j.conbuildmat.2014.07.003.

Belabdelouahab, F., and H. Trouzine. 2014. "Research and Enhancement of Used Tyres, Such as Material Innovative in Algeria." *Physics Procedia* 55: 68-74. doi: http://dx.doi.org/10.1016/j.phpro.2014.07.011.

Bell, F. G., and R. R. Maud. 1995. "Expansive Clays and Construction, Especially of Low-Rise Structures: A Viewpoint from Natal, South Africa." *Environmental & Engineering Geoscience* 1 (1): 41-59. http://www.scopus.com/inward/record.url?eid=2-s2.0-0029480510&partnerID=40&md5=6b69e282f5d8c571b10d621614a6db7d.

Biernacki, JJ, JM Richardson, PE Stutzman, and DP Bentz. 2002. "Kinetics of Slag Hydration in the Presence of Calcium Hydroxide." *Journal of the American Ceramic Society* 85 (9): 2261-2267.

Birss, Fraser W., and T. Thorvaldson. 1955. "The Mechanism of the Hydration of Calcium Oxide." *Canadian Journal of Chemistry* 33 (5): 881-886. doi: 10.1139/v55-106.

Bishop, A. W., and G. E. Blight. 1963. "Some Aspects of Effective Stress in Saturated and Partly Saturated Soils." *Géotechnique* 13: 177-197. http://www.icevirtuallibrary.com/content/article/10.1680/geot.1963.13.3.177.

Bose, Bidula. 2012. "Effect of Curing Period and Temperature on Characteristics of Stabilized Expansive Soil." *International Journal of Emerging trends in Engineering and Development* 4 (2): 704-713.

Bossink, BAG, and HJH Brouwers. 1996. "Construction Waste: Quantification and Source Evaluation." *Journal of construction engineering and management* 122 (1): 55-60.

British Standards. 1975. *Methods of Test for Soils for Civil Engineering Purposes*.

British Standards BS 1377-7. 1990. *Methods of Test for Soils for Civil Engineering Purposes. Shear Strength Tests (Total Stress)*.

Brough, AR, and A Atkinson. 2002. "Sodium Silicate-Based, Alkali-Activated Slag Mortars: Part I. Strength, Hydration and Microstructure." *Cement and Concrete Research* 32 (6): 865-879.

Budhu, M. 2011a. *Soil Mechanics and Foundations (3rd Edition)*.

Budhu, Muni. 2011b. *Soil Mechanics and Foundations*. 3rd ed. U.S.A: John Wiley & Sons.

Chakradhara Rao, M, SK Bhattacharyya, and SV Barai. 2011. " Influence of Field Recycled Coarse Aggregate on Properties of Concrete." *Materials and Structures* 44 (1): 205-220. doi: http://dx.doi.org/10.1617/s11527-010-9620-x

Chen, F. H. 1975. *Foundations on Expansive Soils*. Amsterdam: Elsevier Scientific Pub. Co.

Chen, F.H. 2012. *Foundations on Expansive Soils*. Vol. 12: Elsevier Science.

Chen, Fu Hua. 1965. "The Use of Piers to Prevent Uplifting of Lightly Loaded Structures Founded on Expansive Soils" *Proceeding of International Research and Engineering Conference on Expansive Clay Soils, Texas*,

Chen, Wei. 2006. "Hydration of Slag Cement: Theory, Modeling and Application." University of Twenty, Enschede, Netherlands.

Chen, Wei, and HJH Brouwers. 2007. "The Hydration of Slag, Part 1: Reaction Models for Alkali-Activated Slag." *Journal of Materials Science* 42 (2): 428-443.

Cokca, Erdal. 2001. "Use of Class C Fly Ashes for the Stabilizationof an Expansive Soil." *Journal of Geotechnical and Geoenvironmental Engineering* 127 (7): 568-573.

Cokca, Erdal, Veysel Yazici, and Vehbi Ozaydin. 2009. "Stabilization of Expansive Clays Using Granulated Blast Furnace Slag (Gbfs) and Gbfs-Cement." *Geotechnical and Geological Engineering* 27 (4): 489-499.

D.D. Higgins. 2005. *Soil Stabilisation with Ground Granulated Blastfurnace Slag*. United Kingdom.

Das, Braja M. 2013. *Advanced Soil Mechanics*: CRC Press.

Das, Braja, and Khaled Sobhan. 2014. *Principles of Geotechnical Engineering*. 8 ed: Cengage Learning.

Deer, WA, RA Howie, and J Zussman. 2013. *An Introduction to the Rock-Forming Minerals*. 3rd ed. London: Mineralogical Society of Great Britain & Ireland.

Derek Chisholm. 2011. *Best Practice Guide for the Use of "Recycled Aggregates in New Concrete"*. Wellington, New Zealand.

Edil, Tuncer B, Craig H Benson, M Sazzad Bin-Shafique, Burak F Tanyu, Woon-Hyung Kim, and Aykut Senol. 2002. "Field Evaluation of Construction Alternatives for Roadways over Soft Subgrade." *Transportation Research Record: Journal of the Transportation Research Board* 1786 (1): 36-48.

Environment Protection and Heritage Council (EPHC). 2010. *National Waste Report*. Adelaide, SA: NEPC Service Corporation. http://www.scew.gov.au/resource/ephc-archive-waste-management#National_waste_policy.

EPA. 1992. *Bentonite Mining Lease 70/738 at Gunyidi, Coorow*. Perth: Environmental Protection Authority. http://epa.wa.gov.au/EPADocLib/723_B659.pdf.

Fadl, A. E. 1971. "A Mineralogical Characterization of Some Vertisols in the Gezira and the Kenana Clay Plains of the Sudan." *Journal of Soil Science* 22 (1): 129-135. doi: 10.1111/j.1365-2389.1971.tb01600.x.

Fernández, Raúl, Lorena González, Ana Isabel Ruiz, and Jaime Cuevas. 2014. "Nature of C-(a)-Sh Phases Formed in the Reaction Bentonite/Portlandite." *Journal of Geochemistry* 2014.

Fredericci, C, ED Zanotto, and EC Ziemath. 2000. "Crystallization Mechanism and Properties of a Blast Furnace Slag Glass." *Journal of non-crystalline solids* 273 (1): 64-75.

Fredlund, Delwyn G. 2006. "Unsaturated Soil Mechanics in Engineering Practice." *Journal of geotechnical and geoenvironmental engineering* 132 (3): 286-321.

Gardner, Laura J., Susan A. Bernal, Samuel A. Walling, Claire L. Corkhill, John L. Provis, and Neil C. Hyatt. 2015. "Characterisation of Magnesium Potassium Phosphate Cements Blended with Fly Ash and Ground Granulated Blast Furnace Slag." *Cement and Concrete Research* 74 (0): 78-87. doi: http://dx.doi.org/10.1016/j.cemconres.2015.01.015.

Ghazavi, M, M Hosseini, and M Mollanouri. 2008. "A Comparison between Angle of Repose and Friction Angle of Sand" *Proc. 12th International Conference of International Association for Computer Methods and Advances in Geomechanics (IACMAG)*: Citeseer.

Gruyaert, Elke, Philip Van den Heede, Mathias Maes, and Nele De Belie. 2012. "Investigation of the Influence of Blast-Furnace Slag on the Resistance of Concrete against Organic Acid or Sulphate Attack by Means of Accelerated Degradation Tests." *Cement and Concrete Research* 42 (1): 173-185.

Haha, M. Ben, G. Le Saout, F. Winnefeld, and B. Lothenbach. 2011. "Influence of Activator Type on Hydration Kinetics, Hydrate Assemblage and Microstructural Development of Alkali Activated Blast-Furnace Slags." *Cement and Concrete Research* 41 (3): 301-310.

Hansen, TC. 1986. "Recycled Aggregates and Recycled Aggregate Concrete Second State-of-the-Art Report Developments 1945–1985." *Materials and Structures* 19 (3): 201-246. doi: 10.1007/BF02472036.

Harris, Cyril M. 2005. "Dictionary of Architecture and Construction." edited by Cyril M. Harris, United States: McGraw-Hill. Original edition, 1975.

Hasan, Umair, Amin Chegenizadeh, Mochamad Arief Budihardjo, and Hamid Nikraz. 2015. "Experimental Evaluation of Construction Waste and Ground Granulated Blast Furnace Slag as Alternative Soil Stabilisers." *Manuscript submitted*.

Hausmann, MR. 1990. *Engineering Principles of Ground Modification.* New York.: McGraw-Hill,.

Hebib, Samir, and Eric R Farrell. 2003. "Some Experiences on the Stabilization of Irish Peats." *Canadian geotechnical journal* 40 (1): 107-120.

Hibbitt, Karlsson, and Sorensen. 2005. "Abaqus/Standard User's Manual." USA: HKS Inc. .

Higgins, DD. 2005. *Soil Stabilisation with Ground Granulated Blastfurnace Slag.* United Kingdom.

Hill, Richard C, and Paul A Bowen. 1997. "Sustainable Construction: Principles and a Framework for Attainment." *Construction Management & Economics* 15 (3): 223-239.

Holtz, W. G., and H. J. Gibbs. 1954. *Engineering Properties of Expansive Clays*. 516 vols. Vol. 80: American Society of Civil Engineers.

Horvath, A. 2004. "Construction Materials and the Environment." *Annual Review of Environment and Resources* 29 (1): 181-204. doi: doi:10.1146/annurev.energy.29.062403.102215.

Hosterman, JW, and SH Patterson. 1992. "Bentonite and Fuller's Earth Resources of the United States. Washington, Dc." *US Geological Survey* 45.

Huang, Runqiu, and Lizhou Wu. 2007. "Stability Analysis of Unsaturated Expansive Soil Slope." *Earth Science Frontiers* 14 (6): 129-133. doi: http://dx.doi.org/10.1016/S1872-5791(08)60007-X.

Huleatt, M.B., and A.L. Jaques. 2008. "Australian Operating Mines (1:10 000 000 Scale Map) ", Canberra: Geoscience Australia.

Hyder Consulting. 2011. *Construction and Demolition Waste Status Report* Environment Department of Sustainability, Water, Population and Communities and Queensland Department of Environment and Resource Management. http://www.environment.gov.au/system/files/resources/323e8f22-1a8a-4245-a09c-006644d3bd51/files/construction-waste.pdf.

Indian Standard IS:2720-40. 1977. *Methods of Test for Soils*. Bureau of Indian Standards

Indian Standard IS: 1498. 2007. *Classification and Identification of Soils for General Engineering Purposes*. Bureau of Indian Standards

Inglethorpe, SDJ, DJ Morgan, and David Edward Highley. 1993. *Industrial Minerals Laboratory Manual: Bentonite*: British Geological Survey, Mineralogy and Petrology Group.

J.L. Eades, R.E. Grim. 1966. "A Quick Test to Determine Lime Requirements for Lime Stabilization." *Highway Research Record* 139 (139): 61-72.

Jacob, H, and G Clarke. 2002. "Methods of Soil Analysis, Part 4: Physical Methods." *Soil Science Society of America, Inc. Madison, Wisconsin, USA.*

Jafari, Mohammad, and Mahdi Esna-ashari. 2012. "Effect of Waste Tire Cord Reinforcement on Unconfined Compressive Strength of Lime Stabilized Clayey Soil under Freeze–Thaw Condition." *Cold Regions Science and Technology* 82 (0): 21-29. doi: http://dx.doi.org/10.1016/j.coldregions.2012.05.012.

Ji-ru, Zhang, and Cao Xing. 2002. "Stabilization of Expansive Soil by Lime and Fly Ash." *Journal of Wuhan University of Technology-Mater. Sci. Ed.* 17 (4): 73-77.

Jiang, Hongtao, Baojun Wang, Hilary I. Inyang, Jin Liu, Kai Gu, and Bin Shi. 2013. "Role of Expansive Soil and Topography on Slope Failure and Its Countermeasures, Yun County, China." *Engineering Geology* 152 (1): 155-161. doi: http://dx.doi.org/10.1016/j.enggeo.2012.10.020.

Joint Departments of the Army and Air Force. 1994. "Soil Stabilization for Pavements." USA: TM 5-822-14/AFMAN 32-8010.

Kalinski, Michael E. 2011. *Soil Mechanics Lab Manual*. 2nd Edition ed: Wiley. http://au.wiley.com/WileyCDA/WileyTitle/productCd-EHEP001814.html.

Kariuki, Patrick Chege, and Freek van der Meer. 2004. "A Unified Swelling Potential Index for Expansive Soils." *Engineering Geology* 72 (1–2): 1-8. doi: http://dx.doi.org/10.1016/S0013-7952(03)00159-5.

Karnland, Ola. 2010. *Chemical and Mineralogical Characterization of the Bentonite Buffer for the Acceptance Control Procedure in a Kbs-3 Repository*.

Karunarathne, Aman, E. F. Gad, S. Sivanerupan, and J. L. Wilson. 2012. "Review of Residential Footing Design on Expansive Soil in Australia." In *From Materials to Structures: Advancement through Innovation*, 575-580. CRC Press.

Kasai, Y. 1989. "The Second International Rilem Symposium on Demolition and Reuse of Concrete and Masonry." *Materials and Structures* 22 (4): 312-319. doi: 10.1007/BF02472565.

Kavak, A, G Bilgen, and OF Capar. 2011. "Using Ground Granulated Blast Furnace Slag with Seawater as Soil Additives in Lime-Clay Stabilization." *Journal of ASTM International* 8 (7).

Khalaf, F, and A DeVenny. 2004. "Recycling of Demolished Masonry Rubble as Coarse Aggregate in Concrete: Review." *Journal of Materials in Civil Engineering* 16 (4): 331-340. doi: 10.1061/(ASCE)0899-1561(2004)16:4(331).

Khemissa, M, and A Mahamedi. 2014a. "Cement and Lime Mixture Stabilization of an Expansive Overconsolidated Clay." *Applied Clay Science* 95: 104-110. doi: http://dx.doi.org/10.1016/j.clay.2014.03.017.

Khemissa, Mohamed, and Abdelkrim Mahamedi. 2014b. "Cement and Lime Mixture Stabilization of an Expansive Overconsolidated Clay." *Applied Clay Science* 95 (0): 104-110. doi: http://dx.doi.org/10.1016/j.clay.2014.03.017.

Kim, HS, JW Park, YJ An, JS Bae, and C Han. 2011. "Activation of Ground Granulated Blast Furnace Slag Cement by Calcined Alunite." *Materials transactions* 52 (2): 210-218.

Kodikara, J.K., Choi, X. 2006. "A Simplified Analytical Model for Desiccation Cracking of Clay Layers in Laboratory Tests." *Fourth International Conference on Unsaturated Soils, Carefree, Arizona, United States*: American Society of Civil Engineers. doi: 10.1061/40802(189)218.

Kohler, G, and R Kircher. 1993. "Anlagenkonzepte Zur Herstellung Hochwertiger Recycling-Produkte." *Baustoff Recycling* 94 (95): 93-116.

Kolani, B., L. Buffo-Lacarrière, A. Sellier, G. Escadeillas, L. Boutillon, and L. Linger. 2012. "Hydration of Slag-Blended Cements." *Cement and Concrete Composites* 34 (9): 1009-1018. doi: http://dx.doi.org/10.1016/j.cemconcomp.2012.05.007.

Kumar, S., P. Kolay, S. Malla, and S. Mishra. 2012. "Effect of Multiwalled Carbon Nanotubes on Mechanical Strength of Cement Paste." *Journal of Materials in*

Civil Engineering 24 (1): 84-91. doi: doi:10.1061/(ASCE)MT.1943-5533.0000350.

Lee, A.R. 1974. *Blastfurnace and Steel Slag: Production, Properties, and Uses*: Wiley.

Lenssen, Nicholas, and David M Roodman. 1995. *Making Better Buildings in State of the World 1995*. New York.

Li, Jie, Donald A. Cameron, and Gang Ren. 2014. "Case Study and Back Analysis of a Residential Building Damaged by Expansive Soils." *Computers and Geotechnics* 56 (0): 89-99. doi: http://dx.doi.org/10.1016/j.compgeo.2013.11.005.

Li, RYM, and H Du. 2015. "Sustainable Construction Waste Management in Australia: A Motivation Perspective." In *Construction Safety and Waste Management*, 1-30. Hong Kong: Springer International Publishing.

Li, Xuping. 2008. "Recycling and Reuse of Waste Concrete in China: Part I." *Material behaviour of recycled aggregate*.

Limbachiya, M, MS Meddah, and Y Ouchagour. 2012. "Use of Recycled Concrete Aggregate in Fly-Ash Concrete." *Construction and Building Materials* 27 (1): 439-449. doi: http://dx.doi.org/10.1016/j.conbuildmat.2011.07.023.

Main Roads Western Australia. 2010. *Specification 501 Pavements*. Main Roads Western Australia

Majeed, Zaid Hameed, Mohd Raihan Taha, and Ibtehaj Taha Jawad. 2014. "Stabilization of Soft Soil Using Nanomaterials." *Research Journal of Applied Sciences, Engineering and Technology* 8 (4): 503-509.

Manso, Juan M., Vanesa Ortega-López, Juan A. Polanco, and Jesús Setién. 2013. "The Use of Ladle Furnace Slag in Soil Stabilization." *Construction and Building Materials* 40 (0): 126-134. doi: http://dx.doi.org/10.1016/j.conbuildmat.2012.09.079.

Matias, D, J de Brito, A Rosa, and D Pedro. 2013. "Mechanical Properties of Concrete Produced with Recycled Coarse Aggregates–Influence of the Use of Superplasticizers." *Construction and Building Materials* 44: 101-109.

McCarthy, MJ, LJ Csetenyi, A Sachdeva, and RK Dhir. 2014. "Engineering and Durability Properties of Fly Ash Treated Lime-Stabilised Sulphate-Bearing Soils." *Engineering Geology* 174: 139-148. doi: http://dx.doi.org/10.1016/j.enggeo.2014.03.001.

McGrath, Teresa DH, Jesse F White, and Jerome P Downey. 2014. "Experimental Determination of Density in Molten Lime Silicate Slags as a Function of Temperature and Composition." *Mineral Processing and Extractive Metallurgy (Trans. Inst. Min Metall. C)* 123 (3): 178-183.

Mehta, P Kumar, and Helena Meryman. 2009. "Tools for Reducing Carbon Emissions Due to Cement Consumption." *Structure* 1 (1): 11-15.

Miao, Linchang, Songyu Liu, and Yuanming Lai. 2002. "Research of Soil–Water Characteristics and Shear Strength Features of Nanyang Expansive Soil." *Engineering Geology* 65 (4): 261-267. doi: http://dx.doi.org/10.1016/S0013-7952(01)00136-3.

Miller, Debora J. 1997. *Expansive Soils: Problems and Practice in Foundation and Pavement Engineering*: John Wiley & Sons.

Misra, Anil, Debabrata Biswas, and Sushant Upadhyaya. 2005. "Physico-Mechanical Behavior of Self-Cementing Class C Fly Ash–Clay Mixtures." *Fuel* 84 (11): 1410-1422.

Mitchell, James Kenneth, and Kenichi Soga. 1993. *Fundamentals of Soil Behavior*. 2nd ed. New York, NY: John Wiley & Sons.

Mohr, Otto. 1900. "Welche Umstände Bedingen Die Elastizitätsgrenze Und Den Bruch Eines Materials." *Zeitschrift des Vereins Deutscher Ingenieure* 46 (1524-1530): 1572-1577.

Muntohar, A. S. 2006. "Prediction and Classification of Expansive Clay Soils." *Expansive Soils, Recent Advances in Characterization and Treatment:*: 17.

Murthy, Inampudi Narasimha, Nallabelli Arun Babu, and Jinugu Babu Rao. 2014. "Comparative Studies on Microstructure and Mechanical Properties of Granulated Blast Furnace Slag and Fly Ash Reinforced Aa 2024 Composites." *Journal of Minerals and Materials Characterization and Engineering* 2014.

Nalbantoğlu, Zalihe. 2004. "Effectiveness of Class C Fly Ash as an Expansive Soil Stabilizer." *Construction and Building Materials* 18 (6): 377-381.

Nalbantoglu, Zalihe, and Emin Gucbilmez. 2001. "Improvement of Calcareous Expansive Soils in Semi-Arid Environments." *Journal of Arid Environments* 47 (4): 453-463. doi: http://dx.doi.org/10.1006/jare.2000.0726.

Namdar, Abdoullah. 2010. "Mineralogy in Geotechnical Engineering." *Journal of Engineering Science and Technology Review* 3 (1): 108-110.

NanoScienceWorks. n.d. Types of Carbon Nanotubes. Taylor & Francis Group. Accessed 04/03/2015, http://www.nanoscienceworks.org/Members/siebo/657px-types_of_carbon_nanotubes.png/view.

National Slag Association. 1971. "Processed Blast Furnace Slag, the All-Purpose Construction Aggregate." *NSA J7/-3, Alexandria, Virginia*.

Neeraja, D, and AV Rao Narsimha. 2010. "Use of Certain Mixtures in the Construction of Pavement on Expansive Clayey Subgrades." *International Journal of Engineering Science and Technology* 2 (11): 6108-6114.

Nelson, J.D., and D.J. Miller. 1992. *Expansive Soils: Problems and Practice in Foundation and Pavement Engineering*: J. Wiley.

Nicholson, PG. 2014. *Soil Improvement and Ground Modification Methods*: Butterworth-Heinemann.

Nidzam, RM, and John Mungai Kinuthia. 2010. "Sustainable Soil Stabilisation with Blastfurnace Slag–a Review." *Proceedings of the ICE-Construction Materials* 163 (3): 157-165.

NRC. 2006. *Geological and Geotechnical Engineering in the New Millennium: Opportunities for Research and Technological Innovation*. Washington, DC: The National Academies Press.

NRCS, USDA. 2012. "National Soil Survey Handbook." Title.

Odell, Russell Turner, Thomas Hampton Thornburn, and LJ McKenzie. 1960. "Relationships of Atterberg Limits to Some Other Properties of Illinois Soils." *Soil Science Society of America Journal* 24 (4): 297-300.

Ofori, George. 1992. "The Environment: The Fourth Construction Project Objective?" *Construction Management and Economics* 10 (5): 369-395.

Ortega-López, Vanesa, Juan M. Manso, Isidoro I. Cuesta, and Javier J. González. 2014. "The Long-Term Accelerated Expansion of Various Ladle-Furnace Basic Slags and Their Soil-Stabilization Applications." *Construction and Building Materials* 68 (0): 455-464. doi: http://dx.doi.org/10.1016/j.conbuildmat.2014.07.023.

Oss, Hendrik G. van. 2003. *Slag-Iron and Steel*. United States: US Geological Survey Minerals Yearbook.

Ouf, Mohamed El-Sadek Abdel Rahman. 2001a. "Stabilisation of Clay Subgrade Soils Using Ground Granulated Blastfurnace Slag." University of Leeds, Leeds, UK.

———. 2001b. "Stabilisation of Clay Subgrade Soils Using Ground Granulated Blastfurnace Slag." School of Civil Engineering, University of Leeds. http://etheses.whiterose.ac.uk/id/eprint/327.

Panda, Ranjita. 2013. "Dephosphorization of Ld Slag by Penicillium Citrinum." *Development* 25: 27.

Pandian, NS, and KC Krishna. 2003. "The Pozzolanic Effect of Fly Ash on the California Bearing Ratio Behavior of Black Cotton Soil." *Journal of Testing and Evaluation* 31 (6): 479-485.

PCA. 2001. *Ettringite Formation and the Performance of Concrete*. Illinois, USA.

Petry, Thomas M, and Dallas N Little. 2002. "Review of Stabilization of Clays and Expansive Soils in Pavements and Lightly Loaded Structures-History, Practice, and Future." *Journal of Materials in Civil Engineering* 14 (6): 447-460.

Phani Kumar, BR, and Radhey S Sharma. 2004a. "Effect of Fly Ash on Engineering Properties of Expansive Soils." *Journal of Geotechnical and Geoenvironmental Engineering* 130 (7): 764-767.

Phani Kumar, BR, and RS Sharma. 2004b. "Effect of Fly Ash on Engineering Properties of Expansive Soils." *Journal of Geotechnical and Geoenvironmental Engineering* 130 (7): 764-767.

Pogson, Sara-Rose, and Emma Mountjoy. 2013. "Department of Environment and Conservation Recycling Activity in Western Australia."

Poon, CS, and D Chan. 2007. "The Use of Recycled Aggregate in Concrete in Hong Kong." *Resources, Conservation and Recycling* 50 (3): 293-305. doi: http://dx.doi.org/10.1016/j.resconrec.2006.06.005.

Pourakbar, Shahram, Afshin Asadi, Bujang B. K. Huat, and Mohammad Hamed Fasihnikoutalab. Article In Press. "Stabilization of Clayey Soil Using Ultrafine Palm Oil Fuel Ash (Pofa) and Cement." *Transportation Geotechnics*. doi: http://dx.doi.org/10.1016/j.trgeo.2015.01.002.

Prabakar, J, Nitin Dendorkar, and RK Morchhale. 2004. "Influence of Fly Ash on Strength Behavior of Typical Soils." *Construction and Building Materials* 18 (4): 263-267.

Proctor, DM, KA Fehling, EC Shay, JL Wittenborn, JJ Green, C Avent, RD Bigham, M Connolly, B Lee, and TO Shepker. 2000. "Physical and Chemical Characteristics of Blast Furnace, Basic Oxygen Furnace, and Electric Arc Furnace Steel Industry Slags." *Environmental Science & Technology* 34 (8): 1576-1582.

Puertas, F, A Fernández-Jiménez, and MT Blanco-Varela. 2004. "Pore Solution in Alkali-Activated Slag Cement Pastes. Relation to the Composition and

Structure of Calcium Silicate Hydrate." *Cement and Concrete Research* 34 (1): 139-148.

Puppala, Anand J., Thammanoon Manosuthikij, and Bhaskar C. S. Chittoori. 2013. "Swell and Shrinkage Characterizations of Unsaturated Expansive Clays from Texas." *Engineering Geology* 164 (0): 187-194. doi: http://dx.doi.org/10.1016/j.enggeo.2013.07.001.

———. 2014. "Swell and Shrinkage Strain Prediction Models for Expansive Clays." *Engineering Geology* 168 (0): 1-8. doi: http://dx.doi.org/10.1016/j.enggeo.2013.10.017.

R. Lytton, C. Aubeny, R. Bulut. 2004. *Design Procedure for Pavements on Expansive Soils*.

Rai, Amit, J. Prabakar, C. B. Raju, and R. K. Morchalle. 2002. "Metallurgical Slag as a Component in Blended Cement." *Construction and Building Materials* 16 (8): 489-494. doi: http://dx.doi.org/10.1016/S0950-0618(02)00046-6.

Raman, V. 1967. "Identification of Expansive Soils from the Plasticity Index and the Shrinkage Index Data." *Indian Eng., Calcutta* 11 (1): 17-22.

Regourd, M. 1980. "Structure and Behaviour of Slag Portland Cement Hydrates" *Proceedings of the 7th international congress on the chemistry of cement (7th ICCC)*,

Rogoff, Marc J, and John F Williams. 2012. *Approaches to Implementing Solid Waste Recycling Facilities*: William Andrew.

S. G. Fityus, D. W. Smith, and M. A. Allman. 2004. "Expansive Soil Test Site near Newcastle." *J. Geotech. Geoenviron. Eng.* 130 (7): 686–695. doi: http://dx.doi.org/10.1061/(ASCE)1090-0241(2004)130:7(686).

Saride, S, AJ Puppala, and SR Chikyala. 2013a. "Swell-Shrink and Strength Behaviors of Lime and Cement Stabilized Expansive Organic Clays." *Applied Clay Science* 85: 39-45. doi: http://dx.doi.org/10.1016/j.clay.2013.09.008.

Saride, Sireesh, Anand J. Puppala, and Srujan R. Chikyala. 2013b. "Swell-Shrink and Strength Behaviors of Lime and Cement Stabilized Expansive Organic Clays." *Applied Clay Science* 85 (0): 39-45. doi: http://dx.doi.org/10.1016/j.clay.2013.09.008.

Schanz, T, and MBD Elsawy. 2015. "Swelling Characteristics and Shear Strength of Highly Expansive Clay–Lime Mixtures: A Comparative Study." *Arabian Journal of Geosciences*: 1-9.

Seco, A, F Ramírez, L Miqueleiz, and B García. 2011. "Stabilization of Expansive Soils for Use in Construction." *Applied Clay Science* 51 (3): 348-352.

Seybold, Cathy A, Moustafa A Elrashidi, and Robert J Engel. 2008. "Linear Regression Models to Estimate Soil Liquid Limit and Plasticity Index from Basic Soil Properties." *Soil science* 173 (1): 25-34.

Shillito, Rose, and Lynn Fenstermaker. 2014. *Soil Stabilization Methods with Potential for Application at the Nevada National Security Site: A Literature Review. No. Doe 45255 Doe/Nv/0000939-17*.

Siddique, R, and MI Khan. 2011. *Supplementary Cementing Materials*. Vol. 37, *Engineering Materials*: Springer.

Skempton, A. 1953. "The Colloidal Activity of Clays" *3rd International Conference Soil Mechanic and Foundation Engineering, Switzerland,*

Snellings, Ruben, Gilles Mertens, and Jan Elsen. 2012. "Supplementary Cementitious Materials." *Reviews in Mineralogy and Geochemistry* 74 (1): 211-278.

Solanki, Pranshoo, and Musharraf M Zaman. 2010. "Laboratory Performance Evaluation of Subgrade Soils Stabilized with Sulfate-Bearing Cementitious Additives." *Journal of Testing and Evaluation* 38 (1): 1-12.

Song, S, D Sohn, HM Jennings, and TO Mason. 2000a. "Hydration of Alkali-Activated Ground Granulated Blast Furnace Slag." *Journal of Materials Science* 35 (1): 249-257. doi: 10.1023/A:1004742027117.

Song, S., D. Sohn, H. M. Jennings, and T. O. Mason. 2000b. "Hydration of Alkali-Activated Ground Granulated Blast Furnace Slag." *Journal of Materials Science* 35 (1): 249-257. doi: 10.1023/A:1004742027117.

Song, Sujin, and Hamlin M Jennings. 1999. "Pore Solution Chemistry of Alkali-Activated Ground Granulated Blast-Furnace Slag." *Cement and Concrete Research* 29 (2): 159-170.

Sridharan, A., and K. Prakash. 2000. "Classification Procedures for Expansive Soils" *Proceedings of the Institution of Civil Engineers:* : Geotechnical Engineering.

Standards Australia AS 1289.3.6.1. 2003. *Methods of Testing Soils for Engineering Purposes - Soil Classification Tests - Determination of the Particle Size Distribution of a Soil - Standard Method of Analysis by Sieving*. Standards Australia

Standards Australia AS 1289.3.9.1. 2002. *Methods of Testing Soils for Engineering Purposes - Soil Classification Tests - Determination of the Cone Liquid Limit of a Soil*.

Standards Australia AS 1289.5.1.1. 2003. *Methods of Testings Soil for Engineering Purposes: Method 5.1.1: Soil Compaction and Density Tests-Determination of the Dry Density/Moisture Content Relation of a Soil Using Standard Compactive Effort*.

Standards Australia AS 1289.6.2.2. 1998. *Methods of Testing Soils for Engineering Purposes - Soil Strength and Consolidation Tests - Determination of the Shear Strength of a Soil - Direct Shear Test Using a Shear Box*.

Standards Australia AS 5101.4. 2008. *Methods for Preparation and Testing of Stabilized Materials - Unconfined Compressive Strength of Compacted Materials*.

Standards Australia AS: 1289.3.2.1. 2009. *Methods of Testing Soils for Engineering Purposes - Method 3.2.1: Soil Classification Tests - Determination of the Plastic Limit of a Soil - Standard Method.*

Standards Australia AS: 1289.3.3.1. 2009. *Methods of Testing Soils for Engineering Purposes - Method 3.3.1: Soil Classification Tests - Calculation of the Plasticity Index of a Soil.,*.

Stark, N, AE Hay, R Cheel, and CB Lake. 2014. "The Impact of Particle Shape on the Angle of Internal Friction and the Implications for Sediment Dynamics at a Steep, Mixed Sand–Gravel Beach." *Earth Surface Dynamics* 2 (2): 469-480.

Taha, M. R. 2009. "Geotechnical Properties of Soil-Ball Milled Soil Mixtures." In *Nanotechnology in Construction 3*, eds Zdeněk Bittnar, PeterJ M. Bartos, Jiří

Němeček, Vít Šmilauer and Jan Zeman, 377-382. Springer Berlin Heidelberg.

Taha, Mohd Raihan, and Ting Ying. 2010. "Effects of Carbon Nanotube on Kaolinite: Basic Geotechnical Behavior." *World Journal Of Engineering* 7 (2): 472-473.

Tam, Vivian WY, and Chi Ming Tam. 2008. "Diversifying Two-Stage Mixing Approach (Tsma) for Recycled Aggregate Concrete: Tsma S and Tsma Sc." *Construction and Building Materials* 22 (10): 2068-2077.

Tan, Bo, Rui Zhang, and Yan Ting Lai. 2013. "Analysis on Stability of the Expensive Soil Cutting Slope Based on Ansys" *Applied Mechanics and Materials*: Trans Tech Publ.

Tarrant, Richard. 2010. "Experiment 31 - the Scanning Electron Microscope." Australia: School of Physics - University of Sydney.

Texas Department of Transportation. 1999. "Tex-121-E, Soil-Lime Testing Manual." Texas Department of Transportation online manuals.

———. 2005. "Guidelines for Modification and Stabilization of Soils and Base for Use in Pavement Structures." edited by Soils & Aggregates Branch Department of Transportation. Construction Division Materials & Pavements Section Geotechnical, Texas.

Thyagaraj, T., and S. Zodinsanga. 2014. "Laboratory Investigations of in Situ Stabilization of an Expansive Soil by Lime Precipitation Technique." *Journal of Materials in Civil Engineering* 0 (0): 06014028. doi: doi:10.1061/(ASCE)MT.1943-5533.0001184.

Veith, G. 2000. "Essay Competition: Green, Ground and Great: Soil Stabilization with Slag." *Building Research & Information* 28 (1): 70-72.

Venkatramaiah, C. 2006. *Geotechnical Engineering*: New Age International.

Viswanadham, B. V. S., B. R. Phanikumar, and Rahul V. Mukherjee. 2009. "Swelling Behaviour of a Geofiber-Reinforced Expansive Soil." *Geotextiles and Geomembranes* 27 (1): 73-76. doi: http://dx.doi.org/10.1016/j.geotexmem.2008.06.002.

Walsh, P. F., and D. A. Cameron. 1997. "The Design of Residential Slabs and Footings." SAA HB28-1997; 1997.

Wang, J, Z Li, and VWY Tam. 2014. "Critical Factors in Effective Construction Waste Minimization at the Design Stage: A Shenzhen Case Study, China." *Resources, Conservation and Recycling* 82: 1-7. doi: http://dx.doi.org/10.1016/j.resconrec.2013.11.003.

Wang, Mingwu, and Guangyi Chen. 2011. "A Novel Coupling Model for Risk Analysis of Swell and Shrinkage of Expansive Soils." *Computers & Mathematics with Applications* 62 (7): 2854-2861. doi: http://dx.doi.org/10.1016/j.camwa.2011.07.051.

Whitehouse J., Brownlow J.W., Burton G.R., Ferguson A.C., Glen R.A., Lishmund S.R., MacRae G.P. et al. 2007. *Industrial Mineral Opportunities in New South Wales*: Geological Survey of New South Wales. Bulletin 33.

Wild, S, JM Kinuthia, RB Robinson, and I Humphreys. 1996. "Effects of Ground Granulated Blast Furnace Slag (Ggbs) on the Strength and Swelling Properties of Lime-Stabilized Kaolinite in the Presence of Sulphates." *Clay Minerals* 31 (3): 423-433.

Wong, T. K. 1992. "Use of Granulated Slag as a Stabilising Agent."

Yadu, Laxmikant, and R. K. Tripathi. 2013a. "Effects of Granulated Blast Furnace Slag in the Engineering Behaviour of Stabilized Soft Soil." *Procedia Engineering* 51 (0): 125-131. doi: http://dx.doi.org/10.1016/j.proeng.2013.01.019.

Yadu, Laxmikant, and RK Tripathi. 2013b. "Effects of Granulated Blast Furnace Slag in the Engineering Behaviour of Stabilized Soft Soil." *Procedia Engineering* 51: 125-131.

Yang, Keun-Hyeok, Jae-Il Sim, and Sang-Ho Nam. 2010. "Enhancement of Reactivity of Calcium Hydroxide-Activated Slag Mortars by the Addition of Barium Hydroxide." *Construction and Building Materials* 24 (3): 241-251. doi: http://dx.doi.org/10.1016/j.conbuildmat.2009.09.001.

Yi, Yaolin, Liyang Gu, and Songyu Liu. 2015. "Microstructural and Mechanical Properties of Marine Soft Clay Stabilized by Lime-Activated Ground Granulated Blastfurnace Slag." *Applied Clay Science* 103 (0): 71-76. doi: http://dx.doi.org/10.1016/j.clay.2014.11.005.

Yilmaz, Işık. 2006. "Indirect Estimation of the Swelling Percent and a New Classification of Soils Depending on Liquid Limit and Cation Exchange Capacity." *Engineering Geology* 85 (3): 295-301.

Yilmaz, Işık, and Berrin Civelekoglu. 2009. "Gypsum: An Additive for Stabilization of Swelling Clay Soils." *Applied Clay Science* 44 (1–2): 166-172. doi: http://dx.doi.org/10.1016/j.clay.2009.01.020.

Zha, Fusheng, Songyu Liu, Yanjun Du, and Kerui Cui. 2008. "Behavior of Expansive Soils Stabilized with Fly Ash." *Natural Hazards* 47 (3): 509-523.

Zhang, Xiong. 2005. "Consolidation Theories for Saturated-Unsaturated Soils and Numerical Simulation of Residential Buildings on Expansive Soils." Texas A&M University.

Živica, Vladimír. 2007. "Effects of Type and Dosage of Alkaline Activator and Temperature on the Properties of Alkali-Activated Slag Mixtures." *Construction and Building Materials* 21 (7): 1463-1469.

APPENDIX

PERMISSION FROM PUBLISHER FOR REUSE OF PUBLISHED PAPER

From: Australian Journal Of Basic And Applied Sciences Editor <ajbaseditor@gmail.com>
Sent: Wednesday, 29 July 2015 3:17 AM
To: Hasan
Subject: Re: PERMISSION TO USE COPYRIGHT MATERIAL AS SPECIFIED BELOW

Dear brother,
It is our pleasure to support your thesis and i wish to write statement in your thesis about support our journal to your thesis.

To see more Journal visit our Page:
http://www.aensiweb.com/journals.html

Best Regards

Please visit our page at academia.edu

https://independent.academia.edu/AmericanEurasianNetworkforScientificInformationAENSIPublisher

Editor in Chief

Dr. Abdel Rahman Mohammad Said Al-Tawaha (Ph.D McGill University)

Founder President of American-Eurasian Network for Scientific Information

[Www.Aensiweb.Com]

On 28 July 2015 at 20:46, Hasan <umair.hasan@postgrad.curtin.edu.au> wrote:

Australian Journal of Basic and Applied Sciences

Dear **Publisher,**

It is my understanding that your organisation is the copyright holder for the following material:

"A Review of the Stabilisation", Australian Journal of Basic and Applied Sciences (AJBAS) Vol. 9, Issue No. 7, pp. 541-548, 2015.

I would like to reproduce an extract of this work in a Master's thesis which I am currently undertaking at Curtin University in Perth, Western Australia. The subject of my research is **Experimental Study on Bentonite Stabilisation using Construction Waste and Slag**. I am carrying out this research in my own right and have no association with any commercial organisation or sponsor.

The specific material / extract that I would like to use for the purposes of the thesis is **"whole of the paper mentioned above"**

Once completed, the thesis will be made available in online form via Curtin University's Institutional Repository espace@Curtin (http://espace.library.curtin.edu.au). The material will be provided strictly for educational purposes and on a non-commercial basis.

I would be most grateful for your consent to the copying and communication of the work as proposed. If you are willing to grant this consent, please complete and sign the attached approval slip and return it to me at the address shown. Full acknowledgement of the ownership of the copyright and the source of the material will be provided with the material.

If you are not the copyright owner of the material in question, I would be grateful for any information you can provide as to who is likely to hold the copyright.

I look forward to hearing from you and thank you in advance for your consideration of my request.

Yours sincerely

Umair Hasan

Postgrad Researcher

(MPhil in Civil Engineering)

Department of Civil Engineering

Curtin University